Vikram Kumar
Avinash Kumar Agarwal
Ashutosh Jena
Ram Krishna Upadhyay   *Editors*

Advances in Engine Tribology

International Society for Energy, Environment and Sustainability

Springer

Energy, Environment, and Sustainability

Series Editor

Avinash Kumar Agarwal, Department of Mechanical Engineering, Indian Institute of Technology Kanpur, Kanpur, Uttar Pradesh, India

AIMS AND SCOPE

This books series publishes cutting edge monographs and professional books focused on all aspects of energy and environmental sustainability, especially as it relates to energy concerns. The Series is published in partnership with the International Society for Energy, Environment, and Sustainability. The books in these series are edited or authored by top researchers and professional across the globe. The series aims at publishing state-of-the-art research and development in areas including, but not limited to:

- Renewable Energy
- Alternative Fuels
- Engines and Locomotives
- Combustion and Propulsion
- Fossil Fuels
- Carbon Capture
- Control and Automation for Energy
- Environmental Pollution
- Waste Management
- Transportation Sustainability

Review Process

The proposal for each volume is reviewed by the main editor and/or the advisory board. The chapters in each volume are individually reviewed single blind by expert reviewers (at least four reviews per chapter) and the main editor.

Ethics Statement for this series can be found in the Springer standard guidelines here https://www.springer.com/us/authors-editors/journal-author/journal-author-helpdesk/before-you-start/before-you-start/1330#c14214

More information about this series at https://link.springer.com/bookseries/15901

Vikram Kumar · Avinash Kumar Agarwal ·
Ashutosh Jena · Ram Krishna Upadhyay
Editors

Advances in Engine Tribology

Springer

Editors
Vikram Kumar
Department of Mechanical Engineering
Indian Institute of Technology Kanpur
Kanpur, Uttar Pradesh, India

Avinash Kumar Agarwal
Department of Mechanical Engineering
Indian Institute of Technology Kanpur
Kanpur, Uttar Pradesh, India

Ashutosh Jena
Department of Mechanical Engineering
Indian Institute of Technology Kanpur
Kanpur, Uttar Pradesh, India

Ram Krishna Upadhyay
National Rail and Transportation Institute
Vadodara, Gujarat, India

Preface

Customer demand and stringent emission norms force automotive manufacturers to deliver energy-efficient, economically viable, and environmentally friendly engines. The ask is getting steeper with every passing year. Advanced combustion systems and modified engine dynamics have generated scope for several interdisciplinary research, including engine tribology. Tribology has a key role in the areas of new materials (ceramics, steels, coatings, lubricants, additives) to apply novel fuels, low viscosity, green lubricants, and low heat rejection engines. Without tribological consideration, modern mode of transportation is impossible.

The International Society for Energy, Environment and Sustainability (ISEES) was founded at the Indian Institute of Technology Kanpur (IIT Kanpur), India, in January 2014 to spread knowledge/awareness and catalyze research activities in the fields of Energy, Environment, Sustainability, and Combustion. Society's goal is to contribute to the development of clean, affordable, and secure energy resources and a sustainable environment for society and spread knowledge in the areas mentioned above, and create awareness about the environmental challenges the world is facing today. The unique way adopted by ISEES was to break the conventional silos of specializations (Engineering, science, environment, agriculture, biotechnology, materials, fuels, etc.) to tackle the problems related to energy, environment, and sustainability in a holistic manner. This is quite evident by the participation of experts from all fields to resolve these issues. The ISEES is involved in various activities such as conducting workshops, seminars, conferences, etc., in the domains of its interests. The society also recognizes the outstanding works of young scientists, professionals, and engineers for their contributions in these fields by conferring them awards under various categories.

Fifth International Conference on 'Sustainable Energy and Environmental Challenges' (V-SEEC) was organized under the auspices of ISEES from December 19–21, 2020, in virtual mode due to restrictions on travel because of the ongoing Covid-19 pandemic situation. This conference provided a platform for discussions between eminent scientists and engineers from various countries, including India, Spain, Austria, Bangladesh, Mexico, USA, Malaysia, China, UK, Netherlands, Germany, Israel, and Saudi Arabia. At this conference, eminent international speakers presented

their views on energy, combustion, emissions, and alternative energy resources for sustainable development and a cleaner environment. The conference presented two high voltage plenary talks by Dr. V. K. Saraswat, Honorable Member, NITI Ayog, on 'Technologies for Energy Security and Sustainability' and Prof. Sandeep Verma, Secretary, SERB, on 'New and Equitable R&D Funding Opportunities at SERB.'

The conference included nine technical sessions on topics related to energy and environmental sustainability. Each session had 6–7 eminent scientists from all over the world who shared their opinions and discussed future trends. The technical sessions in the conference included Emerging Contaminants: Monitoring and Degradation Challenges; Advanced Engine Technologies and Alternative Transportation Fuels; Future Fuels for Sustainable Transport; Sustainable Bioprocessing for Biofuel/Non-biofuel Production by Carbon Emission Reduction; Future of Solar Energy; Desalination and Wastewater Treatment by Membrane Technology; Biotechnology in Sustainable Development; Emerging Solutions for Environmental Applications and Challenges and Opportunities for Electric Vehicle Adoption. 500+ participants and speakers from all over the world attended these three days conference.

The conference concluded with a high voltage panel discussion on 'Challenges and Opportunities for Electric Vehicle Adoption,' where the panelists were Prof. Gautam Kalghatgi (University of Oxford), Prof. Ashok Jhunjhunwala (IIT Madras), Dr. Kelly Senecal (Convergent Science), Dr. Amir Abdul Manan (Saudi Aramco) and Dr. Sayan Biswas (University of Minnesota, USA). Prof. Avinash K Agarwal, ISEES, moderated the panel discussion. This conference laid out the roadmap for technology development, opportunities, and challenges in Energy, Environment, and Sustainability domain. All these topics are very relevant for the country and the world in the present context. We acknowledge the support received from various agencies and organizations for the successful conduct of the Fifth ISEES conference V-SEEC, where these books germinated. We want to acknowledge SERB (Special thanks to Dr. Sandeep Verma, Secretary) and our publishing partner Springer (Special thanks to Ms. Swati Meherishi).

The editors would like to express their sincere gratitude to a large number of authors from all over the world for submitting their high-quality work on time and revising it appropriately at short notice. We would like to express our special gratitude to our prolific set of reviewers, Dr. Ram Krishna Upadhyay, Dr. Vikram Kumar, Dr. Leeladhar Nagdeve, Dr. Jitendra Kumar Katiyar, Dr. Santosh Kumar Mishra, Mr. R. Durga Prasad Reddy, Dr. Surya Pratap Singh, Mr. Dhananjay Kumar, Dr. Himadri Sahu, Dr. Suarabh Chandrakar, Dr. Prabhat Chand Yadav, Dr. Pranab Samanta, Dr. Meenu Srivastava, Anastasios Zavos, Dr. Pradeep, Dr. Sunil Kumar Sharma, who reviewed various chapters of this monograph and provided their valuable suggestions to improve the manuscripts. This book is based on Emerging challenges with modern engines, Recent advances in engine tribology, Novel materials for advanced engine design. This book includes the study of friction, wear, lubrication, suitable lubricant additives, and durability of different engine components of alcohol/biodiesel fueled engines. This book deals with different lubrication systems to overcome friction and wear problems of automotive transportation systems. This book also includes chapters of the different materials for future applications in the automotive transport

sector. This book contains the wear of wheels and axels of locomotives. This book contains a review on friction-induced noise and vibration and tribological behavior of texture surfaces. This book contains a review of tribo-corrosion of materials. Chapters include recent results and are focussed on current trends of tribology in the automotive sector. In this book, readers will get an idea about the friction, wear, and lubrication of different engine components and their lubrication approaches. Few chapters are about the application of the composite material for cleaner combustion of engines. Few chapters focused on the review of tribological systems and their behavior of surface texture and tribo-corrosion. We hope that the book would greatly interest the professionals, post-graduate students involved in alternative fuels application in IC engines, friction and wear study of various engine components, lubrication approaches and different additives of lubricants, and novel materials for advanced engine design.

Kanpur, India   Vikram Kumar
Kanpur, India   Avinash Kumar Agarwal
Kanpur, India   Ashutosh Jena
Vadodara, India   Ram Krishna Upadhyay

Contents

Editors and Contributors

About the Editors

Dr. Vikram Kumar is currently at IIT Kanpur. He received his Ph.D. in Mechanical Engineering from Indian Institute of Technology Kanpur, India in 2010 and 2018. His areas of research include Polymer and composite coating; wear, friction and lubrication; IC engine tribology; alternative fuels; advanced low temperature combustion; engine emissions measurement; particulate characterization. Dr. Kumar has edited 1 book and authored 7 book chapters, 16 research articles in international journals and conferences. He has been awarded with 'ISEES Best Ph.D. Thesis Award' (2018), 'Senior Research Associateship under 'SCIRPOOL Scientist' (2018-2021). He is a life time member of ISEES.

Prof. Avinash Kumar Agarwal joined IIT Kanpur in 2001. He worked at the Engine Research Center, UW@Madison, the USA as a Post-Doctoral Fellow (1999 – 2001). His interests are IC engines, combustion, alternate and conventional fuels, lubricating oil tribology, optical diagnostics, laser ignition, HCCI, emissions, and particulate control, 1D and 3D Simulations of engine processes, and large-bore engines. Prof. Agarwal has published 435+ peer-reviewed international journal and conference papers, 70 edited books, 92 books chapters, and 12200+ Scopus and 19000+ Google Scholar citations. He is the associate principal editor of FUEL. He has edited "Handbook of Combustion" (5 Volumes;

3168 pages), published by Wiley VCH, Germany. Prof. Agarwal is a Fellow of SAE (2012), Fellow of ASME (2013), Fellow of ISEES (2015), Fellow of INAE (2015), Fellow of NASI (2018), Fellow of Royal Society of Chemistry (2018), and a Fellow of American Association of Advancement in Science (2020). He is the recipient of several prestigious awards such as Clarivate Analytics India Citation Award-2017 in Engineering and Technology, NASI-Reliance Industries Platinum Jubilee Award-2012; INAE Silver Jubilee Young Engineer Award-2012; Dr. C. V. Raman Young Teachers Award: 2011; SAE Ralph R. Teetor Educational Award -2008; INSA Young Scientist Award-2007; UICT Young Scientist Award-2007; INAE Young Engineer Award-2005. Prof. Agarwal received Prestigious CSIR Shanti Swarup Bhatnagar Award-2016 in Engineering Sciences. Prof. Agarwal is conferred upon Sir J C Bose National Fellowship (2019) by SERB for his outstanding contributions. Prof. Agarwal was a highly cited researcher (2018) and was in the top ten HCR from India among 4000 HCR researchers globally in 22 fields of inquiry.

Mr. Ashutosh Jena is an Master in Thermal Science from NIT Durgapur; currently pursuing Ph.D. in Mechanical Engineering at IIT Kanpur. He has worked on exergy destruction minimisation through fuel-cell integration with combined cycle power-plant for his master's thesis. He is currently working on the development of combustion control strategies through optical diagnosis of advanced combustion concepts in diesel engine. His other area of interests includes high-pressure spray atomisation and combustion, spray and combustion simulation and alternative fuels with special interest to advanced diesel engines. He is a member of ISEES.

Dr. Ram Krishna Upadhyay is currently working as an Assistant Professor at the National Rail and Transportation Institute, Vadodara, established by the Ministry of Railway, Government of India. He has received his Ph.D. and M.Tech from the Indian Institute of Technology (ISM) Dhanbad in Mechanical & Mining Machinery Engineering with a broad specialization in Surface Engineering and Tribology. Before joining NRTI Vadodara, Dr. Ram has worked as Postdoctoral Fellow at the Indian Institute of Technology Kanpur for more than three and half years. His research interests are lubrication and materials wear for industrial application, tribology of additive manufactured parts and nanocomposites. He is a recipient of the SERB-ACS NPDF best poster competition award by the Science and Engineering Research Board, New Delhi, and American Chemical Society, U.S.A. He published several journal papers, book chapters, edited a book, and completed a project funded by the Science and Engineering Research Board, New Delhi.

Contributors

Avinash Kumar Agarwal Engine Research Laboratory, Department of Mechanical Engineering, Indian Institute of Technology Kanpur, Kanpur, India

A. Behera Department of Metallurgical & Materials Engineering, National Institute of Technology, Rourkela, India

Ilyas Hussain Department of Mechanical Engineering, Indian Institute of Technology Bhilai, Raipur, India

R. J. Immanuel Department of Mechanical Engineering, Indian Institute of Technology Bhilai, Raipur, India

Ashutosh Jena Engine Research Laboratory, Department of Mechanical Engineering, Indian Institute of Technology Kanpur, Kanpur, India

Hemalata Jena School of Mechanical Engineering, KIIT Deemed To Be University Bhubaneswar, Odisha, India

Rutvik Kasvekar National Rail and Transportation Institute, Vadodara, Gujarat, India

Jitendra Kumar Katiyar Department of Mechanical Engineering, SRM Institute of Science and Technology, Kattankulathur, Tamil, India

L. A. Kumaraswamidhas Indian Institute of Technology (ISM), Dhanbad, India

Pratyush Kumar National Rail and Transportation Institute, Vadodara, Gujarat, India

Rakesh Kumar Indian Institute of Technology (ISM), Dhanbad, India

Sudarshan Kumar Combustion Research Laboratory, Aerospace Engineering Department, Indian Institute of Technology Bombay, Mumbai, India

Upendra Kumar National Rail and Transportation Institute, Vadodara, Gujarat, India

Vikram Kumar Engine Research Laboratory, Department of Mechanical Engineering, Indian Institute of Technology Kanpur, Kanpur, India

Padeep L. Menezes Department of Mechanical Engineering, University of Nevada, Reno, NV, USA

Santosh K. Mishra Department of Production Engineering, National Institute of Technology, Trichy, India

D. D. Pagar Department of Mechanical Engineering, K. K. Wagh Institute of Engineering Education & Research, Nashik, India

Dipen Kumar Rajak Department of Mechanical Engineering, G H Raisoni Institute of Business Management, Jalgaon, Maharashtra, India

Rashmi Ranjan Sahoo Environmental Engineering Group, CSIR-Central Mechanical Engineering Research Institute (CMERI), Durgapur, West Bengal, India

Saurabh Sharma Aero-Thermo-Mechanics Department, Université Libre de Bruxelles, Brussels, Belgium

Sunil Kumar Sharma National Rail and Transportation Institute, Vadodara, Gujarat, India

Paramvir Singh Combustion Research Laboratory, Aerospace Engineering Department, Indian Institute of Technology Bombay, Mumbai, India

Purushottam Kumar Singh Department of Mechanical Engineering, BIT Sindri, Dhanbad, India

Rahul Sinha School of Engineering, P P Savani University, Surat, India

S. K. Tiwari Indian Institute of Technology (ISM), Dhanbad, India

Ram Krishna Upadhyay National Rail and Transportation Institute, Vadodara, Gujarat, India

Part I
General

Chapter 1
Introduction to Advances in Engine Tribology

Vikram Kumar , **Avinash Kumar Agarwal** , **Ashutosh Jena, and Ram Krishna Upadhyay**

Abstract Customers demands and stringent emission norms have compelled automotive manufacturers to deliver energy-efficient, economically viable, and environmentally friendly engines. The expectations are getting steeper with time. Advanced combustion systems and modified engine dynamics have given rise to scope for interdisciplinary research, including engine tribology aspects. Tribology has a key role in developing newer materials (ceramics, steels, coatings, lubricants, additives) to be applied along with novel fuels, low viscosity, green lubricants, and low heat rejection engines. This book has four sections: Introduction to advances in Engine tribology, Emerging challenges with modern engines, Recent advances in engine tribology, and Novel materials for advanced engine design. The first section is about the advances in tribology of the modern automotive sector. The second section of this book focuses on the emerging challenges in engine tribology related to friction, wear, and lubrication. The third section of this book deals with the development of next-generation materials and lubricating agents. Several studies on the application of composite materials, nanomaterial technology, are studied in the fourth section of this book. Systems like transmission, axle, tribo-corrosion, etc., which indirectly influence engine operation, have been reviewed from tribological aspects. Overall, this book covers all the aspects of tribological studies related to modern engines.

Currently, the modern automotive sector is moving toward the application of biofuels in engines. These fuels include alcohols, ethers, hydrogen, CNG, etc., which face material compatibility and tribological issues. The major problems related to tribological aspects of modern engines are the failure of the existing engines due to

V. Kumar · A. K. Agarwal (✉) · A. Jena
Engine Research Laboratory, Department of Mechanical Engineering, Indian Institute of Technology Kanpur, Kanpur 208016, India
e-mail: akag@iitk.ac.in

R. K. Upadhyay
National Rail and Transportation Institute, Vadodara, India

wear and insufficient lubrication. The recent advances in tribology and novel material selection offer solutions for these limitations. This book attempts to focus on engine tribological limitations and their possible solutions. The first section of this book covers all the sections and their significant outcomes.

The second section of this book covers the friction, wear, and lubrication aspects of different engine components and the wheel and axle wear of a locomotive. In the first two chapters of this section, friction, wear and lubrication of engines are studied. Friction, wear of alcohol-fuelled IC engines are directly linked to the energy losses in various components such as piston assembly, valves, bearings, and pump assembly (Fuks et al. 2010; Santos Filho et al. 2018). Lubrication of various engine components and lubrication regimes influence the friction of engine components, which reduce with the application of alcohol as fuel. However, due to the corrosive nature of alcohols, the wear of alcohol-fuelled engine components is higher than baseline conventional-fuelled engines and increases the lubricating oil contamination and carbon deposits, causing adverse effects on engine components. Routine maintenance is suggested to overcome these issues in alcohol-fuelled engines.

Similarly, the application of biodiesel-blends in the engines affects the life of engine components in the long term (Sinha and Agarwal 2009). It leads to the wear of vital moving engine components such as piston, piston rings, fuel injector, cylinder liner, and cylinder head and carbon deposition on them. The modifications in the engine parameters like compression ratio, injection timing, and injection pressure affect the carbon deposits and wear of the engine parts. In the third chapter, the wear of the SI engine is discussed. Wear is a complicated phenomenon, and its measurement is tricky. In some studies, the concern is expressed regarding the quantitative measurement of wear of machine components. It is, however, difficult to collect data related to quantitative wear measurement. In recent years, attempts have been made to extend the life of such components by altering the mechanical strength of the materials used for these purposes. In the last chapter of this section, the wheel and axle are integrated and form essential parts of a locomotive that supports the overall weight of the wagon. It requires high reliability in terms of power/torque and different types of strength. The study of wear resistance, thermal crack resistance, noise/ vibration, and the performance characteristics of the wagon is required to avoid failure. Hence, more suitable wheels and axle production strategies should be employed to resolve wear related issues.

The third section of this book is about the different technologies of lubrication and additives to overcome friction and wear. The first two chapters of this section cover the boundary lubrication of nano lubricants and nanomaterials lubrication for the transport systems. Nono lubricants are used for lowering the friction and wear of driving interfaces. Nano lubrication is a very recent development in which thick film designs nano/ micro-scale lubrication. In this chapter, the friction and wear of nanoparticles are studied, suspended in oil/water solution. These particles are uniformly distributed in oil/ water along with some additives. The friction and wear properties of these nanoparticles are dependent on their sizes. The second chapter studies different types of lubrication, tribological properties such as friction and wear, the composition of lubricants, and the impact of lubricants on the environment. It

also deals with lubrication systems, the choice of lubricants, properties, and applications of nano particles-based lubrication in the oil medium. This chapter also covers the properties of grease and its suitable applications, particle-based lubrication such as graphene, molybdenum disulfide, boron nitride, boric acid, tungsten disulfide are tested for the actual applications. The properties of Nanocomposite-based lubrication such as epoxy-graphene-molybdenum disulfide (MoS_2), different oils are discussed. The last chapter of this section covers an in-depth review of the influence of friction, noise, vibrations, and acoustics. This chapter deals with the interdependencies and effects of friction-induced noise, vibrations, and acoustic behaviour of rough surfaces under different wear conditions. This review chapter deals with analytical and computational modelling approaches to study the effect of friction-induced noise, vibrations, and acoustics on rough surfaces.

The fourth section of this book is based on the various novel materials like composites for application in the automotive sector, along with the modelling of the transmission system and tribo-corrosion studies of materials. The first two chapters of this section deal with composite materials for future automobiles. The first chapter discusses the composite materials for cleaner engines, which replace conventional materials. These composites are structural materials having enhanced mechanical and tribological performance. These materials are lightweight and can be used for lightweight engine design. This chapter highlights the fundamental aspects of these composite materials and their performance vis-à-vis conventional metallic class materials. This chapter mainly focuses on the role of composite materials in improving the tribological performance of automotive and aerospace engines. The second chapter discussed the material characteristics required for the substitution of composite materials over traditional automotive components. Composite materials exhibit weight reduction properties in an automotive component. This increases the fuel efficiency with reduced emissions. In addition, composite materials offer safety and comfort with improved vehicle performance due to superior mechanical properties over conventional materials. Bio-composites comprising natural metals and polymers have positively impacted environment friendliness by retaining exceptional properties for desired automotive applications. The third chapter of this section deals with modelling the closed-loop hydrostatic transmission system and its control for the automotive sector. The pump and motor are controlled by the physical model of a closed-loop HST (Hydrostatic Transmission) system. A feedback control mechanism is applied using a PID (Proportional, Integral, and Derivative) controller, which keeps track of the decline in rpm of the motor and, through specific control strategies, sends a command signal to the pump. Based on the received feedback signal, the inclination of the swash plate of the pump is varied, resulting in the increase of the flow rate from the pump. An advanced PID controller was constructed based on a neural network that can approximate nonlinearities. The last chapter of this section deals with the tribo-corrosion that occurs during sliding, fretting, rolling, impingement, etc., in a corrosive medium, which is an important study. These materials may be either ceramics or polymers, or alloys. Researchers found that tribo-chemical reactivity of metal is higher than ceramics and polymers. However, polymer coatings help reduce the chemical reactivity of metals in the presence of a corrosive

medium. Therefore, tribo-corrosion is a crucial factor in deciding the application of materials in different environments. This chapter deliberated on the tribo-corrosion on different materials such as alloy, ceramics, and polymers and summarises the remedies suggested by various researchers to avoid tribo-corrosion.

The book contains various lubrication technologies, additives and materials to overcome the wear and friction of different engine components. Particular topics covered in this book are as follows:

- Introduction to Advances in Engine Tribology
- Friction, Wear, and Lubrication studies of Alcohol-fueled IC Engine
- Impact of Biodiesel Blended Fuels on Combustion Engines in Long Term
- Automated SI Engine Wear Parts
- Wear of Wheels and Axle in Locomotive and Measures Taken by Indian Railway
- Boundary Lubrication Properties of Nano lubricants on the Steel Surface for Transportation Application
- Nanomaterials Lubrication for Transportation System
- The Effect of Friction Induced Noise, Vibration, Wear and Acoustical Behavior on Rough Surface: A Review on Industrial Perspective
- Composite materials and their advancements for a cleaner engine of future
- Role of Composite Materials for Automotive Sector: Potential Applications
- Modelling of a Closed Loop Hydrostatic Transmission System and Its Control Designed for Automotive Applications
- Study on Tribo-corrosion of Materials

References

dos Santos Filho D, Tschiptschin AP, Goldenstein H (2018) Effects of ethanol content on cast iron cylinder wear in a flex-fuel internal combustion engine-a case study. Wear 406:105–117

Fuks BPC, Brandão L, de Lemos Alves M (2010) Valuing the switching flexibility of the ethanol-gas flex-fuel car. Ann Oper Res 176(1):333–348

Sinha S, Agarwal AK (2009) Rice bran oil methyl ester fuelled medium-duty transportation engine: long-term durability and combustion investigations. Int J Veh Des 50:248–270

Part II
Emerging Challenges with Modern Engines

Chapter 2
Friction, Wear, and Lubrication Studies of Alcohol-Fuelled Engines

Vikram Kumar and **Avinash Kumar Agarwal**

Abstract There is a significant demand for biofuels as an alternative fuel for existing internal combustion (IC) engines. The long-term effect of these fuels on engine hardware needs to be studied. These studies include friction, wear, and lubrication (tribology) of different engine parts. Tribological studies of bio-fuelled IC engines play a crucial role in scrutinizing legislated particulate matter (PM) emission norms. Wear of the mating interfaces of fuel injection systems and lubricating oils are an originator of PM emissions from the engine exhaust. The application of biofuels in the short term is encouraging. In long-term applications, durability tests resulted in problems with engine failure because of higher carbon deposition and lubricating oil degradation. This review chapter includes a detailed analysis of friction, wear, and lubrication characteristics of bio-fuelled compression ignition and spark ignition engines. The lubricating oils, their properties, and various additives used were assessed for the alcohol-fuelled engines. However, this review does not have any new results, and it highlights the previous studies and projects the future potential of tribology for bio-fuelled IC engines.

Keywords Alcohol · Engine · Friction · Wear · Lubrication

2.1 Introduction

Tribology is a science of study of friction, wear, and lubrication of interacting interfaces of machine components under relative motion. Solid surfaces of the materials meshing with the environment and their relative movement result in the wear of interacting materials. When grouped with friction and lubrication studies, the science is called tribology. Tribology also deals with the reliability and maintenance of the engine components in relative motion. Tribological study of IC engines reduces material wastage and energy losses due to friction and wear of interacting interfaces.

V. Kumar · A. K. Agarwal (✉)
Engine Research Laboratory, Department of Mechanical Engineering, Indian Institute of Technology Kanpur, Kanpur 208016, India
e-mail: akag@iitk.ac.in

9

The tribological study of bio-fuelled IC engines aims to study friction, wear, and lubrication to reduce the effect of biofuels on the engine hardware and longevity.

The use of renewable fuels worldwide is increasing steadily due to the very high prices of petroleum products and limited reserves. Alcohols are a viable substitute for petroleum-based fuels such as diesel and gasoline and can be used as an alternative fuel for IC engines. Applying alcohols as IC engine fuel reduces particulate and net carbonaceous emissions (Fuks et al. 2010; Dutcher et al. 2011). Currently, many countries are using methanol and ethanol as fuel in IC engines by modifying the existing engines to flex-fuel engines. China uses M15 (15% v/v methanol 85% v/v gasoline blend) for large-scale application in the transport sector (Tibdewal et al. 2014). Methanol is also used on a large scale in other IC engines (Kumar et al. 2020; Agarwal et al. 2020). It is produced from renewable resources, biomass, municipal solid waste (MSW), and coal. Carbon capturing technology has exhibited potential for renewable methanol production. It can displace 0–100% diesel or gasoline using different combustion technologies and suitable engine modifications.

On the other hand, ethanol is produced from corn, barley, wheat, sugar cane, and grains. Brazil uses ethanol as fuel on a large scale since 2006 in their flex-fuel engines/ vehicles (Cavalcanti et al. 2012). 85% of vehicles produced in Brazil have flex-fuel engines and use ethanol-gasoline blends. In the United States of America (USA), gasoline blended with 10 to 15% v/v ethanol is used in most vehicles, and ~11 million vehicles are capable of using E85 (a blend of 85% v/v ethanol and 15% v/v gasoline) (US Government 1988). Many European countries like Sweden and Belgium also adopted biofuels such as ethanol in vehicles (Linde and Frode 2010). Currently, in India, most vehicles are using 5% ethanol blends (GSR 412(E) 2015). The Ministry of Road Transport & Highways (MoRTH) has announced the application of 10–15% ethanol blended with gasoline and asked the automotive sector to develop and adapt flex-fuel engines in the vehicles (GSR 881(E) 2019; GSR 682(E) 2016).

The chemical and physical characteristics of the alcohols are given in Table 2.1, which is helpful to explain the tribological characterization of alcohols and their effects on the engine components under relative motion. The presence of oxygen in alcohols causes the degradation of oxidative materials and lubricants, resulting in the wear and corrosion of engine components in contact with the fuel, making them prone to oxidation. Hence, various engine parts in direct contact with fuel should be compatible with alcohol. Alcohols also mix with lubricating oil during the engine operation, causing lubricating oil degradation, suppressing the important lubricating oil properties. The contamination of alcohols in lubricating oil is the cause of tribological concern. Alcohols (methanol and ethanol) have higher latent heat of vaporization, making them more prone to contaminate the lubricating oil than diesel or gasoline during the warmup, cold-start, and short-distance driving (Silva et al. 2011a). 6–25% ethanol was detected in the lubricating oil sump of ethanol fuelled engine during the bench tests (Chui and Baker 1980; Chui and Millard 1981). Hence, lubrication oil degradation enhanced the friction coefficient between the lubricated engine parts, leading to higher wear (Boons et al. 2008; Ferrarese et al. 2010). Very few researchers investigated ethanol's effect on the lubricating oil and reported that ethanol does not affect the friction much; however, the moisture in the

Table 2.1 Chemical and physical characteristics of conventional fuels and primary alcohols (Heywood 1988; www.epa.gov/regulations-emissions-vehicles-and-engines/regulations-greenhouse-gas-emissions-passenger-cars-and, https://en.wikipedia.org/wiki/Bharat_stage_emission_standards, Campos-Fernández et al. 2012; Chen et al. 2010)

Fuel property	Gasoline	Diesel	Methanol	Ethanol	Butanol
Formula	$C_nH_{1.87n}$	$C_nH_{1.7n}$	CH_3OH	C_2H_5OH	C_4H_9OH
Molecular Weight	100–110	200	32.04	46.07	74.12
Octane No (Research)	92–98	–	106	109	98–105
Octane No (Motor)	80–90	–	92	90	85–93
Cetane No	10–15	40–55	2	8	17
Density, kg/L	0.72–0.78	0.81–0.89	0.792	0.785	0.72–0.78
Boiling point, °C	27–225	188–343	65	78	97.6–117.8
Specific Heat kJ/kg K	2.2	1.8	2.5	2.4	2.4
Specific Heat (Vapor) kJ/kg K	~1.7	~1.7	1.5	1.4	1.9–2.6
Viscosity, cst @20 °C	0.37–0.44	2.6–4.1	0.59	1.19	3.6–3.7
Latent Heat of Vaporization, kJ/kg	349	233	1178	923	671.1–707.9
Lower Heating Value, MJ/kg	44.0	41.0	20.0	26.9	33.1
Lower Flammability Limits, Vol%	1.4	0.6	6.7	3.3	1
Higher Flammability Limits, Vol%	7.6	7.5	36.0	19.0	11
Flash Point, °C	−43	74	12	13	26–36
Vapor Pressure, kPa @ 20 °C	48–103	< 0.1	32	15.9	2.2–5.2
Autoignition Temperature, °C	246 -280	210	464	423	343
Stoichiometric Air–Fuel Ratio	14.6	14.4	6.47	9.00	11.21

ethanol contaminates the lubricating oil and reduces the friction (Chui and Baker 1980; Silva et al. 2011b). Ethanol contamination of the lubricating oil suppresses its viscosity, reducing the electrohydrodynamic film thickness. This results in shifting from a full film lubrication regime to a mixed lubrication regime (Costa and Spikes 2015).

The behavior of alcohol contamination of the base oil is different from the formulated lubricating oil. Ethanol-free base oil does not form any film. However, alcohol-containing base oil forms a boundary layer film. The boundary layer formation is due to ethanol oxidation when it comes in contact with hot rubbing surfaces. The boundary layer thickness of a formulated lubricating oil is reduced in the presence of ethanol. The Stribeck curve of the formulated lubricating oil shows that thicker boundary film is formed with increasing engine speed. However, the addition of both anhydrous and hydrous ethanol suppresses the boundary film thickness (Costa and Spikes 2015). Hence, ethanol is more prone to form a tribofilm when added to base lubricating oil. The tribofilm formed protects the wear of rubbing surfaces. Zinc di-alkyl di-thiophosphates (ZDDPs) is an anti-wear additive that forms tribofilm to protect the mating surfaces. However, metal salts, sulfur, and phosphorus oxides

in the ZDDP containing lubrication oil adversely affect exhaust gas after-treatment devices (Taylor et al. 2000).

2.2 Frictional Losses in IC Engines

Mechanical friction of a vehicle can be reduced by interchanging the sliding contacts to rolling contacts, suppressing the weight, reducing the tolerance of piston rings-liner interface, and enhancing the quality of lubrication between the mating components of the engine in relative motion. The main parts of the engine targeted for friction reduction are the valvetrain, crankshaft, crankpin bearings, piston, rings, and fuel pump. This can reduce fuel consumption by up to 1–4 percent. Valvetrain contributes to higher friction at low and high engine speeds. The friction between the sliding contact interfaces of the cam and push rod can be reduced by interchanging with a rolling-type cam-follower design. The use of lightweight materials such as alloys of Titanium or ceramic is another possibility for reducing friction. Valve springs are also made of titanium alloys, which can sustain the heavier load.

Figure 2.1 shows the energy balance and mechanical losses contributed by friction and pumping in an engine. The frictional losses are mainly contributed by the piston assembly, bearings, valve train assembly, and pump assembly. The cylinder liner-piston ring interface contributes approximately 50% of the friction losses. However, the energy lost due to the cylinder cooling was nearly 38%. The main purpose of piston rings is to prevent the leakage of lubricating oil from the crankcase to the combustion chamber and combustion gases from the combustion chamber to the crankcase. Most piston rings are a combination of two compression rings and one lubricating oil ring. Rings are mostly hydrodynamically lubricated, but they make a metal-to-metal contact at the top and bottom dead centers since in these positions, the lubrication regime changes to boundary lubrication. The ring tension of these rings acts as a seal; however, it contributes to the friction. The suppressed stress of the rings reduces the friction by 5–10% and improves the fuel economy by 1–2% (Taylor 1998).

Piston design also affects the contribution to the overall friction in the engine. The skirt of the piston causes higher friction as the friction is directly proportional to the contact area. Hence, the piston skirt size could reduce the contact area with the cylinder liner to reduce friction. A more significant contribution to the friction is from the mass of engine components, which can be reduced by using lightweight materials. Another benefit of the lightweight components, including the piston, is that it reduces engine vibrations. The mass of the connecting rod also contributes to friction, and its mass can also be reduced by using innovative lighter materials. Hence, aluminum alloy or reinforced plastics can be used to manufacture both the piston and the connecting rod. A unique coating on the piston and piston rings can also be used to reduce friction. These materials are molybdenum and diamond-like carbon (DLC), self-lubricating materials that reduce friction by nearly ~5% (Mobarak et al. 2014).
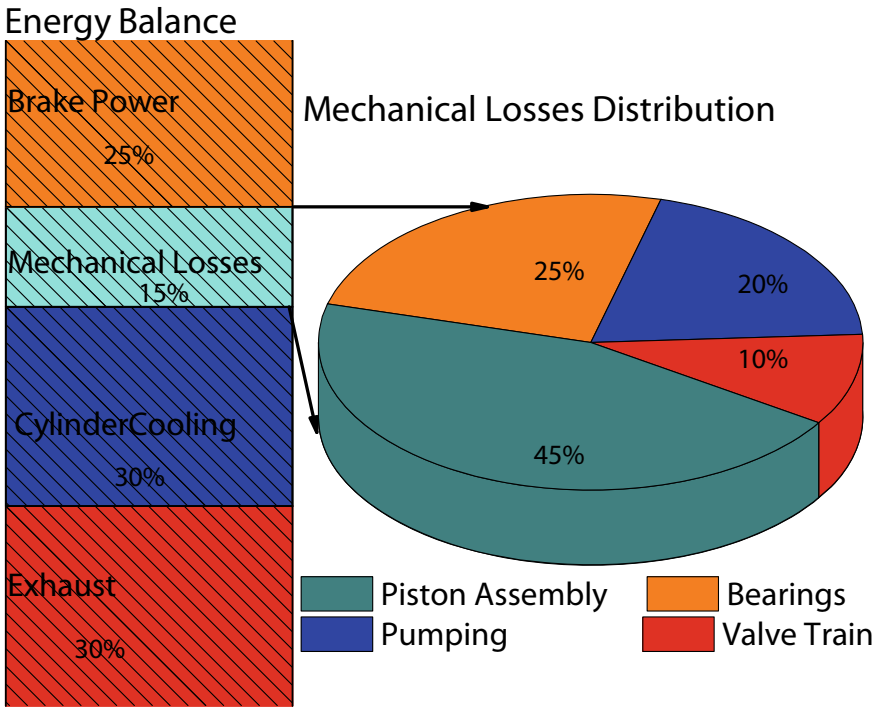
Fig. 2.1   Distribution of fuel energy mechanical losses in an engine (Priest and Taylor 2000; Taylor 1998)

Journal bearings support the crankpin and crankshaft. Crankshaft bearings account for ~25% friction losses, which fully developed lubricating oil films can reduce. A further reduction in friction can be achieved by replacing the journal bearings with roller bearings. Generally, gear-type oil pumps control the flow of lubricating oil. Appropriate design of the oil pump can reduce friction by ~1.5% (Taylor 1998). The lubricating oil selection is also an important aspect to reduce the friction between different engine components. The friction modifiers (like molybdenum compounds) can also be added to reduce the friction without affecting oil consumption.

2.3   Wear Characterization

Wear is an unavoidable phenomenon, which adversely affects the functionalities of the engine components. Relative motion causes continuous material loss between the contacting surfaces (piston ring, cylinder liner, piston, cylinder head, valves, pumps, injectors, etc.). Wear inspection of components is a critical study to assess the engine's reliability in the long run. Quantitative and qualitative studies can perform

wear characterization through image analysis, measurement of wear depth, width, and weight. In general, the wear analysis is performed from time to time by lubricating oil inspection for cost-effective maintenance to enhance reliability and productivity.

2.3.1 Wear Measurement Methods

One of the primary methods for wear analysis is the visual inspection of worn surfaces. Secondly, various imaging instruments are used for the wear inspection of the surfaces. These methods are used to qualitatively assess the wear of different engine components after the long endurance test. Various instruments used for these analyses are digital cameras, microscopes, and scanning electron microscope (SEM) for imaging at different magnification levels. Wear scar diameter is measured through these techniques. The wear volume or wear rate is calculated from 3-D optical images showing wear depth, width, and length, obtained by the optical profiler. The wear rate of worn surfaces can be measured by using the following formula (Bilyeu et al. 2001; Kumar et al. 2019):

$$W_{sp} = \frac{V}{LD} mm^3/Nm$$

Here, V is the wear volume, L is the normal load, and D is the total sliding distance. The wear volume is the multiplication of wear depth, width, and length.

2.3.2 Wear-Metal Analysis of Lubricating Oil Samples

Metallic wear debris from engine components carried by lubricating oil gets accumulated in the oil sump. The lubricating oil samples were drawn at fixed time intervals during the engine testing for further analysis. This analysis quantifies various trace metals (Al, Fe, Mn, Zn Cu, Ni, Pb, Cr, and Mg) present in the lubricating oil. The dry ash extraction method is used to extract metal debris from the lubricating oil (Palus 1998). In this method, a 5-gm lubricating oil sample is kept in the crucible and put on a hot plate at 120 °C to remove the moisture. After that, the sample is placed in a muffle furnace at 450 °C and 650 °C for 2 h and 4 h, respectively. After that, dried ash is dissolved in 1.5 ml concentrated HCl, followed by 100 ml distilled water, forming an aqueous solution. This solution is analyzed using the atomic absorption spectroscopy (AAS) technique, and the trace metals are quantified (Singh et al. 2006). The sources of different metals are given in Table 2.2.

Table 2.2 Different trace metals in lubricating oil and their sources (Nadkarni 2004; Agarwal 1999)

Trace metal	Sources of wear trace metals
Magnesium	Bearings, cylinder liner
Aluminum	Piston, bearing, dirt
Zinc	Bearings, platting, brass components
Chromium	Compression rings, coolant, crankshaft, bearings, plating of cylinder liners
Iron	Engine block, cylinder liner, rings, crankshaft, anti-fiction bearings
Copper	Bearing, piston rings
Nickel	Piston rings, valves
Manganese	Steel shafts, valve
Lead	Bearing

2.3.3   Soot in Lubricating Oil Samples

There is no inorganic carbon (carbonate content) present in the lubricating oil. The base lubricating oil is an organic compound, and additives are complex organometallic compounds. Hence, there is a negligible chance of inorganic carbon formation during the engine operation. The organic carbon originates from the soot gets dissolved in the lubricating oil. The soot in the lubricating oil is measured by quantifying the total carbon content of lubricating oil. The difference in carbon content between used lubricating oil and fresh lubricating oil is the total soot loading to the lubricating oil. Soot emissions are relatively lower from the alcohol-fuelled engines; hence, reduced soot loading enhances the lubricating oil life.

2.3.4   Wear Analysis of Various Engine Components

The wear of engine parts changes periodically by changing the lubricating oil. A thin film of lubricant separates the mating components in an engine. The oil film thickness is relatively lower in an alcohol-fuelled engine. Figure 2.2 shows different types of surface interactions and corresponding wear in engine bearings.

2.3.4.1   Piston Rings and Cylinder Liners

The main components of the power assembly are the piston and rings. There are three types of piston rings: compression rings, oil rings, and middle rings. Different materials are used for each ring. The oil ring is placed at the bottom of the ring pack. It controls the oil film thickness between the cylinder liner and the piston rings. Oil rings help in cooling the piston and cylinder using lubricating oil. It transports the
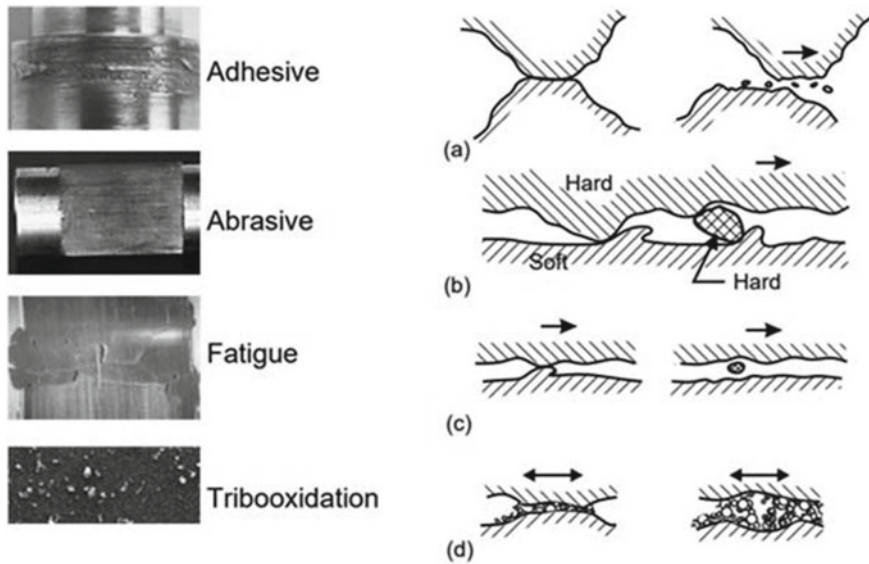
Fig. 2.2 Different types of wear in IC engine bearings (Lakshminarayanan and Nayak 2011)

oil during the reciprocating motion of the piston to lubricate the contact between the cylinder liner and the piston rings. The compression ring restricts the leakage of in-cylinder gases into the lubricating oil sump. The amount of lubricant available at the compression ring is significantly low in quantity, resulting in boundary lubrication. Since the cylinder pressure fluctuates during the cycles, the sealing force of corresponding rings varies dynamically. Hence flexible and light-weight rings are suitable in the engine cylinder.

Several researchers performed a wear analysis of piston ring assembly for alcohol-fuelled engines. Wear of rings and cylinder bore has been reported as a major issue in alcohol-fuelled SI engines under low engine operating temperature (Ryan et al. 1986; Chen and Papadopoulos 2019). The formation of Formic acid from partial oxidation of alcohols increases under low-temperature conditions. It is very reactive with iron and leads to corrosive wear of engine components. The wear of piston rings of methanol fuelled engines is similar to gasoline fuelled engines (Schaefer et al. 1997). Filho et al. (2018) performed an end-to-end engine test to study the wear of the cylinder bore of a flex-fuel engine. Figure 2.3 shows the new piston and piston rings before the test and the carbon deposits formed after the gasoline and ethanol-fuelled engine tests. Ethanol fuelled engine test exhibited lower carbon deposits than gasoline. These carbon deposits led to abrasive (three-body) wear of pistons, rings, and cylinder bore. The localized wear profile of cylinder bore at the top dead center (TDC) and bottom dead center (BDC) is shown in Fig. 2.4 for the gasoline and ethanol fuelled engines. It indicated that higher wear occurred at the upper end of the first ring, which reduced sharply in the direction of the central region of the stroke. The wear increased at the BDC position. The localized wear of

Fig. 2.3 Piston and ring images before and after the test for gasoline- and ethanol-fuelled engine in an end-to-end test of a flex-fuel engine (Santos Filho et al. 2018)
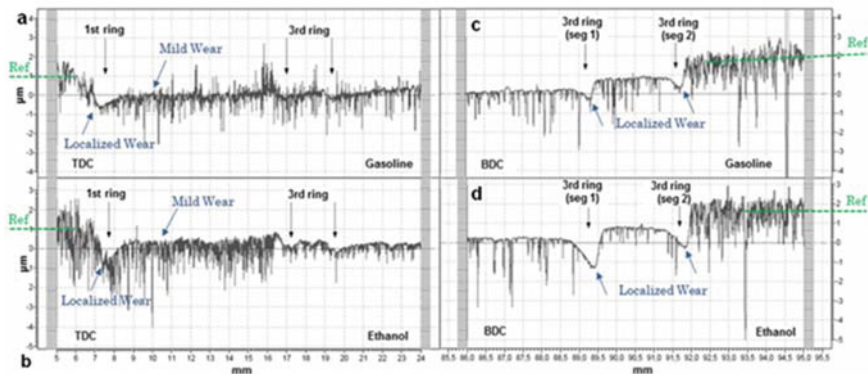

Fig. 2.4 Wear profile of the cylinder liner at the top (**a** and **b**) and bottom (**c** and **d**) dead centers at the reference point, and first and third ring positions in the end-to-end test in a flex-fuel engine (Santos Filho et al. 2018)

cylinder bore was higher at the BDC than at TDC. The maximum wear occurred for the ethanol fuelled engine at the BDC. However, the lowest wear was observed from the ethanol fuelled engine at TDC (Fig. 2.5).

2.3.4.2 Valve Seats and Valve Guides

The wear of valves is affected by the hardness of the material, seating speed, and deflection of valves in high cylinder pressure conditions (Dooley et al. 1997). The valve seat distortion occurs due to mishandling, such as valve seat misalignment, improper cooling, and improper tightening of the cylinder head bolts. Inlet valve wear occurs due to distortion in design, unsuitable fitting, and insufficient lubrication. On the other hand, the exhaust valve wears due to material oxidation under the high-temperature engine operating conditions (Wiles 1965). Other factors which cause valve wear are incorrect installation of spring, higher tappet clearance, higher clearance between the stem and the valve guide, seat grind-in, and valve sticking.

Fig. 2.5 Wear of cylinder bore at the top dead center and bottom dead center in the end-to-end test of a flex-fuel engine (Santos Filho et al. 2018)
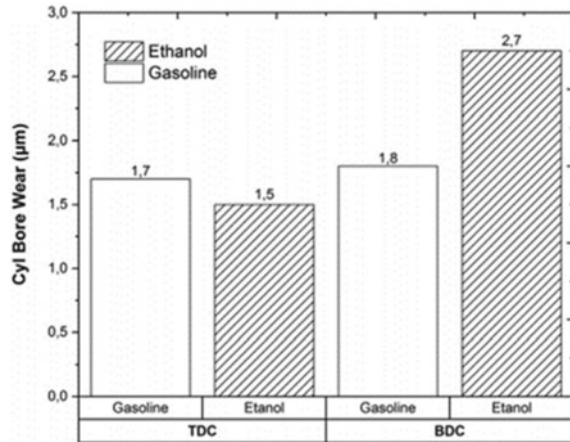
A higher value of the coefficient of friction at the seat angle results in a higher normal force that causes fretting wear during relative motion in the unlubricated conditions (Wang et al. 1995). Exhaust valve seats are exposed to extreme temperatures (up to 1000°C), resulting in thermal stress. Gas engines undergo higher wear than diesel engines (http://www.substech.com/dokuwiki/doku.php?id%C2%BCbearings_in_internal_combustion_engines). Self-lubricating materials can reduce valve wear (Inoue et al. 1993). The wear of the valve train for the M85 (85% v/v/ methanol and 15% gasoline) fuelled engine was higher than the gasoline-fuelled engine at lower temperatures (Schaefer et al. 1997). The presence of methanol and water in the lubricating oil after the combustion promoted the wear of the valve train. The emulsification of lubricating oil by methanol resulted in a mixed lubrication regime, leading to higher cam lobe wear.

2.3.4.3   Bearings

Bearing is a supporting component that allows relative motion between two parts, reducing the power loss (Labeckas et al. 2019). Bearings used in engines are mostly sleeve-type sliding bearings. Bearing always works under lubricated conditions. Surface finish, presence of foreign particles, and misalignment are the main reasons for bearing wear. Due to chemical reactions with surfaces, different types of wear encountered in engine bearings are abrasive wear, adhesive wear, fatigue wear, and chemical wear. The wear of bearings is not significantly affected by lubricating oil contamination as they are lubricated under a hydrodynamic (full-film) lubrication regime. The anti-wear properties of lubricating oil effectively minimize the abrasive wear of bearings for the methanol-fuelled engines (Schaefer et al. 1997).

2.3.4.4   Fuel Injection System

The fuel injection system is the engine's heart, consisting of the fuel pump, fuel filter, and injector. The fuel pump works with very minimal clearance between the mating plunger and barrel. The functioning of the fuel pump depends upon the fuel lubricity. The working pressure of the fuel pump has increased significantly over the years to comply with emission norms, particularly the particulate matter limits. The high fuel injection pressure requires very low clearances (~1 μm) between the metallic components of fuel pumps and injectors to avoid fuel leakage, which increases the chances of wear. When alcohols are used in the high-pressure pump, the wear of the mating surface increased due to the lower viscosity of alcohols. Contaminants such as water and abrasive particles in the fuel increase the component wear.

Methanol is highly susceptible to absorb moisture, forming an aqueous solution. The water may enter during storage or transport. Water contamination may be in the form of free water, dissolved water, or emulsified water. It rapidly oxidizes, catalyzing the wear of steel components because of corrosion and rusting of fuel injection system parts. This leads to the breakdown of fuel metering components, governor, nozzle, and pump. A study reported a 39% reduction in fuel delivery by a pump after 100 h of operation on ethanol-blended diesel (12% ethanol) due to wear of the plunger barrel of the high-pressure pump (Taylor 1998). Despite the lower friction of the ethanol–diesel blends, the wear scar diameter was 10% higher for the ethanol–diesel blend than baseline diesel.

2.4   Different Lubrication Methods

Lubrication of the engine deals with the durability of components and frictional wear. Different engine parts are lubricated under various lubrication regimes shown in Fig. 2.6, as reflected by the Stribeck curve.

Boundary Lubrication: It deals with high load, low speed, and low viscosity. A small amount of lubricant is present between the contacting interface, resulting in higher metal-to-metal contact. In this lubrication regime, friction is rather high, resulting in increased wear and higher temperature rise. Cam followers and rings are generally lubricated under this regime.

Mixed Lubrication: Under a mixed lubrication regime, an abrupt drop in the coefficient of friction occurs. The reduction in coefficient of friction is because of the lower viscosity of lubricant and minimization of the contact area of the mating surfaces. Separation of surfaces increases the viscosity or speed and changes to full film lubrication without any surface contact. It varies from the boundary (asperity contact) to hydrodynamic (full film separation) lubrication. Piston rings (returning from TDC and BDC) are under this regime of lubrication.
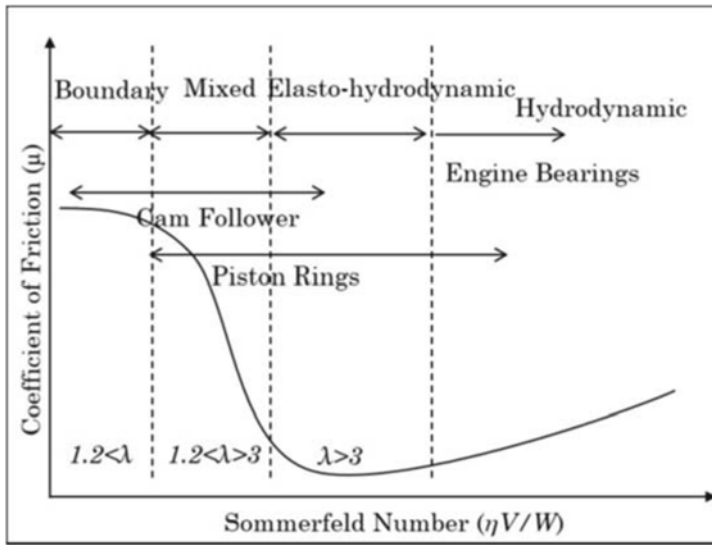
Fig. 2.6 Stribeck curve showing various lubrication regimes, as applicable to different engine components (Kurre et al. 2020)

Elasto-Hydrodynamic Lubrication: In this lubrication regime, contacting surfaces are theoretically separated. However, they are in contact, and a fragile lubricating film is formed. There is an elastic distortion of the mating parts, which is influenced by pressure and viscosity. Cam follower and piston rings are under the elastohydrodynamic regime of lubrication.

Hydrodynamic Lubrication: A full lubricant film is developed between the mating surfaces in the hydrodynamic lubrication regime. Load is carried by the fluid pressure generated by hydrodynamic action dominated by the dynamic viscosity of the lubricant. Most bearings are lubricated under this regime. The piston ring lubrication during the traverse between the dead centers also falls under this regime.

2.4.1 Lubricating Oil Properties and Their Variations

Scheduled analysis of lubricating oil enhances the engine's performance and life. The lubricating oil study also reduces the maintenance cost of the engine. A lubricating oil study is performed for measuring its properties. Many of these properties change with time, and each of them is discussed in this section.

Total Acid Number (TAN): TAN is a measure of the acidity of the lubricating oil. It is measured in mass (in mg) of KOH required to neutralize one gram of lubricating oil. The ASTM D664 standard is used for the titration. For the titration reactions,
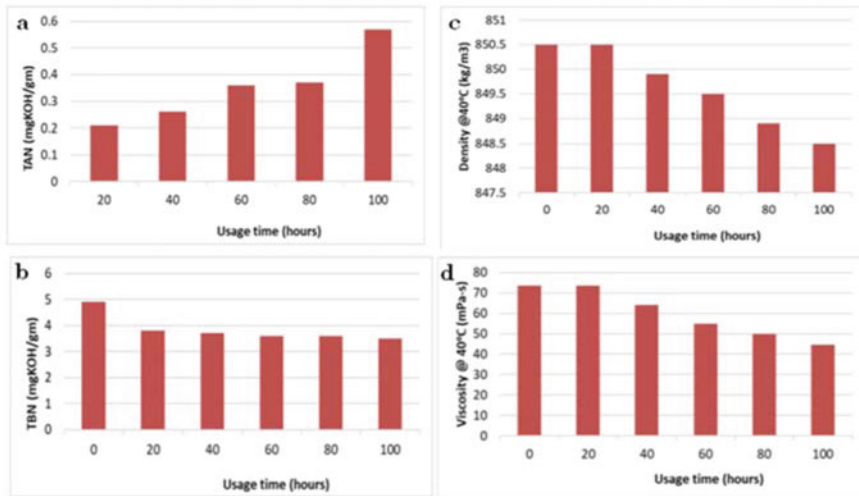
Fig. 2.7 The variations of lubricating oil properties with time for ethanol–diesel-fuelled engine (Dam et al. 1997)

lubricating oil is dissolved in the solution of water, toluene, and isopropanol and then neutralized by KOH. The dilution of ethanol in the lubricating oil increases its TAN, which causes oxidation of lubricating oil, resulting in its degradation. As seen in Fig. 2.7a, TAN increases with the engine's running duration. The maximum allowable TAN of lubricating oil is 3 mg of KOH/g more than the TAN of fresh lubricant (Itoh 2011).

Total Base Number (TBN): It is a measure of the basicity of lubricating oil, which is equivalent to the total mass (in mg) of KOH per gram of lubricating oil that neutralizes the acid (HCl). It is an indication of corrosion prevention by the lubricating oil, which occurs due to oxidation. TBN is measured by potentiometric titration (ASTM D2896), in which lubricating oil is dissolved in the solution of water, toluene, chloroform, and 2-propanol and then treated with acid. Ethanol dilution promotes oxidation, resulting in reduced load-bearing capacity of lubricating oil. TBN of the lubricating oil decreases with the engine running time, as shown in Fig. 2.7b (Dam et al. 1997). The lubricating oil needs to be changed when TBN reduces to 50% of its initial value (Itoh 2011).

Density: Density plays a vital role in the monitoring of the quality of the lubricating oil. The density of lubricating oil is lower than water. Phase separation of oil and water occurs while the engine is stationary. The presence of water in the lubricating oil affects the density and viscosity of the lubricant, resulting in insufficient lubrication of the engine components. Temperature is another parameter that affects the density of the lubricating oil. As the temperature rises, the density decreases. The fuel contamination in the lubricating oil increases its density. Studies have found that

the overall density of the lubricating oil decreases for alcohol-fuelled engines (Kurre et al. 2015).

Viscosity: Viscosity is the measure of the shear force between the two adjacent layers of the fluid. Hence, lubricating oil with higher viscosity requires greater shear force for the relative motion of hydrodynamically lubricated engine parts. Simultaneously, higher viscosity lubricating oil can survive high load due to its high load-bearing capacity. The main purpose of the lubricating oil is the lubrication of engine components to reduce friction and wear of interacting surfaces during the engine operation. The viscosity of lubricating oil decreases with the addition of foreign materials such as fuel and water. It also reduces with increasing lubricating oil temperature. The viscosity of the lubricating oil reduces with the runtime of the engine. Fuel dilution and the thermal oxidation of the lubricating oil are the main reasons for reducing viscosity. The lubricating oil of the alcohol-fuelled engine is diluted by the unburnt alcohol, which condenses over the oil film due to its high latent heat of vaporization. An engine tribological study was performed by blending 6% (v/v) alcohol in gasoline. The viscosity of lubricating oil dropped to 30% of its original value (Khuong et al. 2017). The dilution of alcohol in lubricating oil worsens the friction, but at higher temperatures (>75°C), ethanol evaporates and minimizes its effect on the friction.

2.4.2   Effect of Alcohol on the Lubricating Oil

A large amount of energy is lost in the engine due to a lack of study about friction, wear, and lubrication. Many researchers investigated the friction, wear, and lubrication of alcohol-fuelled engines. Lubricating oils are used to lubricate various engine components. Alcohols (methanol and ethanol) are not compatible with lubricating oils used in engines. Various studies were performed to investigate the effect of alcohols on the lubricating oil used in the engines. Shah et al. (1996) simulated the methanol contamination effect for the injector and crankcase lubricant. Methanol quantity of 1 ml and 200 ml, respectively, in 1000 ml lubricating oil were considered for investigations. The oxidation stability and lubricity of lubricating oil decreased. Banerji et al. (2016) outlined the microlevel mechanism to understand wear and friction. The presence of ethanol in the lubricating oil caused the residue oil layer (ROL), which boosted the degradation of anti-wear additives present in the lubricating oil. So, a specific coating of non-hydrogenated diamond-like carbon (NH-DLC) was recommended to reduce the wear of engine components. This was because of hydroxyl (OH) passivation due to NH-DLC coating, which reduced the coefficient of friction between the mating parts under relative motion. The application of E85 diluted the lubrication oil. It surprisingly minimized the coefficient of friction from 0.11 to 0.08 with NH-DLC coating on the piston rings while maintaining the wear rate nearly constant (Fig. 2.8a and b)). Hence, the development of appropriate materials for coating is responsible for the suppression of friction and wear. Figure 2.8c shows

Fig. 2.8 Coefficient of friction variations with number of cycles for different pairs of materials/coatings for E85 diluted and undiluted lubricating oil and SEM images of oil residue level (Banerji et al. 2016)
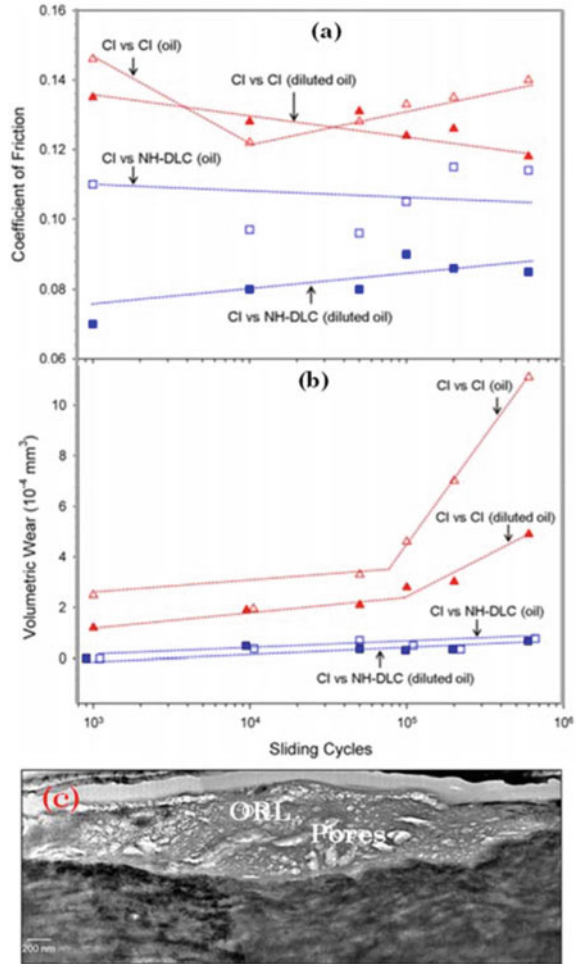
the scanning electron microscopy (SEM) images of the worn surfaces in which ORL and oil pores are demonstrated, confirming the lubricating oil degradation.

The wear of the engine components (piston rings, cylinder bore, cam lobes, and bearings) of the methanol fuelled engine depends on lubricating oil formulation, mainly the detergent chemistry. The wear of methanol-fuelled engine components can be reduced by maintaining the alkalinity of lubricating oil (Crepaldi et al. 2018). The main reason for the wear of methanol-fuelled engines is water contamination and methanol contamination of the lubricating oil. The formulation of methanol-compatible lubricating oil can control the wear by adding greater polar/metal-responsive additives (Crepaldi et al. 2018). The lubricating oil contaminated by ethanol reduced the coefficient of friction between the liner and piston ring by
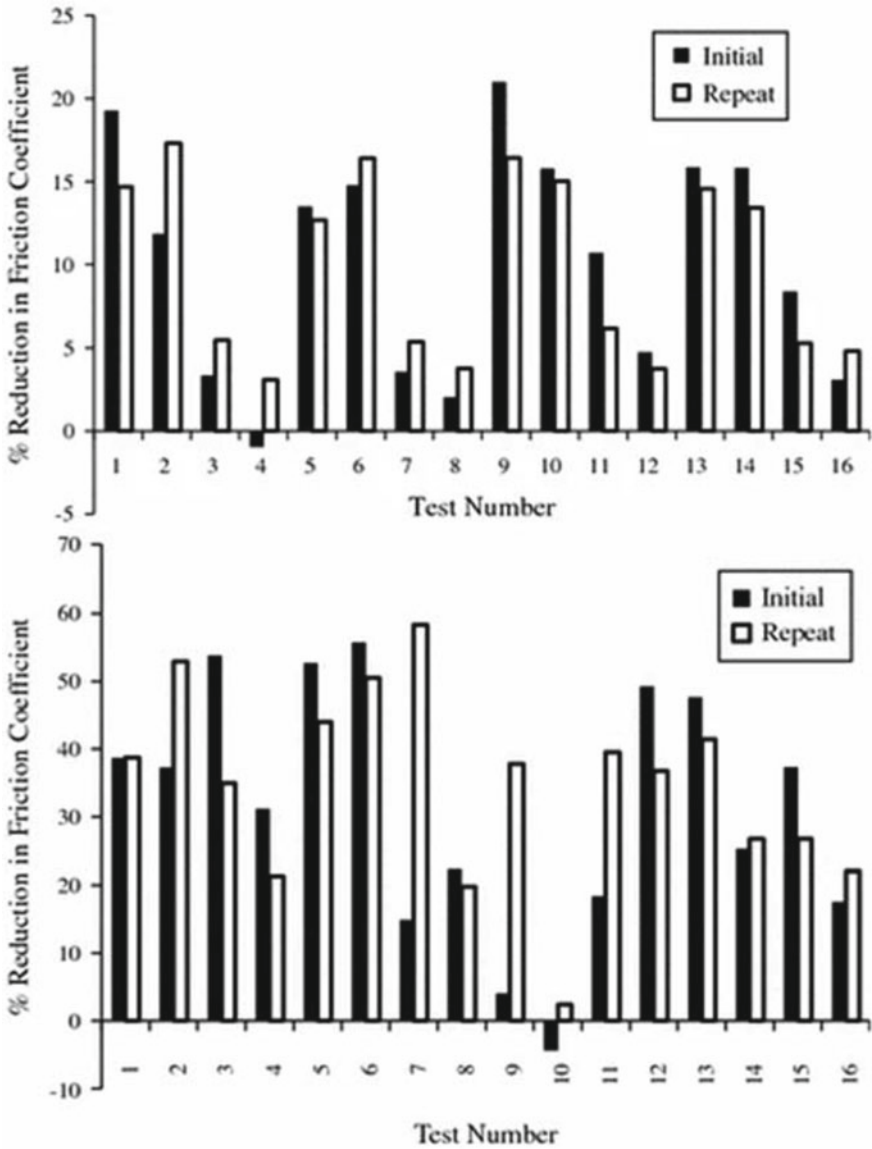
Fig. 2.9 Coefficient of friction reduction (%) for **a** separated phase and **b** sludge phase lubricating oil in comparison to reference formulated lubricating oil (Silva et al. 2011b)

~15% at 50°C. However, at higher temperatures (130°C), the coefficient of friction reduction was lower (almost ~8%) because of the evaporation of ethanol at high temperatures. Hence, the wear of cylinder liner and piston rings was not affected by ethanol contamination (Shukla et al. 1992). Coata and Spikes (2016) investigated the contaminant present in the lubricating oil of an ethanol-fuelled engine. They studied the development of tribo-films and the stability of the lubricating oil containing ZDDP as an anti-wear additive by 5% blending of hydrated and anhydrous ethanol. Tribo-films were solid films formed due to the chemical reaction of lubricants with contacting surfaces They observed that tribo-film thickness reduced with the addition of ethanol, and the reduction of film thickness was more in the case of hydrated ethanol than anhydrous ethanol. These tribo-film destructions caused higher wear of the contacting surfaces.

Bioethanol is an economically viable substitute for gasoline, but it is necessary to study its effect on the existing lubricating oil, cost-effectiveness, and durability. De Silva et al. (2011b) tested different combinations of lubricating oils. They performed tribological and physical property measurement tests for ethanol and water contaminated lubricating oils and compared them with the formulated lubricating oil. The formulated lubricating oil had 5 and 10% ethanol with a combination of 8 and 16% water, respectively. The lubricating oil mixture was separated into two phases: the oil, and the white sludge phase (mixture of water and ethanol). FTIR and viscosity tests analyzed the qualities of these lubricating oil mixtures. There was a significant reduction of coefficient of friction between the cylinder liner and piston ring interfaces in the case of separated phase lubricating oil compared to the reference formulated lubricating oil. Temperature played a dominant role in tribological test conditions of the separated lubricating oil. In contrast, in the case of separated sludge, ethanol alone plays a vital role in the frictional response of the ring-liner interfaces. From Fig. 2.10, it was observed that the percentage reduction of the coefficient of friction with the reference lubricating oil for the separated sludge phase was higher than the separated oil phase.

The self-contamination property of fuel is affected by its porosity. Butanol has low lubricity and porosity (Kuszewski et al. 2021). Hence, butanol is not as self-contaminant fuel like diesel. The durability of injectors is affected by fuel properties at elevated temperatures. The lubricity of the diesel and butanol-diesel blends (5, 15, and 25%) were measured at different temperatures (30, 60, 90, and 120°C) to study the effect of alcohol percentage and temperature. The higher percentage of butanol at elevated temperatures showed superior lubrication properties than lower percentages. This analysis exhibited that 25% butanol at 60°C fulfilled the recommended lubrication properties (Fig. 2.10).

2.5 Carbon Deposits on Engine Components

Various engine components are operated under severe mechanical stresses and at high temperatures. Carbon gets deposited on these components due to oxidative
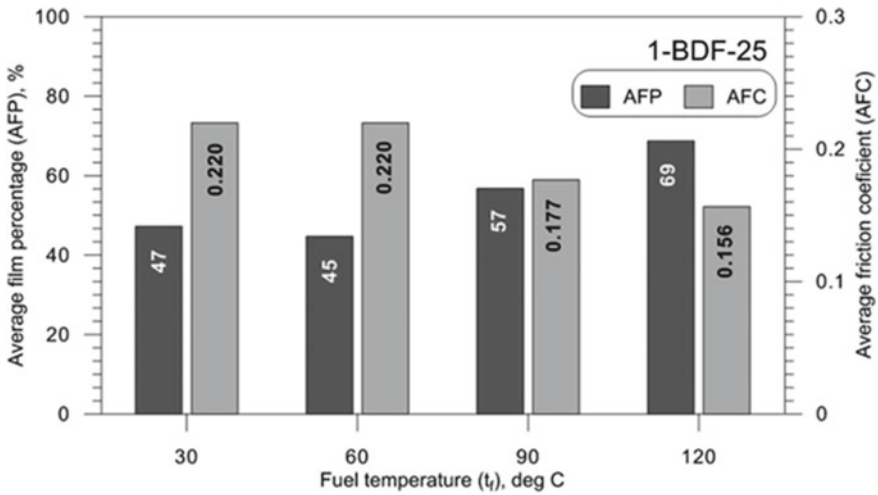
Fig. 2.10 Variations in wear scar diameter and coefficient of friction with the temperature at different butanol percentages (Kuszewski et al. 2021)

and thermal degradation of lubricant or pyrolysis/ incomplete combustion. These deposits on the engine parts reduce the engine's performance and increase downtime. Deposits also cause engine failure. Carbon deposit causes piston ring sticking, injector chocking, lubricating oil degradation, and oil dilution (Agarwal 2007). The formation of carbon deposits is dependent on lubricating oil composition and fuel composition. The increase of lubricating oil consumption increases the carbon deposits. Insufficient mixing of fuel and air, high flash point, and lower volatility cause more carbon deposits (Kalghatgi 1990). Olefins present in fuel increase the carbon deposits (Kalghatgi 1990). The deposits formed due to the presence of lower olefins in the fuel are rather dry and granular. Carbon deposits are higher in alcohol-fuelled engines. The carbon deposits in the methanol-fuelled engine are formed due to the absorption of unevaporated fuel on the existing deposits on the engine parts. The deposits in methanol fuelled engines contain calcium derived from the lubricating oil (Tsukasaki et al. 1990).

2.6 Summary

This study focused on the friction, wear, and lubrication of alcohol-fuelled IC engines. It discussed the energy balance, including losses due to various components such as piston assembly, valves, bearings, and pump assembly. This chapter summarises the effect of alcohol on the friction and wear of multiple engine components. Lubrication of various engine components and lubrication regimes has been discussed as well. The friction of engine components reduces with the application of alcohol as

fuel. However, due to the corrosive nature of alcohols, the wear of alcohol-fuelled engine components is higher than baseline diesel-fuelled engines. The lubrication of engine components is very much affected by the properties of lubricating oil and its additives. The engine operating conditions and fuel type affect the properties of lubricating oil, such as density, viscosity, acidity, and basicity. The temperature of lubricating oil at a high load remains higher, reducing the viscosity and changing the lubrication regimes from hydrodynamic to boundary lubrication. Alcohol applications in engines increase the lubricating oil contamination, causing adverse effects on engine components in contact. However, the coefficient of friction reduces. Carbon deposits on various engine components are higher in alcohol-fuelled engines, deteriorating engine performance and engine life. Routine maintenance is suggested to overcome these issues in alcohol-fuelled engines.

References

Agarwal AK (1999) Performance evaluation and tribological studies on a biodiesel-fuelled compression ignition engine. Ph.D. thesis, Centre for Energy Studies, Indian Institute of Technology, Delhi, India, p 344

Agarwal AK (2007) Biofuels (alcohols and biodiesel) applications as fuels for internal combustion engines. Prog Energy Combust Sci 33(3):233–271

Agarwal T, Singh AP, Agarwal AK (2020) Development of port fuel injected methanol (M85)-fuelled two-wheeler for sustainable transport. J Traffic Transport Eng (english Edition) 7(3):298–311

Banerji A, Lukitsch MJ, Alpas AT (2016) Friction reduction mechanisms in cast iron sliding against DLC: Effect of biofuel (E85) diluted engine oil. Wear 368:196–209

Bearings in internal combustion engines. SubsTech (Substances & Technologies). http://www.substech.com/dokuwiki/doku.php?id%C2%BCbearings_in_internal_combustion_engines.

Bilyeu B, Brostow W, Menard KP (2001) Determination of volume changes during cure via void elimination and shrinkage of an epoxy prepreg using a quartz dilatometry cell. Polimery 46(11–12):799–802

Boons M, Van Den Bulk R. King T (2008) The impact of E85 use on lubricant performance). SAE Technical Paper 2008–01–1763

Campos-Fernández J, Arnal JM, Gómez J, Dorado MP (2012) A comparison of performance of higher alcohols/diesel fuel blends in a diesel engine. Appl Energy 95:267–275

Cavalcanti M, Szklo A, Machado G (2012) Do ethanol prices in Brazil follow Brent price and international gasoline price parity? Renewable Energy 43:423–433

Chen CY, Papadopoulos KD (2019) Ethanol's effects on acid neutralization by motor oils. Tribol Int 132:24–29

Chen CC, Liaw HJ, Shu CM, Hsieh YC (2010) Autoignition temperature data for methanol, ethanol, propanol, 2-butanol, 1-butanol, and 2-methyl-2, 4-pentanediol. J Chem Eng Data 55(11):5059–5064

Chui GK, Baker RE (1980) Lubrication behavior in ethanol-fueled engines

Chui GK, Millard DHT (1981) Development and testing of crankcase lubricants for alcohol-fueled engines. SAE Technical Paper, 811203

Costa HL, Spikes H (2015) Effects of ethanol contamination on friction and elastohydrodynamic film thickness of engine oils. Tribol Trans 58(1):158–168

Costa HL, Spikes HA (2016) Impact of ethanol on the formation of anti-wear tribofilms from engine lubricants. Tribol Int 93:364–376

Crepaldi J, Fujita H, Tomanik E, Galvão C, Balarini R, do Vale JL (2018) A new tribology test procedure to investigate ethanol dilution on engine oils. SAE Technical Paper, 2018-36-0090

Van Dam W, Broderick DH, Freerks RL, Small VR, Willis WW (1997) TBN retention-are we missing the point?. SAE Trans 2398–2403

De Silva PR, Priest M, Lee PM, Coy RC, Taylor RI (2011a) Tribometer investigation of the frictional response of piston rings with lubricant contaminated with the gasoline engine biofuel ethanol and water. Proc Instit Mech Eng Part J J Eng Tribol 225(6):347–358

De Silva PR, Priest M, Lee PM, Coy RC, Taylor RI (2011b) Tribometer investigation of the frictional response of piston rings when lubricated with the separated phases of lubricant contaminated with the gasoline engine biofuel ethanol and water. Tribol Lett 43(2):107–120

Dooley D, Trudeau T, Bancroft D (1997) Materials and Design Aspects of modern valve seat inserts (No. CONF-9704126-). ASM International, Materials Park, OH (United States)

dos Santos Filho D, Tschiptschin AP, Goldenstein H (2018) Effects of ethanol content on cast iron cylinder wear in a flex-fuel internal combustion engine-A case study. Wear 406:105–117

Dutcher DD, Stolzenburg MR, Thompson SL, Medrano JM, Gross DS, Kittelson DB, McMurry PH (2011) Emissions from ethanol-gasoline blends: a single particle perspective. Atmosphere 2(2):182–200

Ferrarese A, Marques G, Tomanik E, Bruno R, Vatavuk J (2010) Piston ring tribological challenges on the next generation of flex-fuel engines. SAE Int J Engines 3(2):85–91

Bastian-Pinto C, Brandão L, de Lemos Alves (2010) Valuing the switching flexibility of the ethanol-gas flex-fuel car. Ann Oper Res 176(1):333-348

GSR 412(E) Dated 19.05.2015. https://morth.nic.in/sites/default/files/notifications_document/Notification_No_G_S_R_412E_dated_19_05_2015_regarding_Flex_fuel_ethanol_vehicles_0.pdf

GSR 682(E) dated 12.07.2016 https://morth.nic.in/sites/default/files/notifications_document/Notification_no_G_S_R_682_E_dated_12_07_2016_regarding_Mass_emission_standards_for_Flex_Fuel_0.pdf

GSR 881(E) dated 26.11.2019 https://morth.nic.in/sites/default/files/notifications_document/G.S.R.%20881%28E%29%2026th%20November%202019%20BS%20VI.pdf

Heywood JB (1988) Internal combustion engine fundamentals. McGraw-Hill, p 915

https://en.wikipedia.org/wiki/Bharat_stage_emission_standards

Inoue K, Ogura H, Igawa S, Takeda K (1993) Effects of lubricant composition on wear in methanol-fueled SI engines. SAE Technical Paper, 932796

Itoh Y (2011) Used engine oil analysis-user interpretation guide: The International Council on Combustion Engines. CIMAC 30:1–34

Kalghatgi GT (1990) Deposits in gasoline engines-a literature review. SAE Trans:639–667.

Khuong LS, Masjuki HH, Zulkifli NWM, Mohamad EN, Kalam MA, Alabdulkarem A, Arslan A, Mosarof MH, Syahir AZ, Jamshaid M (2017) Effect of gasoline-bioethanol blends on the properties and lubrication characteristics of commercial engine oil. RSC Adv 7(25):15005–15019

Kumar V, Sinha SK, Agarwal AK (2019) Wear evaluation of engine piston rings coated with dual-layer hard and soft coatings. J Tribol 141(3):031301

Kumar V, Singh AP, Agarwal AK (2020) Gaseous emissions (regulated and unregulated) and particulate characteristics of a medium-duty CRDI transportation diesel engine fueled with diesel-alcohol blends. Fuel 278:118269.

Kurre SK, Pandey S, Garg R, Saxena M (2015) Condition Monitoring of a Diesel Engine Fueled with a Blend of Diesel. Biodiesel Butanol Engine Oil Analysis Biofuels 6(3–4):223–231

Kurre SK, Pandey S, Khatria N, Bhurata SS, Kumawata SK, Saxenaa S, Kumara S (2020) Study of lubricating oil degradation of CI engine fueled with diesel-ethanol blend. Tribol Indus 43(2):222–231

Kuszewski H, Jakubowski M, Jaworski A, Lubas J, Balawender K (2021) Effect of temperature on tribological properties of 1-butanol-diesel fuel blends-Preliminary experimental study using the HFRR method. Fuel 296:120700

Labeckas G, Slavinskas S, Mickevicius T, Kreivaitis R (2019) Tribological study of high-pressure fuel pump operating with ethanol-diesel fuel blends. Combust Engines 58

Lakshminarayanan PA, Nayak NS (2011) Critical component wear in heavy-duty engines. John Wiley & Sons

Linde R, Frode J (2010) Emissions and experiences with E85 converted cars in the BEST project. Vaxjo, Sweden

Mobarak HM, Masjuki HH, Mohamad EN, Rahman SA, Al Mahmud KAH, Habibullah M, Salauddin S (2014) Effect of DLC coating on tribological behavior of cylinder liner-piston ring material combination when lubricated with Jatropha oil. Proc Eng 90:733–739

Nadkarni RK (2004) Elemental Analysis, Manual 37: Fuels and Lubricants Hand Book, ASTM, Metals Park, OH, pp 707–716

Palus J (1998) Examination of used motor oils by flame AAS for criminalistic purposes: a diagnostic study. Forensic Sci Int 91:171–179

Priest M, Taylor CM (2000) Automobile engine tribology-approaching the surface. Wear 241(2):193–203

Ryan III TW, Bond TJ, Schieman RD (1986) Understanding the mechanism of cylinder bore and ring wear in methanol-fueled SI engines. SAE transactions, pp.1044–1050

Schaefer SK, Larson JM, Jenkins LF, Wang Y (1997) Evolution of heavy-duty engine valves-materials and design (No. CONF-9704126-). ASM International, Materials Park, OH (United States)

Shah R, Klaus E, Duda JL (1996) Development of a bench-scale test to evaluate lubricants for use with methanol-fueled engines. Lubr Eng 52(10)

Shukla DS, Gondal AK, Nautiyal PC (1992) Effect of methanol fuel contaminants in crankcase oils on wear. Wear 157(2):371–380

Singh SK, Agarwal AK, Srivastava DK, Sharma M (2006) Experimental Investigation of the Effect of Exhaust Gas Recirculation on Lubricating Oil Degradation and Wear of a Compression Ignition Engine. 128(4):921–927

Taylor CM (1998) Automobile engine tribology-design considerations for efficiency and durability. Wear 221(1):1–8

Taylor L, Dratva A, Spikes HA (2000) Friction and wear behavior of zinc dialkyl dithiophosphate additive. Tribol Trans 43(3):469–479

Tibdewal SA, Saxena U, Gurumoorthy AV (2014) Hydrogen economy vs. methanol economy. Int J Chem Sci 12(4):1478–1486

Tsukasaki Y, Yasuda A, Ito S, Nohira H (1990) Study of mileage-related formaldehyde emission from methanol-fueled vehicles. SAE Trans:283–288

US Government (1988) Alternative motor fuels act of 1988. 14 O

Wang YS, Schaefer SK, Bennett C, Barber GC (1995) Wear mechanisms of valve seat and insert in heavy-duty diesel engine. SAE Trans:1520–1531

Wiles HM (1965) Gas engines valve and seat wear. SAE Technical Paper, 650393

www.epa.gov/regulations-emissions-vehicles-and-engines/regulations-greenhouse-gas-emissions-passenger-cars-and

Chapter 3
Impact of Biodiesel Blended Fuels on Combustion Engines in Long Term

Paramvir Singh, Saurabh Sharma, and Sudarshan Kumar

Abstract Biodiesel has been investigated in combustion engines for a long time. Numerous studies have been reported on the properties, performance, combustion, and emission analyses of biodiesel and their blended fuels. Mostly, researchers suggested promising blends based on the performance parameters. However, sometimes biodiesel-blended fuel affects the life of engine parts in the long term and leads to the wear of vital moving engine components. There are some studies, which have been focused on this aspect. The present study reviews the effects of biodiesel-blended fuels in the long term. The impact of blended fuels on vital engine parts like piston, piston rings, fuel injector, cylinder liner, and cylinder head in terms of carbon deposition and wear is discussed. The effects of modifications in engine parameters like compression ratio, injection timing, and injection pressure on carbon deposits and wear of the vital parts of the engine are also discussed.

Keywords Biodiesel · Combustion Chamber · Combustion Engines · Endurance · Fuel injector

Nomenclature

AME	Aamla oil methyl ester
BDC	Bottom dead center
CF	Calibration fuel
CME	Castor oil methyl ester
COME	Canola oil methyl ester
CRDI	Common rail direct injection

P. Singh (✉) · S. Kumar
Combustion Research Laboratory, Aerospace Engineering Department, Indian Institute of Technology Bombay, Mumbai 400076, India

S. Sharma
Aero-Thermo-Mechanics Department, Université Libre de Bruxelles, Avenue Franklin Roosevelt 50, 1050 Brussels, Belgium

DEE   Di-ethyl ether
EDS   Energy-dispersive spectrometry
EU   Eucalyptus oil
FAME   Fatty acid methyl ester
HC   Hydrocarbon
IBF   Indonesian biodiesel fuel
JME   Jatropha oil methyl ester
JO   Jatropha oil
KME   Karanja oil methyl ester
LOME   Linseed oil methyl ester
NO_x Nitrogen oxides
PM   Particulate matter
PME   Palm oil methyl ester
RME   Rapeseed methyl ester
ROME   Rice bran oil methyl ester
SAFO   Safflower oil
SE   Non-ionic sunflower oil-aqueous ethanol micro emulsion
SEM   Scanning electron microscope
SME   Sunflower oil methyl ester
SO   Sunflower oil
SOME   Soy methyl ester
TDC   Top dead center
TPO   Tire pyrolysis oil
UHC   Unburnt hydrocarbons

3.1   Introduction

The emissions emanating from the burning of fossil fuels in the transportation sector represent ~20% of the global energy supply and deteriorate the air quality (Chandran 2020). The strict emission norms force the researchers to work on renewable and low emission fuels (Singh et al. 2018a; Singh and Varun 2016; Goel et al. 2018). However, the increment in the number of vehicles adversely affects the overall emission reduction attained through these stringent norms (Singh et al. 2020a). Moreover, the air quality is anticipated to deteriorate in the coming years due to increased population and industrialization (Singh et al. 2016) further. There are two ways to mitigate these issues: 1. To make new advanced engines with the aim of lower emissions, 2. To investigate new clean fuels for the existing engines (Singh et al. 2016). Both steps are essential and need to be implemented in parallel. The present study covers the second perspective and focuses on the feasibility of renewable fuels in diesel engines with existing technology.

Biodiesel is a potential renewable feedstock for diesel engines to meet the demands and mitigate these long-term problems (Singh et al. 2020b). Biodiesel also has better

biodegradation characteristics, availability, low aromatics, no-sulfur, and renewability (Hoang and Le 2019; Singh and Varun 2017a). The properties of biodiesel are very close to diesel properties and can be used in a diesel engine without any significant modifications (Lapuerta et al. 2008; Agarwal 2007; Singh and Goel 2018). Numerous studies report the effect of different biodiesels on engine combustion (heat release rate, cylinder pressure, and rate of pressure rise), performance (brake power, brake thermal efficiency, volumetric efficiency, and brake specific fuel consumption), and emission (carbon monoxide (CO), unburnt hydrocarbon (UHC), particulate matter (PM), nitrogen oxides (NO_x) and carbon dioxide (CO_2)) characteristics (Fazal et al. 2011; Kumar and Varun 2013; Agarwal et al. 2018). In general, neat biodiesel has inferior performance and combustion characteristics than diesel. However, maximum studies found that B20 (20% biodiesel + 80% diesel) is shown to achieve combustion behavior and engine performance in line with diesel fuel (Kumar and Varun 2013; Varun et al. 2017). Moreover, the CO, UHC, and PM emissions are lower from the biodiesel-operated engine than diesel. However, some problems encountered with biodiesel are the cold start, deterioration of rubber seals, higher emissions at cold start, carbon deposition, and fuel injector choking.

The effects of biodiesel or any newer fuel on engine parts regarding deposit and wear are equally important to investigate. There are ASTM and European standards for short-term lubricity tests to study the comparative wear and coefficient of friction from biodiesel and diesel. These short-term lubricity tests can be done using the four-ball tester, high-frequency reciprocating rig, pin-on-disc tribo-tester, etc. (Singh et al. 2018b, c, d; Singh and Varun 2017b). Short-term laboratory tests have been carried out to simulate the wear in moving engine parts (Mosarof et al. 2016; Barsari and Shirneshan 2019). Moreover, some authors have done long-term endurance tests for 300, 512, and 1024 h. Some of them reported promising results with biodiesel in the long-term with lower engine deposits and wear. On the contrary, the problems of higher engine deposit and wear associated with biodiesel in the long term were also reported. Hence, the effect of biodiesel-blended fuels on engine parts needs to be addressed carefully. The impact of biodiesel on lubricating oil degradation is also reported in the literature (Agarwal et al. 2003a; Agarwal 2021; Singh et al. 2019a, 2006). The present article focuses on the effects of various biodiesel fuel blends on the injector, piston top, cylinder head, and piston rings.

3.2 Effects of Biodiesel Blended Fuels on Engine Parts

Wear and friction occurred in all the moving parts, where sliding contacts were involved. Some of the sliding contacts in a diesel engine are lubricated by fuel itself. Hence, the tribological performance of the fuel affects the engine parts in the long term. The effects of fuel lubricity characteristics on combustion chamber deposit, injector, pump plunger, and valves are discussed in this section. The carbon deposition is usually formed due to hydrocarbon (HC) decomposition into elemental carbon and hydrogen at higher temperatures. Secondly, carbon deposits can nucleate and grow

with the polymerization of HCs into larger polynuclear aromatic HC (Liaquat et al. 2013). The carbon deposit is composed of volatile, oxidizing, high boiling point, carbonization substances, and residual ashes (Arifin et al. 2008). High boiling point substances are the medium between the wall surface and particles for the growth of the deposit (Lepperhoff and Houben 1993). The carbon deposit on engine parts negatively affects the engine life and increases the maintenance cost. The carbon deposit on combustion chamber walls affects the heat transfer from the engine cylinder and increases NO_x emissions (Ra et al. 2006). Goldsworthy (2006) and Güralp et al. (2006) reported that the thickness of carbon deposits on the wall of the cylinder could be estimated from the temperature distribution over cylinder walls and fuel impingement area. The presence of olefin in the fuel has the maximum tendency of deposit formation (Ebert 1981).

The long-term test can be done on variable and constant speed engines. The test cycle used for the long-term test as per IS: 10,000 (Part VIII) standard (see Fig. 3.1. The properties of the fuel used for long-term tests are provided in Table 3.1. It can be seen from the table that the properties of fuel used were in specified limits as per the standards. The details of engine type, duration of long-term testing, and investigated components are provided in Table 3.2.

3.2.1 Cylinder Head and Liner

Agarwal and Agarwal (2021b) investigated the effect of Karanja oil methyl ester (KME100) on engine vital parts in realistic conditions during on-field testing of 30,000 km. Scanning electron microscope (SEM) and energy-dispersive spectrometry (EDS) were used to assess the cylinder liner surface. EDS was intended to identify the material transfer between the piston rings and the liner surfaces. SEM analysis was done before and after the on-field testing. The honing marks detected on the liner before the testing was totally removed after the 30,000 km run from the TDC position due to the extent of wear. However, the damage of honing marks was lower with KME100 than diesel, reflecting better lubrication with biodiesel. The dilution of biodiesel in lubricating oil plays a vital role in providing a smoother surface to the moving parts. The dilution was confirmed with atomic absorption spectroscopy (Agarwal and Agarwal 2021c). Moreover, the higher carbon deposit with diesel was reported on the cylinder head compared to biodiesel. Similar results were reported by Singh et al. (Singh et al. 2019c) (see Fig. 3.2).

Higher wear was reported near TDC on cylinder liner because of higher temperature, pressure, and lower piston speed conditions. The boundary lubrication film frequently breaks down at this position, and hence metal-to-metal contact increases. Moreover, the authors also reported higher wear on the anti-thrust side compared to the thrust side. Similar results were reported by Kumar et al. (Kumar and Varun 2015) (see Fig. 3.3). This is due to the contact of piston and cylinder during three strokes at the antithrust side at higher temperature and pressure conditions (Dong et al. 1995) (see Fig. 3.4). Honing marks by abrasive machining are produced on liner
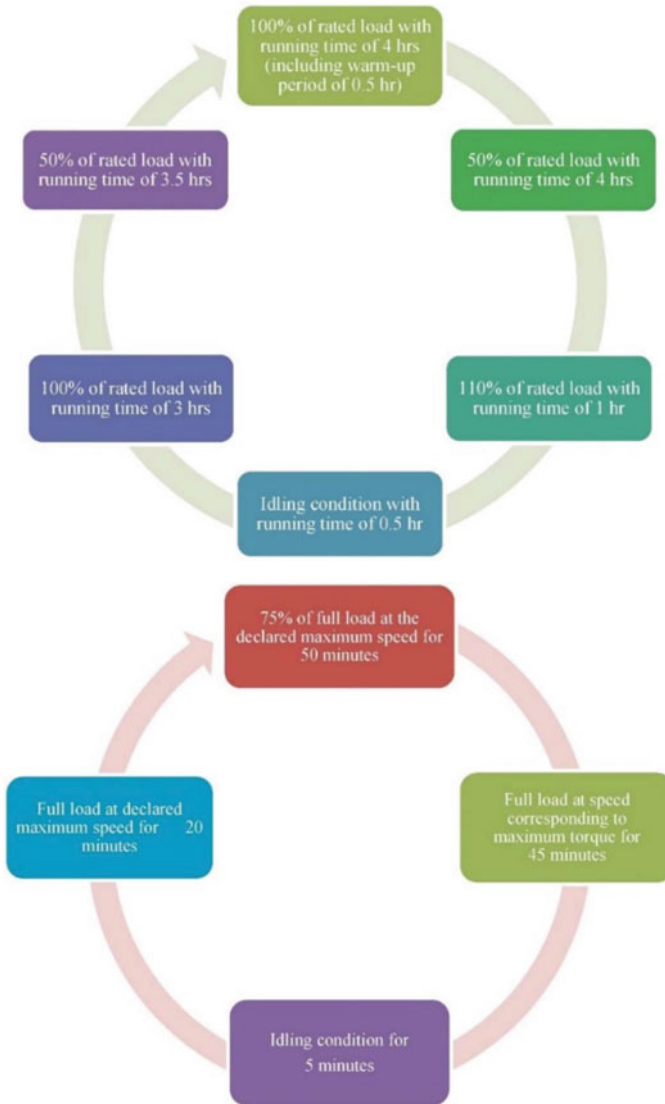
Fig. 3.1 Long-term endurance test cycles for constant and variable speed engine Adapted with permission from M. Sudan Reddy Dandu, K. Nanthagopal (2019) Copyright 2019 Elsevier

for retaining oil on the contact surface for smooth functioning. The honing marks in the cross-hatched pattern can be clearly seen (see Fig. 3.3e) on the anti-thrust side. From the close inspection of Fig, 3.3, the wear lines are visible on the liner surface that shows the abrasive wear in the direction of the piston movement. The crack on

Table 3.1 Properties of the fuel used for long term endurance tests

Properties/Biodiesel	Density (kg/m³)	Kinematic viscosity (mm²/s)	Cetane number	Calorific value (MJ/kg)	Flash point (°C)	Oxidative stability at 110 °C(hr)	Refs.
Diesel	832	2.64	–	–	–	–	Pehan et al. (2009)
RME100	883	4.42	>51	–	–	14.8	
CF	826	2.55	–	–	–	–	Suthisripok and Semsamran (2018)
Diesel	848	–	–	35.9	–	–	
Palm biodiesel	878	–	72.5	32.9	136	–	
COME	881	4.44	45–59	37.5	160	–	Temizer (2020)
Diesel	833	3.32	51	45.6	78	–	Liaquat et al. (2013)
PB20	822	3.62	53.1	43.8	89	-	
SOME100	883	4.27	–	–	–	3.0	Wander et al. (2011)
CME100	913	12.01	–	–	–	9.6	
Diesel	822	3.32	51	45.5	69	–	Liaquat et al. (2014)
JME20	834	3.53	51.9	43.7	74	–	
RME30 winter grade	–	–	–	–	62	23.2	Urzędowska and Stępień (2016)
RME30 summer grade	–	–	–	–	61.5	26.9	
Diesel	–	3.18	51	44.8	–	–	Sinha and Agarwal (2009)
ROME	–	5.29	63.8	42.2	–	–	
Diesel	845	2.92	56.7	47.1	65	-	Hartono and Cahyono (2020)
PME30	856	4.43	69.8	45.5	96	-	

Table 3.1 (continued)

Properties/Biodiesel	Density (kg/m³)	Kinematic viscosity (mm²/s)	Cetane number	Calorific value (MJ/kg)	Flash point (°C)	Oxidative stability at 110 °C(hr)	Refs.
Diesel	–	3.17	–	45.3	72.2	–	Perkins et al. (1991)
RME100	–	5.65	–	40.7	86.7	–	
RME50	–	4.34	–	42.9		–	
Diesel	–	2.44	46.3	–	75	–	Ziejewski and Kaufman (1983)
SO	–	33.9	–	–	274	–	
Diesel	–	2.37	50.1	42.67		–	Ziejewski et al. (1986a, b, 1985)
SO25	–	4.88	45.4	41.1	82.8	–	
SAFO25	–	4.92	47.5	41.1	82.8	–	
SME	–	4.27	46.6	37.2		–	
SE	–	6.31	43	33.6	27	–	
KME100	885	4.65	–	–	169	<5.73	Agarwal and Agarwal (2021a)
Diesel	824	2.55	–	42.6	58	–	Patidar and Raheman (2020)
PME100	874	4.78	–	37.2	143	–	
PME20	837	2.95	–	41.2	69	–	
PME20S10W	850	3.9	–	38.9	75	–	
Diesel	805	–	–	38.7	–	–	Chourasia et al. (2018)
JME100	855	–	–	34.2	–	–	
DEE	704	0.23	–	26.6	35	–	
Diesel	830	3.4	–	42.7	47	–	Singh et al. (2019b)

(continued)

Table 3.1 (continued)

Properties/Biodiesel	Density (kg/m^3)	Kinematic viscosity (mm^2/s)	Cetane number	Calorific value (MJ/kg)	Flash point (°C)	Oxidative stability at 110 °C(hr)	Refs.
AME70EU30	885	3.7	–	41.1	67	–	
Diesel	–	2.6	50	43.8	50	25	Sharma and Murugan (2017)
JME	–	5.6	55	39.4	156	3	
TPO	–	3.35	28	38.1	49	16	
JMETPO20	–	5.2	52	38.82	132	8.2	

*CF: Calibration fuel, SE: a non-ionic sunflower oil-aqueous ethanol microemulsion

Table 3.2 Details of engine type, investigated components, and test duration

Engine type	Investigated components	Long term test duration/distance	Refs.
CRDI 4 stroke turbocharged diesel engine	• Fuel injector • Inlet and exhaust valve • Piston • Cylinder head • Fuel tank • Fuel pump housing • Fuel pump cylinder head • Fuel pump thrust ring • Fuel pump shaft	30,000 km	Agarwal and Agarwal (2021b, 2021c)
MAN D 2566 MUM, 4 stroke, 6 cylinder in line, water cooled bus diesel engine	• Pump plunger surface • Carbon deposits on injectors and in combustion chambers • Nozzle discharge coefficient	5,00,000 km	Pehan et al. (2009)
14-hp Kubota RT140 DI diesel	• Cylinder head • Valves • Piston • Fuel injector • Fuel pump	800 h	Suthisripok and Semsamran (2018)
4- stroke, direct injection diesel engine	• Piston rings	150 h	Temizer (2020)
4-Stroke single cylinder DI diesel engine	• Fuel injector	250 h	Liaquat et al. (2013)
Single cylinder Agrale M93ID direct injection engines	• Fuel injector • Cylinder liner • Intake and exhaust valves • Piston head and rings • Conrod bearings and bushings	1000 h	Wander et al. (2011)
4-Stroke single cylinder DI diesel engine	• Fuel Injector	250 h	Liaquat et al. (2014)

Table 3.2 (continued)

Engine type	Investigated components	Long term test duration/distance	Refs.
Ford Duratorq TdCi 2.0i 16 V four cylinder, four stroke, compression ignition, turbocharged, direct injected engine	• Fuel Injector	300 h	Urzędowska and Stępień (2016)
Mahindra and Mahindra Ltd, India/ MDI 3000 4-cylinder, 4-stroke, DI diesel engine	• Cylinder head • Injector tip • Piston top • Piston ring	100 h	Sinha and Agarwal (2009)
Heavy duty pickup truck with 5.9L diesel engine	• Injector coking • Engine compression • Injector valve performance	1,61,000 km	Peterson et al. (1999)
Dong Feng R180 4-Stroke single cylinder diesel engine	• Piston rings • Piston head • Cylinder head • Fuel injector	200 h	Hartono and Cahyono (2020)
Yanmar 3TN75E-S 3-cylinder, 4-stroke, naturally aspirated DI diesel engine	• Fuel injector • Valve seats and faces • Piston head • Piston rings	1000 h	Perkins et al. (1991)
Yanmar L48 4 stroke, vertical cylinder, air cooled DI diesel engine	• Fuel injector • Intake valve seat • Piston head	200 h	Suryantoro et al. (2016)
Allis-Chalmers 4331 four-stroke DI diesel engine	• Cylinder liner • Piston ring and head • Valves	120 h	Ziejewski et al. (1986a, b, 1985)
Perry & Co., India single-cylinder 4-stroke water-cooled diesel engine	• Cylinder head • Cylinder liner • Piston Ring • Gudgeon pin • Valves • Connecting rod • Big-end bearing • Small-end bush	512 h	Agarwal et al. (2003b)

Table 3.2 (continued)

Engine type	Investigated components	Long term test duration/distance	Refs.
Kirloskar DM-10 4-stroke, single-cylinder, constant speed, water-cooled, DI diesel engines	• Fuel injector • Cylinder head • Piston top • Piston skirt	512 h	Kumar and Atul (2018)
Chetak SDM-14 single-cylinder water-cooled steady rotational speed DI diesel engine	• Cylinder head • Piston top • Fuel injector	100 h	Patidar and Raheman 2020)
Variable compression ignition single cylinder, 4 strokes, DI diesel engine	• Piston head and ring • Cylinder liner • Inlet and exhaust valves • Connecting rod bearing	512 h	Chourasia et al. (2018)
Kirloskar make 4-stroke, single cylinder, water cooled, DI variable compression ratio engine	• Cylinder head • Piston head • Piston ring • Pump plunger • Injector needle	512 h	Singh et al. (2019b)
Kirloskar make 4-stroke, single cylinder, water cooled, DI variable compression ratio engine	• Fuel injector • Cylinder liner • Cylinder head • Piston side and top • Pump plunger	512 h	Kumar and Varun (2015)
Kirloskar (TAF 1 model) single cylinder, naturally aspirated, four stroke, air cooled, DI diesel engine	• Cylinder head and piston crown • Fuel injector and fuel filter • Fuel injection pump components	100 h	Sharma and Murugan (2017)

the surface liner in Fig. 3.3f may be due to thermal shocks with the fuel combustion. The oxidative wear in Fig. 3.3c with biodiesel is due to biodiesel oxidation and black spots are due to corrosive wear. Adhesive wear was reported with diesel (see Fig. 3.3d). This was reported due to the interatomic interaction and welding between the mating surfaces caused by interatomic interactions and the breakdown of the lubricating film (Kumar and Varun 2015). EDS perceives the elemental scattering on the surface. EDS was used to detect the transfer of material during wear from piston

Fig. 3.2 Carbon deposits on the cylinder head from biodiesel and diesel-fueled vehicles after the long-term field test. Adapted with permission from Singh et al. (2019c) Copyright 2019 ASME

rings to cylinder liner. There was no significant material transfer observed after the testing with biodiesel and diesel.

Suthisripok and Semsamran (2018) used the diesel for 100 h and palm biodiesel for 700 h to study the effect of fuel on engine components. They disassembled the engine after testing and visually inspected the parts (see Fig. 3.5). There was no major breakdown, and unusual wear was reported with biodiesel.

Wander et al. (2011) tested soy methyl ester (SOME100), castor oil methyl ester (CME100), and diesel for 1000 h each in the diesel engine. Cylinder liner condition was assessed with a visual inspection, corrosion, and dimension analysis. There were no signs of corrosion; however, higher wear of the cylinder liner was observed (see Fig. 3.6).

The dimension analysis was done at different positions of the cylinder liner. Some of the values (diameter and arithmetic roughness average, R_a) were higher than the specified limits. However, the cylinder liner supplier approved the values after 1000 h test duration. The fax film formation (honing angle) was also found within the acceptable limits. The conrod bearing and bushings were also assessed. The regular wear pattern was observed for all the tested fuels.

Sinha and Agarwal (2009) tested rice bran oil methyl ester (ROME) in a diesel engine for 100 h. They found a lower carbon deposit with biodiesel on the cylinder head compared to diesel. Moreover, the presence of oxygen in biodiesel improves the combustion of fuel and reduces soot formation. To assess the cylinder liner wear at the top dead center (TDC), mid-stroke, and bottom dead center (BDC), surface profiles were evaluated after the long-term test for both fuels (see Fig. 3.7) (Dhar and Agarwal 2014). The values of R_a and R_q at these positions were taken with a surface profilometer. The higher wear was detected at TDC. This is due to the higher temperature and pressure conditions at TDC that break down the lubrication layer. Agarwal et al. (2003b) found comparatively lower wear with linseed oil methyl ester
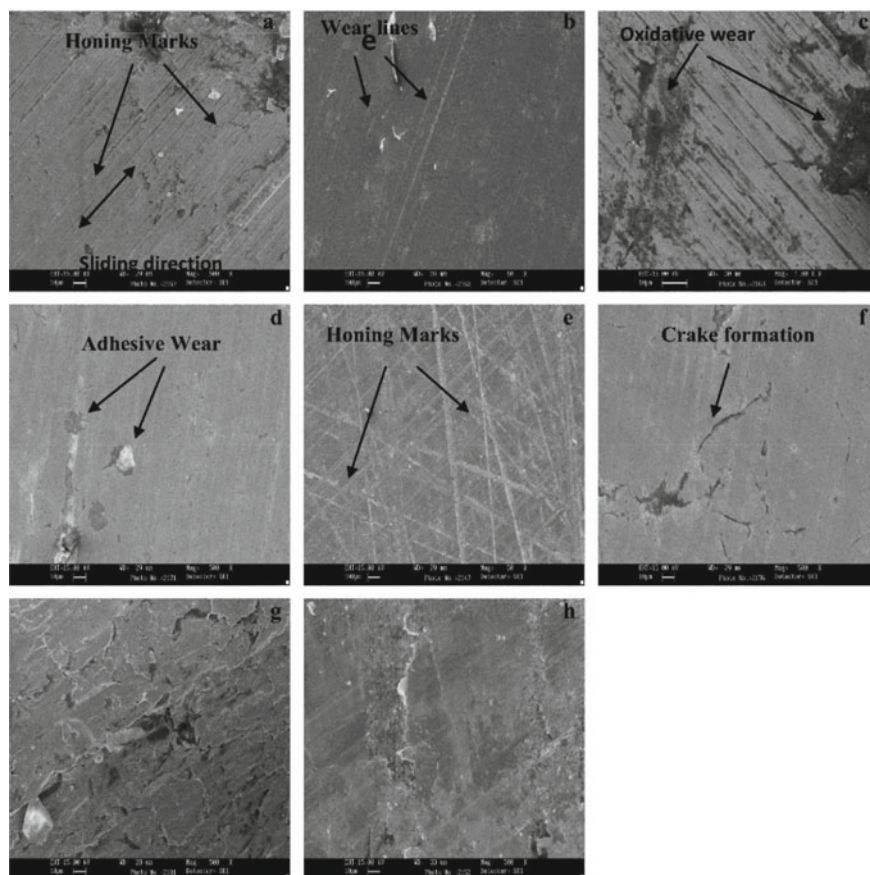
Fig. 3.3 SEM of cylinder liner surface from biodiesel- and diesel-fueled vehicles at **a** TDC thrust side (JB40), **b** TDC thrust side (Diesel), **c** TDC antithrust side (JB40), **d** TDC antithrust side (Diesel), **e** BDC thrust side (JB40), **f** BDC thrust side (Diesel), **g** BDC antithrust side (JB40), **h** BDC antithrust side (Diesel). Adapted with permission from Kumar and Varun (2015) Copyright 2015 Elsevier

(LOME20) than diesel. The percentage reduction in wear of the moving parts is provided in Table 3.3.

Similarly, Hartono and Cahyono (2020) also reported lower carbon deposits with biodiesel. Authors tested PME30 for 200 h in a diesel engine to evaluate the effect of the biodiesel fuel blend on cylinder head deposit. The carbon deposit was 19.5% lower by mass with biodiesel compared to diesel. However, the authors found a corrosive cylinder after disassembling in the case of biodiesel due to the higher water content. Perkin et al. (1991) also reported heavier black carbon deposits throughout the combustion chamber with diesel. Sinha and Agarwal (2010) also reported the higher carbon deposit on cylinder head with ROME20.
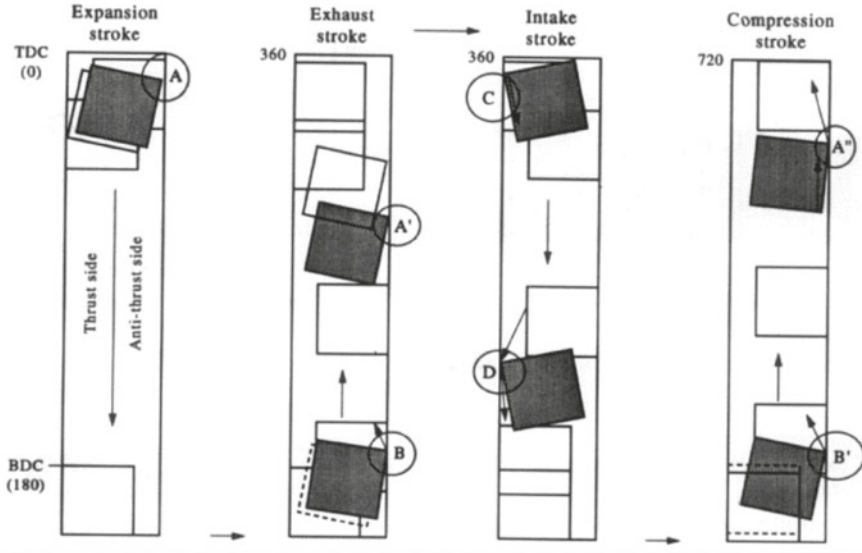
Fig. 3.4 Piston movement in cylinder liner during different strokes. Adapted with permission from Dong et al. (1995) Copyright 1995 Elsevier
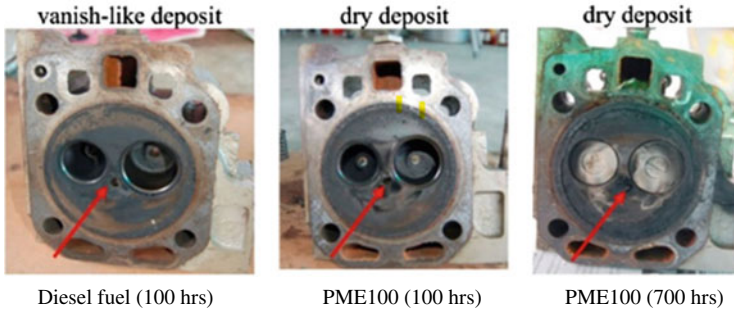

Fig. 3.5 Deposit on cylinder head after long-term test. Adapted with permission from Suthisripok and Semsamran (2018) Copyright 2018 Elsevier

Ziejewski et al. (1986a, b, 1985) have done different studies with sunflower oil (25% v/v with diesel, SO25), safflower oil (25% v/v with diesel, SAFO25), sunflower-oil methyl ester (SOME) and non-ionic sunflower oil-aqueous ethanol microemulsion (SE). Authors found better results with lower deposits on engine vital parts for SAFO25 compared to SO25. However, the transesterification of sunflower oil improves the fuel properties and lowers the carbon deposit with SOME compared to SO25 and SAFO25. Better atomization of SOME due to lower viscosity is one of the reasons for lower carbon deposits. Moreover, larger spatial separations in the ester than in the triglyceride molecules with reduced chemical interaction among the
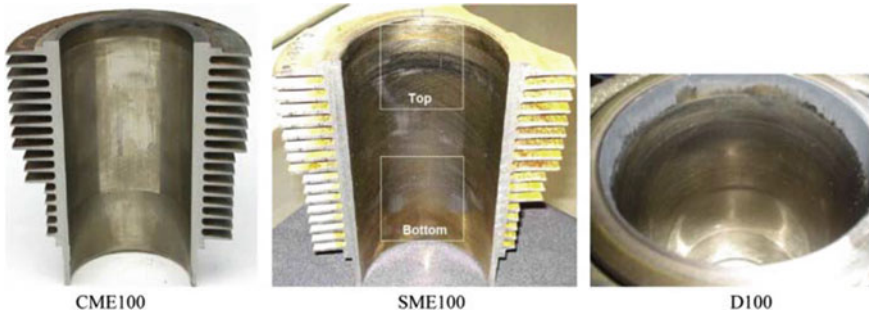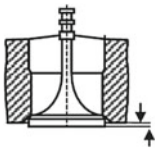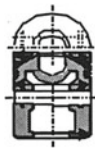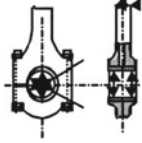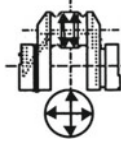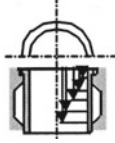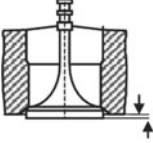
Fig. 3.6 Visual analysis of thrust side of cylinder liner. Adapted with permission from Wander et al. (2011) Copyright 2011 Elsevier

	Diesel (before endurance test)	Diesel (after endurance test)	KOME20 (before endurance test)	KOME20 (after endurance test)
TDC, AT	Ra=1.11, Rq=1.50	Ra=0.81, Rq=1.17	Ra=0.81, Rq=1.05	Ra=0.48, Rq=0.67
TDC, T	Ra=1.04, Rq=1.34	Ra=0.88, Rq=1.17	Ra=0.71, Rq=1.02	Ra=0.50, Rq=0.72
MID, AT	Ra=1.14, Rq=1.51	Ra=0.33, Rq=0.56	Ra=0.92, Rq=1.23	Ra=0.46, Rq=0.76
MID, T	Ra=1.09, Rq=1.38	Ra=0.19, Rq=0.37	Ra=1.02, Rq=1.35	Ra=0.23, Rq=0.34
BDC, AT	Ra=0.92, Rq=1.17	Ra=0.27, Rq= 0.46	Ra=0.86, Rq=1.13	Ra=0.34, Rq=0.63
BDC, T	Ra=1.08, Rq=1.40	Ra=0.60, Rq=0.80	Ra=0.94, Rq=1.36	Ra=0.36, Rq=0.58

Fig. 3.7 Surface profiles of liner surface after endurance test Adapted with permission from Dhar and Agarwal (2014) Copyright 2014 Elsevier

Table 3.3 Comparative physical wear measurements of vital parts Adapted with permission from Dhar and Agarwal (2014) Copyright 2014 Elsevier

Figure of moving part				
Dimensions (percentage change in wear with KME20)	Distance of inlet valve head from mounting flange face (−10)	Diameter of piston at position (−49.5)	Measurement for piston rings (−24.8)	Gudgeon pin, pin bore and small end bush of connecting rod (−10.8)
Figure of moving part				
Dimensions (percentage change in wear with KME 20)	Cnnecting rod bearing bore diameter (+45.16)	Crank pin (+26.5)	Measurement of cylinder bore/cylinder liner (−20.5)	Distance of exhaust valve head from mounting flange face (−55.5)

fatty acids may also be the reason for better results compared to pure oil. However, the deposit was still higher compared to diesel.

Similarly, Suryantoro et al. (2016) also reported higher carbon deposits on cylinder head with B50 fuel. Agarwal and Dhar (Kumar and Atul 2018) used preheated jatropha oil (J50 and J100) and found severe engine deposits with JO100 compared to diesel. Moreover, JO50 showed promising results compared to diesel. The authors suggested JO50 as a potential substitute for diesel with the utilization of waste heat to reduce the viscosity of the fuel blend.

Patidar and Raheman (2020) tested PME 20, diesel and water emulsified biodiesel-diesel fuel blend, PME20S10W (89% PME + 10% water + 1% surfactants by volume). The carbon deposition on cylinder liner was found 18.36 and 32.20% lower than diesel for PME20S10W and PME20, respectively. The presence of oxygen in PME20 helps in better combustion, and hence carbon deposit is reduced. Chourasia et al. (2018) tested JME20A4 (76% Diesel + 20% Jatropha methyl ester + 4% Diethyl ether) in diesel engines for the long term and compared the results with diesel. Authors reported lower deposits and wear in engine parts with JME20A4 than diesel due to the addition of the oxygenated additives. The increase of 63% and 52.7% in wear for cylinder liner and piston was reported with diesel compared to biodiesel-blended fuels.

Sharma and Murugan tested (2017) JMETPO20 (80% JME-20% tire pyrolysis oil) for 100 h in a diesel engine with modified injection timing (24.5°CA bTDC),

injection pressure (220 bar), and compression ratio (18:1). The authors reported a higher carbon deposit with JMETPO20 compared to diesel. However, there was no operational problem encountered during durability analysis. Similarly, Kumar and Varun (2015) reported a long-term endurance test with JME40 for 512 h with modified engine parameters (injection timing (26°CA bTDC), injection pressure (220 bar), and compression ratio (18:1)). The objective of the study was to use a higher biodiesel blend with minor modifications in diesel engine parameters. They found lower engine deposits on engine vital parts with JME40 compared to diesel. The authors reported that modification in engine parameters improved the fuel atomization and combustion of the fuel and reduced the engine deposit. Moreover, the inherent lubricity properties of biodiesel also favor the lower deposit. Singh et al. (2019b) also reported similar results for AME70EU30.

3.2.2 Piston Top, Skirt and Rings

Agarwal and Agarwal (2021b) reported a lower carbon deposit on the piston top with biodiesel compared to diesel. This reflects the better inherent lubrication properties of biodiesel that reduce the deposit formation tendency of biodiesel. However, the white marks were reported on the cylinder head with biodiesel. This is an important concern with the use of biodiesel. The possible reason of white marks is left out traces of catalyst during the transesterification process for biodiesel production. Piston rating was 5 – 15% superior with biodiesel compared to diesel.

Temizer (2020) investigated the effect of 10% canola oil methyl ester- diesel fuel blends and 100% diesel on first and second piston rings. SEM and EDS analyses at 250X magnification were done to analyse the surfaces of piston rings. For both the tested fuels, the condition of piston rings was in the acceptable range after 150 h long-term test. However, the abrasive wear lines are intensified in biodiesel blend compared to diesel. Similarly, higher carbon was detected on the second piston ring with COME10 than diesel due to unburned COME10 fuel (Temizer 2020).

Wander et al. (2011) found a small crack at the upper edge of the piston used in the SME100 fueled engine. The thermal shocks produced in the engine with the combustion of fuel may be the reason for small cracks in the upper edge of the piston. Moreover, high temperature at the upper edge of the piston and relatively low velocity could also be the reason. However, there were no cracks in the piston used with CME100 and diesel. SEM was done to analyse the failure. The better combustion of the fuel is one of the probable reasons of no cracks in the case of diesel and CME100. Microporosity of approximately 45 μm was found in the limit of acceptance for the diesel engine (Wander et al. 2011). Moreover, overall carbon deposit and gum formation were higher with SME100 and CME100 than diesel due to poor combustion. Perhaps, the pistons diameters, groove wear, skirt profile, and pin bore for both the biodiesel were found within the acceptable limits.

Sinha and Agarwal (2009) reported the weight-loss percentage analysis of piston rings. The second compression ring shows maximum weight loss for both the tested

fuels (ROME and diesel) among the piston rings. However, the oil ring had lower weight loss, i.e., 14%, in ROME. ROME showed better results compared to diesel. Better combustion with lower soot emissions, low in-cylinder temperature, and inherent lubricity properties of biodiesel are the possible reasons for promising results with biodiesel. Patidar and Raheman (Patidar and Raheman 2020) reported 28.16 and 40.67% lower carbon deposits on piston tops with PME20S10W and PME20, respectively than diesel.

Hartono and Cahyono (2020) reported the effect of PME30 on piston rings and piston head after a long-term test. There was no significant difference found in the piston rings with a visual inspection. The gap of the piston ring was estimated. The results showed that the gap in the piston ring at TDC is 0.05 mm smaller for PME30. This reflects better lubrication properties of PME30. Moreover, the gaps in the piston rings were within acceptable limits. The authors also evaluated the effect of PME30 on the piston head. Like the cylinder head, there were spots of corrosion reported on the piston head with PME30. This is due to oxidation reactions in the combustion chamber. The reactions are as follows (Hartono and Cahyono 2020):

$$Fe + 3O_2 \rightarrow 2Fe_2O_3 \tag{3.1}$$

$$Fe_2O_3 + 6R'COOH \rightarrow 2Fe(R'COO)_3 + 3H_2O \tag{3.2}$$

$$2R'COOH + Fe \rightarrow 2Fe(R'COO)_2 + H_2 \tag{3.3}$$
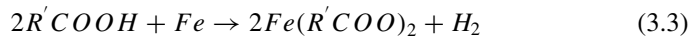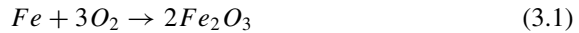
The carbon deposit was 21.8% higher by mass on the piston with PME30 compared to diesel. Similarly, Perkin et al. (1991) found more deposit and discoloration of oil ring with diesel compared to RME50 and RME100. Perhaps, authors found a rust color deposit with biodiesel. This may be due to remained catalysts (KOH and NaOH) left in the biodiesel during production (Perkins et al. 1991). The tendency of piston ring sticking increase with the higher biodiesel contents in the blends (Suryantoro et al. 2016). Also, Suthisripok and Semsamran (2018) reported the varnish-like deposit with diesel and dry deposit with biodiesel on piston top (see Fig. 3.8).

3.2.3   Fuel Injector

The fuel flow rate and injection pattern are highly affected by carbon deposits and need to be studied carefully (Hoang and Le 2019). The condition of the fuel injector was initially endoscopically inspected by Pehan et al. (2009). From photographic view, authors found that the biodiesel-operated engine injector was in better condition than diesel. The authors used an uncleaned diesel injector with biodiesel. They found that carbon deposits remained on the injector tip after diesel was removed to some extent with biodiesel. This may be due to the better solvent action of the biodiesel that
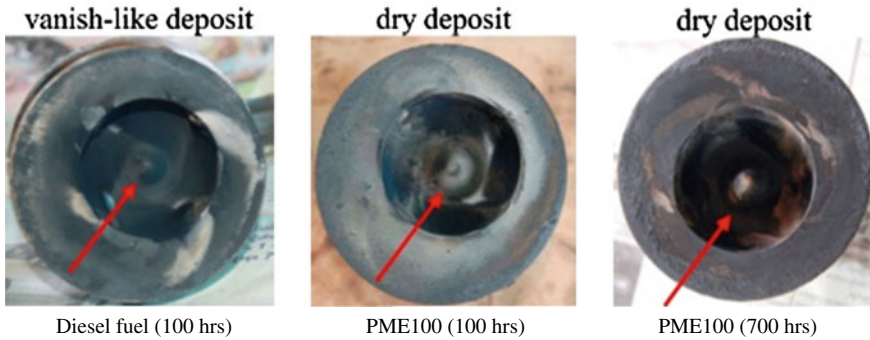
Fig. 3.8 Carbon deposit on piston. Adapted with permission from Suthisripok and Semsamran (2018) Copyright 2018 Elsevier

helps in carbon deposit removal. In all six cylinders, the pattern of carbon deposit was similar. However, the extent of carbon deposit is different for biodiesel and diesel. This is due to the high viscosity and molecular weight of biodiesel that affect the injection parameters (Wander et al. 2011; Liaquat et al. 2014). Despite poor atomization of neat biodiesel, the quantity of carbon deposits was lower with biodiesel than diesel. Suthisripok and Semsamran (2018) found the varnish-like deposit with diesel at the fuel injector tip and dry deposits with biodiesel (see Fig. 3.9).

Liaquat et al. (2013) also inspected the injector nozzle with SEM and energy-dispersive X-ray spectroscopy (EDS). They used PME20 in a diesel engine for 250 h and compared the results with diesel. From visual inspection, they found a higher carbon deposit on the injector used with PME20. Like Suthisripok and Semsamran (Temizer 2020), the dry carbon deposit was observed with PME20 while oily with diesel. From observation through SEM and EDS, the diameter of the holes was reduced in the case of PME20 after the 250 h test, and even some of the injector holes were totally blocked with carbon deposit (see Fig. 3.10).

Fig. 3.9 Carbon deposits on fuel injector. Adapted with permission from Suthisripok and Semsamran (2018) Copyright 2018 Elsevier
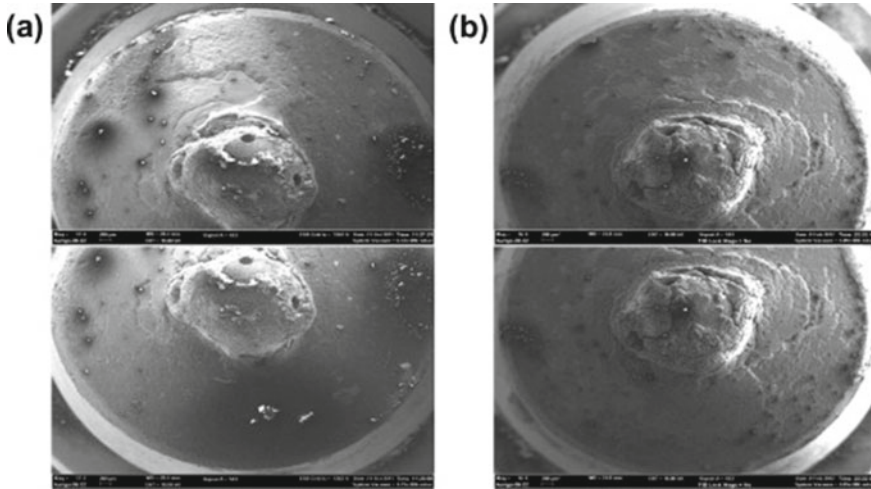
Fig. 3.10 SEM micrographs of deposited injector tips fueled with **a** diesel and **b** PME20. Adapted with permission from Liaquat et al. (2013) Copyright 2013 Elsevier

On the other hand, a thin deposition was observed in the case of diesel compared to PME20. The carbon deposit did not significantly affect the nozzle holes diameter. The higher viscosity and low volatility of biodiesel are some of the major reasons for higher carbon deposits. At higher temperatures, the decomposition of biodiesel during ignition delay may cause a higher carbon deposit at the injector tip.

In another study with JME20, Liaquat et al. (2014) found similar results. They reported substantially higher carbon deposits on injector tip with JME20 compared to diesel (see Fig. 3.11). Reksowardojo et al. (2011) and Birgel et al. (2008) also reported similar results. Patidar and Raheman (2020) also reported 50 and 33% higher carbon deposits on injector tip with PME20S10W and PME20, respectively, compared to diesel. Contrary to these results, Sinha and Agarwal (2009) found lower carbon deposits with ROME due to elemental oxygen in biodiesel, leading to better combustion and lower soot emission.

Urzędowska and Stępień (2016) tested the fuel injector with RME 5 (5% v/v fatty acid methyl ester (FAME)) and two biofuels containing 30% v/v FAME (B30 winter grade and RME30 summer grade). These fuels were prepared with rapeseed FAME. The higher deposition was found with the aged RME30 fuel (see Fig. 3.12). Due to the large number of unsaturated bonds in low volatility, FAME fuel is susceptible to higher carbon deposits (Trobaugh et al. 2013; Lacey et al. 2012; Cook and Richards 2009). There may be other reasons for carbon deposits; perhaps oxidative stability strongly relates to the deposit.

Hartono and Cahyono (2020) also evaluated the deposit formation on the fuel injector. Similar to previous results, the author found a drier fuel injector with PME30. The deposit was evenly distributed in the case of diesel; however, an uneven pattern was observed for PME30. Perhaps, the injectors were found in acceptable limits
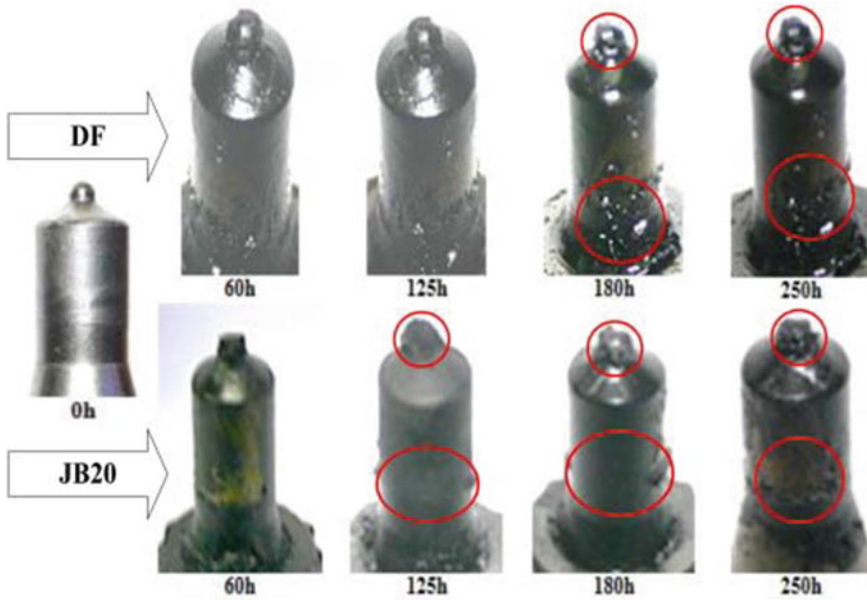
Fig. 3.11 Photographic view of injector nozzles during endurance test. Adapted with permission from Liaquat et al. (2014) Copyright 2014 Elsevier

Fig. 3.12 Injector deposit with **a** RME5 fuel, **b** RME30 fuel, **c** RME30 fuel aged for 16 weeks Adapted with permission from Urzędowska and Stępień (2016) Copyright 2016 Elsevier
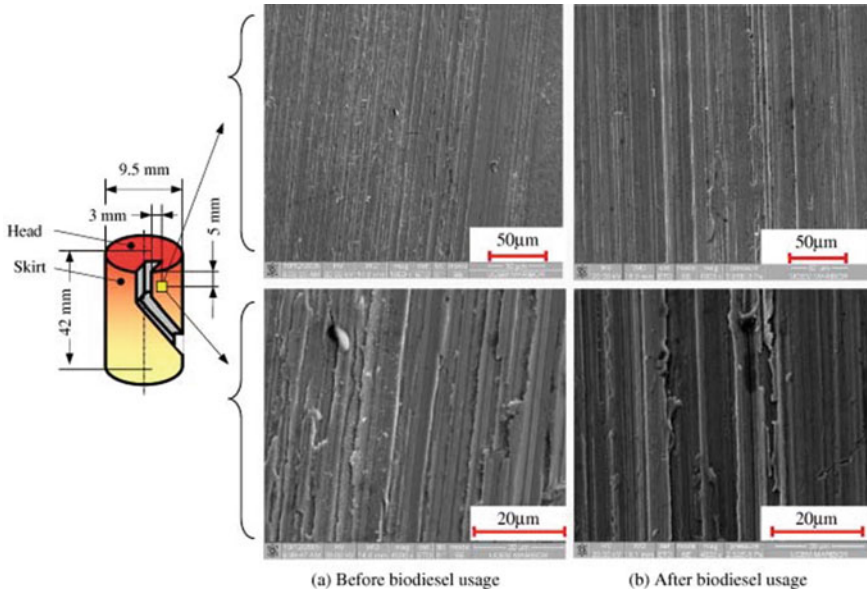
Fig. 3.13 Pump plunger skirt surface before and after biodiesel usage. Adapted with permission from Pehan et al. (2009) Copyright 2009 Elsevier

after the long-term test. Perkins et al. (1991) presented the injector coking results at 200, 400, 600, 800 and 1000 h. To maintain the injection opening pressure, the fuel injector was cleaned after 800 h. No significant change was observed between 400 and 600 h; however, the deposit drastically increased from 600 to 800 h. The result for 200 h and 1000 h were similar for injector coking, as the injector was cleaned after 800 h. Moreover, the internal deposit and wear were found lower for RME100. The discoloration in the injector needle for RME50 was in between diesel and RME100.

Suryantoro et al. (2016) investigated the carbon deposit with gravimetric and photographic methods. Authors reported wear reduction with both the tested fuels i.e., Indonesian biodiesel fuel (IBF, 10% palm biodiesel + 90% diesel) and B50. Similar results were reported by Agarwal et al. (2003b) and Kalam et al. (2004). Moreover, better results were found for IBF compared to PB50 due to efficient combustion (Suryantoro et al. 2016). After 35 h test, the thickness of the soft and wet/oily carbon deposits increased significantly. The presence of fuel residues is the probable reason for the wet nature of the deposit with diesel. The soft and wet/oily carbon deposits are inflammable (Suryantoro et al. 2016). The higher carbon deposition with PME50 is similar as reported previously in the literature (Singh and Varun 2016; Agarwal et al. 2018).

3.2.4 Pump Components

Pehan et al. (2009) used an electron microscope to study the impact of fuels (see Table 3.1 for fuel properties) on the pump plunger surface. They measured the arithmetic (R_a) and quadratic (R_q) roughness averages. Moreover, maximum (R_y) and average (R_z) peak-to-valley heights were also recorded. The measurement was done with mechanical scanning at the top of the pump plunger surface as this region is highly influenced by injection pressure. Results indicated that the biodiesel effect is slightly better on pump plunger skirt with the average root mean square roughness reduction from 0.45a to 0.40a (where a = 0.5 R_z (μm)). This is due to better lubrication with biodiesel. However, the surface roughness is relatively higher at the head of the pump plunger with the biodiesel compared to diesel (see Fig. 3.13). Fortunately, the effect on the pump plunger head is minimal on engine performance. Hence, the higher surface roughness on the head is not alarming but needs to study precisely.

Peterson et al. (1999) tested the RME20 blend in a heavy-duty truck diesel engine for 1,61,000 km. After the testing, the engine was disassembled in the Cummins lab for the evaluation of engine parts. All the parts were found in better conditions as expected. There were slightly higher carbon deposits found on the pump's internal parts; however, no on-field problem was reported with the pump.

Agarwal and Agarwal (2021c) reported brown deposits on the non-moving component of the pump and shaft with biodiesel. The authors found that the brown deposit was iron oxide (rust). However, the performance of the pump after the long run was found satisfactory.

3.2.5 Valves

The effect of fuels on intake and exhaust valves were also reported. Wander et al. (2011) evaluated both the valves with SME100, CME100, and diesel. Both adhesive and abrasive wear were found on the rod and grooves. The wears were within the acceptable limit after 1000 h. Due to insufficient lubrication, the rod used in the experiment with SME100 shows contact fatigue near the retainer. The higher combustion residues were observed at the inlet valve compared to the exhaust valve. Normal abrasive wear was reported at the valve seating (see Fig. 3.14). The irregular contact marks can be seen for CME100 due to irregular wear. A reddish color in the case of CME100 is due to oxidation (Wander et al. 2011).

Like injector tips, Suthisripok and Semsamran (Temizer 2020) reported varnish-like deposits with diesel and dry carbon deposits with palm biodiesel on inlet and exhaust valves (see Fig. 3.15).

Perkins et al. (1991) reported valve seats and faces duller with diesel compared to biodiesel blends. Suryantoro et al. (Suryantoro et al. 2016) reported the deposit formation trends as shown in Fig. 3.16. As seen from the figure, the deposit formation drastically increases up to 100 h for B50. This is due to seal swelling with the higher

CME100 (25x)   SME100 (50x)   D100 (25x)
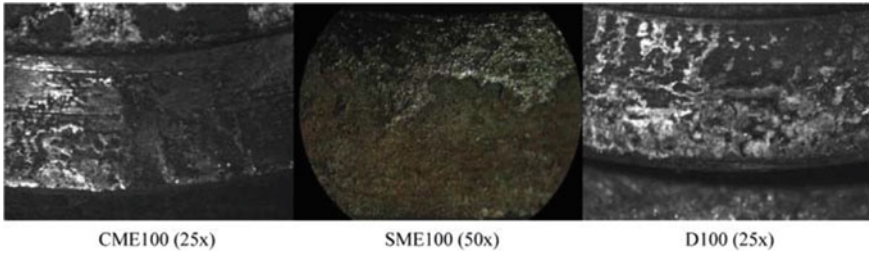
Fig. 3.14 Macrographic photos of exhaust valve seating. Adapted with permission from Wander et al. (2011) Copyright 2011 Elsevier

vanish-like deposit   dry deposit   dry deposit

Diesel fuel (100 hrs)   PME100 (100 hrs)   PME100 (700 hrs)
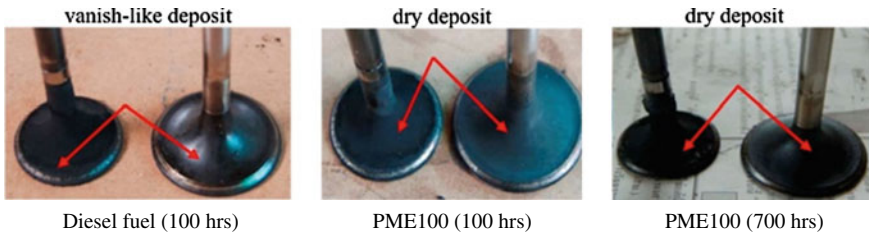
Fig. 3.15 Valves after long term testing with diesel and PME100 Adapted with permission from Suthisripok and Semsamran (2018) Copyright 2018 Elsevier

(a)   (b)
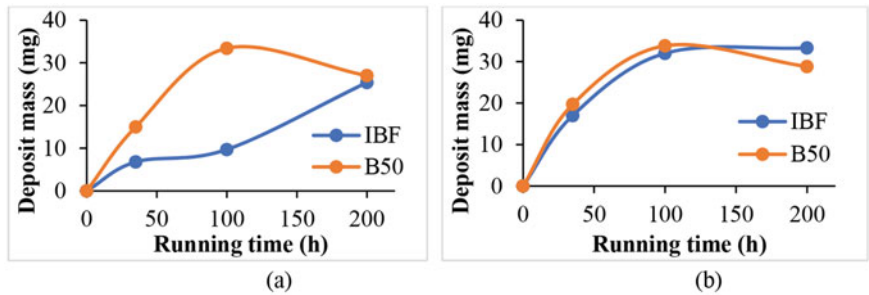
Fig. 3.16 Deposit mass growth trends on, **a** intake and **b** exhaust valve using IBF and B50 Redrawn from Suryantoro et al. (2016)

biodiesel content and oil leakage to the combustion chamber. However, the trend is similar for IBF and B50 for carbon deposit at the exhaust valve. The deposit on the exhaust valve is quite brittle and can be easily removed from the surface. Moreover, Agarwal and Agarwal (2021b) reported erosion wear marks in the case of biodiesel than diesel. However, they have not found any significant difference in valves manifold. They reported that biodiesel compatibility in the long term with test vehicles was satisfactory, and no noticeable durability issues were encountered. This is due to the promising physio-chemical properties of biodiesel and hence proper

combustion.. Ziejewski et al. (1986a, 1985) reported better methyl ester performance than neat oils in terms of lower carbon deposit at valve stems. This is due to the betterment in properties of oil after transesterification. The lower viscosity of methyl ester improves fuel vaporization and combustion. However, the authors have not reported any differences in the carbon deposit on the intake and exhaust valve tulips (Ziejewski and Kaufman 1983). However, significant increase in the carbon deposits on the exhaust valve stem was reported with SO25 compared to diesel.

3.3 Conclusions

It is apparent that prior to suggest a new fuel, it is advisable to perform long-term laboratory and in-field tests that focuses on the deliberation of engine life. In the present study, the following conclusions are made:

- The presence of inherent oxygen atom and superior lubricity in biodiesel helps in reducing the carbon deposits on engine parts due to better combustion. On the other hand, high viscosity and low volatility of biodiesel adversely affect the fuel atomization and combustion, leading to higher carbon deposits.
- Diesel operated engine generates wet carbon deposit (oily, greasy, varnish); however, biodiesel operated engine produces dry deposit.
- High temperature and pressure conditions in biodiesel fueled initiate an early carbon deposition on the fuel injector. Therefore, it is important to do the visual inspection of the fuel injector after the regular interval of time to ensure the long-term performance of the engine.
- Anti-thrust side of the cylinder liner exhibits higher wear compared to anti-thrust side irrespective of the fuel used.
- The area near the top dead center on the cylinder liner is more prone to wear due to the higher temperature and pressure conditions.
- Adjusting the injection timing, injection pressure, and compression ratio is a pathway for biodiesel fueled engines for reducing the carbon deposits.

References

Agarwal AK (2007) Biofuels (alcohols and biodiesel) applications as fuels for internal combustion engines. Prog Energy Combust Sci 33:233–271. https://doi.org/10.1016/j.pecs.2006.08.003

Agarwal AK, Agarwal D (2021a) Field-testing of biodiesel (B100) and diesel-fueled vehicles: Part 1-no load and highway driving emissions, and acceleration characteristics. J Energy Resour Technol. Trans ASME 143:1–7. https://doi.org/10.1115/1.4048307

Agarwal AK, Agarwal D (2021b) Field-testing of biodiesel (B100) and diesel-fueled vehicles: Part 3-wear assessment of liner and piston rings, engine deposits, and operational issues. J Energy Resour Technol Trans ASME 143:1–10. https://doi.org/10.1115/1.4048309

Agarwal AK, Agarwal D (2021c) Field-testing of biodiesel (B100) and diesel-fueled vehicles: Part 4-piston rating, and fuel injection equipment issues. J Energy Resour Technol Trans ASME 143:1–9. https://doi.org/10.1115/1.4048310

Agarwal AK, Bijwe J, Das LM (2003a) Wear assessment in a biodiesel fueled compression ignition engine. J Eng Gas Turbines Power 125:820–826. https://doi.org/10.1115/1.1501079

Agarwal AK, Bijwe J, Das LM (2003b) Effect of biodiesel utilization of wear of vital parts in compression ignition engine. J Eng Gas Turbines Power 125:604–611. https://doi.org/10.1115/1.1454114

A.K. Agarwal, Field-Testing of Biodiesel (B100) and Diesel-Fueled Vehicles: Part 2 — Lubricating Oil Condition Monitoring, 143 (2021) 1–8. https://doi.org/10.1115/1.4048308.

A.K. Agarwal, S. Park, A. Dhar, C.S. Lee, S. Park, T. Gupta, N.K. Gupta, Review of experimental and computational studies on spray, combustion, performance, and emission characteristics of biodiesel fueled engines, J. Energy Resour. Technol. Trans. ASME. 140 (2018). https://doi.org/10.1115/1.4040584.

Arifin YM, Furuhata T, Saito M, Arai M (2008) Diesel and bio-diesel fuel deposits on a hot surface. Fuel 87:1601–1609. https://doi.org/10.1016/j.fuel.2007.07.030

Barsari MAN, Shirneshan A (2019) An Experimental Study of Friction and Wear Characteristics of Sunflower and Soybean Oil Methyl Ester under the Steady-State Conditions by the Four-Ball Wear Testing Machine. J Tribol 141:1–10. https://doi.org/10.1115/1.4042390

Birgel A, Ladommatos N, Aleiferis P, Zülch S, Milovanovic N, Lafon V, Orlovic A, Lacey P, Richards P (2008) Deposit formation in the holes of diesel injector nozzles: A critical review. SAE Tech Pap. https://doi.org/10.4271/2008-01-2383

Chandran D (2020) Compatibility of diesel engine materials with biodiesel fuel. Renew Energy 147:89–99. https://doi.org/10.1016/j.renene.2019.08.040

Chourasia S, Patel PD, Lakdawala A, Patel RN (2018) Study on tribological behavior of biodiesel—Diethyl ether (B20A4) blend for long run test on compression ignition engine. Fuel 230:64–77. https://doi.org/10.1016/j.fuel.2018.05.055

Cook S, Richards P (2009) Possible influence of high injection pressure on diesel fuel stability: a review and preliminary study. SAE Tech Pap 4970. https://doi.org/10.4271/2009-01-1878.

Dhar A, Agarwal AK (2014) Effect of Karanja biodiesel blend on engine wear in a diesel engine. Fuel 134:81–89. https://doi.org/10.1016/j.fuel.2014.05.039

Dong WP, Davis EJ, Butler DL, Stout KJ (1995) Topographic features of cylinder liners - an application of three-dimensional characterization techniques. Tribol Int 28:453–463. https://doi.org/10.1016/0301-679X(95)00010-2

Ebert LB (1981) Chemistry of engine combustion deposits. Plenum Press, New York and London

Fazal MA, Haseeb ASMA, Masjuki HH (2011) Biodiesel feasibility study: An evaluation of material compatibility; Performance; emission and engine durability. Renew Sustain Energy Rev 15:1314–1324. https://doi.org/10.1016/j.rser.2010.10.004

Goel V, Kumar N, Singh P (2018) Impact of modified parameters on diesel engine characteristics using biodiesel: A review. Renew Sustain Energy Rev 82:2716–2729. https://doi.org/10.1016/j.rser.2017.09.112

Goldsworthy L (2006) Computational fluid dynamics modelling of residual fuel oil combustion in the context of marine diesel engines. Int J Engine Res 7:181–199. https://doi.org/10.1243/146808705X30620

Güralp O, Hoffman M, Assanis D, Filipi Z, Kuo TW, Najt P, Rask R (2006) Characterizing the effect of combustion chamber deposits on a gasoline HCCI engine. SAE Trans 115:824–835

Hartono ZA, Cahyono B (2020) Effect of Using B30 Palm Oil Biodiesel to Deposit Forming and Wear Metal of Diesel Engine Components. Int J Mar Eng Innov Res 5:2548–1479

Hoang AT, Le AT (2019) A review on deposit formation in the injector of diesel engines running on biodiesel, Energy Sources. Part A Recover Util Environ Eff 41:584–599. https://doi.org/10.1080/15567036.2018.1520342

Kalam MA, Masjuki HH (2004) Emissions and deposit characteristics of a small diesel engine when operated on preheated crude palm oil. Biomass Bioenerg 27:289–297. https://doi.org/10.1016/j.biombioe.2004.01.009

Kegl B (2008) Effects of biodiesel on emissions of a bus diesel engine. Bioresour Technol 99:863–873. https://doi.org/10.1016/j.biortech.2007.01.021

Kumar AA, Atul D (2018) Experimental investigation of preheated jatropha oil fuelled direct injection compression ignition engine—Part 2, 7:1–15

Kumar N, Varun SR (2013) Chauhan, Performance and emission characteristics of biodiesel from different origins: A review. Renew Sustain Energy Rev 21:633–658. https://doi.org/10.1016/j.rser.2013.01.006

Kumar N, Varun SR (2015) Chauhan, Evaluation of endurance characteristics for a modified diesel engine runs on jatropha biodiesel. Appl Energy 155:253–269. https://doi.org/10.1016/j.apenergy.2015.05.110

Lacey P, Gail S, Kientz J, Benoist G, Downes P, Daveau (2012) Fuel quality and diesel injector deposits. SAE Int J Fuels Lubr 5:1187–1198

Lapuerta M, ARMAS O, Rodriguez Fernandez J (2008) Effect of biodiesel fuels on diesel engine emissions. Prog Energy Combust Sci 34:198–223. https://doi.org/10.1016/j.pecs.2007.07.001

Lepperhoff G, Houben M (1993) Mechanisms of deposit formation in internal combustion engines and heat exchangers. SAE Tech Pap. https://doi.org/10.4271/931032

Leung DYC, Luo Y, Chan TL (2006) Optimization of exhaust emissions of a diesel engine fuelled with biodiesel. Energy Fuels 20:1015–1023. https://doi.org/10.1021/ef050383s

Liaquat AM, Masjuki HH, Kalam MA, Fazal MA, Faheem A, Fayaz H, Varman M (2013) Impact of palm biodiesel blend on injector deposit formation. Appl Energy 111:882–893. https://doi.org/10.1016/j.apenergy.2013.06.036

Liaquat AM, Masjuki HH, Kalam MA, Fattah IMR (2014) Impact of biodiesel blend on injector deposit formation. Energy 72:813–823. https://doi.org/10.1016/j.energy.2014.06.006

Mosarof MH, Kalam MA, Masjuki HH, Alabdulkarem A, Habibullah M, Arslan A, Monirul IM (2016) Assessment of friction and wear characteristics of Calophyllum inophyllum and palm biodiesel. Ind Crops Prod 83:470–483. https://doi.org/10.1016/j.indcrop.2015.12.082

Patidar SK, Raheman H (2020) Performance and durability analysis of a single-cylinder direct injection diesel engine operated with water emulsi fi ed biodiesel-diesel fuel blend. Fuel 273:117779. https://doi.org/10.1016/j.fuel.2020.117779

Pehan S, Jerman MS, Kegl M, Kegl B (2009) Biodiesel influence on tribology characteristics of a diesel engine. Fuel 88:970–979. https://doi.org/10.1016/j.fuel.2008.11.027

Perkins LA, Peterson CL, Auld DL (1991) Durability testing of transesterified winter rape oil (Brassica Napus L.) as fuel in small bore, multi-cylinder, DI, CI Engines. SAE Tech Pap 100:545–556. https://doi.org/10.4271/911764

Peterson GFCL, Thompson JC, Taberski JS, Reece D (1999) Long-range on-road test with twenty-percent rapeseed biodiesel. Appl Eng Agric ASAE 15:91–101

Ra Y, Reitz RD, Jarrett MW, Shyu TP (2006) Effects of piston crevice flows and lubricant oil vaporization on diesel engine deposits. SAE Tech Pap 2006. https://doi.org/10.4271/2006-01-1149

Reksowardojo I, Bui HN, Sok R, Kilgour A, Brodjonegoro T, Soerawidjaja T, Pham MX, Shudo T, Arismunandar W (2011) The effect of biodiesel fuel from rubber (Hevea Brasiliensis) seed oil on a direct injection (Di) diesel engine, ASEAN Eng J Part A 1

Sharma A, Murugan S (2017) Durability analysis of a single cylinder DI diesel engine operating with a non-petroleum fuel. Fuel 191:393–402. https://doi.org/10.1016/j.fuel.2016.11.086

Singh P, Goel V (2018) Effect of bio-lubricant on wear characteristics of cylinder liner-piston ring and cam-tappet combination in simulated environment. Fuel 233:677–684. https://doi.org/10.1016/j.fuel.2018.06.092

Singh P, Varun SR (2016) Chauhan, Carbonyl and aromatic hydrocarbon emissions from diesel engine exhaust using different feedstock: A review. Renew Sustain Energy Rev 63:269–291. https://doi.org/10.1016/j.rser.2016.05.069

Singh P, Varun SR (2017a) Chauhan, Feasibility of a new non-edible feedstock in diesel engine: Investigation of performance, emission and combustion characteristics. J Mech Sci Technol 31:1979–1986. https://doi.org/10.1007/s12206-017-0347-2

Singh P, Varun SR (2017b) Chauhan, Influence of temperature on tribological performance of dual biofuel. Fuel 207:751–762. https://doi.org/10.1016/j.fuel.2017.05.094

Singh SK, Agarwal AK, Sharma M (2006) Experimental investigations of heavy metal addition in lubricating oil and soot deposition in an EGR operated engine. Appl Therm Eng 26:259–266. https://doi.org/10.1016/j.applthermaleng.2005.05.004

Singh P, Varun SR, Chauhan NK (2016) A review on methodology for complete elimination of diesel from CI engines using mixed feedstock. Renew Sustain Energy Rev 57:1110–1125. https://doi.org/10.1016/j.rser.2015.12.090

Singh P, Chauhan SR, Goel V (2018a) Assessment of diesel engine combustion, performance and emission characteristics fuelled with dual fuel blends. Renew Energy 125:501–510. https://doi.org/10.1016/j.renene.2018.02.105

Singh P, Goel V, Chauhan SR (2018c) Effect of phyllanthus emblica biodiesel based lubricant on cylinder liner and piston ring. J Mech Sci Technol 32:1269–1275. https://doi.org/10.1007/s12206-018-0231-8

Singh Y, Singh P, Sharma A, Choudhary P, Singla A, Singh NK (2018d) Optimization of wear and friction characteristics of Phyllanthus Emblica seed oil based lubricant using response surface methodology. Egypt J Pet 27:1145–1155. https://doi.org/10.1016/j.ejpe.2018.04.001

Singh P, Chauhan SR, Goel V, Gupta AK (2019a) Impact of binary biofuel blend on lubricating oil degradation in a compression ignition engine. J Energy Resour Technol Trans ASME 141. https://doi.org/10.1115/1.4041411

Singh P, Chauhan SR, Goel V, Gupta AK (2019b) Binary biodiesel blend endurance characteristics in a compression ignition engine 141:1–11. https://doi.org/10.1115/1.4041545

Singh P, Chauhan SR, Goel V, Gupta AK (2019c) Binary biodiesel blend endurance characteristics in a compression ignition engine. J Energy Resour Technol Trans ASME 141:1–11. https://doi.org/10.1115/1.4041545

Singh P, Sharma S, Almohammadi BA, Khandelwal B, Kumar S (2020a) Applicability of aromatic selection towards newer formulated fuels for regulated and unregulated emissions reduction in CI engine. Fuel Process Technol 209:106548. https://doi.org/10.1016/j.fuproc.2020.106548

Singh P, Chauhan SR, Goel V, Gupta AK (2020b). Enhancing diesel engine performance and reducing emissions using binary biodiesel fuel blend. https://doi.org/10.1115/1.4044058

Singh P, Goel V, Chauhan SR (2018) Effects of dual biofuel approach for total elimination of diesel on injection system by reciprocatory friction monitor. Proc Inst Mech Eng Part J J Eng Tribol 232:1068–1076. https://doi.org/10.1177/1350650117737874.

Sinha S, Agarwal AK (2009) Rice bran oil methyl ester fuelled medium-duty transportation engine: Long-term durability and combustion investigations. Int J Veh Des 50:248–270. https://doi.org/10.1504/ijvd.2009.025010

Sinha S, Agarwal AK (2010) Experimental investigation of the effect of biodiesel utilization on lubricating oil degradation and wear of a transportation cidi engine. J Eng Gas Turbines Power 132:42801-1-42801–9. https://doi.org/10.1115/1.3077659

Sudan Reddy Dandu M, Nanthagopal K (2019) Tribological aspects of biofuels–a review. Fuel 258:116066. https://doi.org/10.1016/j.fuel.2019.116066

Suryantoro MT, Sugiarto B, Mulyadi F (2016) Growth and characterization of deposits in the combustion chamber of a diesel engine fueled with B50 and Indonesian biodiesel fuel (IBF). Biofuel Res J 3:521–527. https://doi.org/10.18331/BRJ2016.3.4.6

Suthisripok T, Semsamran P (2018) The impact of biodiesel B100 on a small agricultural diesel engine. Tribol Int 128:397–409. https://doi.org/10.1016/j.triboint.2018.07.042

Temizer İ (2020) The combustion analysis and wear effect of biodiesel fuel used in a diesel engine. Fuel 270. https://doi.org/10.1016/j.fuel.2020.117571.

Trobaugh C, Burbrink C, Zha Y, Whitacre S, Corsi C, Blizard (2013) Internal diesel injector deposits: theory and investigations into organic and inorganic based deposits. SAE Int J Fuels Lubr 6:772–784. www.jstor.org/stable/26273270

Urzędowska W, Stępień Z (2016) Prediction of threats caused by high FAME diesel fuel blend stability for engine injector operation. Fuel Process Technol 142:403–410. https://doi.org/10.1016/j.fuproc.2015.11.001

Varun P, Singh SK, Tiwari R, Singh NK (2017) Modification in combustion chamber geometry of CI engines for suitability of biodiesel: A review. Renew Sustain Energy Rev 79:1016–1033. https://doi.org/10.1016/j.rser.2017.05.116

Wander PR, Alta CR, Colombo AL, Perera SC (2011) Durability studies of mono-cylinder compression ignition engines operating with diesel , soy and castor oil methyl esters 36:3917–3923. https://doi.org/10.1016/j.energy.2010.10.037

Ziejewski M, Kaufman KR (1983) Laboratory endurance test of a sunflower oil blend in a diesel engine 60:1567–1573

Ziejewski M, Kaufman KR, Pratt GL, Goettler HJ (1985) Fuel injection anomalies observed during long-Term engine performance tests on alternate fuels. SAE Tech Pap 852089

Ziejewski M, Goettier H, Pratt GL (1986a) Influence of vegetable oil based alternate fuels on residue deposits and components wear in a diesel engine. SAE Tech Pap. https://doi.org/10.4271/860302

Ziejewski M, Goettler H, Pratt GL (1986b) Comparative analysis of the long-term performance of a diesel engine on vegetable oil based alternate fuels. SAE Tech Pap 860301. https://doi.org/10.4271/860301

Chapter 4
Automated SI Engine Wear Parts

Rakesh Kumar and Rahul Sinha

Abstract It is very common to witness wear during the operation of SI components. Due to the thin oil film thickness present between the contacting mediums, it encounters serious wear problems in sliding components. Engine performance has greatly improved due to the development of ultralow viscous lubricating oils, however, engine wear has also increased. Wear is always challenging and its measurement is also difficult. In some studies, concern is expressed regarding the quantitative measurement of wear parts of machine equipment. It is, however, difficult to collect the data related to quantitative wear measurement. In recent years, attempts have been made to extend the life of such components by altering the mechanical strength of the materials used for those purposes. The purpose of this paper is to review on ways to improve the wear parts in SI engine.

Keywords Engine Parts · Tribology · Wear · Piston · Engine Bearings

4.1 Introduction

The term "Tribology" was first introduced by Jost (1966). Jost has highlighted the influence of tribology on the economic benefit of the industry. In his published report, another significant term was introduced as the effect of tribology on the emission of carbon dioxide gases and energy consumption. Based on the work of Jost, Holmberg and Erdemir (2017) quantified the global economic benefits towards the fight against tribology. They have considered the four major sectors such as manufacturing, transportation, residential and power generation and concluded that due to tribological contact, total of 23% of world's energy is consumed in which 20% of energy is used to overcome friction and 3% of energy is consumed to remanufacture the parts and equipment which got worn out. It has also been observed that for

R. Kumar
Indian Institute of Technology (Indian School of Mines), Dhanbad 826004, India

R. Sinha (✉)
School of Engineering, P P Savani University, Surat 394125, India
e-mail: rahul.sinha@ppsu.ac.in

the protection against wear damage and application of new replaced material after worn out or by the application of lubrication technologies, in vehicles and other machinery items, it could be helpful in reducing friction and wear. Therefore, taking care of tribological science, Holmberg et al. (2013) reported that the energy could be reduced to 18 to 40% depending on the short-term to the long-term goal. It directly interacts with the effect on annual GDP savings to 1.4%. In a complete statement covered under the report of Holmberg and Erdemir (2017; Holmberg et al. 2017) for energy savings, it is also stated that 25% of energy can be saved from transportation and 20% from power generation. Whereas, approximately of 10% could be saved from the manufacturing and residential sectors. Thus, the application and adoption of advanced tribological technologies can reduce the global challenge of carbon dioxide emission which further can bring one of the biggest advantages in energy savings up to 970,000 million Euros.

While dealing with the term tribology, the demand is to produce the material which not only survives under the tribological environment but also improves the performance of the machine components for energy saving. In this view, industries are always demanding the product which can be best utilized in several applications. In many topics discussed, it is mentioned that wear and friction is not a property of a material. It is mainly the response from a system that is affected by the operating conditions of the contacting surface. In some cases wear is found productive like manufacturing operations where work is performed under a controlled wear environment. However, this can be dangerous to the machine components where some sliding action results in the removal of material from the mechanical parts which leads to the replacement of that component after its failure under wear and friction. If the tribological systems are designed as per their need to perform under the tribological environment then wear and friction can be considered very slow. But wear relatively increases if any debris is left behind the sliding action of two contacting mediums. Under such condition, clearance between the two relatively contacting mediums also influences wear. As wear is classified into abrasive, adhesive, thermal, corrosive, fretting, fatigue, chemical, impact, and percussive types which is represented in Fig. 4.1, so automobile engines and their part has observed some of these wear phenomenon under various circumstances (Bhusan 2013).

With millions of automobile engines registered for use, SI engines have shown great interest based on their performance and reliability. Manufacturers have shown keen interest in improving the power output of the SI engine parts by contributing towards the reduction of harmful greenhouse gases. It further leads to meet the demand of less fuel consumption and more power output (Wong and Tung 2016; Taylor 1998). But with the advancement in technologies, modern engines need to be improved to decrease losses due to wear and friction. Losses due to wear and friction decrease mechanical and thermal efficiency. Figure 4.2 shows the dissipation of energy losses. In Fig. 4.1 Mechanical energy loss contributes to a maximum of 25 to 35% in which losses due to wear and friction also exist (Taylor 1998).

To underpin the losses due to wear and friction it is essential to classify the components of SI engine which can improve the reliability of the machine. Reliability losses
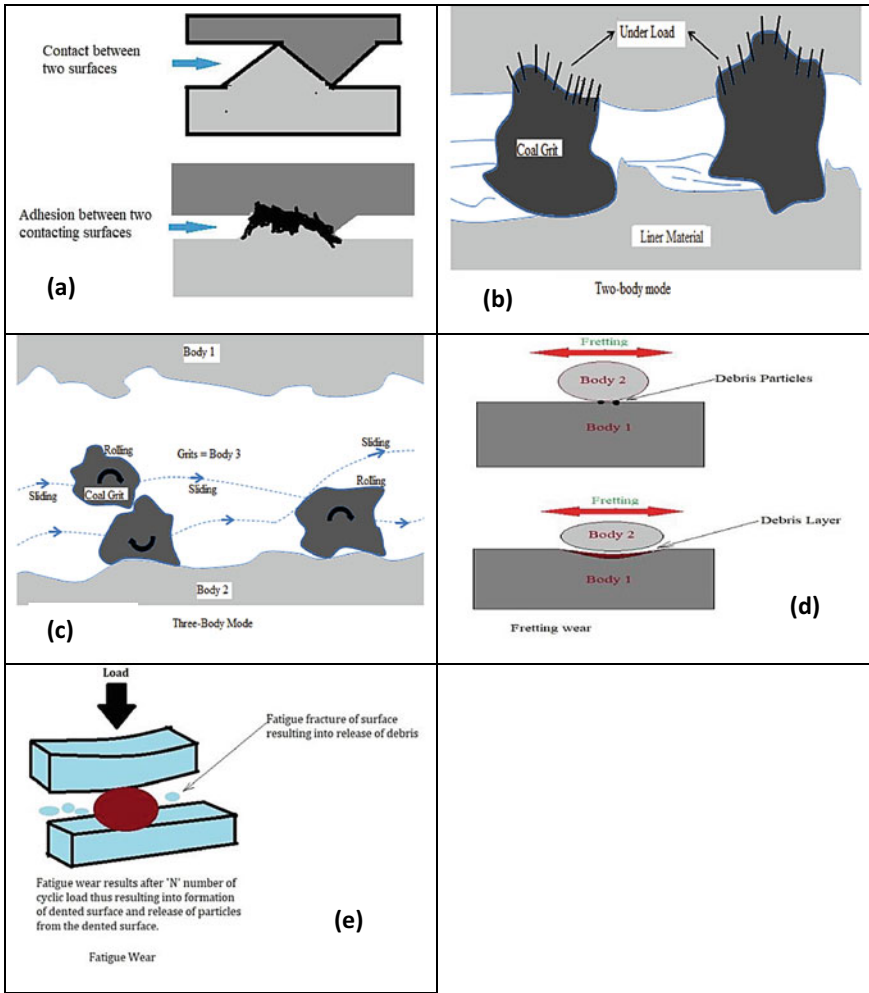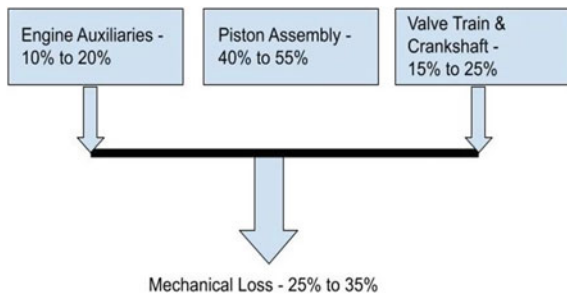
Fig. 4.1 Types of Wear **a** Adhesive wear **b** Two-body Abrasive wear **c** Three body Abrasive wear **d** Fretting wear **e** fatigue wear

Fig. 4.2. Distribution of energy losses (Taylor 1998)

occur due to surface changes observed under the case of wear and friction (Holmberg et al. 2014, 2012). Surface change in major components of automobiles arises due to frictional losses which can be controlled with lubricating oils for the proper functioning of the machine. Moreover, the type of lubrication and lubricating oils can solve the mechanical energy losses due to wear and friction but up to the certain extent. There are different types of lubrication namely hydrodynamic, elastohydrodynamic, mixed lubrication, and boundary lubrication. Therefore, the type of lubrication requirement depends on the type of engagement of engine components. This results in the compromise between reliability, durability, and efficiency of the engine parts. Therefore, industries are always looking to meet the demand for improved performance of engine using lubrication technology (Taylor 1998). Recently, it is being noticed that nano-additives have shown great interest to the industrialist. Sheet thickness of carbon atoms present in graphene is around 0.335 nm which contributes an advantage in the field of nano-tribology for automobile engines (Holmberg et al. 2014). Thus achieving the very small size of this nano-lubricant as additives can be an advantage to mechanical systems of automobiles but it further leads to friction and wear of the sliding parts. This can be considered due to loss of thickness range due to continuous sliding of contacting parts.

4.2 Tribological Components of SI Engine

This chapter discusses common tribological problems occurring in SI engine parts. Mechanical components of automobiles that operate under low stress to high stress include piston assembly, engine bearings, valve train, and gearbox. In most cases of the piston assembly, wear and friction is observed the interface between liner and piston skirt and between piston ring and liner.

4.2.1 Piston Assembly

In an automobile, the piston is one of the components which deliver mechanical energy to automobile machine. It supplies mechanical energy to other mechanical components with the help of reciprocating motion. The reciprocating motion further changes to rotational motion with the help of crankshaft which derives the required output power. Assembly of piston with crankshaft is possible with the help of wrist pin (Wong and Tung 2016). The piston moves from the top dead center to the bottom dead center. In between the two dead centers, the chamber is called as the combustion chamber. This combustion chamber is lined with the liner to protect the inside wall of the combustion chamber and the outside surface of the piston. At the head of piston, there is an arrangement of piston ring. The power delivers by a piston is completed in four strokes. But it delivers nearly about 50% of total mechanical loss due to wear (Ye et al. 2004). If losses due to wear and friction are counted then this energy reduces
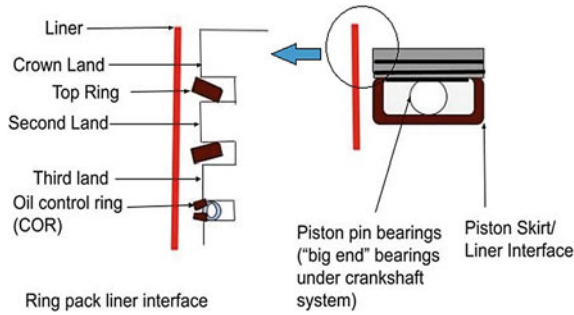
Fig. 4.3 Wear of piston ring

the engine performance at the first stage. Piston-cylinder is generally considered the heart of machine components. Wear of piston crown, piston ring, piston skirt, and cylinder liner is observed under various conditions as shown in Fig. 4.3.

Wear of piston crown is due to the thermal effect, cooling system malfunctioning effect, block of oil injection, and restriction of clearance at the upper surface area of sliding parts which further leads to wear. Sliding may result in mild to severe wear. Therefore, studying the basic parameters like examining of surface roughness is not sufficient to analyze the result that leads to material losses. Some of these effect results into deposition of carbon at the piston crown, crack initiation and insufficient compression which can also be examined as research findings for further references (Green and Lewis 2008).

In piston-cylinder arrangement, the most important part of this component is the piston ring and piston liner. A Piston ring is generally used to maintain sufficient pressure and limit the consumption of oil. This helps the piston to perform effectively inside the cylinder chamber. Based on the material selection for the piston ring it is recommended that it should be light-tight to obtain an even distribution of radial pressure and to avoid uneven wear (Taylor and Eyre 1979; Moughon 2006). When looking at its design part it is either manufactured as negative or positive ovality, as shown in Fig. 4.4. Positive ovality type ring is used in high-speed SI engine as it tends to reduce ring flutter with the help of damping effect observed under vibration. Whereas, negative ovality type ring results to wear and performance losses of the engine but it is more resistant to thermal distortion. Therefore, a proper choice is to be made to improve the engine performance by increasing the performance of the engine. This is achieved by increasing the hardness of the piston ring to prevent early damage due to wear (Taylor and Eyre 1979).

It has been revealed from the studies that cast iron material is more significant to use as piston ring material due to the presence of graphite in laminar form. It is also available in alloyed and coated form as per the requirement and demand for its operation. Thus, this makes the piston ring a self-lubricating type. But this does not ensure the proper life cycle of the piston ring material. Mechanical heat treatment of steels using nitriding process also required for the purpose to improve the life of piston ring material. Alternative to this, PVD coatings of Chromium-based and

A>B for Positive ovality
A<B for negative ovality
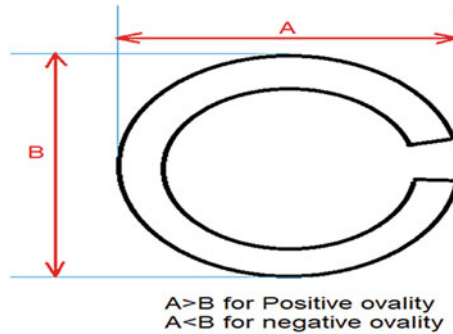
Fig. 4.4 Piston ring ovality (Taylor and Eyre 1979)

DLC (Diamond-like coatings) are trending nowadays (Friedrich et al. 1997; Tung et al. 2003). Tribologists have visualized that how the effect of the abrasive wear mechanism plays a vital role in increasing the wear of piston ring. Studies show that solid particles or contaminants carried through lubricating oil circuits or from the combustion chamber get entrapped in between the interface of piston ring and liner through lubrication results in three-body abrasive wear. Also, poor lubrication can lead to adhesive wear which further results in an increase in friction and scuffing of metal. This is to be the advantageous effect for the improvement of tribological behaviour of the oil lubricants and piston ring coatings to enhance the performance of the machine (Tung et al. 2003).

4.2.2 Engine Bearings

Diagnosing the cause of failure to improve the life span of mechanical components is always required. This can be done using the time to time maintenance. However, premature failure of engine bearing is due to various parameters like dirt, misalignment, overloading, improper lubrication or deficiency in lubrication, corrosion, and improper finish (Wong and Tung 2016). The solution to the premature failure attributes to identifying the cause of failure and performing a better operation to eliminate the problem. To eliminate the problem arising due to wear is required to inspect the appearance of the bearing and take suggestive action against the damage caused by wear. It is also necessary to understand the possible cause of wear for corrective action.

When foreign particles like dirt, as shown in Fig. 4.5, are entrapped in between the contacting surface of bearing and lining then it results in abrasive action (Bhushan 2000; MAHLE 2021). The abrasive actions are the cause of scratch marks on the surface. Macro scratches are easily visible whereas micro scratch needs microscopic examination. The scratches formed to result in displacing of material from the surface and frequent action results in high-spot. High spot results in rupture and breakdown of

Fig. 4.5 Wear action due to foreign particle arrest between bearing and lining (Willn and Bret 1977)
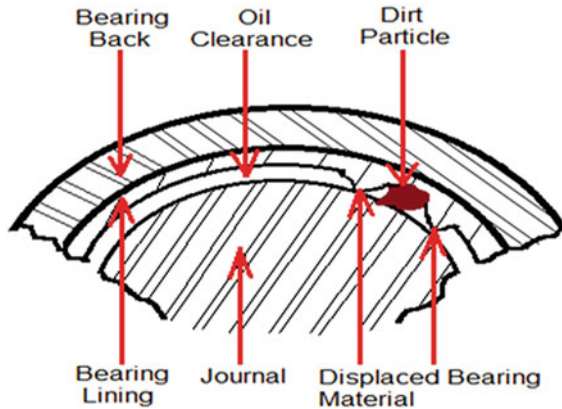
the lining parts of bearing. The scratches are results of abrasive action which is similar to the action of grinding. Another phenomenon observed for the cause of wear in engine bearing is their misassembly which later becomes the factor of a major failure. Bearing failure due to misassembly is pre-processed by wear due to overloading. The formation of fine cracks are the common behaviour observed under this phenomenon. If the issue becomes major then the technician has none other than the replacement of the part. Bearing life also depends on the material used. If the material properties do fall under the category of bearing life span then overloading on the bearing may also result in overlay fatigue. In this case, the surface of bearing appears like a cavity due to displaced crack layers but the displaced material does not get easily removed from the cavity thus resulting in relive of load concentration. If this situation is faced on the entire bearing surface then it indicates the case of overloading due to high friction and wear. Sometimes this situation leads to damage of oil film thickness due to penetration by the rough surface of bearing thus resulting into early failure of the machine parts. To avoid actions of wear damage it is recommended to use dry film coating. It prevents the bearing surface from wear damage by maintaining a low friction coefficient and proposes high strength against wear due to its self-lubricating property, therefore, prevents any change in metallurgical property by not responding to temperature changes (Durak et al. 2008; Williams and Hyncica 1992; Becker and Shipley 2002).

Engine bearing is basically a metallic cylinder that supports the rotating shaft mounted with it. The Performance of automobile engines is reliable on bearing. In an automobile engine, the crankshaft is supported by bearings to allow free rotational movement by minimizing friction. It is designed to work under hydrodynamic lubrication. Generally, bearings are cleft into two half having an upper shell and lower shell. In bearing assembly, oil is supplied through the upper shell having a hole for oil to pass through it. Grooves provided in the upper shell helps to distribute the oil in an even direction. Whereas, the lower shell of the bearing is used to carry

loads and is having no grooves (Branagan 2015). The crankshaft converts motion from reciprocating to rotary thus generating high inertial forces. These inertia forces have resulted through forces experienced under combustion and oscillating of the cylinder between the top dead center (TDC) to bottom dead center (BDC). In this process oil sump constantly supplies lubricating oil to prevent wear and maintain the temperature inside the machine parts (Ligier and Noel 2015). To achieve low friction in engine bearing it is suggested that bearings should operate under elasto-hydrodynamic lubrication (EHL). It is obtained under a set of parameters like speed, load, lubricant type, and type of material (Tamatam 2017). This type of lubrication effect is produced when bearing operates at a high velocity of sliding or the engine is running at the steady idle condition and low contact pressure. Therefore, this type of ideal situation is not always faced by the bearings due to factors like start and stop of the engine, variable load, and change in speed, presence of debris and overheating of lubricant resulting in an aging effect. During the start of the engine, the lubrication effect changes from boundary to mixed and mixed to elastohydrodynamic (Ligier and Noel 2015; Kopeliovich 2016).

In this case, wear is generally produced during boundary lubrication to mixed lubrication as the sliding surface of the bearing is in direct contact. Further, over-heating and thermal aging result in a decrease in viscosity and thickness of oil film also responsible for the transition of lubrication from elastohydrodynamic to mixed and later to boundary type. This condition also facilitates an increase in wear of bearing. Also, debris particles formed either from the bearing assembly or other sliding assembly pairs and carried by the engine oil to different sections of automobile engines thus participates in three-body abrasion (Kopeliovich 2016). As oil filters are used to filer such debris particles from oil but fine debris particles escape this method and therefore they cannot be separated easily. Generally, the size of fine debris particles are less than 10 µm and it can be observed in the engine oil after several days of operation (Williams and Hyncica 1992; Stachowiak and Batchelor 2005; Kerr et al. 2007; Hamid et al. 2017).

For the durability of bearing operation, it is always required that the bearing material should possess high strength for high load-carrying capacity and good wear resistance (Nieuwland and Droste 2001). There are cases of misalignment observed between journal and bearing and to avoid this effect it is recommended that bearing material should possess good conformability. It is also expected that bearing material should possess the property of seizure resistance to avoid the effect of friction welding under sliding action (Ligier and Noel 2015). A better engine-bearing material encompasses with good material selection. As lead is avoided due to its toxic nature and is not recommended for its usage in automobile engine parts. Such a case results in selection of different materials which can possess the same properties as that of lead. Materials containing Bismuth are an alternative to lead. Nowadays Polymers are also used as a bearing material as an alternative to conventional material used as bearing parts (Nieuwland and Droste 2001; Upadhyay 2013; Becker 2004).

4.2.3 Valve Train

Engine oil lubricants and their properties exhibit an important role in improving the engine economy (Rameshkumar and Rajendran 2012). Lubricant behaviour affects the valve train and it is highly recommended to provide good lubricating oil for engine performance. However, this problem is least common in engine due to associated measures, test procedures, and improvements taken for lubricating oil. Some examples of critical engine tests are Sequence VE, Peugeot TU-3, and the Toyota 3A tests (Rameshkumar and Rajendran 2012; Yuan et al. 2000). These tests are meant to examine the wear behaviour of the cam and follower mechanism. Generally, the wear of cam and follower is most likely attracted by abrasive and adhesive. Some cases also showed the existence of corrosive wear phenomena due to temperature differences. The Application of anti-wear additives in engine oil such as zinc dialkyldithiophosphate can reduce the effects of chemical wear (Yuan et al. 2000).

4.2.4 Gearbox Wear

Clutches are generally referred to as synchronizers. As the name suggests, it helps in synchronizing the rotating shaft velocity. Manual, automatic, and dual-clutch transmission engine uses this technology. Generally, brass is used as a material for synchronizer. However, carbon synchronizer is used as a replacement for brass material due to its good wear resistance and durability. It is being noticed that torsional vibration is observed in the case of IC engine in addition to the angular acceleration as the main source is obtained from the order of engine firing. In this respect, if the size of the engine is small then it produces high fluctuations in torsion. This fluctuation is transmitted to the gearbox with the help of a clutch. The gearbox, as mounted on the countershaft, thus excites the idler gear and resulting in the reduction in gap for ring wear.

Allianz Versicherungs (1978) examined the cause of wear in the gearbox and the study revealed that about 65% of the damage occurs in the gear due to faults that arise due to excessive vibration. Moreover, other factors like gear tooth stiffness, time-varying of mesh, tooth face friction, and backlash are also responsible for these effects. Therefore, for getting the best possible result outcome, vibrational analysis has shown a key feature in the improvement of wear of gearbox. In this respect vibration analysis for the case of gear is divided into three main subcategories as time, frequency, and time–frequency domain. In the time domain, the method to examine the vibration is through statistical analysis and the time-synchronous average method. In the time-synchronous average method, the method of the procedure follows is to analyze the average signal over several cycles and synchronize it with the gearbox under running conditions. Thus, this process specifies great importance in improving the background noise of the gearbox which later reduces the wear and tear of the machine parts. Vibration analysis using statistical method consists of examining of

gearbox through kurtosis, skewness, and other relevant method. While the frequency method presents analysis using cepstrum and process spectral density, Short-Time Fourier transform (STFT), wavelet analysis, Cohen distribution, and Wigner-ville.

More or less it is an important consideration that vibration analysis is not an important factor that completely eliminates the major issues occurring due to wear. In this regard for the governing case of environmental concern and sustainable energy growth, the design of gear system for prediction of best mechanical efficiency become a major concern to enrich the solution of wear (Shannon et al. 1996). Therefore, the application of lubricants with optimized solutions can erase the problem of energy conservation and economic factors arising under wear. But frictional losses between gear teeth and lubricants have become a major area of study. As the frictional effect changes the viscosity index of the lubricants, this therefore, increases losses due to churning. The introduction of anti-wear property for minimal significant losses in lubricants can possibly reduce the effect of energy loss occurring in the gearbox. Oil lubricants such as ester oil, polyalphaolefin, polyglycol, and mineral oils show great improvement in increasing the mechanical efficiency of the engine (Kolivand et al. 2010; Bronshteyn and Kreiner 1999; Martins et al. 2008). It is also been noticed by Marques et al. (2009) that lubricating oil with different additive packages and types of base oil generates different power losses even if their viscosity grades are same. Therefore, lubrication properties have a greater influence on fatigue life of the gear. In an experiment on gear tests conducted by Scibbe et al. (1984), it was noticed that extreme pressure (EP) added additives in lubricants resulted in 10 to 50% enhancement in the fatigue life of the gear. In an event of research on EP additives by Hohn and Michaellis (2001), evidence of a decline in resistance in micropitting was observed with mild aging of oil.

Sliding friction during the meshing of gears is also identified as one of the concerns towards power transmission loss (Diab et al. 2006; Diez-Ibarbia et al. 2018). Further, a study was performed by Kaiyue et al. (2016) and examined the effect of oil film thickness and oil length. With the increase in both two factors, i.e. oil film thickness and oil length, consumption of power due to friction reduces. However, it was difficult to establish the ideal working condition of EHL. Moreover, a lubricant with enhanced properties deals with the improvement in the fatigue life of the gear. In continuation with the effect of lubricant on fatigue life, some researchers have revealed that EP additive lubricants give a significant improvement in the fatigue life up to 10 to 50%. This parameter was studied for AISI 9310 made spur gear (Ziegltrum et al. 2017). Some evidence of improvement in fatigue life and wear performance with the aging of lubricant due to temperature rise was observed by Hohn and Michaellis (2001). A conclusion was also drawn over the aging action of lubricant as it deteriorates the resistance of pitting. Alternatively, evidence of decline in wear rate with an increase in lubricant viscosity was one of the major concerns (Diez-Ibarbia et al. 2018). When dealing with the energy consumption due to friction behaviour and considering the key response to a study of wear behaviour, it has come to the notice that fluid pressurization can also have an adverse effect on the fatigue life. Fluid pressurization was observed at the contacting region of high-pressure during gear meshing. Therefore, this advances the crack propagation with the development of

tiny fatigue cracks at the beginning and thus allowing the lubricating fluid to enter into it (Kaiyue et al. 2016). Many discussions have been made to achieve low wear in the gearbox and improving the fatigue life. This accommodates the principle of gear dynamics. Scientific studies on problem faced during gear dynamics, evaluated to control noise and vibration, shows higher viscosity oil improves the fatigue life of gear (Krantz and Kahraman 2005). Studies pertaining to the area of gear dynamics require proper attention. Cases of gear rattle by some researchers were also examined under gear dynamics under highly loaded and unloaded conditions. Evidence shows that the meshing of gear teeth generates gear rattle. It is observed under backlash conditions.

Therefore, it is highly recommended for the frequent replacement of lubricating oil in order to achieve a good quality performance of the engine. As automobile engines have compact transmission systems that degrade the quality of lubrication. This is due to the dissipation of heat and airflow into the gearing system design.

4.2.5 Tire Wear

Among the power transmission elements of IC engine, there exists a unique contribution of tires on the road as it holds safe driving. An automobile is linked with the road through the tires. The tire provides better grip and acceleration by supporting vehicle weight and passenger weight. Mostly used material for a tire is rubber. The application of rubber tires is relying for transportation for many years. Data estimated in 2016 regarding the use of passenger car was near about 1.02 billion which was expected to increase up to 1.3 billion in 2024 (Olver 2005). Tire contains fillers, additive agents, vulcanization agents, softeners, and polymers (both natural and synthetic) (Fietkau and Bertsche 2013). Contents of tires are released to the environment through wear and tear. Researchers have found that microplastic particle (MPP) emitted from tire contributes more than 50% in Denmark (Cinaralp 2017; Lassen et al. (2015), Sommer et al. 2018; Bertling et al. 2018). Scientific studies report the size of microplastic particles ranges in micron from 10 to 80 μm. Wear out microplastic particles emitted from tire gets transported to surface water through various medium. Therefore, the wear of tire is an alarm to the raising concern about the environment. Wagner and Lambert (2018) fetched economic data about the generation of tire wear which was near about 1.3 million tons per year on the roads of Europe. Wear of tire and emission of MPP are mostly influenced by the surface conditions of the road, relative humidity, operation of a vehicle, environment temperature conditions, and properties of tire (Sundt et al. 2014). Therefore, exploring the tribological properties of tire is one of the important issues to solve the governing concern against the environment.

4.3   Engine Condition Monitoring

Wear-related issues occurring in the case of IC engines are high. Technological improvement and advancement of engine parts contribute better reliability life to the engine parts. A governing trend of industry 4.0 allows physical assessment of the engine parts. It also holds better controlling capacity in enriching the reliability of the engine components. This, therefore, provides a promising goal to effectively analyze the variant data from the complexity of multivariable. Thus, an advance in IC engine requires condition monitoring for ensuring better output of power performance. In the gearbox transmission system, about 80% of fault is detected from a system of machinery transmission parts and 10% from a system of rotating machinery parts (Wagner and Lambert 2018). In identifying the issues of fault detection, some of the best approaches have been made to examine faults in decoupling, proper lubrication, misalignment, fluctuation of load, improper gear design, and poor effect of cooling.

There are few literatures available to examine the condition monitoring of the IC engine components for the improvement engine performance. Wakiru et al. (Verucchi et al. 2016) reviewed studies carried on liquid condition monitoring (LCM) and summarized the role of wear debris, carried by lubricating oil, over the fault diagnosis by considering different levels of situation. S. Delvecchio et al. (Saucedo-Dorantes et al. 2017) expressed the views for fault diagnosis of IC engine components. However, timely maintenance of engine components after examining condition monitoring is required for every engine component. Moreover, the study of online visual ferrography (OLVF) technology has been used widely for the diesel engine which contributes on health condition assessment by analyzing through ferrographic image, particle cover area, exhaust temperature, cylinder blow-by etc. (Cao et al. 2018).

Therefore, condition monitoring has become an alternative solution for the problems of wear. In general, friction affects the mechanical surface and its properties, thus accelerating the degradation of the component's life. Methodologies followed for monitoring the faults and diagnosing the problems using artificial intelligence. The most commonly occurring problem due to surface damage, pitting, and chipping occurring in the gearbox can be easily simplified using filters like adaptive wavelets by applying it to the vibration signals. Meanwhile, load torque signature analysis (LTSA) presents a vulnerable solution to diagnose misalignment, mass imbalance, and gears wear (Verucchi et al. 2016). However, there are some limitations to monitoring the gearbox condition and is affected through sensor location and surrounding noise. Certainly, these problem associates confusion in measuring faults. As gear operation includes temperature rise, another technique that proves beneficial in conditioning monitoring is infrared thermography. Using this technique, hot-spot can be easily accessible with an increase in temperature (Saucedo-Dorantes et al. 2017). Although the initial cost of application of this type of technology is high. However, it has great significance in automobile industry.

4.4   Summary

The development in the field of Automotive Tribology is crucial to improve the fuel efficiency of the engine, powertrain durability and the performance of the vehicle. Wear variation is not uniform. Different mathematical models were used for the measurement of wear. Abrasive wear has excessively influence the amount of wear in engine. The wear on the piston ring has been found to be top of the asymmetric crowning when the system is functioning under boundary lubrication. Piston ring wear is comparatively high as compared with the other components of SI engine parts. There are serious problems related to energy consumption and the emission of hazardous gases to the environment in the industrial sector. Tribology not only controls the economic growth but also influences the life of mechanical components when the term is used in a context of reliability and durability of mechanical components. Although, the word tribology is new but it is not necessarily new to the environment of economic growth as it is affecting million-dollars of the world economy. Nowadays, many mechanical components are designed based on tribological concerns. To underneath the situation of economic growth, while dealing with tribology, researchers are finding interest to overtake the wear and tear damages as observed under tribology. With the advancement of modern engines to control and reduce mechanical losses, some developments were also undertaken on lube oils. However, the growing concern of tribology cannot be necessarily meet but some achievements have been made to improve the life of mechanical components. This study concludes that the performance of engine is directly dependent on the wear and friction of the engine components.

References

Allianz Versicherungs AG (1978) Handbook of loss prevention. Springer-Verlag, Berlin
Becker EP (2004) Trends in tribological materials and engine technology. Tribol Int 37(7):569–575
Becker WT, Shipley RJ (2002) Failure analysis and prevention. ASM Handbook International. vol. 11, USA
Bertling J, Bertling R, Hamann L (2018) Kunststoffe in der Umwelt. Mikro- und Makroplastik. Ursachen, Mengen, Umweltschicksale, Wirkungen, Lösungsansätze, Empfehlungen. Kurzfassung der Konsortialstudie. Fraunhofer-Institut für Umwelt Oberhausen
Bhusan B (2013) Introduction to tribology, 2nd edn. John Wiley & Sons, New york
Bhushan B (2000) Principles of Tribology. Modern Tribology Handbook, Vol 1, CRC Press, Florida
Branagan LA (2015) Survey of damage investigation of babbitted industrial bearings. Lubricants 3:91–112
Bronshteyn L, Kreiner J (1999) Energy efficiency of industrial oils. ASLE Trans 42(4):771–776
Cao W, Dong G, Xie Y, Peng Z (2018) Prediction of wear trend of engines via on-line wear debris monitoring. Tribol Int 120:510–519
Cinaralp F (2017) ETRMA statistics report no.9. Technical report, European Tyre and Rubber Industry
Diab Y, Ville F, Velex P (2006) Prediction of power losses due to tooth friction in gears. Tribol Trans 49(2):260–270

Diez-Ibarbia A, Fernandez-del-Rincon A, de-Juan A, Iglesias M, Garcia P, Viadero F (2018) Frictional power losses on spur gears with tip reliefs: the friction coefficient role. Mech Mach Theory 121:15–27

Durak E, Adatepe H, Biyikliog lu A (2008) Experimental study of the effect of additive on the tribological properties journal bearing under running-in and start-up or shut-down stages. Ind Lubr Tribol 60:138–146

Fietkau P, Bertsche B (2013) Influence of tribological and geometrical parameters on lubrication conditions and noise of gear transmissions. Mech Mach Theory 69(8):303–320

Friedrich C, Berg G, Broszeit E, Rick F, Holland J (1997) PVD Cr N coatings for tribological application on piston rings. Surf Coat Technol 97(1/3):661–668. https://doi.org/10.1016/S0257-8972(97)00335-6

Green DA, Lewis R (2008) The effects of soot-contaminated engine oil on wear and friction: a review. Proc I Mech E Part D J Automob Eng 222(9):1669–1689. https://doi.org/10.1243/09544070JAUTO468

Hamid B, Bou-Said B, Lahmar M (2017) The effect solid particle lubricant contamination on the dynamic behavior of compliant journal bearings. Lubr Sci 29:425–439

Hanada K, Murakami Y, Shoji Y, Alhara H, Hirose A (1994) Development of a valve train wear test procedure for gasoline engine oil. Nissan Motor Co. Ltd. International Congress & Exposition, Detroit, Michigan. SAE International. Feb. 28–March 3

Höhn B, Michaellis K (2001) Influence of lubricant aging on gear performance. Materiały 2:363

Höhn BR, Michaelis K, Hinterstoißer M (2009) Optimization of gearbox efficiency. Goriv Maz 48(4):462

Holmberg K, Erdemir A (2017) Influence of tribology on global energy consumption, costs and emissions. Friction 5:263–284. https://doi.org/10.1007/s40544-017-0183-5

Holmberg K, Andersson P, Erdemir A (2012) Global energy consumption due to friction in passenger cars. Tribol Int 47:221–234

Holmberg K, Siilasto R, Laitinen T, Andersson P, Jäsberg A (2013) Global energy consumption due to friction in paper machines. Tribol Int 62:58–77

Holmberg K, Andersson P, Nylund O, Mäkelä K (2014) Global energy consumption due to friction in trucks and buses. Tribol Int 78:94–114

Holmberg K, Kivikytö-Reponen P, Härkisaari P, Valtonen K, Erdemir A (2017) Global energy consumption due to friction and wear in the mining industry. Tribol Int 115:116–139

Jost HP (1966) Lubrication (Tribology)-A report on the present position and industry's needs. Department of Education and Science, H.M. Stationary Office, London, UK

Kaiyue LI, Chen G, Liu D (2016) Study of the influence of lubrication parameters on gear lubrication properties and efficiency. Ind Lubr Tribol 68(6):647–657

Kerr I, Priest M, Okamoto Y, Fujita M (2007) Friction and wear performance of newly developed automotive bearing materials under boundary and mixed lubrication regime. J Eng Tribol 221(3):321–331

Kolivand M, Li S, Kahraman A (2010) Prediction of mechanical gear mesh efficiency of hypoid gear pairs. Mech Mach Theory 45(11):1568–1582

Kopeliovich D (2016) Hydrodynamic journal bearing. http://www.substech.com/dokuwiki/doku.php?id=hydrodynamic_journal_bearing. Accessed 14 July 2021

Krantz T, Kahraman A (2005) An experimental investigation of the influence of the lubricant viscosity and additives on gear wear. Tribol Trans 21(1):138–148

Lassen C, Foss Hansen S, Magnusson K, Norén F, Bloch Hartmann NI, Rehne Jensen P (2015) Microplastics—Occurrence, Effects and Sources of Releases to the Environment in Denmark. Environmental Project No. 1793. Danish Environmental Protection Agency, Strandgade 29, 1401 Copenhagen, DK

Li Y, Li Z, Zhu Y, Li B, Xiong W, Huang Y (2019) Thermal infrared small ship detection in sea clutter based on morphological reconstruction and multi-feature analysis. Appl Sci 9:3786. https://doi.org/10.3390/app9183786

Ligier JL, Noel B (2015) Friction reduction and reliability for engines bearings. Lubricants 3:569–596

MAHLE (2021) https://www.mahle-aftermarket.com/media/local-media-northamerica/pdfs-&-thumbnails/catalogs-and-literature/engine-bearings/ceb-21114-engine-bearing-failures-brochure.pdf. Accessed 05 July 2021

Marques P, Fernandes C, Martins R, Seabra J (2014) Efficiency of a gearbox lubricated with wind turbine gear oils. Tribol Int 71:7–16

Martins R, Cardoso N, Seabra J (2008) Gear power loss performance of biodegradable low-toxicity ester-based oils. Proc Inst Mech Eng J Eng Tribol 222(3):431–440

Moughon L (2006) Effects of piston design and lubricant selection on reciprocating engine friction. M.S. Thesis. Department of Mechanical Engineering, Massachusetts Institute of Technology, Cambridge, MA

Nieuwland P, Droste T (2001) Automatic transmission hydraulic system cleanliness—the effects of operating conditions, measurement techniques and high-efficiency filters. SAE Technical Paper. 01:0867

Olver A (2005) The mechanism of rolling contact fatigue: an update. Proc Inst Mech Eng J Eng Tribol 219(5):313–330

Rameshkumar T, Rajendran I (2012) Mechanical and tribological properties on Al-Sn-Si alloy-based plain bearing material. Tribol Trans 56(2):268–274

Saucedo-Dorantes JJ, Delgado-Prieto M, Osornio-Rios RA, Romero-Troncoso RJ (2017) Diagnosis methodology for identifying gearbox wear based on statistical time feature reduction. Proc Inst Mech Eng Part C J Mech Eng Sci 232(15):2711–2722

Scibbe HW, Townsend DP, Aron PR (1984) Effect of lubricant extreme-pressure additives on surface fatigue life of AISI 9310 spur gears. NASA Lewis Research Center, Cleveland, Ohio, USA

Shannon J, Bell JC, Cadu J (1996) The effect of engine operating temperature on valve train wear: mechanistic understanding through used oil analysis. J Eng Tribol Part J 210(2):145–152

Sommer F, Dietze V, Baum A, Sauer J, Gilge S, Maschowski C, Giere R (2018) Tire abrasion as a major source of microplastics in the environment. Aerosol Air Qual Res 18:2014–2028. https://doi.org/10.4209/aaqr.2018.03.0099

Stachowiak G, Batchelor A (2005) Engineering tribology. Elsevier Butterworth-Heinemann, Amsterdam

Sundt P, Schulze PE, Syversen F (2014) Sources of Microplastics-pollution to the Marine Environment. Norwegian Environment Agency (Miljødirektoaret)

Tamatam LR (2017) Tribological performance of difference crankshaft bearings in conjunction with textured shaft surfaces. M.S. Thesis, Department of Engineering Science and Mathematics, Luleå University of Technology

Taylor CM (1998) Automobile engine tribology-design considerations for efficiency and durability. Wear 221:1–8

Taylor BJ, Eyre TS (1979) A review of piston ring and cylinder liner materials. Tribol Int 12(2):79–89

Thorpe A, Harrison RM (2008) Sources and properties of non-exhaust particulate matter from road traffic: a review. Sci Total Environ 400(1–3):270–282

Tung SC, Gao H, Tung SC, G.H (2003) Tribological characteristics and surface interaction between piston ring coatings and a blend of energy conserving oils and ethanol fuels. Wear 255(7/12):1276–1285. https://doi.org/10.1016/S0043-1648(03)00240-0

Upadhyay R (2013) Microscopic technique to determine various wear modes of used engine. J Microsc Ultrastruct 1:111–114

Verucchi C, Bossio J, Bossio G, Acosta G (2016) Misalignment detection in induction motors with flexible coupling by means of estimated torque analysis and MCSA. Mech Syst Signal Process 80:570–581

Wagner M, Lambert S (2018) Freshwater microplastics: emerging environmental contaminants. Springer International Publishing, Cham

Williams J, Hyncica A (1992) Mechanisms of abrasive wear in lubricated contacts. Wear 152:57–74

Willn JE, Bret PS (1977) Piston ring scuffing during running-in-the influence of lubricants and materials. Proc I Mech Eng 191(1):241–256. https://doi.org/10.1243/PIME_PROC_1977_191_031_02

Wong VW, Tung SC (2016) Overview of automotive engine friction and reduction trends-Effects of Surface, material, and lubricant-additive technologies. Friction 4(1):1–28

Ye ZK, Zhang C, Wang YC (2004) An experimental investigation of piston skirt scuffing: a piston scuffing apparatus, experiments, and scuffing mechanism analyses. Wear 257(1):8–31

Yuan GC, Li ZJ, Lou YX, Zhang XM (2000) Study on crystallization and microstructure for new series of Al–Sn–Si alloys. Mater Sci Eng 280(1):108–115

Ziegltrum A, Lohner T, Stahl K (2017) TEHL simulation on the influence of lubricants on load-dependent gear losses. Tribol Int 113:252–261

Chapter 5
Wear of Wheels and Axle in Locomotive and Measures Taken by Indian Railway

Upendra Kumar, Rutvik Kasvekar, Sunil Kumar Sharma, and Ram Krishna Upadhyay

Abstract A rail wheel and axle is an integrated and essential part of a wheel-set that provides a better and safe operation of rail vehicles. It supports the overall weight of the wagon. It cannot be designed as a safe structure from failure as it has forces acting in many directions. Hence, it requires high reliability in terms of power/torque and different types of strength. Necessary attention on the wear resistance, thermal crack resistance, noise/vibration, and the characteristics and performance of the wagon are required. Maintenance plays a vital role in increasing the life of the wheel and axles. Hence, more suitable wheels and axle production strategies should be started at the earliest to resolve wear issues. Indian railway is working on the Atma Nirbhar Bharat scheme, where the production of these wheels and axles will be implemented in the coming years. This research is about the efforts made by the Indian Railways to indigenize wheels and axle production with minimum wear.

Keywords Wear · Wheels · Axles · Locomotive

5.1 Introduction

Rail wheel is an essential part of railways for movement and carrying different loads to support the overall wagon. Many technological developments have been made, and various studies have been conducted to improve the characteristics of wheels (Joshi 2021; Choudhari et al. 2018). Mainly, two approaches are followed to increase performance: design configuration and the other is material design. This work outlines the various important characteristics of wheels and introduces research and development on these characteristics. This work also discusses the implications of the current issue of the wheels. There are many types of wheels, but we have only discussed solid wheels because they are most widely used globally.

Axles are the twin part of the practical wheel and integrated part of wheeled vehicles. Axles have suspension, which helps transmit torque to the wheel and balance

U. Kumar · R. Kasvekar · S. K. Sharma · R. K. Upadhyay (✉)
National Rail and Transportation Institute, Vadodara, Gujarat 390004, India
e-mail: ram.upadhyay@nrti.edu.in

the wagon body on it. It also maintains the relative position between two wheels. However, the position and angle of the wheel's hub do not depend on the function of the suspension system. The axle also bears the weight of the wagon body along with the cargo weight in the wagon.

5.1.1 Wheel and Axle Problem

Wheels and axles are the essential components of every vehicle. The wheel plays an essential role in making a vehicle more efficient and comfortable. Railroad wheels and axles are the components of wheel-sets that must withstand the higher applied stresses, including impact loads and long-term loads. The operational reliability of the wheels largely determines the safety of the passengers and goods transported, as well as the mass and speed of the train (Choudhari et al. 2018). With a constant increase in the mass and speed of rolling stock, the load on the axle increases, and the reliability and life of the wheel pair must be increased.

One of the significant failures of Indian railways is the deformation of the wheel due to fatigue and stress-inducing in the wheel. Therefore, maintenance becomes an integral part of the integrated system, and it needs to be proper in order to minimize the defect of the wheels. The Indian Railways is the country's lifeline, so the transit should be safe and have minimum failure to have a smooth journey. From 2016, India started manufacturing and using LHB (Linke Hofmann Busch) coaches. LHB coaches are very smooth in operation and can run at high speed as it is very light in weight. As LHB coaches run at high speed, the braking system should work effectively to stop at the right time. Brake damages the wheel in a significantly higher degree of an order (Choudhari et al. 2018). This is a primary concern for Indian Railways as the maintenance of the wheel costs high.

British Rail research carried out a metallurgical survey in 1992 and found out 80% of the wheels were deformed because of the wheel's profile, so they reprofiled the wheel to protect them from thermal stresses, which increases the efficiency of the wheels. They also introduced a wheel-side protection system as a precautionary and preventive tool (Choudhari et al. 2018). Many other causes of wheel failure wear, tear, wheel slide, and tread braking. About 70% of the wheels are reprofiled due to rolling contact fatigue, which helped increase total wheel life, and research and development are going on in this field. A schematic of wheel terminology is presented in Fig. 5.1 (NSW Transport 2021).

5.1.2 Defect Observed on the Wheels

Most of the wheels are made by the technique of casting process, but some of them are made by the technique of forging of carbon steel further heat treated and eventually

Fig. 5.1 Terminology of rail wheel (NSW Transport 2021)
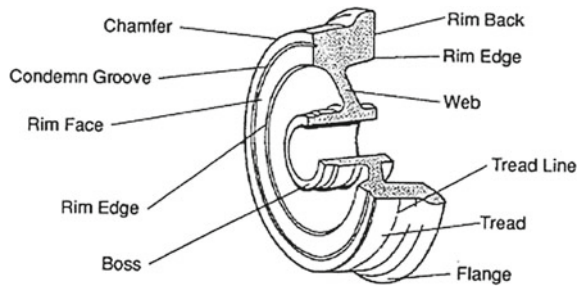
trimmed by machine to get the desired shape. Most of the defects are created during the manufacturing process and are classified into two groups:

- Inherent defects
- Service defects

Inherent Defects:

Manufacturing defects that occurred during the making, shaping, sizing, trimming, machining of low carbon steel result in improper microstructure, chemical composition, segregation, flake, pipe, harmful inclusion, etc. Due to high temperature, the casting process creates many defects like inclusion, blowhole, notch, flatness, porosity, etc. Defects like coarse grain structure arise during fabrication as a result of improper heat treatment.

Service Defects:

Wheel and axles defects occur during the operation/service life due to bad service conditions, leading to improper operation or failure. These kinds of defects are known as service defects.

5.2 Wear of Wheels

Removal of materials from the surface due to abrasion of the wheel on rail causes wear of the wheel. The life of the wheel largely depends on the wear, resistance to wear. Wear also occurs due to rolling contact fatigue (RCF). Wear occurs on the rail as well as on the wheel tread and flange (see Fig. 5.2a).

Fatigue:

The continued loading and unloading of load and forces on the wheel and axles cause fatigue failure (see Fig. 5.2b,c). It is also classified into two types: one is a surface failure, and the other is a subsurface failure. Defects like crack lead and crack head are types of surface fatigue failure, and shelling is a kind of subsurface fatigue failure.

Fig. 5.2 **a** Rolling contact fatigue wear in rail wheel, **b** sub-surface fatigue crack, **c** propagation of sub-surface fatigue crack, and **d** thin flange gauge (Transport 2021)

Hollow Wheel or Deep Flange:

Wear on the wheel tread while moving on the rail track reduces the diameter of the wheel, which gradually leads to an increase in the height of the wheel flange. An increase in the height of the wheel flange starts damaging the points, crossings, fish plates, distance blocks, fishplate bolts, etc. During fatigue wear, cracks are angled across the whole wheel tread area (Fig. 5.2a).

Thin Flange:

Removal of material from the wheel's flange leads to a decrease in the flange's width (see Fig. 5.2d). There should be adequate strength in the flange for maintaining a smooth run of the train because it is subjected to side thrust while turning the wagon. As the flange becomes thin, it gets weak, and there are some cases when it could not sustain the side thrust, which is very dangerous for any vehicle and may cause accidents.

Thin Wheel:

Continuous wearing, tearing, and material removal of the wheel make the wheel thin. Thin wheels are very dangerous and unsafe because further hammering of the wheel on the rail track at joints makes the wheel thinner and may lead to cracking and breakages of the wheel.

Sharp Flange:

The tip of the flange of the wheel has a radial profile that traces the rail track profile. But with time, due to material wear and tear, the wheel's flange gets sharp and loses its radial profile. The sharp profile is hazardous for moving a wagon at the crossing when a train switches its path from one track to another, which may lead to a significant accident.

Wheel Flat:

Skidding off the wheel on the rail track after the brake is applied for some distance causes flatness of the wheel surface. Excessive flatness causes improper rolling of the wheel on the track, which results in unpleasant noise and discomfort to the passengers. The flat wheel also causes breakage, skidding, and derailment of the train. Also, it causes a false flange on the tread.

Shattered Rim:

Removal of a big part of the material from the corner of the wheel due to thermal stress or localized load causes shattered rim.

Spread Rim:

It is an internal defect that is spread only for a short distance where the rim widens out on the front face of the wheel, which usually happens due to flattening of the tread and may lead to crack propagation on the wheel's surface.

Shelled Tread:

Shelling occurs when localized thermal stress on the face of the wheel due to breakage or wear out of material forms to notch on the surface around the wheel's rim. They look like minor skid marks or a spot notch.

Thermal Cracks:

Crack formation and propagation (Fig. 5.3) around the rim on the wheel's surface due to intense heating and cooling of the wheel induced by severe brake binding creates thermal stress, leading to thermal crack on the wheel's surface.

Heat checks:

Heat checks are a special kind of thermal crack which are not so deep and are not clearly visible and are formed adjacent to the braking surface. These are usually denser than the thermal cracks.
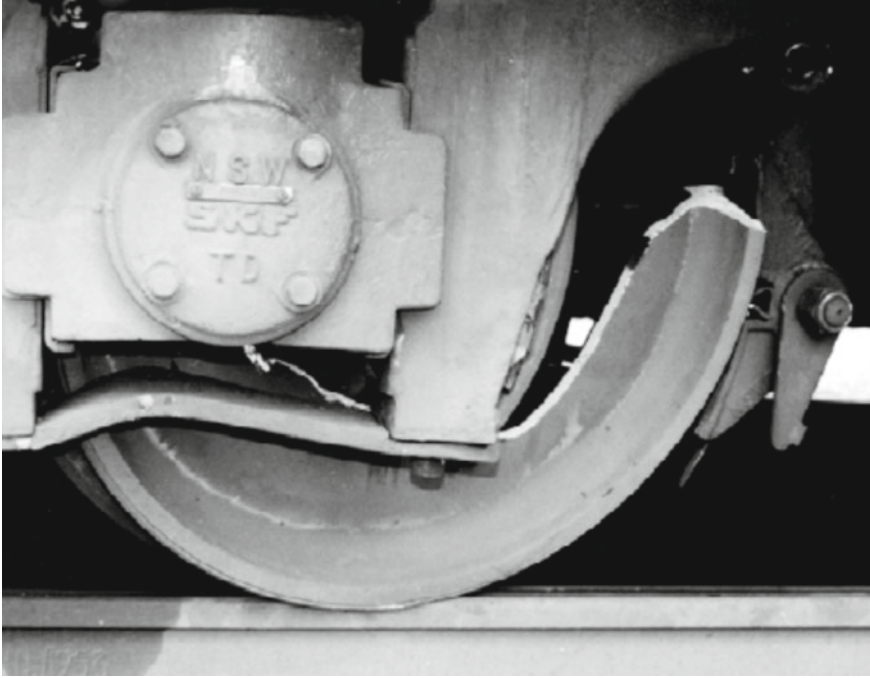
Fig. 5.3 Fracture of rail-wheel due to thermal crack (NSW Transport 2021)

Sliding defect:

During sliding of the wheel on the rail track, the uneven force acting on the wheel, like retarding force by the wheel on the brake, causes a sliding defect on the wheel surface.

Wheel spalling defect:

After the long service of the wheel spalling defect (Fig. 5.4a,b), many crack networks that may be parallel or perpendicular to the surface occur on the side of the wheel in the form of minor visible flaws/patches.

5.3 Defect Observed on the Axles

Most of the defects on the axles arise during the manufacturing of the axles and service of the axles due to service conditions, which they are subjected to stress. Defects on axles form during:

- Heat-treatment operation
- Machining operation

Fig. 5.4 a, **b** Spalling of
rail-wheel (Transport 2021)

(a)

(b)
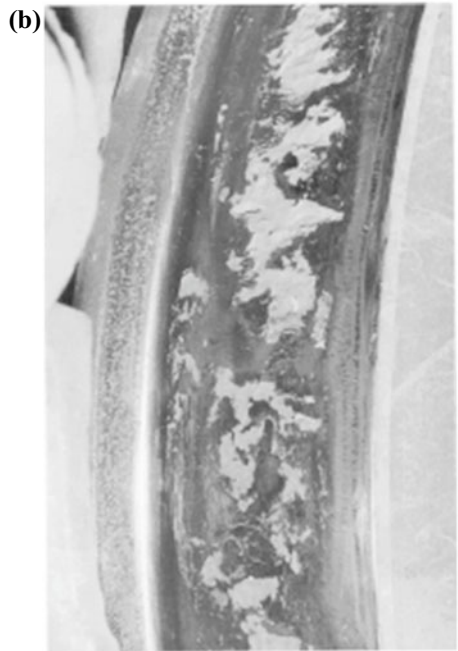
- Repair practice
- Assembly operation
- Steel-making and shaping operation
- Maintenance practice and
- Corrosion.

Major defects in the axle are segregation, cracks, laps, seams, piping, slag inclusions, etc., mainly occurs during the steel making process. There are many defects like overheated or burnt structure, decarburization, surface defects, non-uniform microstructure, etc. are occur during the heat treatment process. These all defects can be minimized by proper machining and a controlled heat treatment process. If heat treatment is not carried out properly, it may result in a rough surface finish like turning marks, tool marks, insufficient fillet radii, etc. Some defect also occurs during welding of axles due to improper mixture of oxygen and acetylene flame, which also reduces the life of the axles.

We can maintain the axle boxes properly by lubricating them and also by tightening torque, tightening force, and ingress of foreign matter. They are much prone to corrosion as axle boxes are exposed to air. The formation of pits on the axles creates stress concentration areas, leading to the failure of the axles. Sections like a journal, inner wheel seat, transition zones, or fillets are the most vulnerable locations for fracture axle sets. Short fillet radii, tool marks can cause notches on the axles, leading to fillet failure in the inner ring edges.

5.3.1 The Problem Associated with Axles

Increased axle loads and train speeds over the last year have also allowed increased wheel-rail contact force. In addition, a study has been carried out to optimize the wheel-rail configuration in order to save money and increase performance. These patterns have shifted the primary cause of tyre rim damage away from wear and toward fatigue. In contrast to the gradual degradation caused by wear, fatigue results in wheel cracks or material failure on the tread surface. These failures may result in rail injury, train suspension damage, and, in severe cases, train derailment. Railroad wheel fatigue, also known as rolling contact fatigue, occurs due to the rolling motion's repetitive contact tension. Hence, it is necessary to examine various failure processes in detail, including split rims, longitudinal brake rims, and thermal cracking. Shattered rim failures are triggered by extensive subsurface fractures that extend almost parallel to the tyre tread surface. Shattered rim failures are triggered by extensive subsurface fractures that extend almost parallel to the tyre tread surface. Thermal cracking typically results in removing a section of the wheel tread, while a broken rim compromises the wheel's integrity, making it more dangerous. The objective of the fundamental analysis is to investigate the spread of subsurface cracks (shattered rim). The majority of current rolling contact fatigue models use a more straightforward method for stress estimation, such as a Hertz analytical solution or a simplified finite

element analysis with applied Hertz contact strain. Due to its complicated configuration of the wheel/rail touch field, a 3D finite element method is more appropriate for measuring the stress response of mechanical components.

A railway wheel-set serves many critical roles by bearing the train's weight, transmitting its momentum and braking powers to the tracks, and guiding the vehicle on the track. In these conditions, it is clear that wheel-set reliability is a required field. A wheel-set breakdown during service may have severe social and economic consequences, and in the worst-case situation, it may result in serious structural loss and even death. Additionally, wheel loss can have a detrimental effect on other vehicle components (e.g., suspension) and the track (e.g., rail).

Between April 2018 and January 2019, the Indian Railways experienced a high number of infrastructure accidents, prompting concerns about the national transporter's safety strategy. The accidents are classified as 'rail fracture,' 'train parting, "signal and weld breakdown,' and so on. Additionally, 2,313 instances of overhead electric (OHE) system failure occurred, while 97,520 instances of signal system failure occurred. The term 'coach detachment' was reported 1,302 times in the results. There were 2,059 incidents of wagon detachment and 643 instances of 'train parting' in the area, resulting in disrupted regional railway operations. There were 3,001 rail fractures and 1,633 weld faults recorded up to January 2019, comprising 4,634 injuries. For reference, the fiscal year 2018 had a total of 4,369 rail and weld fractures. In the fiscal year 2017, 3,546 such occasions were registered.

Today, about 45–50 million railway wheels are in use worldwide. Allowing for a one-in-1000 annual failure rate will result in 45,000–50,000 failed wheels each year. It is self-evident that if the term 'failure' applies to a total fracturing of the wheel rendering the train inoperable, railways are not an effective mode of transportation. In fact, the majority of wheel fatigue-related failures are less 'dramatic' in nature. Cracks are typically mitigated until they become wide enough to trigger catastrophic failures. Nonetheless, wheel fatigue may have significant economic and organizational effectiveness. Additionally, the fact that wheel fatigue failures appear to occur in epidemics, creating significant economic and organizational disruptions, contributes to this. Without countermeasures, wheel fatigue problems are likely to worsen as rail speeds, and axle loads rise, as does train fleet use. Due to the enormous amount of operating wheels and axles and the shrinking margins for operational failures, there is a tremendous opportunity for cost reduction by better material fatigue control. Additionally, marginal cost reductions associated with routine maintenance extended fatigue life, and improved wheel and axle reliability add to significant cost savings. As mentioned previously, injuries involving wheel or axle fractures are uncommon. Although tragic incidents are rare, they are often heavily reported by the media, which may lead passengers to abandon rail travel. This has a significant negative impact on the company, as a decline in rail transportation, whether due to questionable protection, decreased operating efficiency, or decreased economic viability, attracts passengers and freight to automobiles, trucks, and airlines. These are substandard modes of transportation in terms of socioeconomics, the atmosphere, and protection. From an operating standpoint, it is critical to comprehend and apply information about wheel and axle fatigue. However, the topic is often fascinating

from a scientific standpoint. Throughout history, fatigue study and railroads have been inextricably related. Railways incorporated complex forces of ample magnitude and length to induce fatigue failures. In the 1850s, the first formal analysis of material fatigue was conducted on railway axles. Since then, considerable expertise has been obtained, but fatigue in general, and fatigue of railway wheels and axles in particular, remains an unsolved issue.

The wear and tear on wheels and axles significantly affect the cost and performance of railway transportation networks. Since the inception of railways, wheel and axle profiles have been motivated by the need to fix strength and wear issues and ensure ride protection and efficiency. Excessive profile changes must be restored by grinding the wheel to its initial profile. A wheel may only be reprofiled a finite number of times until the rim's height is decreased to an unsuitable value for the wheel's mechanical resistance. When this cap is hit, it is necessary to replace the wheel. Since wheel reprofiles and repairs have a substantial impact on maintenance costs, numerous studies have been undertaken to address this problem. The word 'wheel wear' is commonly used to refer to any harm to the rolling surface of a railway wheel that results in material loss. This may be caused by adhesive or abrasive wear, rolling touch fatigue (RCF), or (to a lesser extent) substrate relocation caused by plastic deformation.

Normal railway wheel wear occurs due to the wheel's frictional forces being exchanged with the track. Thus, vehicle operating conditions involving high frictional forces on the tyre, such as traction, accelerating, and curve negotiating, are especially applicable to regular wear creation. When in traction and braking, longitudinal tractive braking forces cause wear, which appears to accumulate in the center of the tyre tread. Wear forming during curve negotiation is a dynamic mechanism that includes both longitudinal frictional forces produced by the gap in rolling radius between the internal and external wheels and transversal frictional forces produced by the wheel-set traveling along the curve direction with an angle of attack greater than zero in the event of a strong wheel assembly. As a result of this dynamic wheel-rail touch state, the wheel profile exhibits two distinct wear regions: one on the thread and another on the flange. The rate of wear in these two areas is directly related to various variables, including the vehicle's configuration, the condition of the touching surfaces, and the service profile. Several techniques are reported to identify rail wheel wear, such as machining learning and using ultrasonics (Krummenacher et al. 2018; Mudgal et al. 2014).

5.4   Possible Solution Adopted by Other Country

Through the usage of modeling techniques, including computer simulation, the method for designing the wheel structure has also been enhanced. Additionally, the wheel's durability has been dramatically increased by the advancement of hot rolling technologies for producing solid wheels. The wheel technology has continuously been researched and innovated by countries like Japan, the USA, and Europe.

However, their inventions are mostly based on commuter cars in Europe and Japan, including high-speed automobiles. On the other side, there is a disparity in the way the United States of America's expectations are thought. Since the turn of the twentieth century, EN Standards for wheels and axles have been developed in Europe one after the other. They are set for uniform implementation around the E.U. Their foundation principles are UIC (International Union of Railways) standards; however, some new requirements were introduced during the conversion to EN norms. A new classification of Categories 1 and 2 was defined for a typical case for high-speed and conventional-speed wheels.

The wear trait of the tread has a direct impact on the wheel's life; as such, it is a critical economic feature, namely repair costs. The main factor impacting wear characteristics is carbon content. The greater the percentage of carbon, the heavier it is. However, since increased carbon content appears to increase thermal risk, international guidelines for wheel materials often span a number of steel grades ranging from low to high carbon content. The carbon content and hardness of each steel grade as defined by the Association of American Railroads (AAR) Standard in the United States of America, Japanese Industrial Standards (JIS) and the EN Standard in Europe are shown in Table 5.1 (Okagata 2013). By contrast, the Japanese specification for wheel material requires only one steel classification with a carbon content of 0.60 percent or greater, as shown in the Fig. 5.5. As listed below in the table, there is a historical context. They came to an unlikely discovery after almost seven years of inquiry. Increased carbon content in a wheel decreases wheel and rail wear.

The outcome of wear percentage due to different combinations shown in Fig. 5.5 (Okagata 2013). For each mix, the wheel material was chosen from a range of three carbon content levels, and the rail material was chosen from a range of three carbon content levels. The following explanation explains how this decision was reached.

Table 5.1 Different steel grades specification by EN, AAR and JIS

Region	Specification	Steel grade		Carbon content (%)	Hardness HB
Europe	EN 13,262	ER6		$\leq$0.48	234–270 *
		ER7		$\leq$0.52	247–282 *
		ER8		$\leq$0.56	258–296 *
		ER9		$\leq$0.60	300–350 *
North America	AAR M-107/ M-208	Class L		$\leq$0.47	197–277
		Class A		0.47–0.57	255–321
		Class B		0.57–0.67	302–341
		Class C		0.67–0.77	321–363
		Class D			341–415
Japan	JIS E 5402–1	SSW	QS	0.60–0.75	246–307
			QR		311–363
			QRH		295–347

(* Equivalent hardness according to specified tensile strength) (Okagata 2013)

Fig. 5.5 Rail and wheel abrasion tests by miniature vehicle (Okagata 2013)
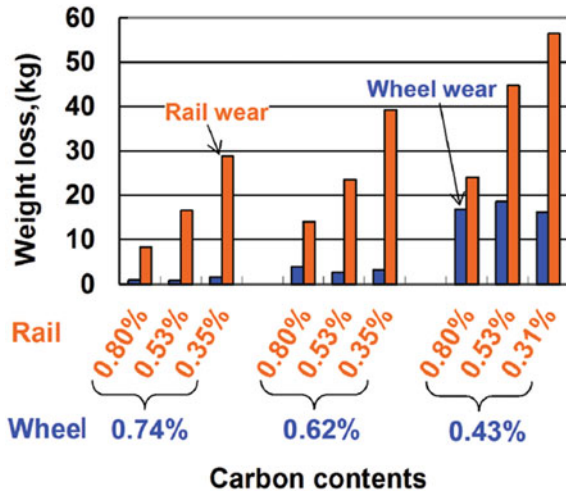
Due to the fact that the fine particles extracted from the wheel or rail surface act as an abrasive material between the tread and rail, they accelerate wheel and rail wear. This ensures that less wear on a wheel decreases the amount of abrasive material on the track, which reduces rail wear. It was concluded that increasing the carbon content of a wheel would never reduce rail life but rather boosts.

5.5 Wheel and Axle Problem in Indian Railways

Indian Railways are the most cost-effective and convenient form of long-distance and regional passenger means of transport and have contributed significantly to the growth and development of industries. Due to the growth of the railway network in Mumbai, Kolkata, and Jharkhand, their local industry like the textile industry, jute industry, and mining industry has been growing exponentially. These growths can be seen in other parts of the country. Via their railway network, railways assist in supplying raw materials and other services to these manufacturing sites and finished products to the consumer. Agriculture, too, owes a great deal of its prosperity to railways. Nowadays, small farmers may even export their agricultural goods and offer them on the global market at profitable rates.

Additionally, Indian Railways contributes to closing the divide between cities and rural areas and has been instrumental in disseminating inventions and ideas. Railways are particularly well-suited for lengthy commutes and have an efficient means of national integration. Railways are critical in easing human misery in the event of extreme situations such as droughts, hurricanes, food shortages, and earthquakes. This is achieved by the transportation of vital equipment, relief, and emergency workers to affected areas in order to relieve hunger and malnutrition. Railways often

assist with dealing with man-made disasters such as social, political, rebellion, and religious disruptions. It enables the free flow of citizens, police, soldiers, and military machinery, among other things. Railways' critical role in defending the country's independence and sovereignty against foreign aggression has been demonstrated numerous times. Railways preserve the British heritage by connecting large ports to their hinterlands, thus contributing to the coastal areas' overall prosperity. The arrival of superfast trains and container services in a number of Indian cities has meant that men and goods can travel quickly and easily. Railways are particularly well-suited to long-haul transportation of bulky commodities such as coal and petroleum.

While Indian Railways have experienced impressive qualitative and quantitative advancements over the last few decades, this infrastructure continues to be troubled by various issues that demand urgent attention. Numerous accomplishments have been made, but still more remains to be accomplished. Several of the significant issues confronting Indian Railways are explained in the next section.

The wheel and the axle shaft are mounted in two ways:

1. Cold press-on.
2. Shrink fitting.

Usually, the production employs the cold press-on process, while maintenance suggests shrink fitting (Knothe and Stichel 2017). The Indian Railways previously used the IRS (Indian Railway Standard) wheel profile, as illustrated in Fig. 5.6 (The Investigation of Derailments 2021). However, Rail interaction with the IRS wheel profile resulted in the accelerated flange and root flange wear during the initial phases, prior to acquiring a wear-adopted/worn wheel profile. As a result of wheel fatigue, the worn wheel profile accrued during the operation was significantly reduced. Since then, the worn wheel profile has been adopted for modern wheels as well (Knothe and Stichel 2017).

When a wheel's profile deteriorates, it can hit dangerously low levels in the following situations:

- Thin flange
- Sharp flange
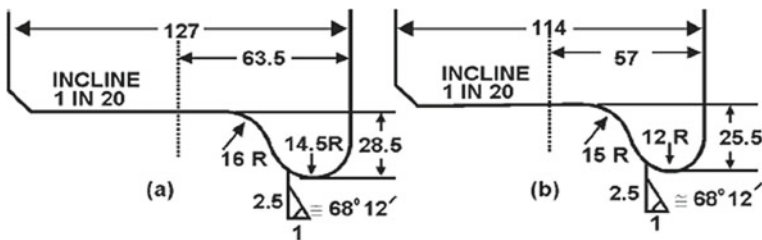- Worn root
- Deep flange

Fig. 5.6 IRS wheel profile: **a** broad gauge wheel and **b** meter gauge wheel (The Investigation of Derailments 2021)

- Hollow tyre or false flange
- Flat tyre

5.6   Stakeholders and Interests

The global market of rail wheels and axles is projected to rise by 1.2% in CAGR in the 2020–2025 projection. By 2025, the market would have grown to USD 3094.2 million, up from USD 2944.9 million in 2019. To maintain a competitive edge, stakeholders in the global Railway Vehicle Wheels and Axles industry rely on mergers and acquisitions and new product releases.

Stakeholder of Railway Vehicle Wheels Market:

Bochumer Verein Verkehrstechnik (BVV), Germany.

Rail Wheel Factory, India.

Rail wheel plant, India.

Lucchini R.S., Italy.

Nippon Steel and Sumitomo Metal Corporation (NSSMC), Japan.

Interpipe, Ukraine.

Amsted Rail, United States.

The interest of Stakeholder of Railway Wheels and Axles:

Organizational Framework:

An organizational framework is a mechanism that describes how such tasks are designed to accomplish an organization's objectives. These tasks can involve enforcing the rules, assigning duties, and delegating responsibilities.

Internal Business processes:

The internal process viewpoint concerns the processes that produce and supply the proposal for consumer value.

- Concern for process time measurement
- Impact of continuous improvement of the production process
- Effectiveness of preventive maintenance schedules
- Effectiveness of continuous feedback mechanism
- Quantum and impact of research in-house to improve the product

Cost planning:

The mechanism for managing and monitoring the spending of a company is called cost management.

- Elimination of non-value addition activities
- Effect of JIT in production costs reduction
- Impact of product improvement through a reduction in rework on costs
- Understanding of non-conformance costs of production by all staff

Management of suppliers:

Vendor management is a practice that enables companies to control costs, maximize service delivery, and mitigate risk throughout the course of their operation.

- Efforts at improvements in vendor relationships
- Encouragement to long term vendor relationships
- Effect of cumbersome procedures in building vendor relationships
- Vendor rating system efficacy
- Prequalified vendor's system efficacy
- Inventory management

Employee productivity:

Employee productivity is a measure that compares the amount of production generated by a project to the amount of time required to complete it.

- Learning & Growth perspective
- Motivational issues

5.7 Organizational Implications

An environmental management system (EMS) is a framework for coordinated, detailed, planned, and recorded management of the environmental initiatives of an organization. It encompasses the operational framework, personnel, and preparation necessary to formulate, enforce, and manage Environmental Impact Analysis policies. Alternatively, the environmental management framework means a system and database integrate systems and practices for personnel, reporting, summarizing, and communicating advanced environmental performances to internal and external partners of a company.

To use and recognize the environmental management system process, the International Organization for Standard (ISO) is generally used. Environmental Management Information Systems (EMIS) are digital information solutions monitored by organizations to handle environmental data as part of their overall environmental management system.

The EMS follow process depicts the steps involved in designing an environmental agenda, preparing the EMS, and then putting it into action. The framework depends upon analyzing and solution of the problem. This process is called Plan Do Check Act (PDCA). The framework is in development, and an environmental management

system (EMS) is a program of constant improvement through which a company usually reviews and revises its system.

This paradigm applies to a broad variety of organizations, ranging from industrial plants to retail sectors and government departments. They have specific standards because of their ability to enact growth, profitability, and cost savings. Reduced waste further improves an organization's personnel efficiency and sets ISO expectations for continuous growth and consumer success.

ISO 14001 lays down the environmental management system guidelines (EMS). It does not include criteria for environmental performance but rather lays out a framework for a business or agency to implement in order to establish an appropriate EMS. It is important to any business that wishes to increase resource utilization, minimize duplication, and reduce costs. Through implementing ISO 14001, managers, staff, and external partners will be assured that environmental impact is being evaluated and strengthened within the organization. ISO 14001 may also be integrated into other compliance tasks, assisting businesses in achieving their sustainable and economic objectives.

ISO 14001, along with the other ISO 14000 specifications, is a voluntary standard whose primary objective is to continuously enhance and assist organization efficiency and productivity while complying with any applicable legislation. Organizations are accountable for defining their priorities and success metrics. The norm assists them in achieving their objectives and goals and tracking and measuring their progress toward achieving these objectives and goals.

The norm applies to all enterprise levels, from the corporate level down to the product and service level; rather than relying on precise environmental sustainability metrics and targets, the standard emphasizes what a company would accomplish to achieve the objectives.

ISO 14001 is often referred to as a conventional management framework specification, which means that this applies to any enterprise that wishes to develop and handle its personnel more efficiently. This contains the following:

- Businesses ranging in size from a single location to massive multi-national conglomerates
- Moving from high-risk businesses to low-risk support organizations
- Sectors of manufacturing, processing, and operation, plus local governments
- All industrial industries, both public and private
- Makers of the original machinery and their retailers.

In India, cast steel wheels are manufactured using a pressure pouring manufacturing process (Sharma et al. 2018; Mandal and Ghosh 2018; Rail Wheel Factory 2021). It is produced in the Rail Wheel Factory, Bengaluru. The procedure starts with pedigree scrap, which consists of old used wheel-sets, axles, and other components that have been discarded by the Railways as inappropriate for usage. Melting this scrap steel takes place in an ultra-high frequency arc furnace. A spectrometer is used to determine the ideal chemistry of molten metal alloy. Finally, the wheels are poured into preheated and sprayed graphite molds. After a fixed specified period has passed, the mold is cut in half, and the risers and cast wheel are immediately separated.

The wheel is then put into a series of heat-treatment procedures. Cleaning, inspecting, peening, and different consistency and examination phases are performed on the wheel. There is no requirement of machining and trimming except precession boring of the central hole in which the axle needs to be fitted.

The axle production method is as follows. First Rail wheel factory buys vacuum steel blooms degassed. The blooms passed through the long forging process to achieve accuracy. In the revolving hearth furnace, billets are heated to forging temperature. Gas cutting is used to cut the forged steel to the desired length for the axles. The axles are then heat processed using a variety of different heat treatment methods, and their physical properties are checked before machining. To achieve greater accuracy and surface smoothness, the axles are machined on various machines. Rough spinning, end machining, finish turning, machining centers, grinding, and burnishing are also used in the smoothening process. Axle consistency is checked using internationally standardized measurements such as ultrasonic, magnetic particles, and others.

5.8   Atma Nirbhar Scheme of Indian Railways

The billet is utilized instead of the liquid form of material in the forged wheel production process. The material is shaped by compressive force in this procedure. Forging processes may be classified into two categories: hot and cold forging. The billet is preheated to red hot, and the material can be drop forged, which shapes the slugs through repetitive impact. After achieving the desired shape, it then goes through the cooling process. For the Indian Railways, the forged wheel should contain Carbon 0.56% max., Molybdenum 0.08% max., Phosphorus 0.020 max., Sulphur 0.015 max., and Vanadium between 0.05 to 0.015%. Steel should have hydrogen and oxygen concentration of no more than 2 and 15 parts per million, respectively. At the DSP factory, the wheels are manufactured by rolling blocks and pressing processes. After this process, wheels go through heat treatment and machining.

Forged axle manufacturing is done by using a series of heat treatments, forging, and machining processes. This process uses billet as a raw material. The billet is cut to the required dimension and heated. The compressive force of the repetitive hammer converts raw material into fitted dimensions. After the cooling process, the rough axles are subjected to heat treatment. Some properties include:

- Produce superior mechanical properties
- A more complex structure can forge

  Advantages of the forged technique.

- Production rates are very high.
- No oxidation occurs
- Can handle shock loading
- Hardness can increase by the heat treatment process

The disadvantage of the forged technique.

- Stronger tooling needed
- Residual stress may occur
- Less surface bonding due to density of structure molecular

SAIL-DSP is the only forged wheel and axle supplier for the Indian railways. The company can manufacture more than 70,000 forged wheels and axles. Steps were taken to indigenize this wheel through Steel Authority of India Limited (SAIL) Durgapur as well as Rashtriya Ispat Nigam Ltd. (RINL) Vishakhapatnam. Currently, Indian Railways import forged wheels and axles from China, but actions are taken to develop locally and assured off-take contract with RINL for 80,000 wheels per year. SAIL Durgapur has started manufacturing LHB wheels—400-odd wheels are on trial. SAIL Durgapur has a capacity for 60,000 forged wheels of all types (coaching max 30,000). A new axle forging plant is coming up at RWF and is expected to be operational by 2022. SAIL Durgapur has submitted a proposal to supply 12,000 axles per year from 2021–22 onwards.

Implementing this scheme will benefit Indian Railways in many ways. As Indian Railways are planning to incorporate more such assemblies, the import costs and reliance on China would only rise if the wheel and axel forging is not indigenized at a large scale. This could cost us millions of rupees in forex. Implementing this scheme will not only reduce the cost of imports but also reduce dependency on other countries. China has proven to be a non-reliable partner because of its Debt-trap diplomacy. Currently, India has received a lot of goodwill worldwide for its diligence in the supply of the CoVID-19 vaccines. India indigenizing such key technology could be a stepping stone for India's Africa outreach. India has the potential to capture the markets of Africa in this field. Since the cost of production in India is low, we can easily export to African countries. Exploiting the same would also yield economic benefits. If imports are curtailed, and factories are set up in India, it would boost the local economy and generate job opportunities. Finally, it will help India to become Atma-Nirbhar.

5.9   Summary and Conclusion

Vibration caused by faulty wheels and axles evokes a range of stimuli and reactions, from enjoyment or annoyance to disruption of tasks, damage, and disease. Individual responses to vibration can be estimated if the vibration is 'evaluated, "measured,' and 'assessed' using information gleaned from human response studies. The assessment of the vibration amplitude that results in while working, at recreation, or when traveling can be forecast using evaluation techniques that consider human susceptibility to various magnitudes, frequencies, paths, and durations of vibration, thus assisting in the improvement of wheel and axle structure. The evaluation methods allow complex simulations of the vehicles to be optimized before manufacturing prototypes. They assist in prototyping, research, and configuration, as well as vehicle manufacturing.

Where a driver or passenger's opinion is affected by variables other than the sensation being analyzed and analyzed, vibration evaluation may also produce imprecise forecasts of discomfort. Vibration analysis can identify variations that are not observable subjectively since testing and appraisal can detect minor changes more quickly than subjective assessment.

The goals of new technologies are to improve safety through intervention and improved asset reliability and, at the same time, reduces cost, as the most costlier technology may not be necessarily the safest in this upgrading world. In this direction, rail-wheel interaction has to be the thrust area to reduce wear and tear of both wheels and axles. More significant association of technologies, industries, R&D institutions, and the Department of Science & Technology (Ministry of HRD) will have to be ensured in developing new technology to improve the condition of rail wheels in the Indian Railway. The increased periodicity or reduced frequency of maintenance will be another priority area as it is essential in this self-reliant world.

For over seven decades, Bhartiya Rail's strategy has been to be self-sufficient or Atmanirbhar. Among Bhartiya Rail's numerous 'Atmanirbhar' projects is the 1950-founded Chittaranjan Locomotive Works, which began manufacturing steam locomotives before transitioning to electric locomotives in 1972. The backbone of both of these joint efforts has always been 'technology transition,' which allowed Railways to provide a technology foundation for upgrading in the coming years. The RDSO, the Indian Railways' research and development arm based in Lucknow, has played a significant role in this 2021 toward self-reliance. Before the series output begins, a completely computerized design and construction cell with state-of-the-art computer facilities performs strain gauge and squeeze tests on wheels and axles. Railways are now preparing to accelerate electrification, which would boost demand for better wheels and axles, necessitating a scaling-up of wheel and axle manufacturing. This is consistent with the Prime Minister's latest initiative to transform the country into a 'manufacturer to the world.

References

Choudhari SU, Badwaik RR, Kavre SR, Pardi MT, Barange PS, Achre SG (2018) Review on wheel defects in indian railways. Int J Res Appl Sci Eng Technol (IJRASET) 6(1):3013–3014
Joshi HC (2021) Hand book for C&W supervisors. https://ncr.indianrailways.gov.in. Accessed 13 July 2021
Knothe K, Stichel S (2017) Rail vehicle dynamics, 1st edn. Springer International Publishing, Heidelberg
Krummenacher G, Ong CS, Koller S, Kobayashi S (2018) Wheel defect detection with machine learning. IEEE Trans Intell Transp Syst 19(4):1176–1187
Mandal GK, Ghosh A (2018) Turnaround challenges in a manufacturing unit: a case study of wheel & axle plant of durgapur steel plant, SAIL, India. Int J Sci Eng Res 9(7):1873–1887
Mudgal LK, Sharma RK, Singh M (2014) Defects in wheels and axles and detection by Ust. Int J Eng Manag Res 4(2):176–180
NSW Transport (2021) Wheel defect manual, https://www.transport.nsw.gov.au/industry/asset-standards-authority/find-a-standard/wheel-defect-manual-12, Accessed 13 July 2021

Okagata G (2013) Design technologies for railway wheels and future prospects. Nippon Steel Sumitomo Metal Techn Report 105:26–33

Rail Wheel Factory (2021) Indian Railways, https://rwf.indianrailways.gov.in/view_section.jsp? lang=0&id=0,295,402,416. Accessed 13 July 2021

Sharma A, Murtaza MA, Murtaza MI (2018) Rail Road Wheel Requirements and Manufacturing Processes. Int J Mech Prod Eng Res Develop 8(2):93–102

The Investigation of Derailments, Indian Railways Institute of Civil Engineering. Accessed 13 July 2021

Part III
Recent Advances in Engine Tribology

Chapter 6
Boundary Lubrication Properties of Nanolubricants on the Steel Surface for Transportation Application

Ram Krishna Upadhyay and Rashmi Ranjan Sahoo

Abstract Nanolubricants immersed in a liquid medium can be vital for interacting surfaces to compensate driving forces for low friction and wear properties. These two properties are essential for transportation vehicles because their components continuously interact with another part of the vehicle, which causes material wear. Hence, a lubricant film is required to protect these surfaces. If the lubricant film thickness drops or becomes too small to provide full fluid separation of the two interacting surfaces, rough surface asperities start to contact one another. Asperities are initially coated with a film of oxide, such as iron oxide on iron or steel, aluminum oxide on aluminum. As surface asperities rub against each other, there develops a tendency of adhesion. As rubbing continues, the oxide film is removed from the surface, which in turn causes high friction and severe wear. Boundary lubrication occurs when the lubricating film thickness equalizes with a thickness of surface roughness, leading to pure asperities contact between the surfaces. The work delivers recent developments in lubrication concepts and those essential for nanolubrication properties. It intends to support surface properties at nano/micro scales for various nanometric scale thick lubrication film design. Different nanoparticle friction behavior is studied in water/oil medium as nanosuspensions and as an additive with grease matrix with a pin-on-disc (POD) tribometer. The particle suspension and its dispersion were used to control by the surfactants/dispersants. The friction data of suspensions indicated that the particle size is an essential parameter in controlling the friction and wear.

Keywords Nanolubricants · Friction · Wear · Grease

R. K. Upadhyay (✉)
National Rail and Transportation Institute, Vadodara, Gujarat 390004, India
e-mail: ram.upadhyay@nrti.edu.in

R. R. Sahoo
Environmental Engineering Group, CSIR-Central Mechanical Engineering Research Institute (CMERI), Durgapur, West Bengal 713209, India
e-mail: rr_sahoo@cmeri.res.in

6.1 Introduction

The boundary lubrication (BL, see Fig. 6.1) mechanism can be defined either by direct surface contact or liquid mediate contact, whose thickness is too small to separate the contacting surfaces (Guiggiani 2020; Sahoo et al. 2010; Sahoo and Biswas 2009, 2014; Upadhyay and Kumar 2019; Liu et al. 2020; Sahoo and Patnaik 2005). In this case, rough asperities of the surface will interact with each other as the lubrication film thickness drops. Numerous attempts have been made to make lubricant work more efficiently to decrease lubricant consumption and minimize wear and tear in machines. Multiple researchers have adopted particular methods like the addition of various colloids and polymers.

The significance of disulfides in enhancing the lubricity of lubricants cannot be ignored. Disulfides have been the focus of study by various researchers for improving the efficiency of lubricants. Joly-Pottuz et al. (2004) have carried out an experimental study on lamellar materials of metal disulfide, such as molybdenum disulfide (MoS_2), Tungsten disulfide (WS_2), Niobium disulfide (NbS_2) to investigate their lubrication catalyzing properties. One of the most efficient anti-friction additives currently used in automotive lubrication is the molybdenum dithiocarbamate (MoDtc) in solution in oil. With the increase in temperature and pressure, this molecule breaks up to form a thin film of MoS_2 on the surfaces to induce a lamellar mechanism of lubrication.

Any material with a particle size less than 100 nm (0.1 μm) is defined as a nanoparticle. Nanoparticles have a very high surface area to volume ratio. Thus when a material is made into nanoparticles, its reactivity increases. As the component scale moves from macro to micro to nano, the surface contact nature is dominated by surface forces, typically dwarfed by mechanical loading. In boundary lubrication regimes, the surfaces of the material are not perfectly smooth. The nanoparticle penetrates deeper inside the two asperities zone and provides better lubrication. However, in thick film lubrication, nanoparticles are not effective because the load is purely supported by a film, depending on a system's sliding velocity. Under low temperature and low load, lubricant viscosity enhances close to contacting surface, but lubrication mechanism effect is moderate. For low temperature and high load, friction can be minimized by adsorbed mono-molecular layers of surfactant. In the case of high temperature and medium load, adequate wear debris amorphous layer formation occurs by the reaction between additives and metal surface. However, as

Fig. 6.1 Boundary lubrication of two surfaces separated by the thin lubricating film
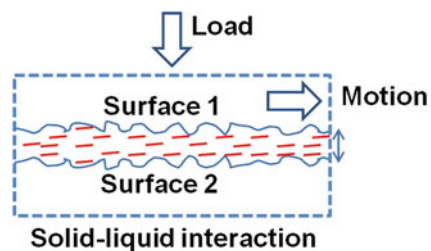
the load increases, the reaction between lubricant additives and metal surface occurs, forming inorganic material sacrificial films on the worn surface, preventing metal to metal contact and any other severe wear situations.

6.2 Materials and Experiment

The effect of the particle size of solid particles suspended in liquid or grease with or without dispersant on the friction and wear property of metal contacts have been discussed in this report. The nanoparticles are chosen based on their morphology and chemistry. Nanoparticle belongs to three different categories, i.e., Layered structure nanoparticle (molybdenum disulfide, boron nitride, kaolin), Oxides nanoparticle (boric acid) and Metallic nanoparticle (copper). The following methodology was followed to fulfill the research objectives.

First, the described nanoparticles were suspended in an oil medium with surfactant (SPAN 80), dispersant (PIBS), and without dispersant/surfactant, with the help of an ultrasonic processor. The resulting particle size was measured by a Nano-zeta sizer (Malvern Instruments). Further, the frictional behaviour of the suspensions between metal to metal (steel) contacts was investigated by Pin on Disk (POD, DUCOM Bangalore) Tribometer. The particle suspensions in paraffin oil (viscosity: 64 cSt) and water medium were prepared by an ultrasonicator (VCX-500, 20 kHz frequency). The prepared solution is then taken for the chemical and tribological related analysis.

Second, the above nanoparticles were suspended in a water medium with surfactant (Cetrimonium bromide (CTAB), Sodium dodecyl sulfate (SDS), Sodium hexametaphosphate (SHMP), and TWEEN 20) and without surfactant, with the help of an ultrasonic processor. The resulting particle size was measured by a Nano-zeta sizer (Malvern Instruments). Further, the frictional behaviour of the suspensions between metal to metal (steel) contacts was investigated by Pin on Disk Tribometer.

Third, the lithium stearate grease's lubricating behavior and the above particle effect on the lubrication behaviour when impregnated in the grease matrix were investigated. The grease sample's FTIR spectra were recorded on Perkin Elmer FT-IR Spectrum 100 using a spectrum reflectance accessory. At the last effect of particle size and concentration on the particle's lubrication behaviour, greases were studied. Frictional behaviour of the greases between metal to metal (steel) contacts were carried out by Pin on Disk Tribometer. Experimental conditions are shown in Table 6.1.

6.2.1 Pin-On-Disk Tribometer

Figure 6.2 shows the pin-on-disk machine (DUCOM, Bangalore) to test the tribological performance of prepared nanolubricants under sliding conditions. The operating conditions of the machine are listed in Table 6.2. Hardened stainless steel was used

Table 6.1 Nanomaterials and its composition used in tribological tests

Nano material	Oil suspension	Water suspension	Grease
MOLYBDENUM DISULFIDE	Heavy Oil Heavy Oil + Span 80 Heavy Oil + PIBS	Water + MoS_2 Water + CTAB Water + SDS Water + SHMP Water + TWEEN 20	Lab Grease + MoS_2 Lab Grease + (MoS_2 + PIBS)
BORIC ACID	Heavy Oil Heavy Oil + Span 80 Heavy Oil + PIBS	Soluble in Water	Lab Grease + Boric Acid
BORON NITRIDE	Heavy Oil Heavy Oil + Span 80 Heavy Oil + PIBS	Water + BN Water + CTAB Water + SDS Water + SHMP Water + TWEEN 20	Lab Grease + Boron Nitride
KAOLIN	Heavy Oil Heavy Oil + Span 80 Heavy Oil + PIBS	Water + kaolin Water + CTAB Water + SDS Water + SHMP Water + TWEEN 20	Lab Grease + Kaolin (2%) Lab Grease + Kaolin (10%) Lab Grease + (Kaolin + PIBS)
COPPER	Heavy Oil Heavy Oil + Span 80 Heavy Oil + PIBS	Water + Cu Water + CTAB Water + SDS Water + SHMP Water + TWEEN 20	Lab Grease + Copper Lab Grease + (Copper + PIBS)

for both pin and disk material. The chemical composition was C: 0.15 wt.%, Mn: 1 wt.%, P: 0.04 wt.%, S: 0.03 wt.%, Si: 1 wt.% silicon, and Cr: 11.5–13.5 wt.%. The Rockwell hardness of steel substrate material and pin was between 50 and 60 HRC.

6.2.2 Preparation of Grease

Plain/lab grease was prepared in a vessel using stearic acid (C18H36O2) and lithium hydroxide (LiOH.H_2O). At first instance, the ultrasonic bath was preheated up to 70 °C, stearic acid (C18H36O2) of 1 gm quantity was added in 10 ml of the mineral oil. Once the temperature is raised to 90 °C, the lithium hydroxide (LiOH.H_2O) mixture was added to the oil mixture. After a while, a soap was formed then the temperature of that vessel was raised from 70 °C to 180 °C for an hour to remove the extra water content from the grease. After the complete formation of grease, this was then stored in the container for tribological investigation. The same procedure was followed for the particle-based grease preparation. The particle size was controlled using PIBS as a dispersant in the oil suspension for controlling particle size.
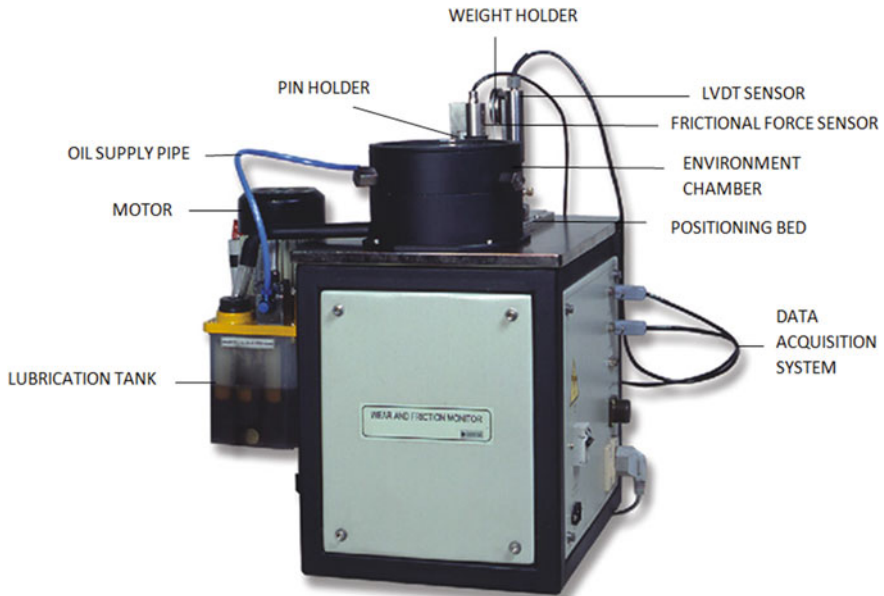
Fig. 6.2 Schematic of pin-on-disk machine

Table 6.2 Operating parameters for pin-on-disk (POD)

Serial No	Parameter	Specification
1	Wear Disc Diameter	Dia 100 mm, 6–8 mm thick
2	Pin Diameter, Length	4–8 mm, 20–30 mm long
3	Wear Track Dia	Min:50 mm and Max 80 mm
4	Disc Speed	100 RPM to 1000 RPM
5	Normal Load	Min:10 N and Max 100 N
6	Frictional Force	Max 100 N

6.3 Results and Discussions

6.3.1 Nanoparticles in an Oil Suspension

The principal parameters of nanoparticles are their shape, size, and the morphological sub-structure of the substance. Nanoparticles are presented as an aerosol (mostly solid or liquid phase in the air), a suspension (mostly solid in liquids), or an emulsion (two liquid phases). In the presence of chemical agents (surfactants/ dispersants),

the particle surface and interfacial properties can be modified. For nanoparticles suspended in liquids, particle charge can be stabilized by electrochemical processes at surfaces.

A lubricant was prepared by suspending the nanoparticles particles in the oil. The particle suspensions were prepared in oil medium without and with the presence of PIBS, span 80 as dispersants. With the ultrasonic processor's help, the particle suspensions in oil use dispersants to control their size and dispersion before the suspension is used as a lubricant in tribology.

Figures 6.3, 6.4, 6.5, 6.6 and 6.7 shows the particle size distribution of MoS_2, kaolin, BN, BA, and Cu in the presence of PIBS, span 80 and without dispersant, respectively. The addition of the dispersant to the suspension decreases the particle size with PIBS has a dominant effect compared to span 80.

Figure 6.8 shows the comparison of all the tested particle sizes with and without the dispersants. The fragmentation of the particles with the ultrasonic processor without the dispersants varies from particle to particle, where MoS_2 and BN, which are more hydrophobic than others, provide smaller particle sizes, which can be attributed to their different wetting behaviour and needs further investigation.
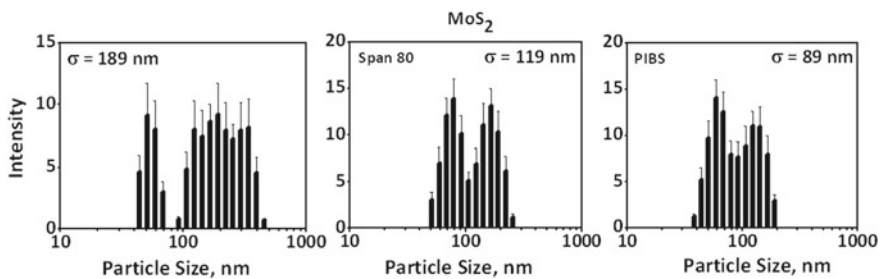

Fig. 6.3 Molybdenum disulfide (MoS_2) particle size distribution in oil suspension without dispersant and span 80 PIBS, using DLS
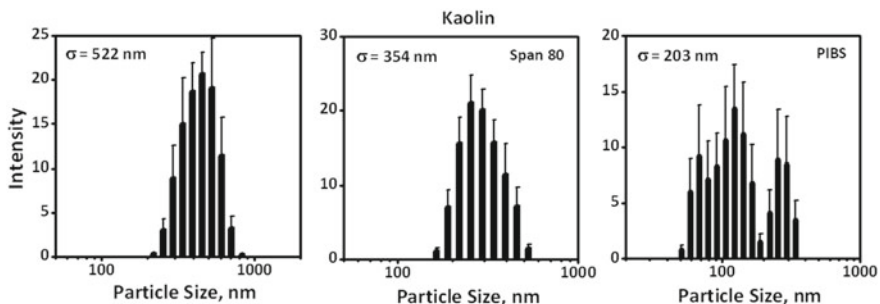

Fig. 6.4 Kaolin particle size distribution in oil suspension without dispersant and span 80 PIBS, using DLS
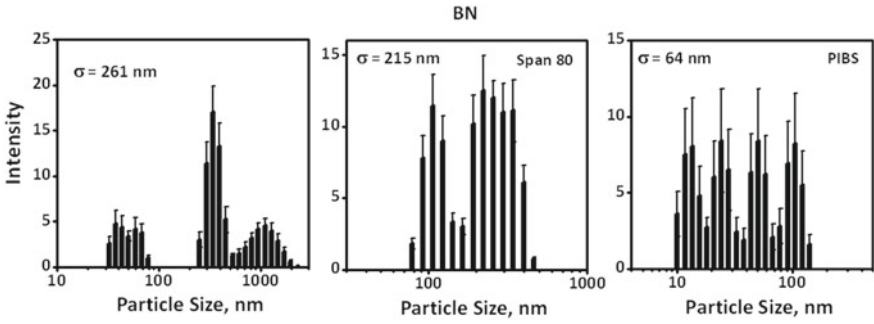
Fig. 6.5 Boron nitride (BN) particle size distribution in oil suspension without dispersant and span 80 PIBS, using DLS
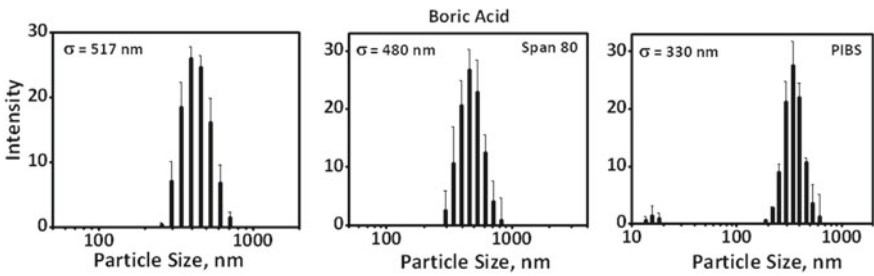

Fig. 6.6 Boric acid particle size distribution in oil suspension without dispersant and span 80 PIBS, using DLS
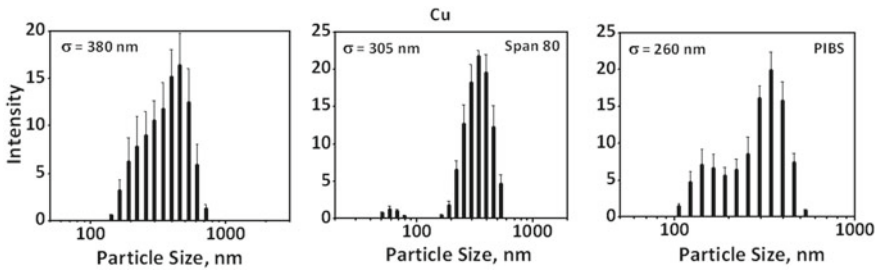
Fig. 6.7 Copper (Cu) particle size distribution in oil suspension without dispersant and span 80 PIBS, using DLS

The suspensions were sprayed on the steel substrate, and tribological tests were done using those particle suspensions as a lubricant. Figure 6.9 shows the effect of nanolubricants on the friction properties of steel-to-steel contact. The friction coefficient was primarily affected by the particle size. The decrease in the particle size decreases the friction coefficient and attains minimum value. Particle suspensions with PIBS as dispersant give the least coefficient of friction value when these five

Fig. 6.8 Particle size comparison in the oil medium

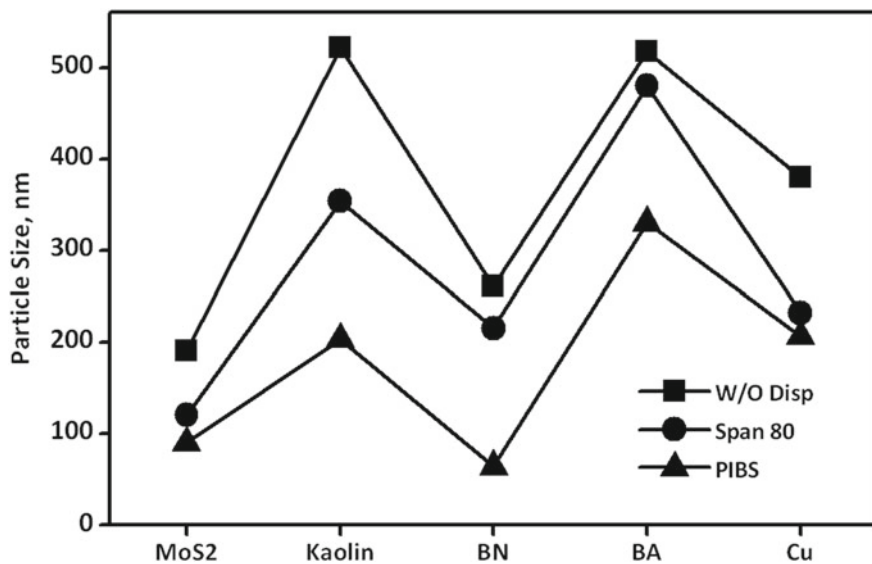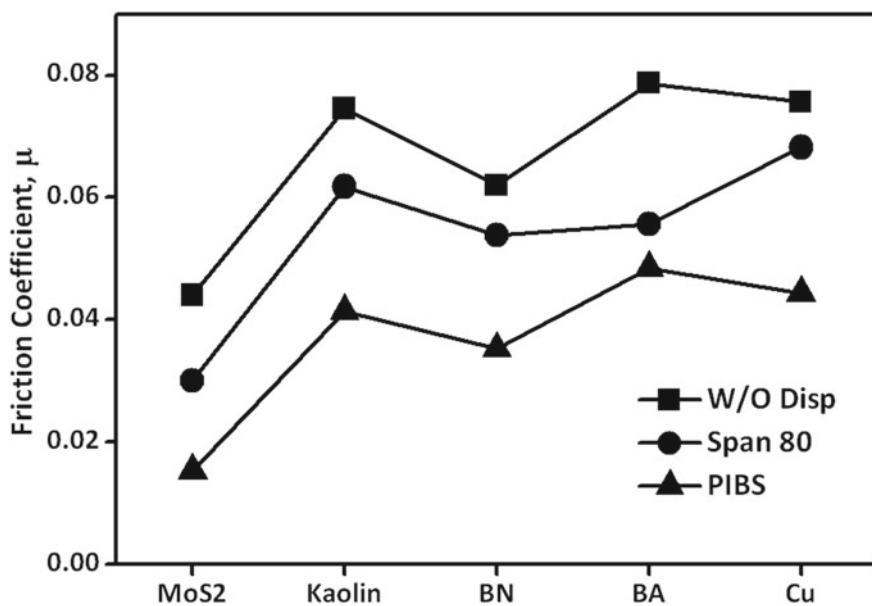**Fig. 6.9** Friction coefficient of nanoparticles suspended in oil medium

particles are compared, MoS_2 having less frictional co-efficient (~ 0.02) than other nanoparticles, where the observed friction co-efficient are ~ 0.04 – 0.05.

6.3.2 Nanoparticle in Water Suspension

Nanolubricants are solid powders of nanoparticles, often containing micron-sized nanoparticle agglomerates. These agglomerates can be re-dispersed upon fragmentation using ultrasonic processing. Nanoparticle dispersions are suspensions of nanoparticles in water or organic solvents. Nanoparticles in dispersions often settle upon storage, which is more horrid in water than oil, which hinders their use as lubricants. In nanosuspensions, the liquid medium helps transport the suspended particles between the contacting bodies for smooth sliding. The solid particles adhered to the contacting interfaces and developed a steady-state low friction regime.

Agglomeration is the main problem in justifying the above mechanism for any practical application. Due to smaller particles' large surface area to volume ratio, they attract and form agglomerates. Practically, these agglomerates do not accommodate within the contacting surfaces. Hence, the potential beneficial outcome of the layered structure is not achieved. PIBS as liquid dispersants is therefore played an essential role in providing lubrication effect to the surface where nanoparticles are generally used as an additive for property modifier. Organic dispersants contain a polar functional group and are attached to a lengthy bulky hydrocarbon group. They mainly utilize oxygen or nitrogen polarization without containing metal ions. This helps in adsorption on the particles for non- agglomeration and supports keeping particles in the suspension form. They create opposite repulsion forces to keep the particles at a distance and help stabilize immersed particles. Thus, additives based on surfactants can offer improved performance for nanoparticles immersed in a medium than without surfactants for a broader range of applications (Scamehorn 1986; Rosen and Hua 1982). It is interesting to see the effect of the largest dispersed quantity of water with the provided low surfactant quantity for any liquid medium (Shinoda and Kunieda 1977). Investigation of four nanoparticles such as MoS_2, kaolin, BN, Cu is carried in water suspension using DLS and POD. DLS obtains average particle sizes of these nanomaterials, whereas the frictional properties of the nanolubricants are investigated by POD tribometer.

Figures 6.10, 6.11, 6.12 and 6.13 shows the particle size distribution of MoS_2, kaolin, BN, and Cu in water medium without dispersing CTAB, SDS, SHMP, and Tween 20, respectively. The addition of the dispersant to the suspension decreases the particle sizes, but no definite trend was observed with a particular surfactant for the particle reduction.

The particle size comparison of these four particles is demonstrated in Fig. 6.14. The average particle size of the particles in the presence of dispersants is reduced. The particle fragmentation in the water medium without any dispersant is less than oil and can be attributed to the different wetting behaviour in oil and water medium. The ultrasonic wave can be dissipated into the particles and rupture the particles into
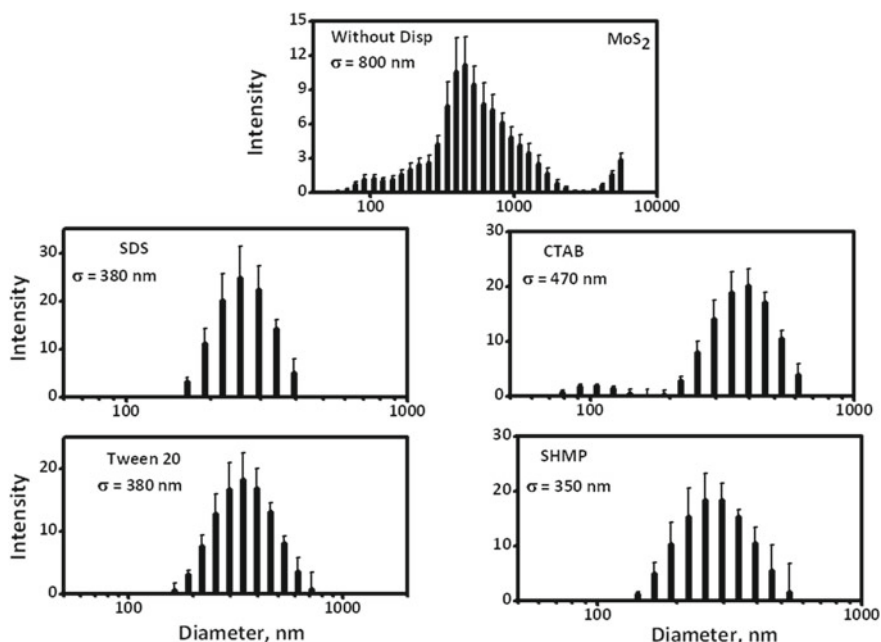
Fig. 6.10 Molybdenum disulfide (MoS_2) particle size distribution in water suspension without dispersant and SDS, CTAB, Tween 20, and SHMP, using DLS

very small parts, whereas water only partially wet the particles, therefore fragmenting only from the surfaces.

Further, the aqueous particle suspensions were sprayed on the steel substrate, and tribological tests were done with the POD tribometer. Figure 6.15 shows the average friction coefficient recorded for the particle suspensions between the steel-to-steel contacts. Contrary to the oil medium, the friction coefficient's performance in the water medium's case is not valid. Because no dependency of particle size on the water dispersion is established. On the other hand, it is worth notifying that the particle suspensions with additive (SDS) have a better effect on the friction response. SDS reduces the friction to some extent and achieves the least friction coefficient value of < 0.1, which is in all cases can be compared to the friction response of the oil medium. While SDS surrounding the particles has a negative charge and these particles are transporting towards a negatively charged steel substrate, these above data are particularly an unusual finding. They need further investigation in particle chemistry, particle – surfactants interaction, particle transport, etc.
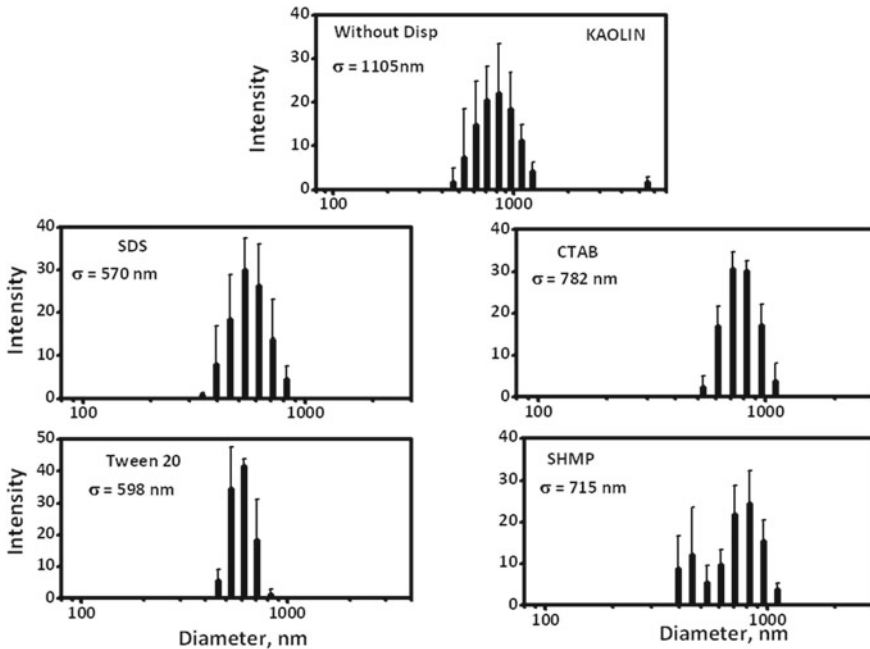
Fig. 6.11   Kaolin particle size distribution in water suspension without dispersant and SDS, CTAB, Tween 20, and SHMP, using DLS

6.3.3   Grease Analysis Using FTIR

The lithium stearate soap-based lubricating greases were prepared in dense paraffinic oil, and its FTIR analysis was conducted. The dispersion of lithium stearate soap in the oil medium was excellent. Figure 6.16 shows the prepared grease FTIR structure and its corresponding chemical bonding's at particular frequencies. FTIR is a versatile means to explore chemical elements present in the grease structure in the form of used oil, any performance modifier additives, and liquid soap itself (Fuks et al. 1972). The achieved spectrum gives a clear picture of the grease performance, and sometimes it is essential to know the exact modifications required for better uses. The various FTIR spectra for a tested grease was found for the following regions.

(i)   3000–2800 cm-1: 2928, 2852 cm-1: CH2 antisymmetric and symmetric stretching vibrations.
(ii)   1500–1300 cm-1: 1456, 1378 cm-1: CH2 and CH3 deformation vibrations.
(iii) 900–700 cm-1: 721 cm-1: Indicative of lengthy paraffinic chains.
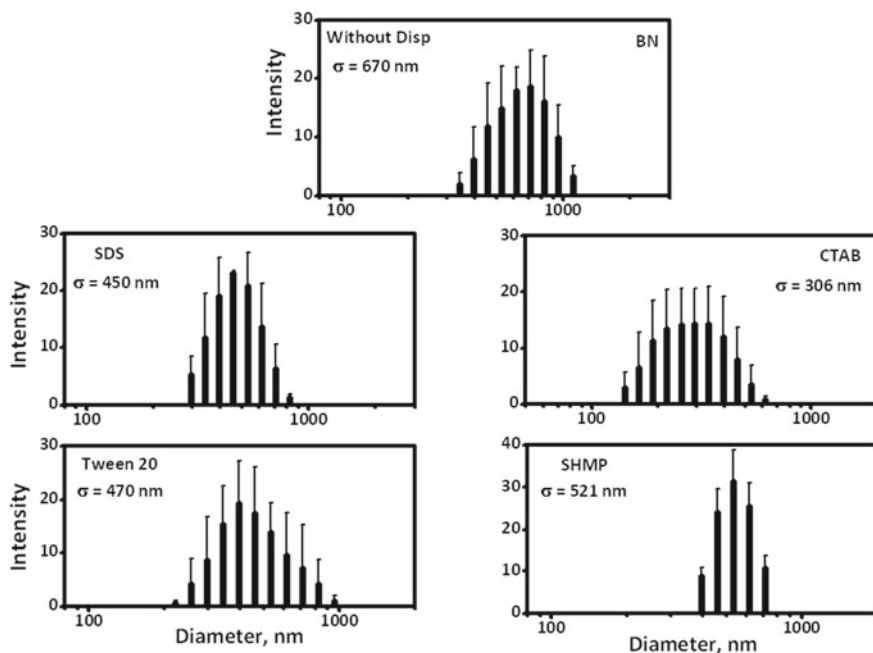(iv)   1600–1500 cm-1: –COOM metal carboxylate group.

Fig. 6.12 Boron nitride (BN) particle size distribution in water suspension without dispersant and SDS, CTAB, Tween 20, and SHMP, using DLS

In this present study, the IR spectra peak values between 1578 and 1562 cm-1 correspond to the—COOLi, which is well justified with the earlier reported data (Fuks et al. 1972).

Lithium stearate prepared grease was then subjected to tribological analysis. The grease was added to the steel sliding contact interface, and tribological experiments were done on this coating. Figure 6.17 compares the prepared lab grease's friction coefficient with that of the parent oil and commercial grease. The friction coefficient recorded for the oil was found to increase with time. However, as the stearic acid molecules were suspended in an oil medium, the soft soap transformed into a highly thick grease matrix. At this stage, the friction coefficient (~ 0.08) is almost constant with the sliding time and found to perform better than the commercial grease (~0.1).

Figure 6.18 shows the variation in friction coefficient with sliding time for the various prepared particle-based greases. Figure 6.19 shows a relative comparison of particle greases, oil alone as a lubricant, commercial grease, and lab/soft grease. Infusion of the nanoparticles into the grease matrix reduces friction coefficient significantly for the fixed duration of sliding time. The recorded friction values are consistently lower than their respective oil suspensions, indicating that the grease matrix has a much better load-bearing ability than the mere oil.
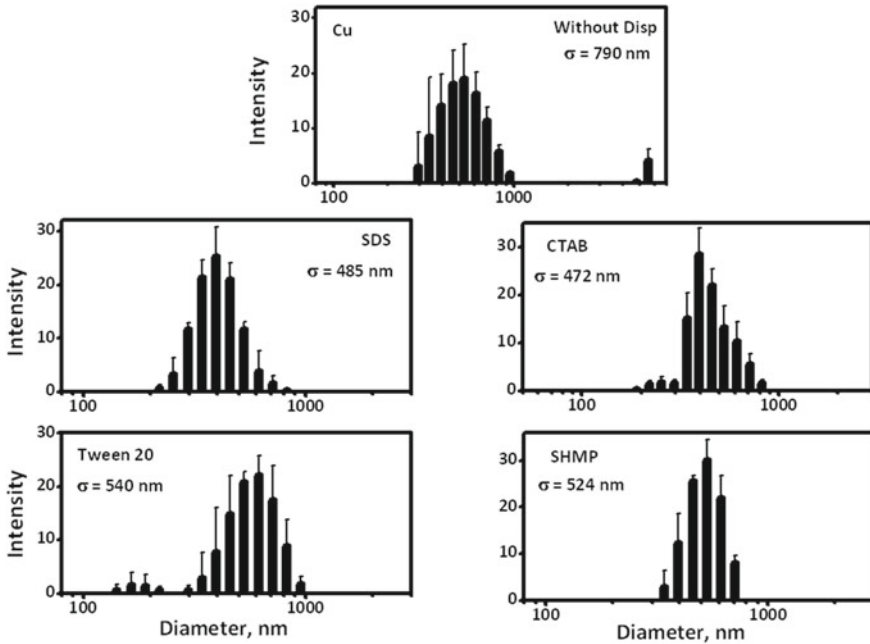
Fig. 6.13 Copper (Cu) particle size distribution in water suspension without dispersant and SDS, CTAB, Tween 20, and SHMP, using DLS

Figure 6.20 shows the effect of initial particle size fed to the oil suspension before preparing the grease on the particle grease's tribological performance. The oil suspension was prepared without and with PIBS as a dispersant to control the particle size, followed by the grease preparation. The results showed a modest effect of the particle size on friction (see inset Fig. 6.20), indicating the initial particle size does not affect tribological behaviour as the particles might get agglomerated again on the course of the preparation of the grease.

Figure 6.21 shows the effect of particle concentration on the oil suspension before preparing the grease on the particle grease's tribological performance. The oil suspension was prepared without dispersant with 0.2% and 1% w/v of the particle, followed by the grease preparation. The results showed a little effect of the particle concentration on friction at the test's initial point (see inset Fig. 6.21). For 0.2% kaolin, the friction values slowly drop down with time initially, after which it became independent of time. However, for higher concentration kaolin, the friction values are almost independent of time from the starting of the test.

Fig. 6.14 Comparison of particle sizes of the particles used in the water medium
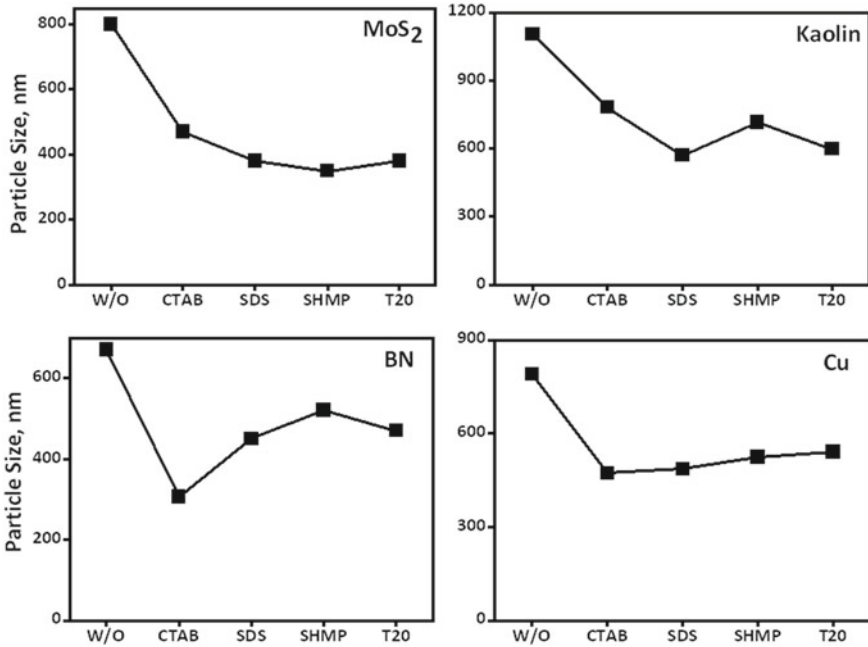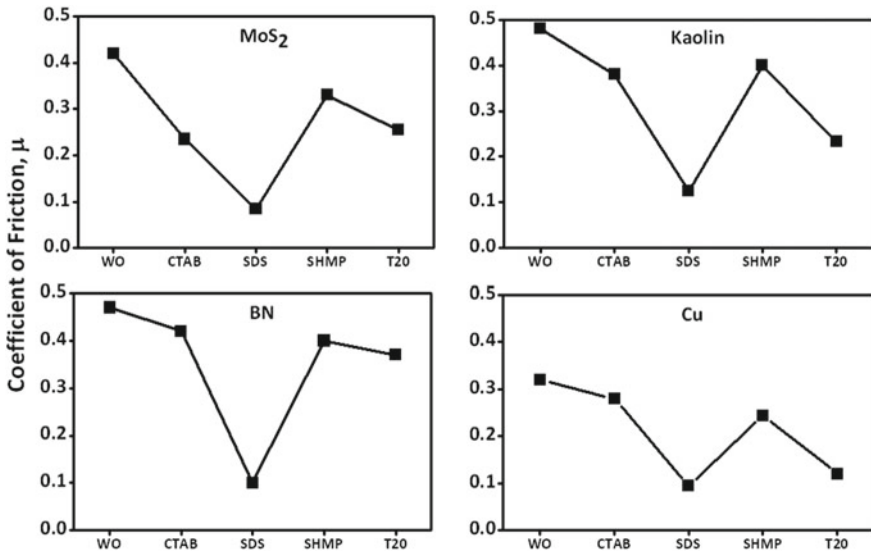

Fig. 6.15 Friction Coefficient of particles suspended in the water medium
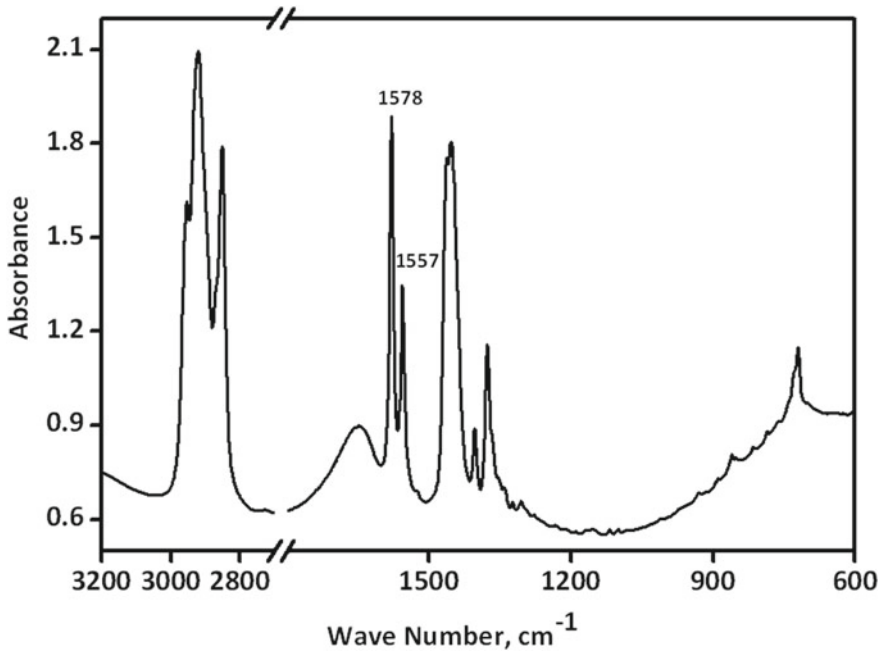
Fig. 6.16 Lithium stearate soap FTIR spectra prepared with the help of heavy paraffin oil

Results show that nanoparticle lubrication plays a vital role in reducing surface friction and wear. The present work focuses on the tribological behaviour of nanoparticle modified lubricants potentially to be used for lubrication. The results of boundary lubrication properties can be used for automotive or other related transport vehicles such as railway, marine, and aerospace applications. Nanolubricants are resistant to a wide variety of fluids in space application where an extensive range of temperature and conventional lubricant was evaporated. Nanolubricants have found wide use in aerospace equipment, primarily because they are better suited to aerospace applications' more demanding requirements than mineral oil-based materials. The primary condition that makes aerospace applications so demanding is the requirement to operate over an extremely wide temperature range. Industrial applications of nanolubricant are bearing, engine oils (automotive, diesel), gas turbine (aircraft), gears (machinery, helicopters), two-cycle engines (scooters). This work can be further detailed by synthesizing more specialized materials for the nanotribological application. The detailed wetting analysis is also crucial for identifying the surface's real behaviour, which needs to be investigated in detail.
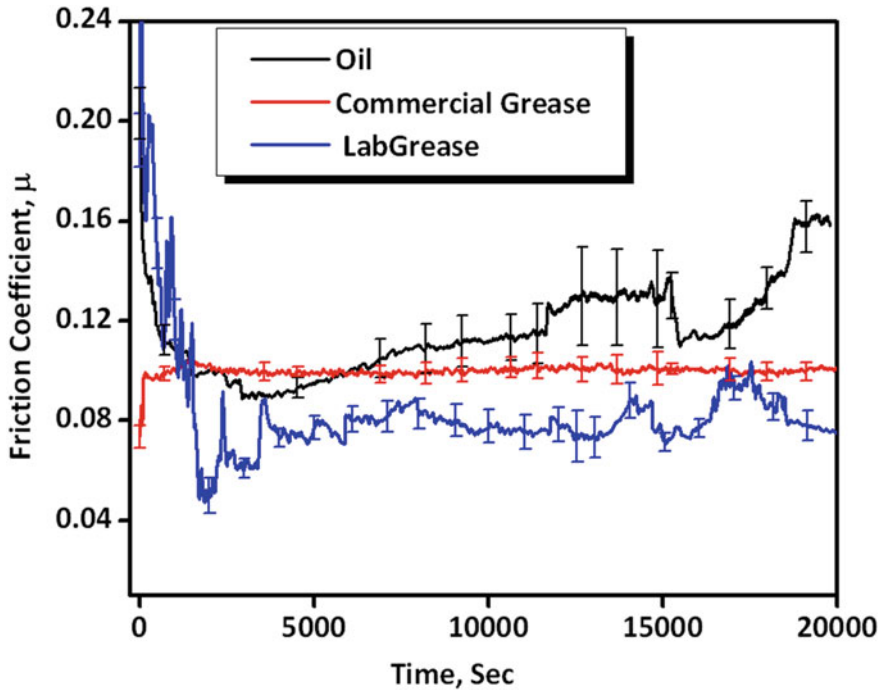
Fig. 6.17 Comparison in variation in friction coefficient of the prepared lab grease with that of the parent oil and commercial grease with sliding time

6.4   Conclusions

In this study, three areas of investigation were considered. Firstly, the effect of nanolubricants on the surface of a material in oil suspension was studied. Secondly, nanoparticles in water suspension and lastly, the nanoparticles blended with grease matrix were studied. The results obtained from these experiments led to the following conclusions.

- It was found that the use of dispersants/surfactants in a medium can stabilize the suspension and control the particle size.
- The addition of dispersant tends to reduce the particle size in the suspension, and the decrease in particle size reduces the friction for the oil suspension.
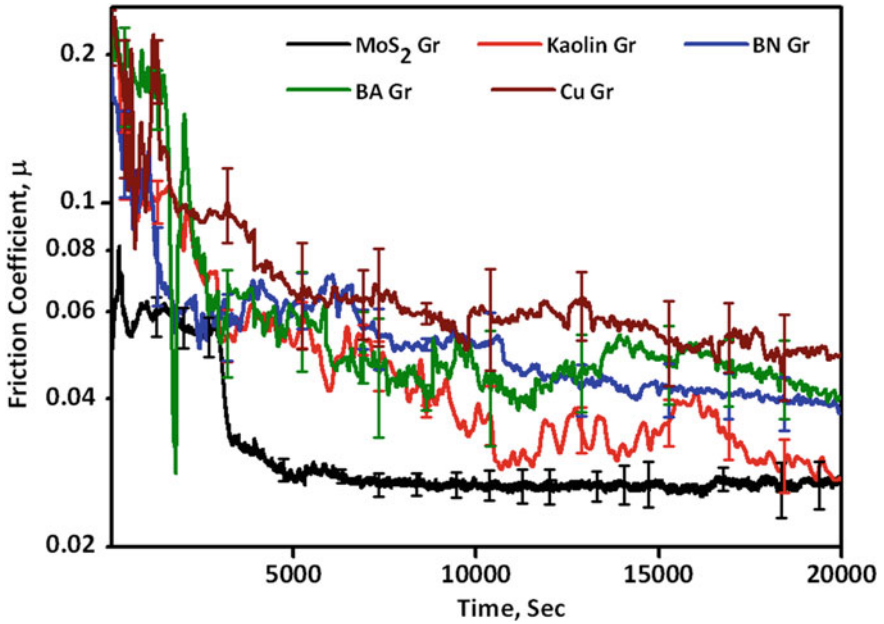
Fig. 6.18 Variation in friction coefficient of the prepared particle grease with time
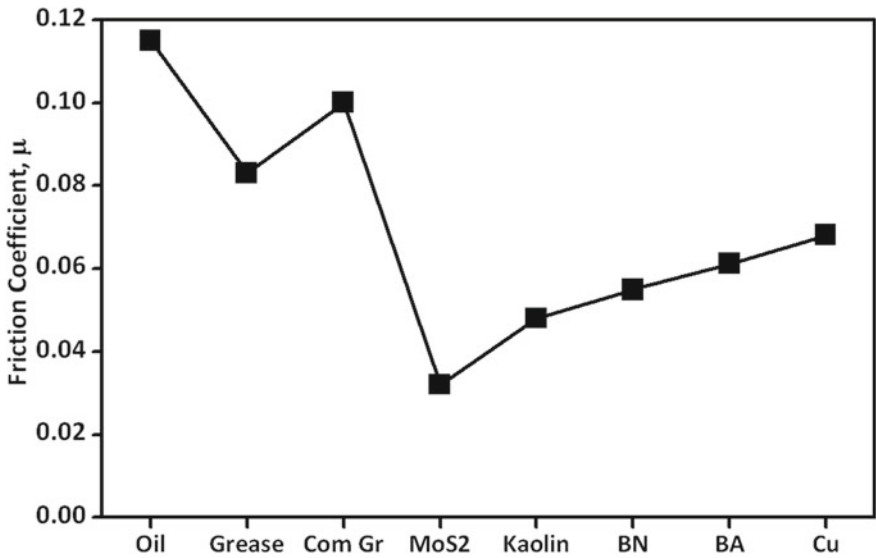
Fig. 6.19 Comparison in friction coefficient of the prepared lab grease, particle grease with that of the parent oil, and commercial grease available
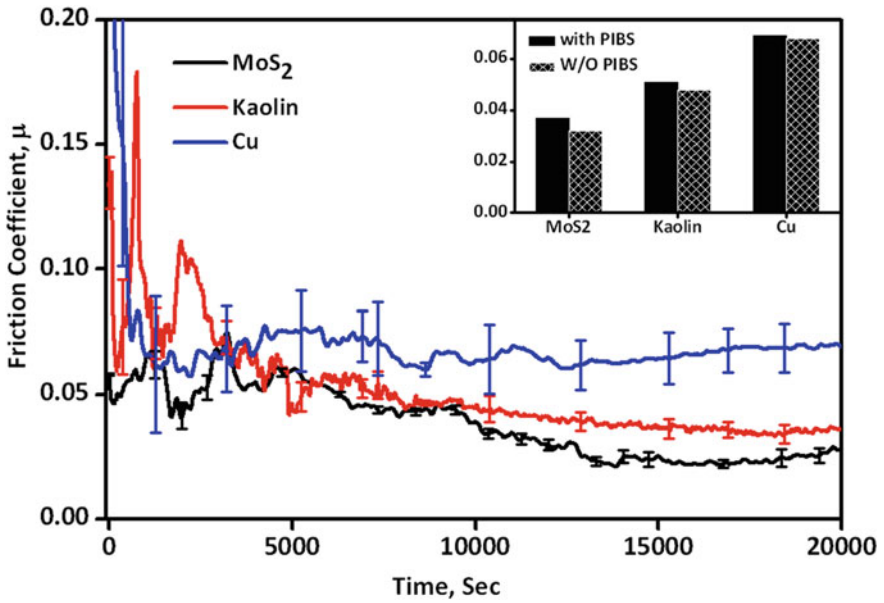
Fig. 6.20 Comparison in friction coefficient of the prepared particle grease with variant particle size

- In the water medium, irrespective of their particle size, SDS suspension provides the least friction coefficient.
- Oil and grease alone give high frictional values. However, when mixed with particles, the reduction in friction values is substantial.
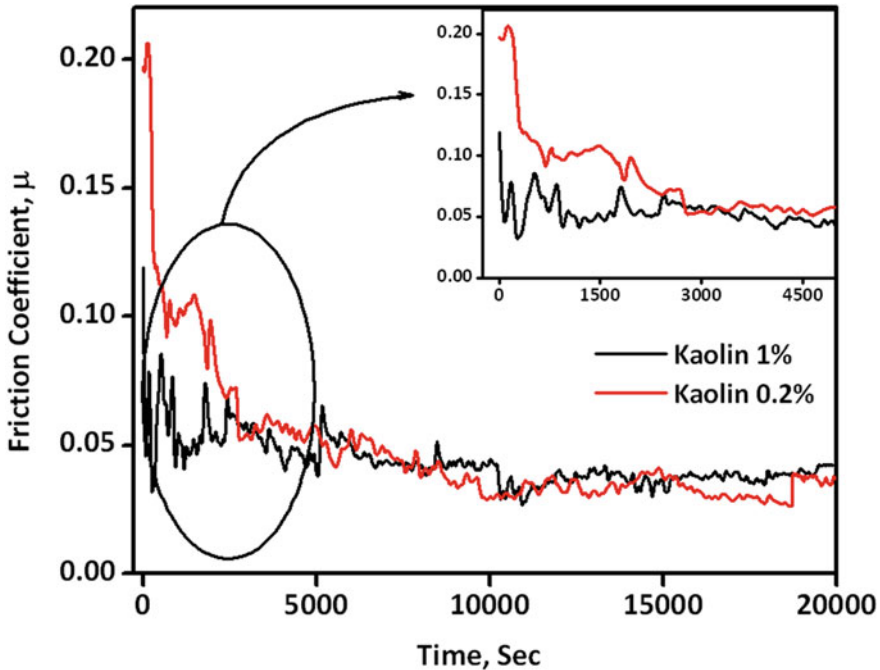
Fig. 6.21 Comparison in friction coefficient of the prepared kaolin grease with different concentrations of particle sizes

References

Fuks IG, Medvedeva TV, Ishchuk YL (1972) Application of IR spectroscopy in studying grease composition and properties. Chem Technol Fuels Oils 8:152–155

Guiggiani M (2020) Lubrication problems solved by the boundary element method. Eng Anal Boundary Elem 119:183–188

Joly-Pottuz L, Dassenoy F, Vacher B, Martin JM (2004) Ultralow friction and wear behaviour of Ni/Y-based single wall carbon nanotubes (SWNTs). Tribol Int 37(11–12):1013–1018

Liu Y, Ge X, Li J (2020) Graphene lubrication. Appl Mater Today 20:100662

Rosen MJ, Hua XY (1982) Synergism in binary mixtures of surfactants: II. Some experimental data. J Am Oil Chem Soc 59:582–585

Sahoo RR, Biswas SK (2009) Frictional response of fatty acids on steel. J Colloid Interface Sci 333:707–718

Sahoo RR, Biswas SK (2014) Effect of layered MoS_2 nanoparticles on the frictional behavior and microstructure of lubricating greases. Tribol Lett 53:157–171

Sahoo RR, Patnaik A (2005) Surface confined self-assembled fullerene nanoclusters: A microscopic study. Appl Surf Sci 245(1–4):26–38

Sahoo RR, Math S, Biswas SK (2010) Mechanics of deformation under traction and friction of a micrometric monolithic MoS_2 particle in comparison with those of an agglomerate of nanometric MoS_2 particles. Tribol Lett 37:239–249

Scamehorn JF (1986) Phenomena in mixed surfactant systems. Anal Chem 58(12):1250A

Shinoda K, Kunieda H (1977) Microemulsions: Theory and practice, 1st edn. Academic Press, New York

Upadhyay RK, Kumar A (2019) Boundary lubrication properties and contact mechanism of carbon/MoS$_2$ based nanolubricants under steel/steel contact. Colloid Interf Sci Commun 31:100186

Chapter 7
Nanomaterials Lubrication for Transportation System

Pratyush Kumar and Ram Krishna Upadhyay

Abstract This work presents detail about lubrication, different types of lubrication, tribological properties such as friction and wear, the composition of lubricants, and the impact of lubricants on the environment. Further, it covers types of the lubrication system, choice of lubricants, properties, and applications of nano particles-based lubrication in oil mediums. It also explains the properties of grease and its suitable applications, particle-based lubrication such as graphene, molybdenum disulfide, boron nitride, boric acid, tungsten disulfide. Nanocomposite-based lubrication properties of epoxy-graphene-molybdenum disulfide (MoS_2) under dry sliding contact are discussed in detail. Oil properties and their use, different oils, their viscosity, influencing parameters affecting the oil viscosity, viscosity and temperature relationship, methods to measure viscosity, and basics of absolute and kinematic viscosity are discussed. Significant rail components such as Elastic Rail Clips (ERC), Sealing linear, Switch Expansion Joint (SEJ) for effective lubrication methods are presented.

Keywords Friction · Wear · Lubrication · Nanoparticles

7.1 Introduction

7.1.1 Lubrication

Any machinery with rolling elements or ball bearings needs adequate lubrication to prevent wear and tear of the machinery components. Engine oils and grease are commonly used as lubricants in all heavy machinery, including automotive, heavy earthmoving machinery, marine, aerospace, and railways (Jain 2021). Grease is a semi-solid substance that is particularly suitable for heavy-load machine parts where stresses are very strong at the point with touch with metallic surfaces. At low-pressure interactions between metal sheets, grease has a viscosity that fits the Newtonian fluid equation for shear stress and shear strain. The pressures and

P. Kumar · R. K. Upadhyay (✉)
National Rail and Transportation Institute, Vadodara, Gujarat 390004, India
e-mail: ram.upadhyay@nrti.edu.in

temperature-dependent viscosity equation but lubricating grease properties show its non-Newtonian behavior.

The mechanism or practice of utilizing a lubricant to minimize wear, tear, and friction when two surfaces come in contact is referred to as lubrication. Lubrication is a section of tribology that focuses on the study of lubrication. Solids such as molybdenum disulfide (MoS_2), dispersions of solid/liquid (solid/oil mixture), liquids (water or oil), dispersions of liquid–liquid, or gases could also be used as lubricants. The applied load is carried partly or entirely by hydrostatic or hydrodynamic pressure in fluid-lubricated systems, preventing solid body interactions (consequently wear and friction). Different lubrication regimes can be differentiated based on the degree of surface isolation. Adequate lubrication helps system elements to operate smoothly and continuously, reduces wear, and prevents unnecessary pressures or shakes at bearings. Components will rub disruptively against one another lubrication fails, causing fire, local welding, disruptive damage, and failure. A lubricant's essential functions are as follows (Lubrication increases the efficiency and life-expectancy of machines 2021):

- Producing a layer between contacting materials to minimize friction.
- Keeping the machine from running out.
- Corrosion resistance.
- Cooling by heat dissipation from surfaces.
- Sealing.
- Contaminating particles are transported to filters for cleansing.

7.1.2 Lubrication Classification

7.1.2.1 Manual Lubrication

Manual lubrication necessitates the use of a grease gun or other conventional lubrication instrument by a technician. This form of lubrication has a range of disadvantages, including increased system downtime, high repair costs, and inadequate lubrication (too much, too less, or not frequently enough). Manual lubrication is incompatible with today's cost-cutting and proactive maintenance issues. As in a grease gun, a traditional lubrication device cannot ensure optimum lubrication by delivering the correct volume of lubricant to the machines at the right place and in the correct spot – typically when the machine is running. Manual lubrication procedures expose you to the possibility of under-lubrication or over-lubrication, all of which have detrimental consequences for the machine's parts, reliability, and total costs (Lubrication increases the efficiency and life-expectancy of machines 2021; Pitfalls of manual lubrication 2021). Its disadvantages are:

- When lubricating hard-to-reach bearings, safety is a concern
- Specific devices are unsafe to lubricate when they are working
- Lock-out and tag-out processes take time and result in production losses

Excessive lubrication can lead to:

- Deposition of unnecessary heat
- Spoilage of goods
- Harm to the bearing seal
- Issues of cleanup
- Downtime has improved.

Low lubrication can lead to:

- Item wear has grown
- Injury of bearing
- Failure that happens too fast
- Increased oil consumption
- Operating and repair expenses have soared

7.1.2.2 Automatic Lubrication

An automatic lubrication device applies the right amount of lubricant to the machines at the right place and in the correct position, usually when the process is working. It takes the place of a standard lubrication device, resulting in longer machine life, less wear, and lower maintenance costs (Lubrication increases the efficiency and life-expectancy of machines 2021). Its advantages are:

- Increased durability of equipment: Automatic lubrication eliminates wear and increases the life of your equipment by supplying the right volume of lubricant at the right place and in the correct place. To prevent moving machine parts from rubbing against each other, automatic lubrication forms a thin layer between them. The components will be insulated from wear, and it will last longer if direct metal-to-metal interaction is avoided.
- Decrease in lubrication intake: Automatic lubrication devices provide small volumes of lubricant more often, reducing lubricant use. This not just saves money on oil and grease, but it also helps the atmosphere.
- Decreased maintenance expenses: You can save money on replacement parts, and automatic lubrication increases machine longevity by reducing wear. Furthermore, since the equipment doesn't require manual point-by-point lubrication by specialists, you can significantly reduce the repair costs. Compared to the 15-min testing and filling time of an auto-lube device, lubing using a grease gun is time-consuming for technicians.
- System downtime is minimized: It's important to prevent the installations from coming to a halt if you want to maximize your overall efficiency. Automatic lubrication devices, unlike manual lubrication, do not need the machine to be turned off in order to inject more oil. Lock-out and tag-out operations can be stopped. The equipment can continue to operate as the lubrication mechanism ensures that the proper volume of lubricant is used for optimum lubrication. As a result, automated lubrication significantly decreases labor and downtime.

- Workplaces that are safer and healthy: A machine mechanic uses a grease gun to lubricate the required machine parts in manual lubricated conditions. Any critical machine sections are challenging to reach and require climbing on the device, which can also be done while still working. This raises significant safety issues, which can be mitigated by adding an automatic lubrication system. Auto lube also eliminates the risk of falling out while avoiding human interaction with lubricants and leaked oil on the concrete.
- Improvements to the environment: Automatic systems determine the precise quantity of lubricant necessary. Waste, degradation of products, as well as housecleaning problems are also significantly minimized. Improved bearing, gear, and chain lubrication ensure less friction and less energy usage.
- Adaptable to any situation: Several different types of automatic lubrication systems, such as single-line parallel, series progressive, dual-line, and multi-line, each with its own set of benefits and implementation areas (significant advantages of automatic lubrication 2021). Because of all this broad variety, an automated lubrication device can lubricate almost every application.

7.1.3   Preventing Low and Excessive Lubrication

The implications of inadequate lubrication are well known: increased part wear, premature loss, higher energy demand, and higher operational and repair costs. However, the implications of unnecessary lubrication may be almost as harmful. It wastes lubricant, raises downtime, and may induce unnecessary heat build-up. It also places tension on lube points. The response is self-evident: optimum lubrication.

There are several reasons for bearing failure. The highest percentage is because of inadequate lubrication, i.e., 34.4%. 19.6% is because of contamination, 17.7% due to installation errors, 6.9% due to bearing overload, 2.8% due to storage and handling errors, and the remaining 18.6% for other reasons. There is a general question that why do we require lubrication. So, to answer this question, we can say that it reduces friction, allowing moving machine parts to float around one another smoothly. One of the most critical preventive maintenance tasks is lubrication. Maintaining the appropriate pace for this operation is critical because it enables maintenance shutdowns to be arranged without disrupting scheduled output and guarantees that the system runs at maximum efficiency. The following are some of the features of a quality lubricant (Lubrication increases the efficiency and life-expectancy of machines 2021):

- To remain liquid over a broad temperature spectrum, it must have a high boiling point and a low freezing point
- The viscosity index is high
- Thermal Consistency
- Stability of the hydraulic system
- Possibility of demulsification
- Preventing corrosion
- Oxidation tolerance is high.

7.2 Lubricants Reducing Friction and Wear

As two objects are in motion, lubrication decreases the heat produced. It improves performance and efficiency by creating a layer between contact objects that reduces friction. Based on the design of the application, lubricants can reduce or increase friction. Lubricants also caused a spike in resistance on straight joints. If the grease forms a layered film between the sliding surfaces, higher friction is needed. However, if only a small amount of lubricant, such as a monolayer film, is present between the surfaces, lubricant reduces friction significantly. As a result, by use of lubricant reduces the total friction of the structure. Friction mitigation lowers heat output and reduces the aggregation of fumes, as well as improving proficiency. When applied as a layer between two heavy surfaces, a lubricant is described as a material similar to the oil that reduces friction, heat, and wear. It's usually added to minimize friction between surfaces that come into contact, which decreases the warmth produced as the parts pass. When the lubricant is applied to a machine, it extends between the two surfaces, scouring them against each other and removing any defects on the surface. It often forms a thin film between the surfaces in contact. As a result, the lubricant coating replaces the interaction between the two hard surfaces, reducing the friction force substantially. How Do These Lubricants Help in The Reduction of Friction Between System Moving Parts? Lubricants aid in the smoothing of machine parts with grating surfaces. As a consequence, the level of resistance is decreased. When the lubricant is applied between the rubbing sections of a system, it forms a thin film of grease that polishes the two granting surfaces (How Lubricants Combat Friction and Wear. 2021). Since this coating of oil divides the two giving pieces a bit, the resistance is significantly diminished. The tension between the machine parts reduces, and the flow becomes more elastic.

7.3 Types of Lubrication

7.3.1 Boundary Lubrication

The metal surfaces in a lubricated device can contact each other during initial start-up or under heavily loaded conditions, such as in gearsets. Lubricants must have the proper viscosity as well as the required anti-wear or extreme-pressure additive chemistry to prevent (or reduce) frictional wear during this lubrication condition (How Lubricants Combat Friction and Wear 2021). The chemical properties of the additive package will be just as critical as the physical properties of the oil, especially viscosity, in boundary conditions. Still, operating conditions like temperature will influence both.

7.3.2 Mixed Lubrication

Mixed lubrication (h > 0.1 μm) is a transition stage between boundary and hydrodynamic lubrication state. In a mixed lubricated contact regime, surface roughness has a significant impact on the contact's performance. It may happen where partial contact lubrication is used, such as when journal bearings are lubricated.

7.3.3 Hydrodynamic Lubrication

When an oil film supports a rotating part, such as a shaft, it prevents the shaft from touching the supporting bearing. A hydrodynamic lubrication state happens between the contacting parts. This occurs as a mechanism begins spinning, and the speeds and loads are such that a wedge of oil passes between the shaft and bearing surfaces, moving the shaft away from the bearing surface. A crankshaft and journal bearing in a vehicle engine or a turbine are examples of typical applications. The oil's viscosity must be such that the hydrodynamic state is retained under all operating conditions, such as high speed and high load, low speed and low load, and so on, for hydrodynamic lubrication to get successful. In relation to boundary conditions, hydrodynamic lubrication necessitates preserving the oil's physical properties, especially its viscosity, under all circumstances. If the viscosity is reduced too much due to the operating conditions, metal-to-metal contact between the high spots or asperities can occur (How Lubricants Combat Friction and Wear 2021). When the oil's viscosity is so high (thick), the internal resistance to the shearing of the oil molecules limits operating performance and allows temperatures to rise significantly.

7.3.4 Elastohydrodynamic Lubrication

A lubrication state known as elastohydrodynamic lubrication (EHL) is prevalent in equipment that has system components with localized areas with very high-pressure contacts, such as roller and ball bearing applications (How Lubricants Combat Friction and Wear. 2021). As a standard oil approaches the interaction zone between the moving elements, EHL conditions exist. As oil approaches the touch zone between a ball and a raceway, the oil pressure increases dramatically. This friction increases the viscosity of the crude, which raises the pressure even more. The strain builds up to the point that the oil becomes pseudo-solid. This can subtly bend the elements' touch fields, impacting the rolling element's contact areas elastically.

Around the same time, the oil film thickness can avoid surface high points or asperities from cracking the oil film as the rolling components pass across the contact region, ensuring the oil's physical characteristics such as viscosity and viscosity index are suitable for the application. Since temperature directly impacts an oil's

viscosity, incorrect or irregular operating temperatures can hinder the forming of the elastohydrodynamic lubricating film. In bearings, the forming of EHL films is often followed by a rise in temperature. Extreme harm will occur if the temperature increases high enough to decrease the viscosity of the oil significantly.

7.4 Composition of Lubricants

Lubricants usually contain 90% base oil (mostly petroleum fractions, also known as mineral oils) and less than 10% additives. Base oils may be vegetable oils or industrial liquids, including hydrogenated polyolefins, esters, silicones, fluorocarbons, among many others. Decreased friction and wear, high viscosity, enhanced viscosity index, corrosion and oxidation tolerance, aging or contamination resistance, and so on are all advantages of additives.

Powders (dry graphite, PTFE, molybdenum disulfide, tungsten disulfide, and other non-liquid lubricants, for example), PTFE tape used in piping, air cushion, and other non-liquid lubricants are examples. Dry lubricants, including MoS_2, graphite, and tungsten disulfide, can lubricate at temperatures up to 350 °C, where oil and liquid-based lubricants cannot (Lubricant 2021). Low friction properties of compacted oxide glaze layers formed at hundreds of degrees Celsius in metallic sliding systems have piqued interest. However, practical use is still several years away due to their mechanical brittleness.

7.5 The Impact of Lubricants on Climate Change and the Environment

Environmental issues are becoming more important in our society. Given how quickly our world is being poisoned with various contaminants, every reduction is welcome. Lubricants are not particularly harmful to the environment since they are close to many other chemical components. A significant portion of lubricants pollutes the environment during use. This may be desired (total-loss lubrication) or the result of mishaps such as emissions, leaks, spillages, or other problems (Mang and Dresel 2007).

Because of their widespread usage, lubricants and mechanical fluids pollute the environment in small, commonly dispersed amounts and, on rare occasions, massive, concentrated quantities. The language used in conjunction with environmental compatibility needs to be divided between the contextual and the objective (Mang and Dresel 2007):

Subjective parameters (non-measurable):

• Eco friendly

- Eco compliant

Objective parameters (measurable or provable):

- Biodegradability
- Water solubility, water pollution
- Toxicity to the environment and physiological protection
- Oil change intervals, performance, and permits
- Increased efficiency and reduced oil demand
- Use of less energy results in lower emissions
- Compatibility with generic lubricants and materials
- The usage of environmentally friendly raw materials
- Environmental awards

At least 60 percent of biodegradability according to OECD 301 or at least 80 percent as per CEC L-33-A-93 is typically considered an important objective requirement for Bio-Lubricants. However, in the immediate future, the other parameters may become increasingly important.

About 40–50 percent of Europe's almost 5 million tonnes of used lubricants pollute the environment per year until the lubricant ends. This interaction with the ecosystem, and the resulting pollution of the atmosphere, groundwater, and water is either potentially desirable (total-loss lubrication) or occurs due to leakage or other problems (Mang and Dresel 2007). The roughly 40 percent of mineral oil-based lubricants that are not appropriately disposed of causes most of the pollutants produced by these lubricants.

7.6 Properties of Nano Particles-Based Lubrication in Oil Medium

Nano lubricant additives are primarily used to boost the tribological properties of lubricants. Anti-wear, anti-friction, and extreme pressure additives are the most popular applications. Nano additives reduce friction and wear between mating surfaces while increasing lubricant thermal conductivity, reducing heat build-up, and increasing fuel consumption in vehicle engines. Strict environmental standards to limit sulfur content and particulate pollution from diesel fuels have culminated in a reduction in sulfur and phosphorus-containing lubricating oil additives. This decreases the lubricating strength of diesel oil and speeds up the wear of engine parts. Nano chemicals have been used to increase the lubricity of engine oil. When boundary films fail or split under boundary lubrication conditions, solid nano additives may improve the tribological properties of slipping contact surfaces, bear the load, and function as backup lubricating films. The degree to which nanomaterials can increase the base oil's tribological properties is determined by a variety of variables, including the form of substrate, size, and nanomaterial loading. The usage of thin, uniformly spaced nanomaterials greatly enhances tribological properties. Larger

particles improve abrasiveness and avoid forming a defensive coating on the lubricating surface, resulting in inferior tribological properties. To achieve the desired improvement in tribological properties, an optimal concentration of nanomaterials is also needed. This is because the development of a continuous protective film is hindered at low concentrations, and crowding of nanoparticles results in increased abrasiveness at concentrations higher than the optimum value, both of which result in weaker tribological properties (Deepika 2020). Applications of nano particles-based lubricants in different industries are presented below.

7.6.1 Automotive Oils

Engine oil lubricants account for approximately half of the lubricant industry, and they have received a lot of attention. Lubricant formulators use low viscosity engine oils and new, more effective friction modifiers to increase fuel efficiency. Its essential functions are as follows (Deepika 2020):

- Maintains a constant oil flow between sliding surfaces and ensures efficient engine activity over an extensive temperature range
- Protecting engine parts from rust and corrosion
- Removing sludge from engine components
- Preventing foaming

7.6.2 Railroad Engine Oils

Diesel engines are commonly used in railroad applications. In the area of diesel engine lubrication, significant progress is being made. In the operating atmosphere of diesel locomotive engines, high mechanical and thermal pressures are imposed on different engine components, including the lubricant. New problems for designing high-performance lubricants for railroad applications have arisen due to increased demand for more horsepower per cylinder and tougher nitrous oxide and particulate matter pollution regulations. Its fundamental properties and functions are as follows:

- To minimize piston deposits, it has strong detergency and dispersant properties.
- Excellent oxidation and thermal stability to avoid oil degradation and the formation of sludge.
- Excellent wear resistance.
- Alkalinity is high, which helps to neutralize acids created during standard engine service.

7.6.3 Marine Engine Oils

The use of fuel oils has risen dramatically due to the rapid production of newer and larger marine diesel engines. Concurrently, to aid in marine engine management's design and manufacturing phase, improving the standard of lubricating oils is essential. Its fundamental properties and functions are as follows (Deepika 2020):

- Engine sections are protected from rust and corrosion.
- Alkalinity is high, and it can carry a lot of weight. Water separation properties that work.
- Demulsibility properties that are effective.

7.6.4 Industrial Oils

Hydraulic engines, generators, compressors, bearings, open and closed gears, machine tool slideways, pneumatic equipment, and automotive transmissions are only a few devices that use industrial lubricants (Deepika 2020). Lubricant formulations differ in composition depending on the requirement and application.

7.7 Base Oil

Base oils are used to render lubricating greases, fuel oil, and metal grinding fluids. Different oil compositions and properties are needed for different products. The viscosity of the liquid at different temperatures is one of the most significant considerations. The abundance of base oil compounds and how quickly they can be removed determine whether or not a crude oil is appropriate for making into a base oil. The process of extracting crude oil yields base oil. This relates to the heating of crude oil in order to distinguish different distillates from one another. Light and heavy hydrocarbons are separated during the heating process; petrol and other fuels can be produced by refining the lighter ones, while the heavier ones can be used to make bitumen and base oils. Base oils are made from a wide variety of crude oils that are mined all over the world. A paraffinic crude oil is the most well-known, although there are also naphthenic crude oils that include goods with increased solubility and low-temperature properties. Hydrogenation technology, in which sulfur and aromatics are removed using hydrogen under high pressure, may provide highly pure base oils. When it comes to maintaining quality, these base oils are the way to go (Base oil 2021). Additives are chemical components added to base oils to meet the durability requirements for end goods, such as friction and cleaning properties. Certain types of motor oils have a higher than 20% additive content.

7.7.1 Categories of Base Oil

Base oils are grouped into five different groups by the American Petroleum Institute (API) (Base Oil Groups Explained 2021). The first three classes are made from petroleum crude oil that has been refined. Total synthetic (polyalphaolefin) oils make up Group IV base oils. Most other base oils not used in Groups I and IV fall under Group V. Lubricating oils start as one or more of these five API classes before adding additives.

7.7.1.1 Group I

Base oils in Group I have a viscosity index of 80 to 120 and less than 90% saturates, more than 0.03 percent sulfur, and less than 90 percent saturates. These oils can tolerate temperatures of 32 °F to 150 °F. Solvent fermentation is used to refine Group I base oils. As a result, they are the most inexpensive base oils available.

7.7.1.2 Group II

More than 90% saturates, less than 0.03 percent sulfur, and a viscosity index of 80 to 120 characterize Group II base oils. Hydrocracking, a more complicated method than that used to make Group I base oils, is often used in their production. Group II base oils have more robust antioxidation properties since all of the hydrocarbon compounds are saturated. In contrast to Category I base oils, they have a lighter color and cost more. Group II base oils, on the other hand, are becoming more popular on the market, and they are priced similarly to Group I oil.

7.7.1.3 Group III

Group III base oils contain more than 90% saturates, less than 0.03 percent sulfur, and a viscosity index of more than 120. These oils are refined much more than Group II base oils and are usually hydrocracked severely (higher pressure and heat). This method aims to obtain a purer base oil. Group III base oils are often referred to as-synthesized hydrocarbons, even though they are made from crude oil. These oils, including Group II base oils, are becoming more popular.

7.7.1.4 Group IV

Polyalphaolefins make up Group IV base oils. Synthesizing is the method used to create these synthetic base oils. They have a much broader temperature spectrum, making them ideal for use in both extreme cold and high heat environments.

7.7.1.5 Group V

Silicone, phosphate ester, polyalkylene glycol (PAG), polyolester, biolube, and other base oils are known as Group V base oils (Base Oil Groups Explained 2021). To improve the oil's properties, these base oils are often combined with other base stocks. A PAO-based compressor oil combined with a polyolester falls into Group V. Esters are popular Group V base oils used to enhance existing base oils properties in various lubricant formulations. Compared to a PAO synthetic base oil, ester oils can withstand more abuse at higher temperatures and have superior detergency, allowing for more hours of use.

7.8 Viscosity

The viscosity of lubricating oil or grease is perhaps the most important property. The shear stress and the rate of shear in most fluids in laminar flow have a linear relationship. The viscosity, or more precisely, the dynamic viscosity, as opposed to the kinematic viscosity, determined by the viscosity-to-density ratio, is the proportionality constant (Guide and to Measuring Oil Viscosity 2021). Several parameters influence the viscosity of the oil.

- Contamination of water: Chemically, free water and oil do not combine. Under some conditions, however, they combine to create an emulsion that resembles coffee with cream. This emulsion would improve the kinematic viscosity of the oil.
- Additives: Oil formulations may include additives. For example, excluding naturally high VI base oils, Due to more excellent fluid solvency, multigrade mineral-based engine oils produce a springy additive that is lightweight at low temperatures and spreads at high temperatures.
- Soot: In diesel engines, one of the most common problems is soot. It's a type of particle that causes a colloidal suspension in oil. The dispersant in the oil is intended to avoid the growth and aggregation of the soot particles, allowing a colloidal suspension to form.
- Temperature variations: A lubricating oil's viscosity index measures how much its viscosity varies as a function of temperature. A low VI means that the viscosity of the oil changes substantially as a result of temperature changes. At the same time, a high VI indicates that the viscosity of the oil changes very little. The VI of oil whose viscosity does not alter much between 40 °C and 100 °C is greater than that of oil whose viscosity change is comparatively higher. The Viscosity Index Test measures the oil's kinematic viscosity at 40 °C and 100 °C, or 104°F and 212 °F (ASTM D 2270). The viscosity index of 95 or higher is deemed vital in general. Oils with a large VI support fragile components best over a broader temperature spectrum.

- Oxidative and thermal degradation by-products: Although these are insoluble by-products, the oil retains a stable suspension of them (Guide and to Measuring Oil Viscosity 2021).

7.8.1 Viscosity Versus Temperature

While it is well understood that oil can thin out or become less viscous as the temperature rises, the theoretical rule governing the shift in viscosity with temperature is unclear, necessitating the use of analytical methods (Herschel 1922). The temperature coefficient of viscosity, or the change in viscosity as a function of temperature, is different for different oils. A small coefficient is ideal for lubricating oil from a practical standpoint because it reduces the risk of seizure when the temperature of a bearing is unintentionally raised above its expected operating value. It's worth noting that when German engineers were considering potential replacement lubricants, the temperature coefficient of viscosity was the one feature they stressed.

Effect of temperature on the viscosity of graphene and molybdenum disulfide (MoS_2):

The effects of volume concentration (0.05%, 0.1%, and 0.15%) and temperature (10–90 °C) on the viscosity and surface tension of graphene–water nanofluid were analyzed (Ahammed et al. 2015). The surfactant sodium-dodecyl-benzene sulfonate is used to keep graphene in a stable suspension. The researchers discovered that as the temperature rises, the viscosity of the graphene–water nanofluid decreases. In another study, MoS_2 viscosity properties were studied (Vattikuti and Byon 2015). Results showed that as the temperature increases, the viscosity decreases, and viscosity increases with a decrease in the temperature of MoS_2.

7.8.2 10.2Multigrade Versus Monograde Oil

As the temperature rises, all liquids thin out, but a multigrade oil (10 W-40) maintains viscosity at optimal levels within a defined temperature range. Low temperatures are not needed for monograde oils. As a result, they thicken much faster than comparable multigrade oils as the temperature drops. They thin out uniformly over a temperature spectrum as the temperature rises (SAE 30) (Oil 2021). Since there are no viscosity index improvers in monograde engine oils, shear is not a problem. Most manufacturers will define a Summer and Winter oil viscosity grade for their vehicles before introducing multigrade oils. Both were Mono Grade viscosities, with a lower viscosity in the winter (SAE 30) and a higher viscosity in the summer (SAE 50). Summer and Winter grades were made obsolete with the advent of Multigrade oils, which allowed for a starting viscosity and a high temperature running viscosity.

7.9   Grease

Grease is a solid to semi-solid liquid made from oil, and a thickening agent blended up to 35%.Grease is typically used on equipment that operates daily or has been in storage for a long time. Since the grease is still there, a lubricating film will form almost instantly. Machinery that is difficult to lubricate regularly. High-quality greases can lubricate disconnected or difficult-to-reach components for extended periods without requiring re-filling. These greases are also found in permanently sealed systems, including electric motors and gearboxes. Extreme conditions necessitate special devices, such as high temperatures and stresses, shock loads, or slow speeds under heavy loads. Components that are worn out (Wright 2021). Grease can prolong the life of worn parts previously lubricated with oil by retaining thicker films in clearances widened by wear.

Grease acts as a sealant, preventing leakage and keeping pollutants out. Grease serves as a sealant to avoid lubricant leakage and the entry of corrosive chemicals and foreign materials due to its consistency. It also preserves the efficacy of deteriorated seals. Grease is less complicated to control than gasoline. Oil lubrication can be costly, requiring a complicated system of circulating equipment and retention systems (Wright 2021). On the other hand, grease is easily contained by easy, less expensive containment devices due to its rigidity. Strong lubricants are suspended in grease. In high-temperature or intense high-pressure applications, finely ground solid lubricants, for example, graphite and molybdenum disulfide, are combined with grease. Solids stay suspended in grease, but they settle out of oils. It is not necessary to regulate and track the fluid level.

7.10   Graphene Based Lubrication

Graphene is a 2-D material and offers unique friction (in humid air and dry nitrogen, few layers showed low and stable friction with a frictional coefficient equal to 0.15). It has wear properties that are generally not seen in conventional materials. It has excellent thermal, optical, electrical, and mechanical properties. It can serve both as a colloidal or solid–liquid lubricant. It is highly chemically inert, has too much strength, easily shearable, densely packed, and very smooth surface, making its tribological behavior impressive. Even with many layers, it is very, very thin. Hence, we can apply it to nano or micro-scale systems, such as nanoelectromechanical systems abbreviated as NEMS and microelectrochemical systems abbreviated as MEMS with oscillating, sliding, and rotating contacts reduce wear and friction (Berman et al. 2014).

Graphene is the world's most robust material: graphene has a specific strength of 48 000 kN m kg1, which is over 300 times that of steel (steel specific strength = 154 kN m kg1) while remaining extremely light. Graphene has a high thermal conductivity of about $3000\,W\,mK^{-1}$, compared to $400\,W\,mK^{-1}$ for copper. Graphene can withstand extremely high current densities (a million times higher than copper).

Graphene functionalization makes it very flexible and allows it to be integrated into various devices and materials depending on the application (Davies et al. 2021). It is resistant to any atomic or molecular species except hydrogen ions.

Zhang et al. (2021) have studied multilayer graphene for reducing friction and wear in water-based sand cleaning liquid under a uniform load of 5 N. The effects of various multilayer graphene concentrations on the coefficient of friction (COF) were investigated. Figure 7.1a shows the friction coefficient curves for the various concentration of graphene particles. In Fig. 7.1b, we can divide into two stages, the concentration of multilayer graphene as less than 0.05% and above 0.05%. The wear decreases sharply when the concentration is more than 0.05 percent, indicating that the first step of friction reduction has begun. In the second level of friction reduction, the wear reduces and stabilizes as the concentration increases to 0.5 percent. Viscosity experiments were performed on each solution, and it was discovered that adding graphene to a water-based sand cleaning solvent did not affect its viscosity. As a
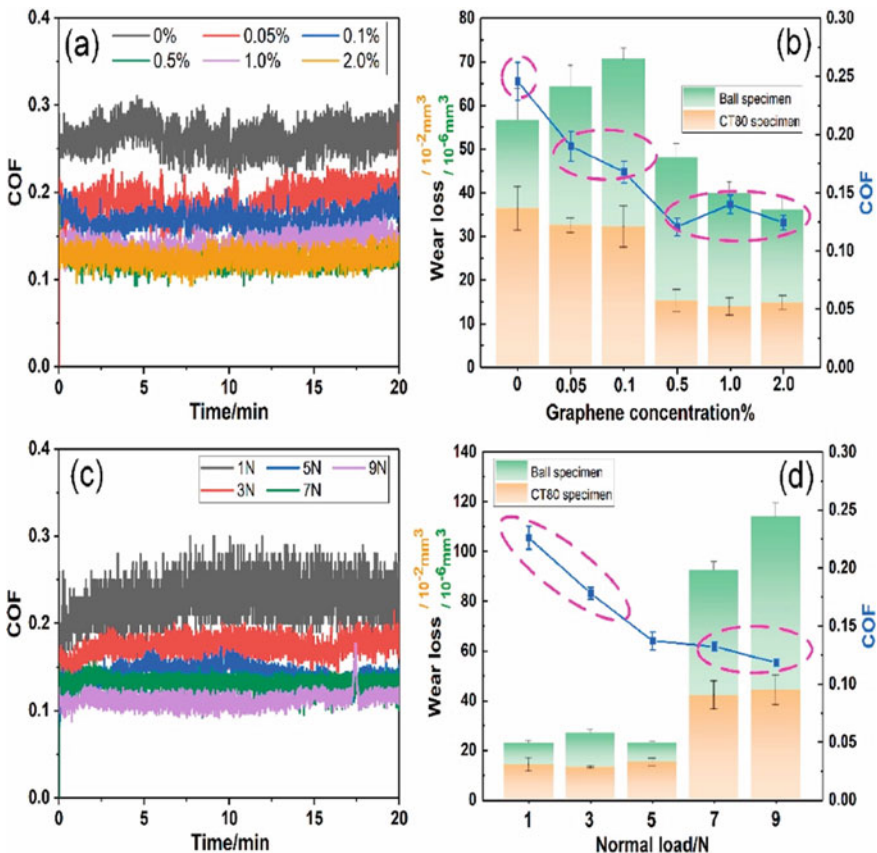

Fig. 7.1 a–d CT80 coiled tubing friction and wear performance with varying concentrations of graphene under different loads. Reprint with permission from Zhang et al. (2021)

result, it's possible that the anti-friction was due to multilayer graphene's lubrication effect. Friction and time curves under various loads can be seen in Fig. 7.1c. Since the COF's vibration amplitude under 1 N is considerably higher than other loads, the friction process occurs only at the rugged peaks of two contact surfaces. In addition, as the normal load rises, the COF gradually decreases in two stages: swift and steady. It's worth remembering that the tipping point is 5 N for both wear loss and COF. The COF decreases to a minimal value of about 0.11 as the load rises to 9 N (see Fig. 7.1d).

Additional wear measurements were carried out using different concentrations and loads, as shown in Fig. 7.2 (Zhang et al. 2021). At various multilayer graphene concentrations, several turning points were found within the continuum of experimental parameters. The turning point changed in the direction of increasing load as the concentration rose. In general, in extreme wear operation, the ultimate load of CT80 content was inversely proportional to the concentration of multilayer graphene.

Figure 7.3 shows how as an additive in a water-based sand cleaning solution, multilayer graphene prevents friction and wear (Zhang et al. 2021). The friction and wear control mechanisms and the formation of the lubrication film are divided into two parts. The addition of sodium cholate dispersant to improve multilayer
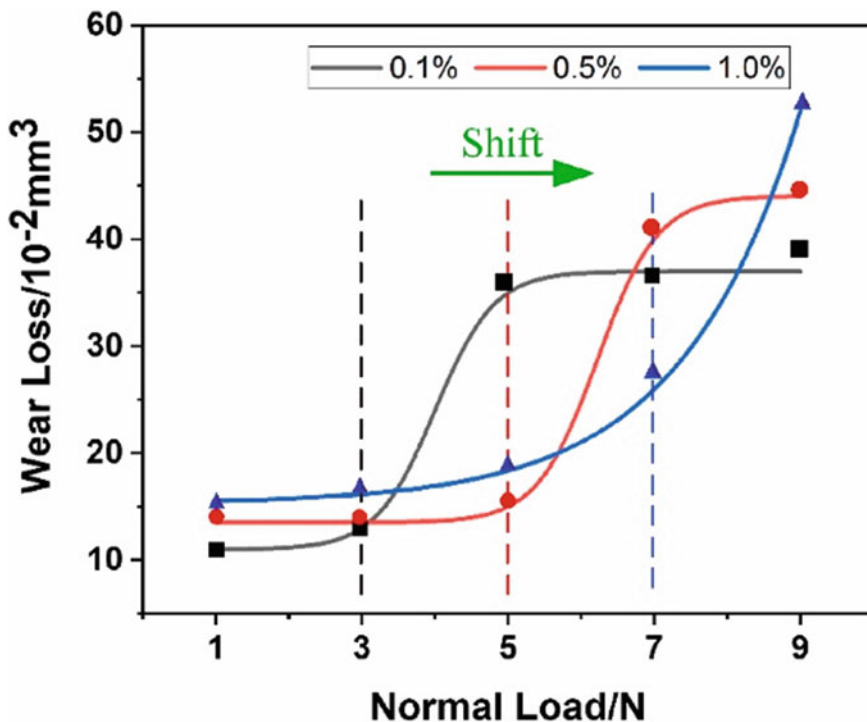

Fig. 7.2 Effect of graphene concentration on the normal load and wear performance. Reprint with permission from Zhang et al. (2021)
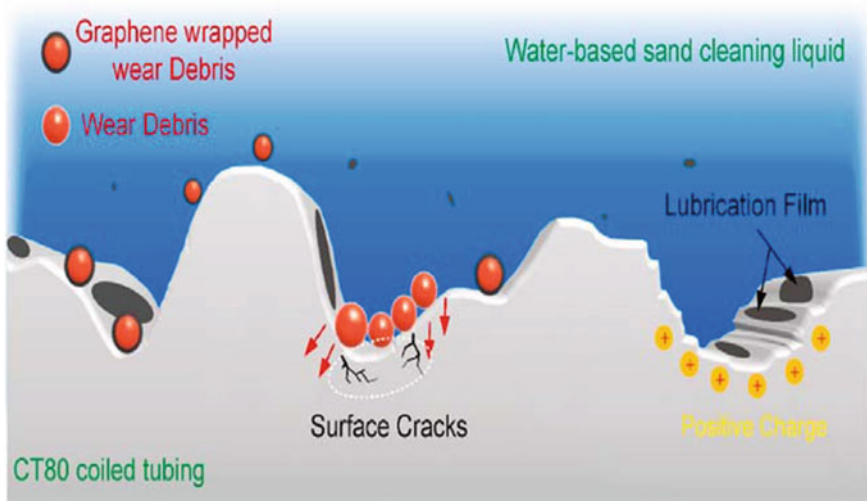
Fig. 7.3 Multilayer graphene as an additive in water-based sand cleaning liquid for friction and wear reduction. Reprint with permission from Zhang et al. (2021)

graphene dispersion performance in water-based sand cleaning liquid for lubrication film formation makes it easier to penetrate the frictional contact zone. The emulsifier molecules can dissociate the anions in the water-based sand cleaning solvent. Static electricity attracts these molecules to multilayer graphene, where they combine with the positively charged metal friction surface to form the graphene lubrication film. Furthermore, unlike deionized water, the water-based sand cleaning solvent contains a surfactant that lowers the solution's surface tension and reduces the angle of interaction with the CT80 coiled tubing content. The hydrophobic and hydrophilic model of the lubricating fluid on the surface of friction helps create a lubricating film on the touch surface. The multilayer graphene will progressively adsorb on the touch surface, creating a lubricating film that can be used to control friction and wear locally. In multilayer graphene, chemical bonds hold C–C atoms together. The force of Van der Waals, combined with an insufficient interlayer force, prevents sliding, lowering shear stress, and improving friction reduction in frictional touch wear resistance. Furthermore, the experiments were conducted in sand cleaning the liquid atmosphere, water-based rather than ordinary deionized water. The abrasive particles produced during the friction process will be suspended in the solution for a more extended period, enabling them to attach to the dispersed multilayer graphene. As a result, the wrapped particles of multilayer graphene can speed up sliding, spinning, or collision action, reducing debris accumulation in the frictional contact region and thereby reducing abrasive wear. Friction often results in a significant number of bruises on the CT80's surface. The appearance of these bruises aggravates the material's wear and tear. While specific multilayer graphene will fill in scratches on a worn surface, reducing wear and friction dramatically. Because of the volatility of

lubricating film-forming, the COF has a lower limit that must be maintained. While multilayer graphene may minimize friction and wear, once the CT80 material has passed the turning point, the load may be the most important factor deciding the wear condition.

7.11 MoS$_2$ Based Lubrication

Charoo et al. (2017) studied tribological Properties of MoS$_2$ Particles as lubricant Additive on EN31 alloy Steel sliding against AISI 52,100 steel ball. The objective was to find the tribological behavior of EN31 alloy steel roller bearings under lubricated conditions with different sizes of MoS$_2$ particles (0.5% to 1%). These particles were suspended in conventional lubricant SAE 20W40. On a tribo-pair consisting of EN31 steel disc and AISI 52,100 steel ball, four sizes of MoS$_2$ particles, such as 35 µm, 7 µm, 3 µm, and 90 nm, were used as additives in the lubricant SAE 20W40.

Tests were conducted at room temperature with a steady sliding speed of 0.03 m/s and various loads to determine the coefficient of friction under dry and lubricated conditions. In contrast, the base lubricant SAE 20W40 was evaluated at the same operational conditions with different amounts of MoS$_2$ particles (0.5 wt percent, 1.0 wt percent). For a 10-min test period, Figs. 7.4, 7.5 and 7.6 indicates the difference in COF of different concentrations of MoS$_2$ additive lubricant under various loading conditions. As opposed to base oil, the lubricant with additives has a lower coefficient of friction. The decrease in COF may be due to the impact of ball bearing, where
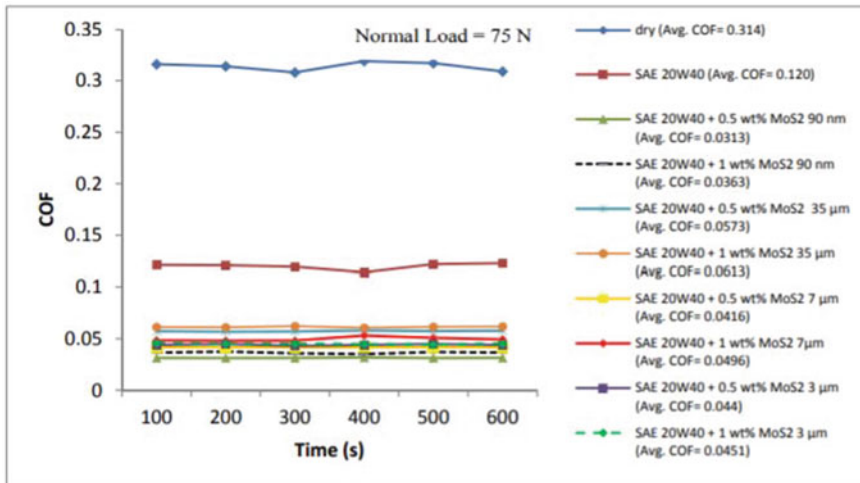
Fig. 7.4 Coefficient of friction performance under the dry and lubricated condition in the presence of MoS$_2$ particles as additives and under normal load of 75 N. Reprint with permission from Charoo et al. (2017)
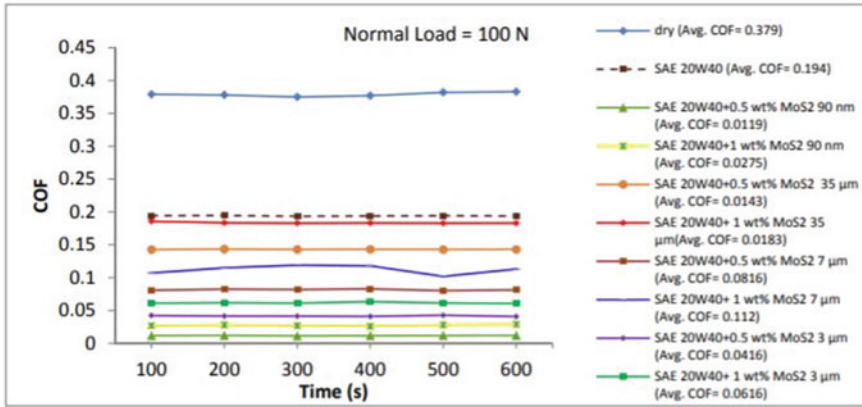
Fig. 7.5 Coefficient of friction performance under the dry and lubricated condition in the presence of MoS$_2$ particles as additives and under normal load of 100 N. Reprint with permission from Charoo et al. (2017)
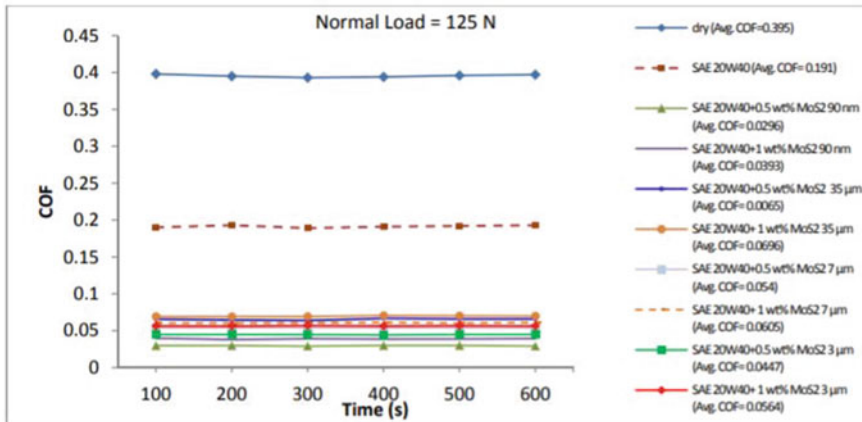
Fig. 7.6 Coefficient of friction performance under the dry and lubricated condition in the presence of MoS$_2$ particles as additives and under normal load of 125 N. Reprint with permission from Charoo et al. (2017)

strong particles scattered in the lubricant on the touching surfaces, based on the findings.

It was also discovered that as the load increased, the coefficient of friction also increased. Increased COF may be caused by a decrease in the thickness of the lubricating film between the touching surfaces while the touches are in the boundary lubrication regime. The magnitude of the COF of MoS$_2$ nanoparticles in lubricant is smaller than the base oil under all loading conditions. It is thought that this is due to the hexagonal configuration of MoS$_2$, where the layers of MoS$_2$ shear off when

a load is applied. These layers form a defensive coating on the surface. Overall, the friction coefficient decreased as the particle size decreased due to the rolling of the small-sized particles in the touch-field. Thus, the concentration of particles, scale, and load in the lubricant SAE 20W40 determine the coefficient of friction.

7.12 Boron Based Lubrication

Wan et al. (2015) investigated the tribological behavior of lubricant oil containing boron nitride (BN) nanoparticles. The friction system's temperature was increased as the test progresses. The viscosity of the lubricating oil, which changes dramatically with temperature, significantly impacts the flow condition and oil film thickness throughout the frictional phase. Figure 7.7 depicts the various viscosities of lubricating oils as a function of BN nanoparticle additives concentration at a shear rate of 100 s^{-1} and temperatures ranging from 20° to 60°. As the temperature increases, the viscosities of all oils, whether without or with the additives of BN nanoparticle, decreases rapidly. Both nano-BN oils, however, showed no significant increase in
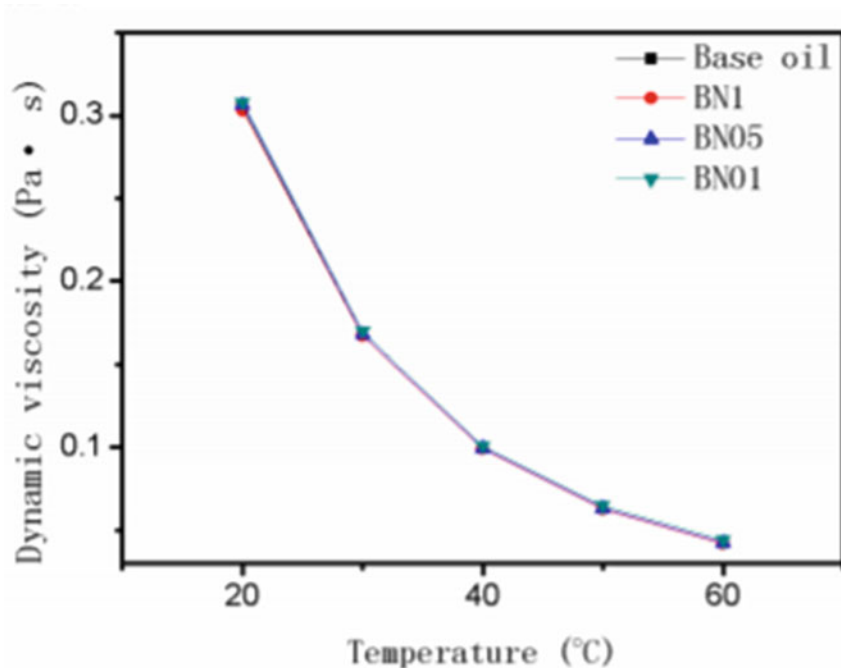
Fig. 7.7 Dynamic viscosity as a function of temperature. Reprint with permission from Wan et al. (2015)
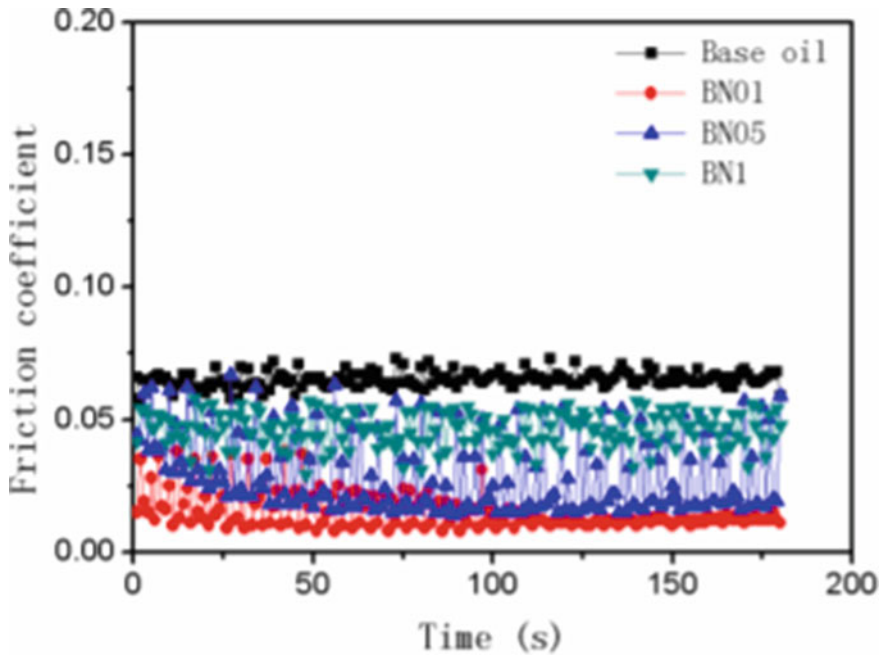
Fig. 7.8 Base oil and nano-BN oil's friction coefficient as a function of time. Reprint with permission from Wan et al. (2015)

viscosity at 1.0 wt.% concentration. It suggests that the viscosity of the lubricant's tribological efficiency can be insignificant at the same temperature.

Figure 7.8 depicts the COF of the nano-BN oils and base oil throughout the frictional procedure. As it is shown, the nano-BN oils friction coefficient values are smaller than that of base oils during the experiment. As the concentration of BN nanoparticle additives grows, the friction coefficient of nano-BN oils rises. The COF curves of samples BN1 and BN05 show noticeable fluctuation with test time, while the curves of sample BN01 appear to remain stable. The average friction coefficients for the base oil, BN01, BN05, and BN1 throughout the experiments were 0.065, 0.047, 0.030, and 0.015, respectively. The COF of BN01, BN05, and BN1 was lowered by 76.9%, 53.8 percent, and 27.7%, respectively, compared to the base oil. Adding BN nanoparticles to the base oil will significantly boost its anti-friction properties.

Viscosity for both the nano-BN oil and the base oil viscosity reduced dramatically as the temperature rose, with little discernible difference between them. Nano-BN oils significantly improved the anti-wear and anti- friction properties of the base oil, and lower nanoparticle concentrations resulted in better tribological efficiency.

Songfeng et al. (2020) had investigated the tribological properties of boron nitride by bioinspired polydopamine modification. Results showed that both hydroxylation and PDA alteration would potentially lower the COF and wear rate of the BN as a

water additive. However, as the testing time lengthens, the friction coefficient has lower COF values. In Fig. 7.9, curves of COF (Fig. 7.9a), average values of COF (Fig. 7.9b), width, and depth of wear (Fig. 7.9c), and the rate of wear (Fig. 7.9d) are seen for water-based lubrication, other mixtures, respectively. The COF raises when BN is applied to water, but the wear pressure, wear distance, and depth decrease. Consequently, BN is a strong wear-resistant substance with a limited effect on reducing friction. Both the BNO and BNO-PDA have lower COF levels than pure water and BN since the BN is oxidized in air and then modified by PDA. The average COF of the BNO-PDA24 is the lowest, while the average COF of the BNO, BNO-PDA6, and BNO-PDA48 are all the same (Fig. 7.9b). However, the COF curves in Fig. 7.9a show that from 1200 to 1800, the COFs of BNO-PDA are lower than those of BNO. In terms of friction reduction, the PDA changed BNO outperforms the unmodified BNO after the additional testing time. As seen in Fig. 7.9c and d, the BNO-PDA and BNO have narrower wear depths, widths, and rates than water and BN Fig. 7.9d.

Furthermore, in terms of distance, depth, and pace, the BNO-PDA6 shows the least amount of wear. The BNO-PDA24 and BNO-PDA48, on the other side, reveal more wear than the BNO, which may be attributed to the severe PDA modification, and can quickly result in wear residue. According to the tribological studies, both the BNO-PDA and BNO have good tribological behavior compared to BN. As the testing period increases, however, all BNO-PDA samples display lower COF values than BNO.

7.13 Boric Acid Based Lubrication

The friction and wear performance of boric acid lubricant in extended duration operations were evaluated by Deshmukh et al. (2006). Extended wear tests established the relative efficacy of boric acid. The calculated COF values were plotted as a function of the sliding distance for all of the lubrication cases examined to provide a benchmark for performance comparison. The sliding of the base materials in the absence of lubricant resulted in the highest COF over the measured sliding distance (Fig. 7.10). The COF rose exponentially from 0.125 to more than 0.6 at a distance of 2000 m. This tendency can be clarified by the fact that there is significant asperity activity between components in the absence of lubricant. As steady-state sliding is achieved, the levels of sliding resistance down with time as the peaks of the disk asperities plastically distort to become more rounded, as seen in the chart. These work-hardened rounded peaks provide consistent resistance to slipping motion and enable a low-shear-strength lead film to form naturally inside the interface to provide some lubrication. The creation of soft lead films, on the other hand, had little effect on minimizing friction during the experiments.

As shown in Fig. 7.11, the COF in the combined canola oil and boric acid tests were equal to the transmission oil and combined transmission fluid and boric acid
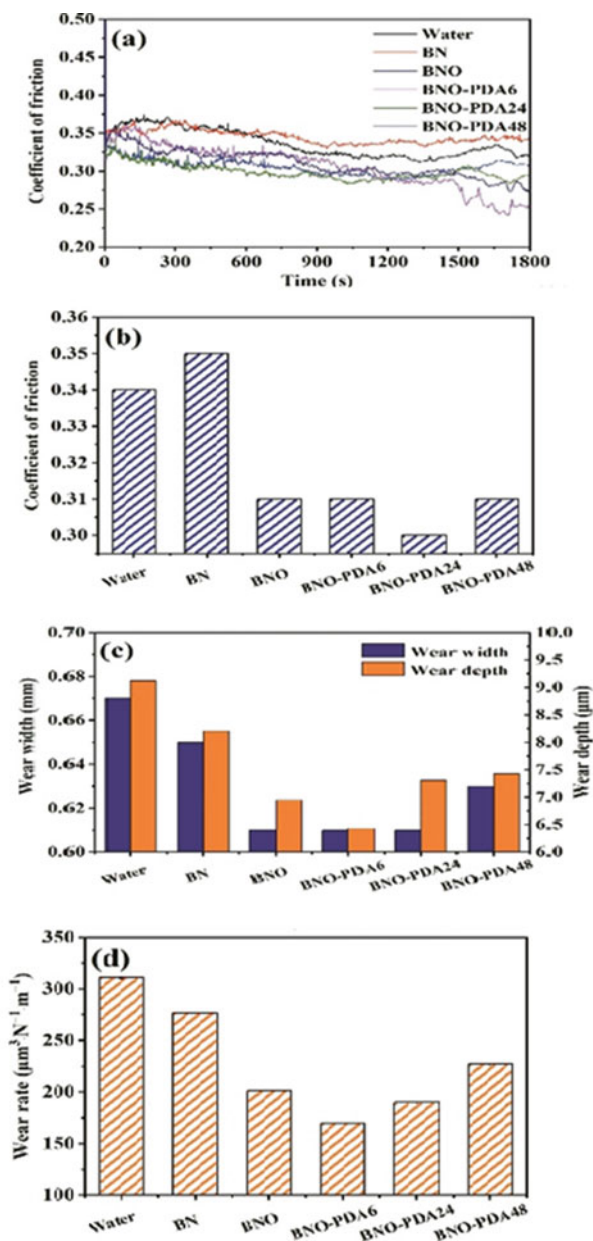
Fig. 7.9 **a** Friction coefficient curves, **b** average values of COF, **c** width and depth of wear, and **d** wear rates of water and all samples. Reprint with permission from Songfeng et al. (2020)
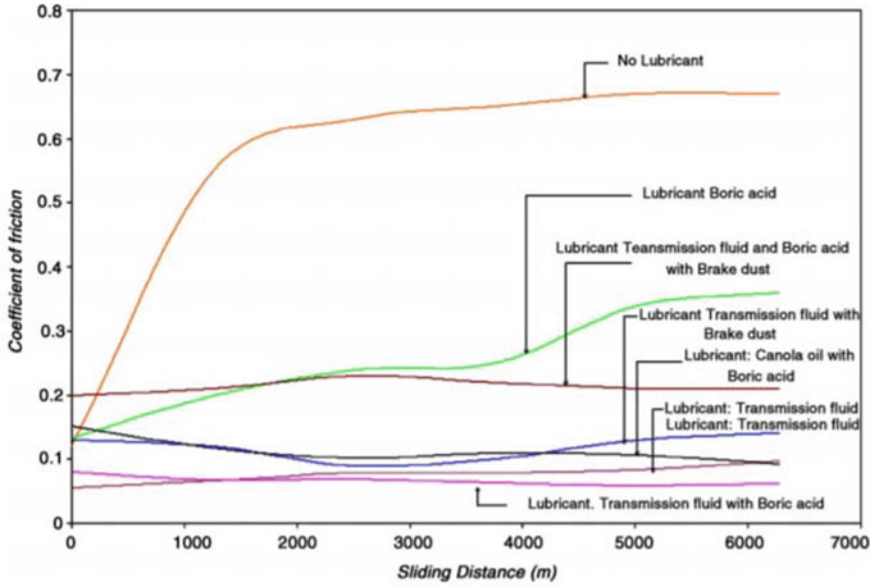
Fig. 7.10 Variation of coefficient of friction with sliding distance. Reprint with permission from Deshmukh et al.(2006)
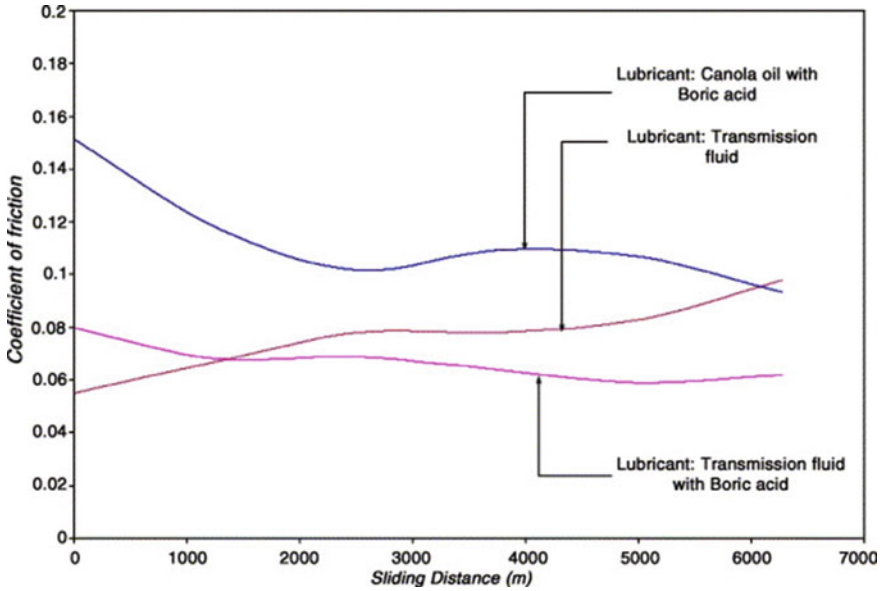

Fig. 7.11 Boric acid and canola oil friction results. Reprint with permission from Deshmukh et al. (2006)

Fig. 7.12 Wear scar of boric acid and canola oil. Reprint with permission from Deshmukh et al. (2006)
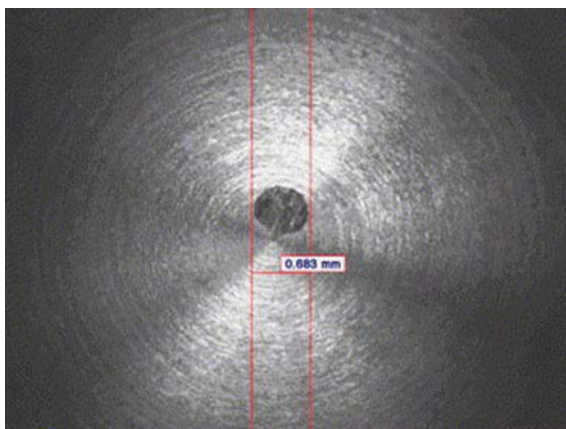
(Deshmukh et al. 2006). The lubricant mixture of boric acid and canola oil demonstrated little deterioration across the full spectrum of sliding samples, which was a fascinating trend. In particular, the all-natural lubricant mixture had a consistently declining COF value during the conditions evaluated, unlike all of the other lubricants. The COF in the boric acid and canola oil case reduced under 0.1 at the end of the slipping experiments, lower than the transmission fluid-only case (Fig. 7.11). The average wear efficiency of the natural lubricant mixture was more remarkable than the friction activity of the canola oil and boric acid combination.

The mixture of canola oil and boric acid generated the least wear rate among all tested lubricants (Fig. 7.12). In reality, compared to the next best case of transmission fluid and boric acid, the wear incidence was nearly 50% lower. The fact that the boric acid and canola oil did not decay over the full spectrum of sliding tests accounts for the improved wear efficiency. This is important since the lubricant will be used in long-term installations where replenishment is impossible. Furthermore, it demonstrates that the lubricant mixture could be utilized in various other uses, including industrial processes where disposal of non-environmentally safe lubricants is sometimes prohibitively costly. However, it is necessary to note that the natural lubricant mixture cannot be used unless further research has been completed. Both boric acid and canola oil, for example, are considered to degrade at high temperatures, limiting their use in industrial processes to stamping operations.

Boric acid proved to be an insufficient lubricant during sliding tests, especially when it came to wear. The bad wear quality is attributed to the assumption that if the boric acid in the touch interface is not replenished, it is quickly squeezed out. Additionally, the boric acid is assumed to inhibit the natural formation of a film of lead between the copper components of the brake valve assembly. The synthesis of boric acid and canola oil was tested as an environmentally safe lubricant. This lubricant also has good wear properties and has been suggested as a natural lubricant solution in some engineering applications.

7.14 Tungsten Disulfide Based Lubrication

Paturi et al. (2016) had conducted measurement and analysis of surface roughness for WS$_2$ solid lubricant-assisted minimum quantity lubrication (MQL). Turning of Inconel 718 experimented for the MQL application, micron-sized tungsten disulfide (WS$_2$) strong lubricant particles were dispersed (0.5 wt.%) in an emulsifier oil-based cutting solution (20:1). Turning experiments were carried out to determine the finished consistency of the machined surface in the presence of WS$_2$ stable lubricant. Using a mathematical design technique, the influence of cutting parameters on the finish quality of the work surface is assessed. Compared to MQL machining alone, results indicate that the surface strength of machined work content improved by around 35 percent during WS$_2$ solid lubricant-assisted MQL machining.

The residuals were plotted in Figs. 7.13 and 7.14 (Paturi et al. 2016) against the estimated surface roughness using the Anderson–Darling test and normal probability plots for MQL machining and WS$_2$ strong lubricant assisted MQL machining, respectively. Both Figs. 7.13 and 7.14 show data that roughly resembles the straight line. The null hypothesis is that the data distribution law is normal, whereas the alternate hypothesis is non-normal. If the *p*-value is more significant than 0.05 (level of significance), the null hypothesis cannot be rejected (i.e., the data follow a normal distribution). Consequently, the models proposed for estimating the surface finish state of machined work content are adequate in both the machining and
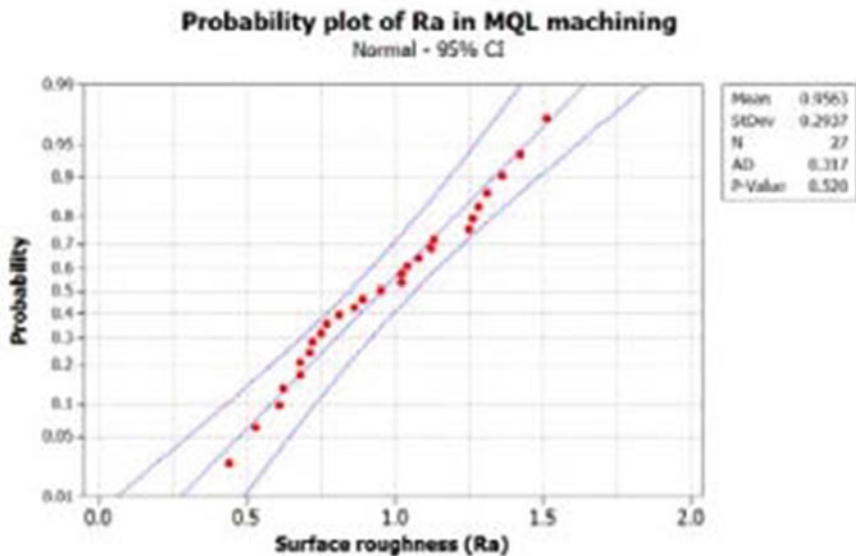
Fig. 7.13 In MQL machining, normal probability plots for average surface roughness (Ra) calculated on the machine work material. Reprint with permission from Paturi et al. (2016)
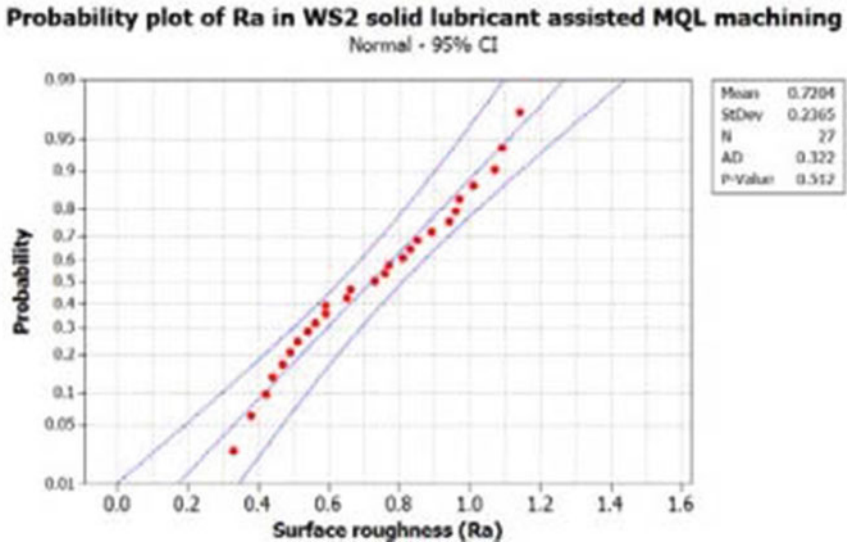
Fig. 7.14 In WS$_2$ strong lubricant aided MQL machining, normal probability plots for average surface roughness (Ra) measured on the machine work material. Reprint with permission from Paturi et al. (2016)

the machining. Consequently, it seems that WS$_2$ strong lubricant may be added to emulsifier oil-based cutting fluids as a potential additive.

Aldana et al. (2016) studied the WS$_2$ nanoparticle's anti-wear and friction-reducing properties on the rough surfaces in the presence of ZDDP additive. The effect of WS$_2$ nanoparticles used as lubricant additives in PAO alone and the presence of ZDDP additive on the lubrication of rough surfaces was examined at 100 °C under the boundary lubrication regime. Compared to PAO base oil, the use of nanoparticles in PAO base oil eliminates wear and friction. The effect of WS$_2$ nanoparticles on rough surface lubrication was first tested in a base oil. Under the same test conditions, the findings were similar to those obtained when the surfaces were lubricated solely with PAO. Figure 7.15 shows the friction curves for PAO and WS$_2$ immersed nanoparticles in PAO oil. The friction performance was highly repeatable. The PAO alone had a COF of around 0.37 ± 0.02, while the sample comprising the nanoparticles had a COF of around 0.10 ± 0.01. This suggests that using tungsten disulfide nanoparticles in the lubrication of rough surfaces can result in a 70 percent reduction in friction. Previous experiments utilizing the same WS$_2$ nanoparticles used in this analysis, carried under the same conditions and on smooth surfaces, produced a COF of 0.08 percent. Figure 7.16 shows wear scars on the pins after sliding. The pin lubricated with PAO had a wear scar diameter of around 630 µm, while the probe with nanoparticles had a wear scar diameter of around 230 µm. This demonstrates that wear is significantly decreased in a later stage. When lubricating the surfaces with nanoparticles instead of only base oil, the results proved that both COF and wear could be decreased by about 70%.
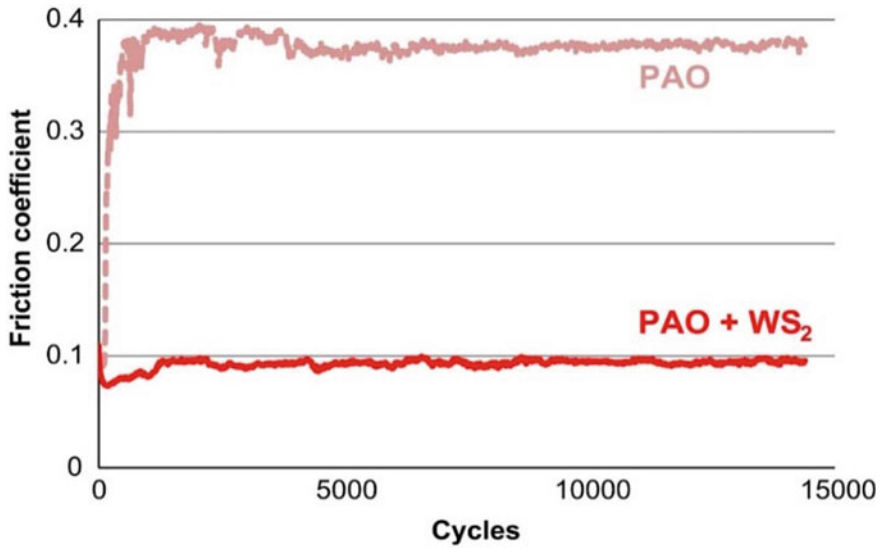
Fig. 7.15 Friction curves at 100 °C for the reference sample (PAO) and nanoparticles immersed in PAO. Reprint with permission from Aldana et al. (2016)
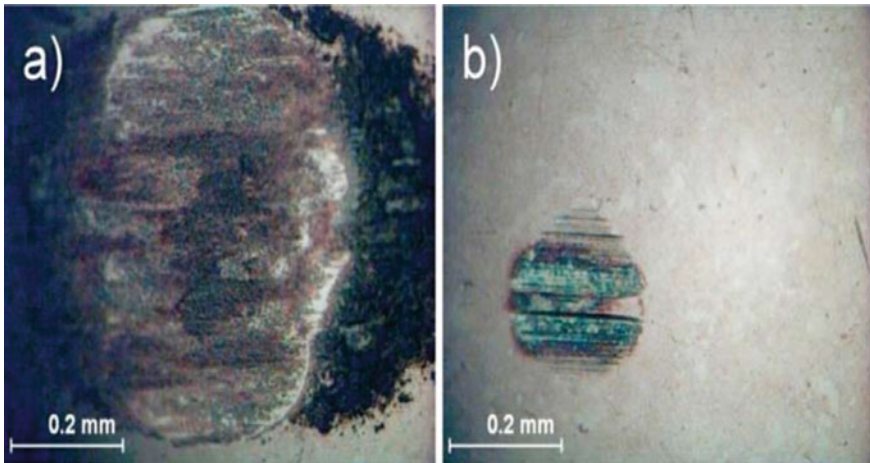
Fig. 7.16 Wear scars after friction testing on rugged surfaces at 100 °C. (a) PAO alone and (b) WS$_2$ in PAO base oil. Reprint with permission from Aldana et al. (2016)

7.15 Lubrication of Rail Track Components

By reducing wear and tear, the lubrication of various track components extends their longevity. To raise visibility and ensure that proper practices are adhered to in the

sector (https://rdso.indianrailways.gov.in/Lubrication). It is essential to adhere to the following lubricant instructions:

7.15.1   Lubricating Elastic Rail Clip (ERC) CLIPS

ERCs with MCI inserts should be greased and oiled on a routine basis to avoid degradation and capture. Material required is Graphite grease of IS-408–1981. There are some specific instructions (https://rdso.indianrailways.gov.in/Lubrication):

- Grease cannot be applied during the hot summer months or when there is a lot of rain.
- Only one ERC can be taken down at the moment. To be sure of this, one pre-greased key should be carried by the keyman corresponding ERC greased with a '0' number grease composed of a graphite
- Oiling and greasing can be done by Keyman @ 20 sleepers, i.e., 80 ERCs per day.
- Extra men may be hired to grease ERCs to complement Keyman's efforts, as Keyman will not be able to finish the job on his own.
- If ERC mass lubrication is used, at least 15 sleepers must remain intact between two sleepers where ERC has been removed.
- ERC should be lengthened to its original length.

  The procedure should be followed as:

- After removing the ERC, clean the eye of the insert with an appropriate brush. Clean the inside of the insert with this brush. With a wire brush and emery paper, clean the rail foot below the liner spot. Wire brush and emery paper can be used to clean the ERCs.
- After brushing, grease graphite should be added to the inside of the insert's eye and the ERC's Ieg.
- The ERC should be switched from inside and outside.

7.15.2   Greasing and Sealing Linear Contact Area

After washing, the rail liner seat in corrosion-prone areas should be greased with graphite grease according to RDSO specifications. Greasing and sealing liner touch areas shall be performed once a year on the gauge face side and once every two years on the non-gauge face of rail to avoid the ingress of toilet droppings in the space between the liner and rail foot.

7.15.3 Lubricating Switch Expansion Joints (SEJs)

The frequency of lubrication should be fortnightly. There are some specific instructions:

- The SEJ will be oiled and greased by Keyman.
- If required, Keyman will check and tighten fastenings at SEJ.
- When the LWR is distressed, the following method for oiling and greasing the SEJ under traffic control must be followed.

  The procedure should be followed as:

- Oiling and greasing the tongue and stock rails of the SEJ and securing the fastenings must all be performed at the same time. The keyman is responsible for oiling and greasing the SEJ regularly without dismantling or interfering with it. Externally, on the fishing planes of various sections of SEJ, the required oil/grease should be added.
- Complete oiling and greasing of SEJ shall be performed only when the concerned Long Welded Rail (LWR) is de-stressed by dismantling the SEJ. The work must be completed in the order outlined below under traffic block:

(i)   SEJ's nuts and chairs must be replaced.
(ii)   After cleaning the faces with a wire brush, a gap between the tongue and the stock rail must be formed, and their interfaces must be greased.
(iii)   Chair and tongue rail interfaces and chair and stock rail interfaces should be greased during brushing.
(iv)   The tongue rail stock must be reset.
(v)   After removing the seats, the bolts and nuts must be oiled and tightened.

7.15.4 Lubricating Point and Crossings

Tongue Rail: Once a week, grease the gauge face of tongue tracks, the outer rail of the turn-in-curve, and the emergency cross-over.

Cleaning and lubricating points:

(i)   Signal workers for points interlocked with signals or provided with locks must regularly clean and lubricate slide chairs. (Usually up to the third sleeper from the switch's toe).
(ii)   SSE/P Way on hand-operated stages, with the remaining slide chairs of all points interlocked with signals or fitted with locks.
(iii)   Frequency: Every two weeks.
(iv)   In addition to those mentioned above, oiling brackets and lugs can be performed simultaneously, as the touch area of these members with the stretcher bar erodes, causing the thickness of stretcher bar bolts to decrease and jam.

7.15.5 Lubricating Rail Joints

Purpose: To help expand rail joints and reduce wear on the rails' and fish plate's fishing planes. Allow for visual inspection of rail ends for any cracks or flaws. One of the ways to avoid low joints is to reduce the wear on fishing flights.

Frequency:

(i) Once a year, after the monsoon, during the coldest month of the year (i.e., from October to February).
(ii) When the rail temperature is between td + 150C and td-150C, and the average distance value is between 3 and 12 mm, the joints in buffer rails must be lubricated twice a year.
(iii) Keyman provides spare joggle fishplates for use in an emergency once a month.
(iv) Joggle fishplates: Once a year, following the monsoon season.

Material: Plumbago (graphite) and kerosene oil made into a hard paste. Fish bolts and nuts can be made of black or recycled oil. The following is the material minimum in kilograms for 100 single joints:

- Plumbago—5kgs
- Kerosine oil—3.5 kg
- Black or reclaimed oil—2.75 kg

There are some specific instructions:

(i) Lubrication should not be performed in excessively hot or cold conditions or while it is raining.
(ii) Creep in heavy areas must be adjusted before joint lubrication.
(iii) Rail joint lubrication is usually done by a permanent way gang under the close direction of a trained permanent way supervisor.
(iv) According to IRPWM 806 (2), the lubrication work should be done under a warning order and the safety of engineering signals.
(v) At no point can two consecutive joints on the same rail or two opposite joints be opened for lubrication. If working, two gangmen could sit diagonally opposite joints facing the direction of the rail.
(vi) Each gangmen lubricating rail joint should also have a magnifying glass and a mirror on hand to check rails for cracks or defects.
(vii) Lubrication should be done in such a manner that after lubrication, all bolt heads should be on the inner side in even years and on the outer side in odd years.

The procedure should be followed as:

Greasing the fishing planes of rails and fish plates and oiling the fish bolts were all part of the rail joint lubrication process. This can be done in the following manner:

(i) Unscrew the nuts and mount them on the opposite side of each bolt to prevent them from interchanging when being reinstalled.
(ii) Remove the inside fishplate by lightly tapping it.

(iii) Use a wire brush to clean the fishing surface of the rails and fish plate, then use waste cotton to scrub away the rust.

(iv) Using a magnifying glass and a mirror, examine the rails and the fish plate's cleaned surface for any cracks.

(v) Paint a thin coat of plumbago and kerosene oil mixed to make a fine paste on the rail's fishing planes and fish plates.

(vi) Remove the fish bolts one at a time and oil them before reinstalling them in the opposite direction.

(vii) Clear the outside fish plate with a light tap.

(viii) Treat the other fish plate and the rails' fishing surface in the same manner.

(ix) Substitute a fish plate and nuts. Tighten the inner two bolts first, without over-stretching the bolts, with the regular fish bolts spanner to the most significant degree possible.

(x) Care should be taken to ensure that there is only one fish plate and at least three fish bolts without the two rails being linked.

   When a train approaches the worksite, all fish plates should be mounted, and at least one fish bolt and nut on either side of each joint should be tightened. This must be completed before the worksite's banner flag is requested to be replaced.

(xi) Specifics of lubrication work completed with dates should be registered in the Permanent Way Inspector's section Register.

7.15.6 Certificate of Lubrication

SSE/P Way should apply a Certificate of lubrication of fish-plated joints with exceptions, if any, to the Assistant Engineer every year in April (https://rdso.indianrailways.gov.in/Lubrication). AENs can forward copies of these licenses, along with statements, to the DEN/Sr. DEN/DSE for review and record.

7.16 Conclusions and Future Directions

The present study focuses on the lubrication system which is currently being used in Indian Railways. It discusses the benefits of lubricating the materials in contact, such as friction, wear, surface roughness, viscosity, etc. This work discusses the effects of various multilayer graphene concentrations on the COF performance of graphene. It shows that as the load increases, the COF value decreases. Additional experiments were performed on other turning points based on the concentration and load parameters which showed that the ultimate load of CT80 material in intense wear activity was inversely proportional to the concentration of multilayer graphene. The tribological behavior of MoS_2 was also discussed. Results suggest the difference in friction coefficient of different concentrations of MoS_2 additive lubricant under various loading

conditions. As opposed to base oil, the lubricant with additives has a lower coefficient of friction. Boron nitride tribological performance is also discussed in this paper. The friction system's temperature rises as the test progresses. The viscosity of the lubricating oil, which changes dramatically with temperature, significantly impacts the flow condition and oil film thickness throughout the frictional phase. The complex viscosities of lubricating oils as a feature of the concentration of BN nanoparticle additives at a shear rate of 100 s^{-1} for temperature varying from 20 to 60 °C were studied. As predicted, the viscosities of all oils, whether with or without BN nanoparticle additives, decrease rapidly as the temperature rises. The calculated friction coefficient values of BN were plotted as a function of the sliding distance for all of the lubrication cases, examined to create a benchmark for output comparison. The sliding of the base materials in the absence of a lubricant generated the highest friction coefficients. At a distance of 2000 m, the coefficient of friction increased rapidly from 0.125 to more than 0.6. The creation of soft lead films, on the other hand, had little effect on minimizing friction during the experiments. The tungsten disulfide tribological performance was studied at 100 °C under the boundary lubrication regime. The effect of WS_2 nanoparticles was used as lubricant additives in PAO alone and the presence of ZDDP additive on rough surfaces to study their tribological properties. Compared to PAO base oil, the use of nanoparticles in PAO base oil eliminates both wear and friction by about 70%. The various procedures for track lubrications such as ERC clips, points, and crossings are suggested for better lubrication. In the future, more complex nanocomposites with different materials can be used to make ternary composites for lubrication. Other compositions, including self-lubricating materials, can also play an essential role in manufacturing lubricants to reduce friction.

References

Ahammed N, Asirvatham L, Wongwises S (2015) Effect of volume concentration and temperature on viscosity and surface tension of graphene–water nanofluid for heat transfer applications. J Therm Anal Calorim 123(2):1399–1409

Aldana P, Dassenoy F, Vacher BL, Mogne T, Thiebaut B (2016) WS_2 nanoparticles anti-wear and friction reducing properties on rough surfaces in the presence of ZDDP additive. Tribol Int 102:213–221

Base Oil Groups Explained (2021) https://www.machinerylubrication.com/Read/29113/base-oil-groups, Accessed 05 Apr 2021

Base oil (2021) https://en.wikipedia.org/wiki/Base_oil. Accessed 05 Apr 2021

Berman D, Erdemir A, Sumant A (2014) Graphene: a new emerging lubricant. Mater Today 17(1):31–42

Charoo M, Wani M, Hanief M, Rather M (2017) Tribological properties of MoS_2 particles as lubricant additive on EN31 alloy steel and AISI 52100 steel ball. Mater Today Proc 4(9):9967–9971

Davies P, Tzalenchuk A, Wiper P, Walton S (2021) Summary of graphene (and related compounds) chemical and physical properties. Accessed 16 Apr 2021

Deepika (2020) Nanotechnology implications for high performance lubricants. SN Appl Sci 2(6):1128

Deshmukh P, Lovell M, Sawyer W, Mobley A (2006) On the friction and wear performance of boric acid lubricant combinations in extended duration operations. Wear 260(11–12):1295–1304

How Lubricants Combat Friction and Wear. Accessed 20 Mar 2021

A Guide to Measuring Oil Viscosity (2021). https://www.azom.com/article.aspx?ArticleID=12878. Accessed 15 Mar 2021

Herschel W (1922) The change in viscosity of oils with the temperature. J Ind Eng Chem 14(8):715–722

https://rdso.indianrailways.gov.in/Lubrication of Track Components. Accessed 04 July 2021

Jain A (2021) Implementation of Gauge Face Lubrication on Mountainous Tracks on Indian Railways. http://www.iricen.gov.in/iricen/ipwe_seminar/2011/anirudh_jain_8.pdf, last Accessed 16 Apr 2021

Lubricant (2021). https://en.wikipedia.org/wiki/Lubricant. Accessed 05 Apr 2021

Lubrication increases the efficiency and life-expectancy of machines. Accessed 20 Mar 2021

Mang T, Dresel W (2007) Lubricants and lubrications, 2nd edn. Wiley VCH, Weinheim

Penrite Oil (2021) https://www.penriteoil.com.au/knowledge-centre/Engine%20Oil%20Types/189/what-is-the-difference-between-multigrade-and-monograde-oils/411. Accessed 15 Mar 2021

Paturi U, Maddu Y, Maruri R, Narala S (2016) Measurement and analysis of surface roughness in WS2 solid lubricant assisted minimum quantity lubrication (MQL) turning of inconel 718. Proc CIRP 40:138–143

Pitfalls of manual lubrication. Accessed 20 Mar 2021

7 Significant advantages of automatic lubrication. Accessed 20 Mar 2021

Songfeng E, Ye X, Wang M, Huang J, Ma Q, Jin Z, Ning D, Lu Z (2020) Enhancing the tribological properties of boron nitride by bioinspired polydopamine modification. Appl Surf Sci 529:147054

Vattikuti S, Byon C (2015) Synthesis and characterization of molybdenum disulfide nanoflowers and nanosheets: nanotribology. J Nanomater 2015:1–11

Wan Q, Jin Y, Sun P, Ding Y (2015) Tribological behaviour of a lubricant oil containing boron nitride nanoparticles. Proc Eng 102:1038–1045

Wright J (2021) Grease basics. https://www.machinerylubrication.com/Read/1352/grease-basics. Accessed 13 Mar 2021

Zhang Z, Guo Y, Han F, Wang D, Zhang S (2021) Multilayer graphene for reducing friction and wear in water-based sand cleaning liquid. Wear 470–471:203619

Chapter 8
The Effect of Friction Induced Noise, Vibration, Wear and Acoustical Behavior on Rough Surface: A Review on Industrial Perspective

S. K. Tiwari and L. A. Kumaraswamidhas

Abstract This paper presents in-depth review on the influence of friction, noise, vibration and acoustical behavior and their relationship with different approaches in past. The interdependencies and effect of friction induced noise, vibration and acoustical behavior are analyzed on the rough surface at different asperitical level. The origination of frictional (noise, vibration, acoustical behavior), its dependencies on rough surface under different wear conditions are critically reviewed. The review concludes that an analytical and computational modelling approach is necessary to study the effect of friction induced noise, vibration and acoustical behavior on the rough surface.

Keywords Friction induced noise · Vibration · Wear · Acoustical emission · Rough surface

8.1 Introduction

Frictional noise is easily produced if the vibration is generated between two rough surfaces. Noise is called flutter, chatter when f < = 1 kHz while noise is called squeal when f = 1−20 kHz (Akay 2002). The noise with low pressure level can be easily controlled, while the noise with high pressure level, e.g., automobile brake, wheel of mass transient system, mechanical gear, sliding bearing, gearboxes, artificial joint, hinge joint may create many challenges (Ghazaly et al. 2014; Kang and Kim 2010; Kang 2015, 2011; Sinou et al. 2013; Nam et al. 2016). Frictional noise is transient and unsteady in nature and depend on many factors. As per some research, the phenomenon of surface topography is the main reason in creation of noise. Rusli and Okama (2007) investigated contact parameters of the structure and suggested that surface topology can affect frictional noise by destabilizing the system mode coupling. Ben Abdelounis et al. (2010) established numerical models using ABAQUS with varying roughness parameters. The study estimated vibration level at different nodes to calculate the changing trend of sliding speed and surface roughness with

S. K. Tiwari (✉) · L. A. Kumaraswamidhas
Indian Institute of Technology (ISM), Dhanbad 826 001, India

frictional noise. Eriksson et al. (1999) performed analysis on relationship between generation of squeals and surface topography. Bergman et al. (1999) studied about the influence of short blasted disc in origination of brake squeal and this squeal can be generated when the coefficient of friction exceeds the critical value of 0.4. However, considering the complexity, there is a need to find an optimum way for reduction of squeal, based on the irregular characteristics of topography and correlation of microscopic surface topography. The frictional noise is often called roughness noise when surface roughness is exposed to normal vibration. There are some studies on the effects of surface roughness on friction induced noise (Abdelounis et al. 2010, 2011; Othman and Elkholy 1990; Othman et al. 1990; Dang et al. 2013; Stoimenov et al. 2007; Bartolomeo et al. 2017; Kchaou et al. 2016). Although, the experimental setup of these studies are different but it seems an acceptance to a power law,

$$E_a \propto S_a^\alpha V^\beta \tag{8.1}$$

where, E_a represents the acoustic power, S_a represents the surface roughness and V is the sliding velocity. α and β are the power coefficient. But in certain cases where the friction is induced in the larger surface area, the generalized power law is presented as:

$$E_a \propto S_a^\alpha V^\beta S^{\lambda/10} \tag{8.2}$$

where S is the apparent contact area between the two surfaces/solids. The exponential component λ is expressed in dB/ scale. There has always been distinction between actual and apparent contact areas. In the field of tribology, the friction is relatively supervised through actual contact surface which is well known fact.

Likewise, wear also create several challenges in industry because it reduces the machine life and replacement of machine proves to be very costly (Khan et al. 2009). The friction induced in worn-out surfaces have impact on wear processes. The basic principle of wear processes depends on physical geometrics, type of load applied, surface contact and mechanical properties (Wang et al. 2016). However, some efforts have been made by researchers on empirical relationships (Hadfield and Brebbia 2012). These relationships are accurate and précised based on laboratory measurements and generate wear under real operating conditions (Bayer 1976). Moreover, many wear processes can be explained reasonably and afterwards applied in the industry. But, their accuracy remains questionable when complex situation arises (such as the worn-out components, use of lubrication). This is due to several mechanisms adopted by which wear can occur. Different mathematical models have been advanced to analyse relationship between friction and wear (Blau 2009). This is important because frictional work is linked with roughness changes, wear particle generation, tribo-material evolution, and microstructural alteration (Park and Salmeron 2014). Having a similar coefficient of friction doesn't indicate that frictional processes are identical (Blau 2001). This is due to difference in wear generation. More ever, in other research cases, the generation of wear will impact

frictional processes too and analysed by embedding friction models in wear models. For industrial purpose, Archard's wear model are widely used on analytical work and experimental evidence on wear and friction (Gnecco and Meyer 2015).

Hence, in most of the studies friction, wear, noise and vibration are treated independently and in-depth review of their inter-dependencies is still logging. The main objective of this review is to provide a critical analysis of existing friction induced noise, vibration, wear and tribological models and their dependencies on each other.

8.2 Concept of Physical Contact Surface

The idea behind contact surface is first studied by Bowden et al. (1951). They concluded that the friction between two rough surfaces is generated by the contact between the two asperities. The actual contact area is unalike from the apparent area of contact which is shown in Fig. 8.1.

According to coloumb's first law, the frictional force between the two surfaces is independent of the apparent contact area (Persson et al. 2008). Bowden and Tabor model assumed number of asperities to be constant. Archard (1953) introduced a model defining asperities in terms of load dependent number instead of constant number. Greenwood and Williamson (1966) refined the model introducing an exponential and a guassian distribution of asperities.

The basic idea of friction and wear is the molecular attraction between these asperities for both metal and polymer (Briscoe and Tabor 1972; Myshkin and Kovalev 2009). The Johnson–Kendall–Roberts (JKR) model utilizes hertz model for the elastic solid surfaces to analyse surface energy which create attraction between the surfaces that is shown in the Fig. 8.2. The deformation on the surface are so microscopic that the surface roughness gives a low measurement values. This model can be applied with experimental results for the surface like gelatine and rubber and the deformation varies to such limit that surface roughness become negligible. The another model like DMT model is introduced to analyse the impact of molecular
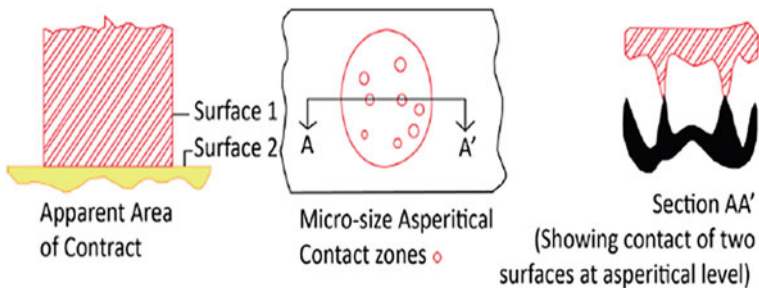
Fig. 8.1 Apparent contact area and real contact area. Permission from Creative Commons CC BY license (Lontin and Khan 2021)
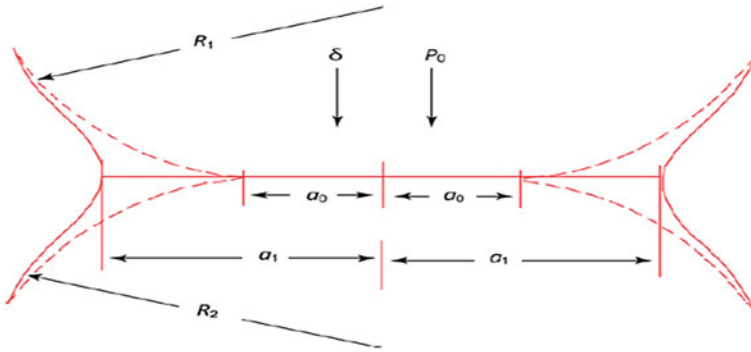
Fig. 8.2 Solid contacts in presence and absence of surface force. Contact radius a_1 in presence of forces and contact radius a_0 in absence of forces. Permission from Creative Commons CC BY license (Lontin and Khan 2021)

interaction and contact deformation between a ball and a plane (Derjaguin et al. 1975). The DMT model is more suited to micro-sized and small metal spheres, that are elastic in nature. An improved model (Muller et al. 1994) which uses Lennard–Jones potential to determine the magnitude of force between two surfaces is shown in Fig. 8.3.

here,

z = distance of two planes and.

z_0 = distance between planes in equilibrium state.

The research analyses that the number of asperities is highly sustained on the real contact area that are contacting on both surfaces. There is no adequate research to know the variation of friction in terms of number of contacting asperities, or noise or vibration and wear processes. The variation in asperitical contacts will influence the
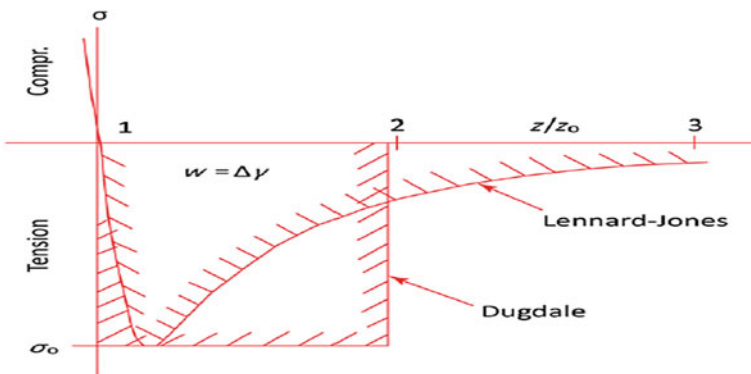
Fig. 8.3 Dugdale and Lennard–Jones approximation. Permission from Creative Commons CC BY license (Lontin and Khan 2021)

frictional processes, noise, vibration, wear, and the tribological behaviour. The investigation of the friction processes at the small level or microscopic level is important so as to understand the true change in asperitical contacts.

8.3 Friction Noise Due to Wear

The noise generated during wear and friction processes are divided into two categories: (1) airborne noise, and (2) acoustic noise. In this section we will discuss about these two categories of noise produced during the friction process. This section will describe about the impact and relationship of airborne/ acoustic noise with respect to the wear process.

8.3.1 Airborne Noise and Wear

The energy is transferred in the form of work done during friction process. This will result in two type of deformation. First is the elastic deformation and second is the plastic deformation. In elastic deformation the energy is transferred into noise while in plastic deformation, the energy is transferred into no noise. Stoimenov and Kato (2003) determined experimentally that wear has an impact in generation of noise. In the study, contact area is monitored using frictional sound analysis. In the analysis, when the load is varied from 1 to 7 N, audible sound is measured in a single pass. The power spectrum is correlated with the distance measured between the lumps as shown in Fig. 8.4.

Chen et al. (2002) categorised squeal generation under wear into four different phases. In the 1st stage, no squeal is produced. In the 2nd stage, squeal is not emitted. In the 3rd stage, squeal is emitted as coefficient of friction increases. In the 4th stage, finally the squeal gets disappear. Some of the researchers studied about the effect of temperature on wear (Hu 2017; Jacko et al. 1984; Newcomb and Spurr 1971; Rhee 1974). As the temperature increases, wear rate also increases exponentially as shown in Fig. 8.5.

8.3.2 Acoustic Emission and Friction

As wear is linked to noise, it is possible to correlate wear with acoustic emission. Acoustic emissions are stress waves produced by the rapid release of strain energy. Boness and McBride (1991) studied about acoustic emission generated in different wear conditions which is shown in Fig. 8.6. In case of unlubricated contact RMS signal is high while for lubricated contact, the RMS signal is low. Boness et al. (1990) studied about the variation of acoustic emission which is shown in Fig. 8.7.
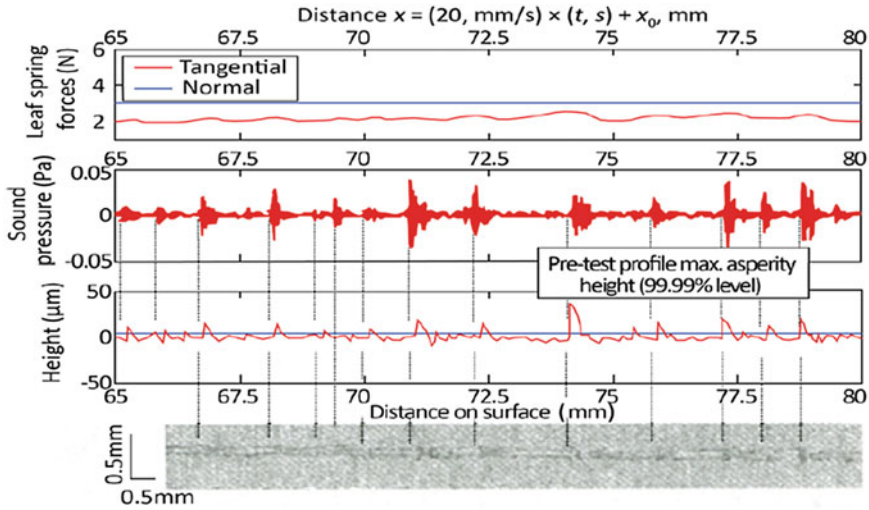
Fig. 8.4 Sound pressure signal together with height and leaf spring force of measured elastic forces. Permission from Creative Commons CC BY license (Lontin and Khan 2021)
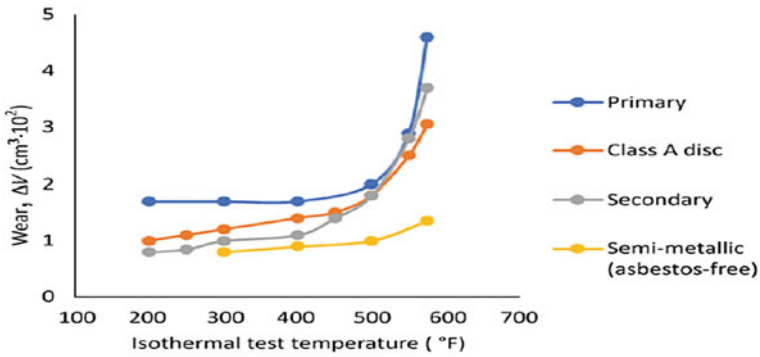
**Fig. 8.5** Variation in wear with isothermal test temperature. Permission from Creative Commons CC BY license (Lontin and Khan 2021)

Benabdallah and Aguilar (2008) investigated about the relationship between wear of surface and acoustic emission. The acoustic emission increases as the frictional coefficient and wear rate increases.
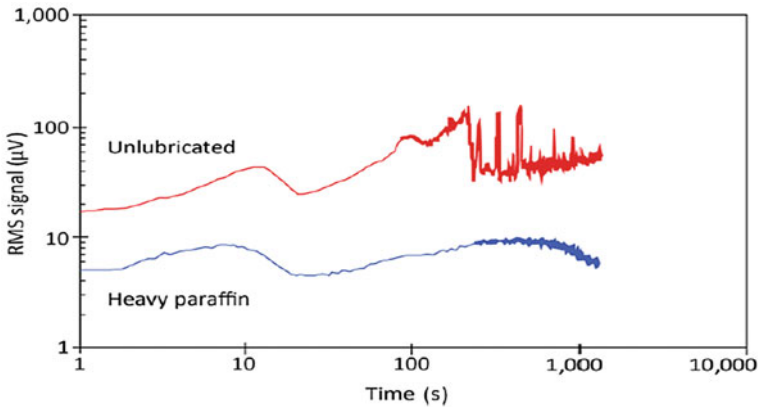
Fig. 8.6 Variation of RMS with time for acoustic emission. Permission from Creative Commons CC BY license (Lontin and Khan 2021)
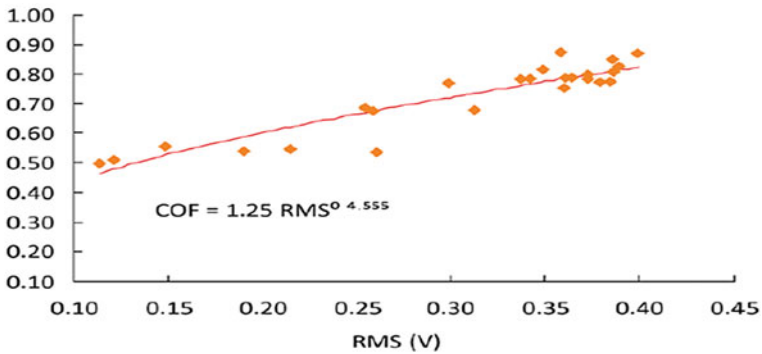
Fig. 8.7 Relationship between RMS value and Coefficient of friction (COF). Permission from Creative Commons CC BY license (Lontin and Khan 2021)

8.4   Modelling Techniques

8.4.1   Wear Models

There has been comprehensive research done on different wear models. Meng and Ludema (1995) and Yadav et al. (2016) provided a brief literature study and the origin of different wear models. The wear depends on lot of factors but all of them are not considered for modelling. Barwell (1958) studied about the wear formation and mechanism related to it in different application domain. The literature illustrates four mechanisms of wear such as scuffing, fretting, corrosion, rolling contacts, and simple sliding. Some of the wear models are used by the researchers is described in Table 8.1.

Table 8.1 Sliding wear models (Lontin and Khan 2021)

Model	Author	Conclusion
Numerical	Shen et al. (2010)	Calculation of parameters are calculated using ABAQUS software
Numerical	Hassan and Mohammed (2016)	Modelling of sliding wear acquires high efficiency using ANN
Empirical	Rhee (1970)	Input parameters are provided and a proper correlation between the parameters proves to be good
Empirical	Archard and Hirst (1956)	Once the equilibrium is reached the model will correlate well
Theoretical	Archard (1959)	The model analyses the flash temperature as a deciding factor during the wear process
Theoretical	Silva and Jr (2008)	The Archard model in terms of (IVP) is modified by initiating an uncertainty on the wear coefficient
Empirical	Quinn (1971)	The model provides better results for the wear in unlubricated conditions of metals
Numerical	Öqvist (2001)	The outcome of this model is exact and quick at each time step
Numerical	Mukras et al. (2009)	The computational time reduces drastically at the end of a cycle in the geometry providing reasonable accuracy
Empirical	Savio et al. (2009)	The surface roughness prediction through the polishing process gives satisfactory result in this model

8.4.2 Friction Models

The main limitation of coulomb law is that it over-simplifies the frictional processes. This is reason that friction models are developed as a substitute to coulomb model. Frictional models are divided into two categories: (1) Emperical models, and (2) Physics-based models which is shown in Table 8.2.

8.4.3 Empherical Models

More advanced version of coulomb model includes strikbeck model and viscous friction model. The stribeck model include frictional force as the function of sliding velocity while viscous friction model includes frictional force as a proportionate to the sliding velocity. But to analyse a complex problem all the features should be allowed for a dynamic behaviour. So most of the models are based on empherical models instead of scientific knowledge models (Mate 2008) and are divided into two

Table 8.2 Physics-based models (Lontin and Khan 2021)

Author	Advantages of the model	Drawbacks
Emami et al. (2017)	Considering the impact of adhesion, the model models provides a good result along with hysteresis	Limited up to certain velocities range
Eriten et al. (2012)	The model deals with friction phenomena which are critical like Damping, stick–slip, and pre-sliding friction. Moreover, the model exhibits characteristics which provide optimum predictive potentiality	The parameters are not dependent on time and needs withdrawal with asperity and surface height and distributions
Dankowicz (1999)	This model can speculate physics-based explanations and dynamics that agrees with other models for the friction processes	The model parameters values determination is a complex task and need to be estimated, along with state variables
Moerlooze et al. 2010)	The model accounts for several studies such as normal creep, pre-sliding hysteresis, static coefficient of friction, frictional lag, Stribeck dynamical oscillations, viscous effect, and stick–slip	Lubrication and Wear are not reviewed in this model

categories: (1) steady state, and (2) dynamic model. The steady state and the dynamic models are summarized as follows in Tables 8.3 and 8.4.

8.5   Conclusion

A comprehensive review on different methods to analyse friction induced noise, vibration, wear and acoustic emission is provided in this paper. This is validated by the experimental and theoretical based studies. A brief discussion of coulomb's models and its categories such as physics- based model and empirical models are developed as an alternative. These models rely on lot of factors which is not understood theoretically. However, the wear models and frictional models are studied experimentally. The existing literature can be utilized by the industry and can provide significant contribution in dealing with the industrial limitation.

Table 8.3 Different dynamic models. Permission from Creative Commons CC BY license (Lontin and Khan 2021)

Model	Parameters	Karnopp (1985)	Canudas de Wit et al. (1995)	Dahl (1968)
Pre-sliding displacement	✔	✘	✔	✔
Coulomb friction	✔	✔	✔	✔
Viscous friction	✔	✔	✔	✔
Negative viscous friction	✔	✘	✔	✔
Rising static friction	✔	✔	✔	✔
Dwell time	✔	✘	✔	✔
Frictional memory	✔	✘	✔	✔
Drawbacks	Complex and non-linear parameters cannot be determined	Some of the parameters are not considered	The results analyses some kind of discrepancies	The study does not deal with Stribeck Effect

Table 8.4 Steady-state models. Permission from Creative Commons CC BY license Permission from Creative Commons CC BY license (Lontin and Khan 2021)

Model	Different friction phenomena	Drawbacks
Tustin Model	Viscous, Coulomb, and Static friction	At maximum or threshold velocity, rupture occurs
Stribeck model	Viscous, Coulomb, and Static friction	Hysteresis and pre-sliding are not found in this model

References

Abdelounis HB, Bot AL, Perret-Liaudet J, Zahouani H (2010) An experimental study on roughness noise of dry rough flat surfaces. Wear 268(1):335–345

Abdelounis HB, Zahouani H, Bot AL, Perret-Liaudet J, Tkaya MB (2011) Numerical simulation of friction noise. Wear 271(3):621–624

Akay (2002) Acoustics of friction. J Acoust Soc Am 111(4):1525–1548

Archard JF (1953) Contact and rubbing of flat surfaces. J Appl Phys 24(8):981–988

Archard JF (1959) The temperature of rubbing surfaces. Wear 2(6):438–455

Archard JF, Hirst W (1956) The wear of metals under unlubricated conditions. Proc R Soc Lond A 236(1206):397–410

Bartolomeo MD, Lacerra G, Baillet L, Chatelet E, Massi F (2017) Parametrical experimental and numerical analysis on friction-induced vibrations by a simple frictional system. Tribol Int 112:47–57

Barwell FT (1958) Wear of metals. Wear 1(4):317–332

Bayer RG (1976) Selection and use of wear tests for metals. ASTM International, West Conshohocken (USA)

Ben Abdelounis H, Le Bot A, Perret-Liaudet J (2010) An experimental study on roughness noise of dry rough flat surfaces. Wear 368:335–345

Benabdallah HS, Aguilar DA (2008) Acoustic emission and its relationship with friction and wear for sliding contact. Tribol T 51(6):738–747

Bergman F, Eriksson M, Jacobson S (1999) Influence of disc topography on generation of brake squeal. Wear 225:621–628

Blau PJ (2001) The significance and use of the friction coefficient. Tribol Int 34(9):585–591

Blau PJ (2009) Embedding wear models into friction models. Tribol Lett 34(1):75–79

Boness RJ, McBride SL (1991) Adhesive and abrasive wear studies using acoustic emission techniques. Wear 149(1–2):41–53

Boness RJ, McBride SL, Sobczyk M (1990) Wear studies using acoustic emission techniques. Tribol Int 23(5):291–295

Bowden FP, Tabor D, Palmer F (1951) The friction and lubrication of solids. Am J Phys 19(7):428–429

Briscoe BJ, Tabor D (1972) Friction and adhesion. Surface forces in friction and adhesion. Faraday Spec Discuss Chem Soc 2: 7–17

Canudas de Wit C, Olsson H, Astrom KJ, Lischinsky P (1995) A new model for control of systems with friction. IEEE Trans Autom Control 40(3):419–425

Chen GX, Zhou ZR, Kapsa P, Vincent L (2002) Effect of surface topography on formation of squeal under reciprocating sliding. Wear 253(3–4):411–423

da Silva CRÁ, Jr PG Jr (2008) Uncertainty analysis on the wear coefficient of Archard model. Tribol Int 41(6):473–481

Dahl PR (1968) A solid friction model. In: Technical Report TOR-0158(3107-18), El Segundo, USA

Dang VH, Perret-Liaudet J, Scheibert J, Bot AL (2013) Direct numerical simulation of the dynamics of sliding rough surfaces. Comput Mech 52(5):1169–1183

Dankowicz H (1999) On the modeling of dynamic friction phenomena. ZAMM 79(6):399–409

de Moerlooze K, Al-Bender F, Van Brussel H (2010) A generalised asperity-based friction model. Tribol Lett 40(1):113–130

Derjaguin BV, Muller VM, Toporov YP (1975) Effect of contact deformations on the adhesion of particles. J Colloid Interface Sci 53(2):314–326

Emami A, Khaleghian S, Su C, Taheri S (2017) Physics-Based friction model with potential application in numerical models for tire-road traction. In: Proceedings of the ASME 2017 dynamic systems and control conference. Tysons, USA

Eriksson M, Bergman F, Jacobson S (1999) Surface characterization of brake pads after running under silent and squealing conditions. Wear 232(2):163–167

Eriten M, Polycarpou AA, Bergman LA (2012) A physics-based friction model and integration to a simple dynamical system. J Vib Acoust 134(5):051012

Ghazaly NM, El-Sharkawy M, Ahmed I (2014) A review of automotive brake squeal mechanisms. J Mech Des Vib 1(1):5–9

Gnecco E, Meyer E (2015) Fundamentals of Friction and Wear on the nano-scale. Springer, Berlin (Germany)

Greenwood JA, Williamson JB (1966) Contact of nominally flat surfaces. Proc R Soc Lond A 295(1442):300–319

Hadfield M, Brebbia CA (2012) Tribology and Design II. WIT Press, Southampton

Hassan AKF, Mohammed S (2016) Artificial neural network model for estimation of wear and temperature in pin-disc contact. Univ J Mech Eng 4(2):39–49

Hu B (2017) Friction and wear of automotive and aircraft brakes. In ASM Handbook. Totten G E, Ed. Materials Park: ASM International, pp 969 –983

Jacko MG, Tsang PHS, Rhee SK (1984) Automotive friction materials evolution during the past decade. Wear 100(1–3):503–515

Kang J (2011) Theoretical model of ball joint squeak. Sound Vib 330(22):5490–5499

Kang J (2015) Friction-induced noise of gear system with lead screw and nut: mode coupling instability. J Sound Vib 356:155–167

Kang J, Kim K (2010) Squeak noise in lead screw systems: self-excited vibration of continuous model. J Sound Vib 329(17):3587–3595

Karnopp D (1985) Computer simulation of stick–slip friction in mechanical dynamic systems. J Dyn Syst Meas Control 107(1):100–103

Kchaou M, Lazim ARM, Bakar ARA, Fajoui J, Elleuch R, Jacquemin F (2016) Effects of steel fibers and surface roughness on squealing behavior of friction materials. Trans Indian Inst Met 69(6):1277–1287

Khan MA, Cooper D, Starr A (2009) BS-ISO helical gear fatigue life estimation and wear quantitative feature analysis. Strain 45(4):358–363

Lontin K, Khan M (2021) Interdependence of friction, wear, and noise: a review. Friction 1–27

Mate CM (2008) Tribology on the small scale: a bottom-up approach to friction, lubrication and wear. Oxford University Press, Oxford (UK)

Meng HC, Ludema KC (1995) Wear models and predictive equations: Their form and content. Wear 181–183:443–457

Mukras S, Kim NH, Sawyer WG, Jackson DB, Bergquist LW (2009) Numerical integration schemes and parallel computation for wear prediction using finite element method. Wear 266(7):822–831

Muller VM, Yushchenko VS, Derjaguin BV (1994) On the influence of molecular forces on the deformation of an elastic sphere and its sticking to a rigid plane. J Colloid Interface Sci 45(1):91–101

Myshkin NK, Kovalev AV (2009) Adhesion and friction of polymers. In Polymer Tribology. Sujeet K Sinha, Ed. London: Imperial College Press, pp 3–37

Nam J, Choi H, Kang J (2016) Finite element analysis for friction noise of simplified hip joint and its experimental validation. J Mech Sci Technol 30(8):3453–3460

Newcomb TP, Spurr RT (1971) Friction materials for brakes. Tribology 4(2):75–81

Öqvist M (2001) Numerical simulations of mild wear using updated geometry with different step size approaches. Wear 249(1–2):6–11

Othman MO, Elkholy AH (1990) Surfaces roughness measuring using dry friction noise. Exp Mech 30(3):309–312

Othman MO, Elkholy AH, Seireg AA (1990) Experimental investigation of frictional noise and surface-roughness characteristics. Exp Mech 30(4):328–331

Park JY, Salmeron M (2014) Fundamental aspects of energy dissipation in friction. Chem Rev 114(1):677–711

Persson BNJ, Sivebaek IM, Samoilov VN, Zhao K, Volokitin AI, Zhang ZY (2008) On the origin of Amonton's friction law. J Phys Condens Matter 20(39):395006

Quinn TFJ (1971) Oxidational wear. Wear 18(5):413–419

Rhee SK (1970) Wear equation for polymers sliding against metal surfaces. Wear 16(6):431–445

Rhee SK (1974) Wear mechanisms for asbestos-reinforced automotive friction materials. Wear 29(3):391–393

Rusli M, Okuma M (2007) Effect of surface topography on mode-coupling model of dry contact sliding systems. J Sound Vib 308:721–734

Savio G, Meneghello R, Concheri G (2009) A surface roughness predictive model in deterministic polishing of ground glass moulds. Int J Mach Tools Manuf 49(1):1–7

Shen X, Cao L, Ruyan L (2010) Numerical simulation of sliding wear based on archard model. In 2010 International Conference on Mechanic Automation and Control Engineering, Wuhan, China, pp 325–329

Sinou JJ, Loyer A, Chiello O, Mogenier G, Lorang X, Cocheteux F, Bellaj S (2013) A global strategy based on experiments and simulations for squeal prediction on industrial railway brakes. J Sound Vib 332(20):5068–5085

Stoimenov BL, Maruyama S, Adashi K, Kato K (2007) The roughness effect on the frequency of frictional sound. Tribol Int 40(4):659–664

Stoimenov BL, Kato K (2003) The relationship between frictional sound and lumps build-up at the contact interface in singlepass dry sliding between Aluminium pin and flat. In Tribology Series. Elsevier, Amsterdampp 159–164

Wang XC, Mo JL, Ouyang H, Wang DW, Chen GX, Zhu MH, Zhou ZR (2016) Squeal noise of friction material with groove-textured surface: An experimental and numerical analysis. J Tribol 138(2): 021401

Yadav G, Tiwari S, Rajput A, Jatola R, Jain ML (2016) A review: erosion wear models. In International Conference on Emerging Trends in Mechanical Engineering, Bhopal, India, pp 150–154

Part IV
Novel Materials for Advanced Engine Design

Chapter 9
Composite Materials and Its Advancements for a Cleaner Engine of Future

Ilyas Hussain and R. J. Immanuel

Abstract Composites form a modern class of structural materials that are increasingly replacing the conventional materials in various engineering domains due to the reduced density along with simultaneous enhancement in mechanical and tribological performance. Specific to the combustion engine application, usage of lighter materials becomes imperative as it yields greater fuel efficiency, bringing down the pollution related problems and leading to cleaner energy. Metal-based composite materials are found to be a potential solution to such problem owing to its higher strength to weight ratio achieved by tailoring the reinforcement-matrix composition and distribution. This chapter attempts to highlight the fundamental aspects of these composite materials and their performance against the conventional metallic class of materials along with the recent development in advanced composite materials. To rightly align with the central theme of this book, this chapter mainly focus on the role of composite materials on the improvement in tribological performance of automobile and aerospace engines. Special attention is given to the advanced composite materials that are of current research focus for improved tribological and high temperature performance in aerospace engine applications. A complete survey on the available work in this direction is being presented along with the challenges and future prospect.

Keywords Composite materials · Classification of composites · Properties of composites · Automotive and aerospace applications · Light weighing composites

I. Hussain · R. J. Immanuel (✉)
Department of Mechanical Engineering, Indian Institute of Technology Bhilai, Raipur 492 015, India
e-mail: jose@iitbhilai.ac.in

9.1   Introduction

9.1.1   Need for Composites

Composite materials find their place in engineering applications where the structure and properties of standard materials are insufficient. When the conventional materials reach their upper threshold beyond which no improvement is practically feasible, different materials are combined to form composites that give unique properties and superior performance than their constituents (Allemang et al. 2014). For example, concrete, which is a mixture of sand and gravel with cement, has excellent compressive strength but brittle with negligible tensile strength on its own. The strength of concrete structure is increased by addition of reinforcement. Steel rods, wires, bars (rebar), or mesh are commonly used for this purpose and as a result, the structure can withstand higher tensile, compressive, and shear loads (Harker 2018). Another example of more relevance is in the highly competitive airline business, which is continuously in search of methods and techniques to reduce the total build mass while maintaining/improving the stiffness and strength of the aircraft's components (Zhang et al. 2018; Dursun and Soutis 2014). This is being accomplished in the recent decades by using composite materials in place of various traditional materials.

Knowledge of different types of composites and their performance with respect to their structure, distribution/geometry of reinforcements, and properties of constituent phases is essential for optimal selection and design of materials (Allemang et al. 2014). This chapter gives a fundamental insight on different types of composites with a special focus on their application in automotive and aerospace industries in general and their engines in specific.

9.1.2   History and Background

Composites were found to have their existence as early as fifteenth century BC. Early Egyptians and Mesopotamian immigrants used a combination of mud and straw to make strong and sturdy buildings. Ancient utility items, such as pottery and boats, continued to be reinforced with straw. The individual component elements, straw and clay, were unable to execute the function on their own, but they were able to do so when combined. Some believe the straw was used to soften the jagged fissures in the dried clay, while others say it was used to keep the clay from splitting (Ngo 2020).

The Mongols developed the first composite bow in 1200 AD. Bows were pressed and wrapped with birch bark using a mixture of wood, bone, and animal glue. These bows yielded a lot of power and were incredibly accurate. Genghis Khan's military domination was aided by composite Mongolian bows, which were the most powerful weapon on the planet until the invention of gunpowder ("thoughtco history of composites.pdf". xxxx).

Birth of the "Plastic Era". When scientists invented plastics, the modern era of composites began. Until then, the only glues and binders available were natural resins produced from plants and animals. Plastics such as vinyl, polystyrene, phenolic, and polyester were invented in the early 1900s. These synthetic compounds outperform the naturally available resins used at that time. For some structural applications, however, plastics alone are insufficient. Additional strength and stiffness were needed, which required further reinforcement. The first glass fibre was introduced in 1935 by Owens Corning. When glass fibre was mixed with a plastic polymer, a remarkably robust and lightweight structure resulted. The Glass Fibre Reinforced Polymer (GFRP) industry began here ("thoughtco history of composites.pdf"; "History.pdf").

WWII—a catalyst for the development of composites. Several significant developments in composite materials have come as a result of wartime need. Wartime propelled the FRP industry to mass production from the laboratory research on composites, just like the Mongols did with the composite bow. Unconventional materials were required for use in military aircraft to make it lightweight. Engineers quickly discovered that composites had additional advantages besides being lightweight and robust. Fibreglass composites, for example, were discovered to be radio frequency transparent, and the material was quickly adopted for use in shielding electronic radar equipment (Radomes) ("thoughtco history of composites.pdf"; Nagavally 2017).

Modifying Composites: "Space Age" to "Everyday". The small-scale specialist composites sector was at peak by the end of WWII. With the decline for military products, the remaining composites developers were attempting to break into new sectors. One obvious product that profited was boats. In 1946, boat hull was released as the first composite commercial. In 1947, a whole composite automobile body was built and analysed. The 1953 Chevrolet Corvette was born as a result of this. The invention of the vehicle brought in a slew of novel moulding techniques, including compression moulding of sheet moulding compound (SMC) and bulk moulding compound (BMC). For the automotive sector and other industries, the two processes have appeared as the primary technique of moulding. Brandt Goldsworthy, known as the "grandfather of composites" at the time, pioneered several novel production methods and products, including the surfboat made of fibreglass, which modernized the sport forever. Goldsworthy moreover pioneered the pultrusion fabrication process, which enables for consistently strong fibreglass reinforced products. Ladder steps, tool handles, pipelines, arrow shafts, armour, train floors, and medical gadgets are all made using this technology ("History.pdf").

Continued Advancement in Composites. Though the first carbon fibre was patented in 1961, carbon fibre composites did not became available commercially for several years. Carbon fibre has been used to develop components for a variety of industries, including aeronautical, automobile, and consumer goods. With the composites sector began to mature in 1970s, improved plastic polymers and reinforcing fibres have started being produced. Due to their low density (light in weight) and high

tensile strength, an aramid fibre, Kevlar was developed by DuPont, which has become the priority in body armour. Carbon fibre was also introduced about this period, and rapidly being used to replace elements that were formerly made of steel. The composites sector is continuously expanding, with a lot of it now centred on renewable power. Blades of wind turbine, in particular, are continuously pushing the envelope in terms of size, demanding the use of novel composite materials ("History.pdf"; Nagavally 2017; Dawoud and Saleh 2019).

Looking Ahead. The composites sector is continuously evolving. FRP composites have now revolutionised the nautical, automobile, and aeronautical industries (Harker 2018; Zhang et al. 2018) (Gheorghe et al. 2021). Similarly rapid transformations have occurred in many specific applications of infrastructure and chemical processing industries. As the sector takes advantage of the flexibility in design, robustness, light in weight, corrosion resistance, and other features that offered by composites, there is a significant potential for a comparable technology change in the architectural and construction sectors. The Institute for Advanced Composites Manufacturing Innovation, a $259 million public–private partnership, was announced by the US Department of Energy in 2015. The Institute's focus will be on making advanced composites at lower cost with less energy to manufacture, as well as more recyclable. The development of novel reinforcements will enable composites to be used in even more applications. As composites feed the requirement for stronger, lighter, and environmentally friendly goods, environmentally friendly resins will combine recycled plastics and bio-based polymers. Composite materials will continue to make the world a superior place ("History.pdf".).

9.1.3   What Are Composites?

A composite material is made up of two or more chemically different and unsolvable phases with a distinct boundary, which are combined in such a way that their characteristics and underlying performance outperform the constituents functioning alone. The distinct phases are classified as *reinforcement* and *matrix* (Allemang et al. 2014; Aboudi et al. 2013). Reinforcements are the strengthening phases among the constituents, while matrix is the one which binds and places the reinforcement together. Reinforcement materials exist in fibre, particulate, or flake form within the matrix which is usually continuous. Concrete strengthened with steel and epoxy polymer strengthened with graphite fibres, are examples of composite material (Aboudi et al. 2013).

Composite materials are not brought to this world for the first time by human being. The core strength of a plant/tree - the stem (which we call as wood) is made up of one polymer species—strong and rigid cellulose fibres—covered in a sticky matrix of another polymer, the polyose lignin. This naturally occurring composite is strong, but only along the longitudinal axis. Human, with the available intelligence modified the natural wood to create another composite, by suitably arranging multiple layers

of wood that gets rid of the said disadvantage which is the well-known plywood. Nature does much improved job of design and production than we do. Other natural composites include bone, teeth, and mollusk shells, which combines natural polymer matrix and hard ceramic reinforcing phases (Harker 2018).

Composite materials which are conventionally been employed in the aircraft industry are known as advanced composites. These composites have thin-diameter high-performance reinforcements in a matrix material like aluminium or low-density polymer (Zhang et al. 2018; Dursun and Soutis 2014). Graphite/epoxy, Kevlar/epoxy, and boron/aluminium composites are some of the commercially known examples of advanced composites (Aboudi et al. 2013).

Materials are blended in composites to make better use of their merits while reducing the impacts of their defects to some extent. This optimization approach can free a designer from the constraints that come with selecting and manufacturing traditional materials. This helps material engineer to customize the material to be stronger and lighter with superior qualities, meeting the application demand (Allemang et al. 2014; Dawoud and Saleh 2019).

9.1.4 Composites Against Metals

Metals and alloys that are monolithic in nature that has been the primary material for centuries in various engineering application. However, with the rapid advancement of technology in various fronts, these materials cannot always match the current needs. One way to achieve the performance requirements of modern engineering is to combine several materials to get a synergetic benefit.

Composites are more efficient in several cases. In airline business, for example, one is constantly seeking for methods to reduce the aircraft mass while maintaining the strength and rigidity of its elements. This can be accomplished by using composite materials instead of traditional metal alloys by blending light-weight reinforcement to traditional alloys. Even if the cost of composite materials is higher, the cost savings in fuel make them more lucrative. A reduction of approximately half kg in mass in a commercial aircraft can save up to 1360 L of fuel per year. Fuel expenses account for 25% of a commercial airline's overall operating costs and hence the principal cost incurred in usage of composite is outperformed.

Composites provide a number of other benefits over traditional materials. Enhanced strength, stiffness, fatigue and endurance to impact load, thermal conductivity, resistance to corrosion, and other properties may be among them (Harker 2018; Aboudi et al. 2013).

9.1.5   Limitations in Use of Composites

Just like two faces of a coin, composited do possess certain demerits. Some of the primary limitations of composites are the following.

- Higher cost of composite production is a significant problem (Kumar et al. 2015). Extensive research is being carried out on the processing and manufacturing techniques of composites to improve the quality while reducing the overall cost. Manufacturing techniques like SMC (sheet moulding compound) and SRIM (structural reinforcement injection moulding) have already reached commercialization that reduces the time and cost in making automotive parts from composites (Aboudi et al. 2013).
- The characterization and testing of composite structures are difficult and complex as compared with their metallic counterpart. This acts as one of the prime factor behind the reduced momentum in development of novel composite materials.
- When compared to metals, composites require more effort to repair. In composite structures, major faults and fissures can sometimes go undetected.
- In comparison to metals, composite materials exhibit poor combination of strength and fracture toughness (Aboudi et al. 2013).

9.2   Classification of Composites

Form of reinforcement and material of matrix are two major components based on which composites are classified in general (Fig. 9.1).

The principal forms of reinforcements are:

(a)   Particulate
(b)   Flake
(c)   Fibre

　　　i.   Continuous
　　　ii.   Discontinuous

The most widely used matrix materials are:

(a)   Metal
(b)   Ceramic
(c)   Polymer
(d)   Carbon

Particulate Composites contains particles of reinforcements distributed in the matrix. Because of the random distribution of particulates, the properties it yield are usually isotropic (Allemang et al. 2014). Particulate composites offer advantages such as enhanced strength, elevated working temperatures, and resistance to oxidation, among others. Aluminium particles used in rubber; particles of silicon carbide (SiC)
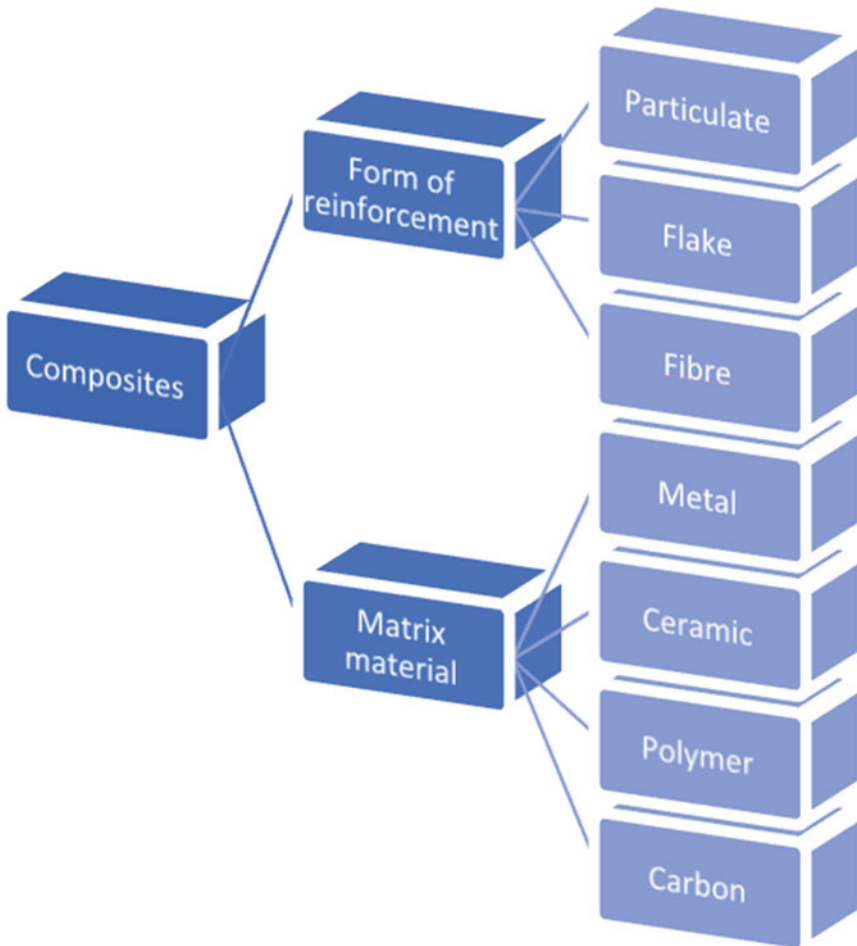
Fig. 9.1 Classification of composites

used in aluminium are few common examples of this type of composites (Jin et al. 2018).

Flake Composite consists of matrices with flat platelets as reinforcements. Glass, mica, aluminium, and silver are common materials used as flakes (Allemang et al. 2014). Flake composites have several advantages, including a high out-of-plane flexural modulus, enhanced strength, and a minimal cost. Flakes, on the other hand, are not easy to line up, and hence possess limited applications till date.

Fibre Composites Short (discontinuous) or long (continuous) fibres are embedded to enhance strength of matrices in fibre composites. Carbon, glass and aramid fibres are few examples of fibres used as reinforcement. Unidirectional or woven fibre laminae are the basic building blocks of continuous fibre matrix composites. To

make a multidirectional laminate, laminae are piled on top of one another at different angles. Such an arrangement not only improves the strength of the composite, but also reduces the anisotropy (Aboudi et al. 2013; Soutis 2005).

9.2.1 Metal Matrix Composites

Metal matrix composites (MMCs), as the name indicates, have metal/alloy as the matrix. Aluminium, aluminium–lithium alloy (lighter than aluminium), magnesium, copper, titanium, and superalloys are some common MMC matrix materials currently in use. Graphite, aluminium oxide, silicon carbide (SiC), boron, molybdenum, and tungsten are the commonly used reinforcements in MMC either in particulate or in fibre form (Tjong and Ma 2000).

Non-metallic fibres have elastic moduli ranging from 200 to 400 GPa and tensile strengths ranging from 2000 to 3000 MPa. Metals are typically strengthened to increase or decrease their characteristics to meet design requirements. As an instance, inclusion of SiC fibres in Aluminium can boost the elastic stiffness and strength of the material while reducing significant coefficients of thermal expansion and thermal and electric conductivities (Gecu and Karaaslan 2018).

Advantages of Metal Matrix Composites. MMC are primarily utilised to improve the strength of light weight low-strength materials. Excellent specific strength and modulus can be achieved by reinforcing aluminium and titanium alloys, which are low-density materials (Ma 2020).

Certain application domains such as automobile engine demands material that can work in a wide range of temperature without significant physical distortion. This physical phenomena is quantified as coefficient of thermal expansion (CTE). In such applications lower CTE is beneficial. The light weight low strength materials shall be replaced by its composites in such applications where reduction in its coefficient of thermal expansion (CTE) is synergistically achieved by strengthening the matrix with low CTE fibres like graphite, etc. (Baradeswaran and Perumal 2014).

Compared to polymer matrix composites, MMCs have a number of advantages some of which are the following:

- Higher elastic characteristics
- Higher service temperature
- Higher electric and thermal conductivities
- Better wear, fatigue, and defect resistance

On the other hand, MMCs have higher processing temperatures and density than PMCs, which are considered to be their disadvantages (Aboudi et al. 2013).

9.2.2   Ceramic Matrix Composites

Ceramic matrix composites (CMCs) are classified under advanced materials because of their durability in extreme working conditions such as high temperature and corrosive environments. Ceramics are robust and rigid, and they can withstand elevated temperatures, but lack toughness (Krenkel and Berndt 2005). Silicon carbide, silicon nitride, aluminium oxide, and mullite (a compound of aluminium, silicon, and oxygen) are commonly used matrix materials that maintain their strength to elevated temperatures of about 1700 °C (Padture 2016; Tang and Hu 2017). Carbon and aluminium oxide are the most common fibre materials. Jet and automobile engine parts, mining equipment used in deep-sea, pressure vessels, structural components, cutting tools, and dies for metal extrusion and drawing are some examples for the application of CMC.

Advantages and disadvantages of CMCs. Higher strength and stiffness, elevated working temperature, inertness to chemicals, and low density are few advantages of CMCs. Ceramics, on their own, have poor fracture toughness and fail catastrophically under tensile or impact force. Strengthening reinforcements improve their fracture toughness making CMCs more appealing for applications that requires high mechanical qualities and intense working temperatures (Aboudi et al. 2013).

9.2.3   Polymer Matrix Composites

Polymer matrix composites (PMCs) are the most popular and well-established composites, comprising of a polymer (e.g., epoxy, polyester, urethane) strengthened by fibres (e.g., glass, graphite, aramids, carbon, boron) of diameters in microns. As a result, on a weight-for-weight basis PMCs are at least five times stronger than steels (Aboudi et al. 2013; Ku et al. 2011). Various classifications of PMCs based on the reinforcements are—Glass Fibre-Reinforced Polymer (GFRP) Composites, Carbon Fibre-Reinforced Polymer (CFRP) Composites and Aramid Fibre-Reinforced Polymer (AFRP) Composites.

The most conventional fibre reinforcements used in polymer matrices are glass, carbon, and aramids. Boron, silicon carbide, and aluminium oxide are other fibre materials that are sparsely used (Ku et al. 2011). Military aircraft components, helicopter rotor blades, and various athletic products have all used boron fibre-reinforced polymer composites. Tennis rackets, circuit boards, military armour, and rocket nose cones all use silicon carbide and aluminium oxide fibres.

Advantages and drawbacks of Polymer Matrix Composites. Low cost of material and fabrication, great strength, and simple manufacturing routes are among the reasons for PMCs to be the most popular composites. The disadvantages of PMC involve low operating temperatures, high coefficients of thermal expansion, and anisotropic performance (Aboudi et al. 2013; Cho et al. 2014).

9.2.4 Carbon–Carbon Composites

Carbon–carbon composites (CCC) are made up of carbon fibres that are embedded in a carbon matrix. These composites are around 20 times stronger than graphite fibres while being 30% lighter, and they can withstand temperatures of up to 3315 °C (Aboudi et al. 2013; Gradl et al. 2017).

Advantages of Carbon-Carbon Composites. Carbon, like ceramics, is brittle and susceptible to flaws. The capacity to endure elevated temperatures, lower creep rate, light in weight, good tensile and compressive strengths, high fatigue resistance, high thermal conductivity, and high coefficient of friction are all advantages of using a carbon matrix to reinforce a composite. Disadvantages include high cost, poor shear strength, and susceptibility towards oxidation and subsequent degradation in performance at elevated temperatures (Joel et al. 2018).

9.3 Properties of Composites

The domain of composites is so vast that generalisation in any form is difficult and close to impossible. In general composites are developed to have greater strength, higher stiffness long with low density and ability to perform in extreme environmental conditions. The placement of composites among various other engineering materials in terms of strength and density is shown in Fig. 9.2.

When comparing with monolithic materials, each class of composite has its unique set of characteristics. CMCs, for example, offer excellent corrosion, oxidation, and wear resistance, as well as the capacity to withstand high temperatures (Tang and Hu 2017).

Low CTEs are helpful in applications that require consistency in dimensions. This is very crucial in engine parts where different parts are subjected to different temperature at different time. Under this complex condition, the materials are required to maintain its dimensional stability which can be achieved only when the CTE of the materials are maintained as low as possible. Composites are feasible to be produced with close to-zero CTEs by using the right reinforcements and matrix materials. The ability to modify the coefficient of thermal expansion reduces the thermal strains and alterations that occur when unlike materials are connected (Zweben 2015).

Another unique feature of certain composites is their unusually high heat conduction, which is becoming increasingly relevant. Carbon nano-tubes are a special class of reinforcement material that significantly improves the conductivity even in the highly conductive aluminium and copper alloys (Prakash et al. 2017). As a result, composites are increasingly being used in situations where heat dissipation is a major design factor. Furthermore, composites' low densities and high strength, as can be seen in Fig. 9.2, make them particularly useful in temperature management applications where weight is a factor, such as mobiles, tablets, laptop, computers, and spacecraft modules.
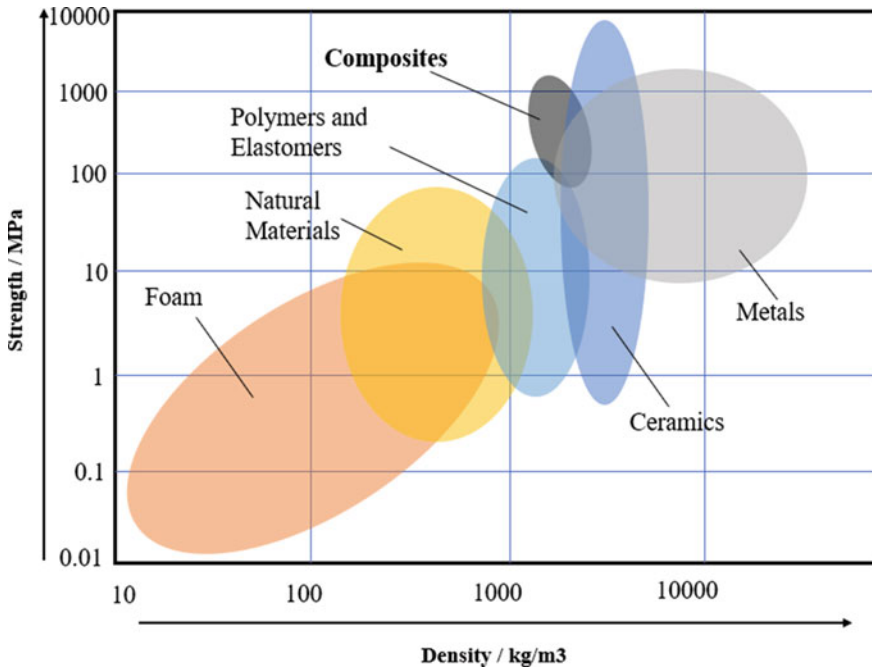
Fig. 9.2 Comparison of strength against density for different materials

9.3.1 Metal Matrix Composites

In mechanical systems, metals and its alloys are the commonly used materials. Novel materials are produced with superior or improved qualities, such as higher strength and modulus, improved resistance to wear, and lower CTE, by strengthening them with continuous and discontinuous fibres, whiskers, and particulates (Zweben 2015; Arunachalam et al. 2018).

Research indicates that continuous fibres provide the maximum gain in strength and modulus for MMC. However, the comparatively expensive continuous strengthening fibres and the complex fabrication routes has limited their utilisation. Discontinuous fibres or particles are commonly utilised as reinforcements to strengthen MMCs as they are cheaper, readily available and easier to disperse it in the matrix and relatively uniformly distributed in the matrix (Zweben 2015; Arunachalam et al. 2018; Yu et al. 2018). This trend can change in future when different, lesser-cost continuous fibres and methods are established in future. Therefore, in subsequent section, we focus on certain particle reinforced MMCs that are commonly used for various engineering applications.

Mechanical Properties of Titanium Carbide Particle-Strengthened Steel. For many years, titanium carbide (TiC) reinforced steel alloys are employed in engineering applications like cutting blades, tools and dies, and parts undergoing wear.

"Ferro-Tic" is the brand name for these products. Let's say a composite composed of austenitic stainless steel strengthened with 45% by volume TiC particles to demonstrate the effect of particulate reinforcements. The composite has a modulus of 304 GPa, whereas the homogeneous solid base metal has a modulus of 193 GPa. The composite has a specific gravity of 6.45, which is roughly 20% lesser than that of solid matrix. As a result, individual stiffness of composite is nearly double to that of unreinforced metal. Because of the lighter weight, guide rollers made of this MMC can go faster than those made of base metal, resulting in less wear. Furthermore, because of the TiC particles, the composite has a better intrinsic wear endurance, high thermal stability and fatigue strength (Zweben 2015; Almangour et al. 2017; Hayat et al. 2019).

Mechanical Properties of Silicon Carbide and Alumina Particle-Strengthened Aluminium. One of the important MMC is aluminium strengthened with ceramics particles like SiC and alumina (Al_2O_3) particles (Maurya et al. 2019). The properties of composites are altered due to geometry of particle, volume percentage of particle, the matrix material used and manufacturing process employed. Alumina particles do not react as quickly with the matrix as SiC particles do at high temperatures, so they are utilised to strengthen aluminium (Maurya et al. 2019; Muraliraja et al. 2018). As a result, alumina-reinforced composites are more versatile in terms of process development and applications (Reddy and Vijaya 2017). The rigidity and heat conduction of alumina, on the other hand, are lower than those of SiC, and these become the drawback of Alumina reinforced MMC. SiC has lower density than alumina and other titanium-based reinforcements used in aluminium matrix, but alumina has CTE near to matrix material aluminium as shown in Fig. 9.3, which increases wettability between matrix and reinforcement and produces more homogeneous composite (Gecu and Karaaslan 2018; Ma 2020; Gupta et al. 2018; Chen et al. 2018).

As a result, high strength and stiffness, better homogeneity, low density, high thermal conductivity and excellent abrasion resistance with good fatigue endurance is achieved by particulate reinforcing. The composites have much higher moduli and specific moduli than monolithic aluminium, titanium, and steel. One example of Al composite reinforced with SiC particles is presented in Table 9.1 for better understanding (Aboudi et al. 2013; Zweben 2015; Gupta et al. 2018).
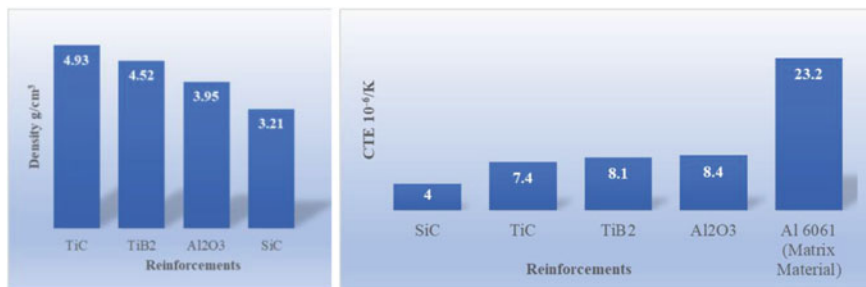

Fig. 9.3 Comparison of Density and CTE for various conventional reinforcements

Table 9.1 Mechanical and Physical properties of Al_2O_3 and SiC particle-reinforced Al-6061 (Aboudi et al. 2013; Zweben 2015; Gupta et al. 2018)

Property	Aluminium (6061)	SiC (55 vol.%) Particle-Reinforced AA6061
Modulus, GPa	69	186
Tensile yield strength, MPa	275	495
Tensile ultimate strength, MPa	310	530
Elongation (%)	15	0.6
Density, g/cm^3	2.77	2.96
Specific Modulus, GPa	25	63
CTE, 10^{-6}/K	23	10.4
Thermal Conductivity, W/m K	218	160–220

9.3.2 Ceramic Matrix Composites

CMC are the advanced grade of composites that are least used in current engineering application among the composite materials inspite of its ability to work in elevated-temperature and resistance to corrosion environment. Ceramics, being known for their great stiffness and hardness, as well as their endurance to wear, corrosion, and oxidation, and their ability to operate at high temperatures, would have been the right choice for engine application (Arai et al. 2018). However, they have certain demerits that have strictly restricted their use in applications involving substantial tensile pressures. Ceramics have poor fracture toughness, which renders them extremely vulnerable to minor faults (Li 2018).

Ceramic materials are poor in fracture toughness which is improved by addition of reinforcements in fibre, whisker, or particulate form to create CMCs. This also enhances the thermal and mechanical shock resistance of the CMC. The use of continuous fibres is found to yield maximum benefit as compared with other form of reinforcements (Zoli et al. 2018).

This is clearly demonstrated through the data available on various alloys, monolithic ceramics and CMCs as presented in Table 9.2. It is evident from the table that by suitably incorporating long fibres, SiC fibres reinforced SiC matrix CMC lead to improved fracture toughness that are comparable to aluminium alloys. This makes CMC a suitable candidate for various components of aerospace and rocket engines (Zweben 2015; Li 2018; Ruggles-wrenn and Lee 2016).

Ceramic matrix composites come in a variety of forms and are in varying stages of development (Wang et al. 2019). SiC fibre-reinforced SiC (SiC/SiC) is one of the most established systems, with a very low density of 2.5 g/cm^3 and CTE of 3 ppm/K, the in-plane thermal conductivity is 19 W/mK, and the through-thickness value is 9.5 W/mK for a fabric-strengthened composite with 40% of fibre volume fraction (Zweben 2015).

Table 9.2 Comparison of fracture toughness SiC reinforced CMC with alloys and monolithic SiC (Zweben 2015)

Matrix	Reinforcement	Fracture Toughness, MPa m$^{1/2}$
Aluminium	–	14–30
Steel	–	40–65
Al$_2$O$_3$	–	3–5
SiC	–	3–5
Al$_2$O$_3$	Zirconia (Zr) particles	6–14
Al$_2$O$_3$	SiC whiskers	5–10
SiC	Continuous SiC fibres	24–30

9.3.3 Carbon–Carbon Composites

Carbon–carbon composites have a long history of being employed for the reason that it has superior resistance to erosion at elevated-temperature. Early materials had modest strengths and stiffness, but these qualities have continuously improved through time (Windhorst and Blount 1997).

Oxidation is one of the extreme drawbacks of carbon–carbon composites, which occurs at a temperature of around 370 °C for isolated materials. The threshold is dramatically raised when oxidation inhibitors are added to the matrix and coatings of reinforcements. Carbon–carbon composites can withstand 1380 °C of temperatures in inert atmospheres or vacuum (Zweben 2015; Jin et al. 2018).

SiC fibre-reinforced carbon has been employed in the construction of aviation gas turbine engine flaps in recent years (Windhorst and Blount 1997). This material has a CTE that is nearer to that of ceramic coatings such as SiC, which reduces cracking of coating and spallation (Jin et al. 2018).

Carbon matrices have low stiffness with extreme hardness. As a result, unidirectional carbon–carbon composites have low traverse and across-thickness elastic moduli and strength properties. The through-thickness direction of fabric-reinforced materials is weak. Three-dimensional reinforcement forms are frequently utilised as a result of this. It is feasible to achieve moduli as high as 340 GPa, tensile strengths as high as 700 MPa, and compressive strengths as high as 800 MPa in the direction of fibre reinforcement. Elastic moduli of 10 MPa, tensile strengths of 14 MPa, and compressive strengths of 34 MPa are found in directions perpendicular to fibre directions (Zweben 2015).

Carbon–carbon composites can be fabricated to a wide range of shapes and sizes, with a wider scale of physical properties. The properties of the matrix are determined by the type of fibres utilised, as well as the precursors and techniques used to create it. Densities typically range from 1.4 to 1.8 g/cm^3. Thermal conductivities in plane varies from less than 10 to around 350 W/mK. Conductivities through-thickness are often relatively small. CTEs are also quite low, varying from −1 to + 1 ppm/K on average (Manocha 2003).

9.3.4 Polymer Matrix Composites

Polymers, as previously stated, are generally weak and low-strength materials. It is necessary to strengthen materials with continuous or discontinuous fibres in order to obtain mechanical characteristics suitable for structural applications. When particles of ceramic or metals are added to polymers, the modulus of the material increases. Strength, on the other hand, does not improve considerably and often reduces. To make materials conductive both electrically and thermally, metallic particles such as silver and aluminium are combined (Krishna et al. 2019). In some applications, these materials have taken the place of lead-based solders. Magnetic composites can also be created by adding ferrous particles into a variety of polymers. Magnetic tape, used in recording audio and video, is a common example.

Though the usage of PMC is restricted from engine application, PMCs, strengthened with symmetrically arranged continuous fibres are the most effective structural materials. Temperature has a considerable effect on the properties of PMC, particularly their strengths. Temperature affects polymer characteristics in a variety of way (Guo et al. 2019). This is true for epoxy formulas with varying cure and glass transition temperatures (Forintos and Czigany 2018). Polyimides, for example, offer good elevated-temperature characteristics, allowing them to emulate with titanium. Polyimide matrices are used in components of aviation gas turbine engine with working temperatures as high as 290 °C (Zweben 2015).

9.4 Application of Composites

The application domains of composite materials are increasing day by day. In this section, a brief overview on the usage of composites in various industries is presented to give a bird-eye view on the significance of composites to the readers.

9.4.1 Metal Matrix Composites

As stated in our earlier section, a number of MMC, such as TiC particle-strengthened ferrous alloys, tungsten carbide particle-strengthened cobalt, and diamond particle-strengthened cobalt, have been utilised commercially for decades.

MMC with continuous fibre reinforcement are relatively costly and have seen reduced but notable use. The mid-fuselage part of the space shuttle orbiter is made up of beam trusses made of boron fibre-strengthened aluminium tubes. The Space Telescope's high-gain antenna waveguides are composed of carbon fibre-strengthened aluminium and protrude out from the main telescope tube frame. They have a superior axial strength and a minimal axial CTE, thus antenna pointing precision is

maintained. Because of their extraordinarily high axial moduli and strength, SiC fibre-strengthened titanium tubes are employed in aeroplane actuators.

Alumina (Al_2O_3) fibre-strengthened aluminium, which is utilised in electrical transmission lines, is the most well-known MMC commercial material that uses continuous fibres. Because of its high stiffness-to-density and strength-to-density, support towers can be positioned widely at a distance in new construction and existing systems can be expanded.

One of the most important applications of SiC particle-strengthened aluminium, as previously indicated, is in packaging and electrical and photonic thermal control. These materials are known as AlSiC in the electronic/photonic packaging business. Low CTE and density are two of AlSiC's key advantages over conventional materials. Thermal conductivity of one formulation is 255 W/mK, which is much higher than that of aluminium alloys. Manufacturers of these composite claims that replacing copper baseplates in power modules with AlSiC reduces thermal tensions between the aluminium nitride substrate and base plate, effectively, eliminating fatigue failure.

Electronic packaging also uses silicon–aluminium composites. The conductivity of AlSiC composites is much lower than that of copper, which is a severe disadvantage. As a result, MMC materials with superior thermal conductivities are still being developed. Aluminium and copper strengthened with carbon fibres and graphite flat platelets, as well as aluminium, copper, and silver reinforced with diamond particles, are some examples of high-conductivity composites.

In Military sector dimensional stability is required for components working on high precision missile control systems, which means that the geometries or positioning of the components cannot vary in use. MMC with high microyield strength, such as SiC/aluminium composites, meet these criteria. Furthermore, the volume fraction of SiC can be changed to get a coefficient of thermal expansion that is compatible with the rest of the system.

Aerospace industries primarily rely on MMC because of its improved yield and fracture strength, low thermal expansion, and appropriate endurance to wear. Metal matrix composites are also currently being used to make lighter car engines than their metal counterparts. MMC are also used in gas turbine engines due to their great strength and low weight. Discontinuous ceramic fibres strengthened MMC have been utilised to replace cast iron inserts in automobile and truck engines to increase wear resistance in internal cylinder surface and piston wall and to provide high-temperature strength. To improve wear resistance and lower the friction coefficient, Honda blends ceramic and carbon fibres to create MMCs. In engine valves, titanium boride particle-are used to strengthen titanium based MMCs (Miracle 2005).

SiC particle strengthened aluminium MMC are used in aerospace, automotive, and optical structural applications. In microelectronic and photonic applications, it has become a standard material. F-16 aircraft replacement fuel access doors, gas turbine engine fins, and rotor blade sleeves of helicopter are among the aerospace/defence applications (Frankovic et al. 2005).

Silicon particle-strengthened aluminium is employed in automobile engine cylinder liners for wear resistance. Brake calliper of modern automobiles are made using an aluminium alloy that was locally strengthened with continuous ceramic fibre

precast composite inserts. A nanocrystalline alumina fibre with a diameter of 10 to 12 pm and a fibre volume fraction of 65% makes up the fibre. Finite element analysis confirmed the reinforcement placement and amount, resulting in a design that met minimal design criteria and matched cast-iron calliper deflections in a packaging limited environment (Schmid and Kalpakjian 2009).

9.4.2 Ceramic Matrix Composites

As explained in previous section, continuous fibres strengthening of ceramics can make them effective structural materials. Fracture toughness is also improved by discontinuous fibres and whiskers (elongated single crystals), but to a lesser extent.

In a growing number of aerospace optical systems, Carbon/SiC composites are being used. There are only a few commercial ceramic matrix composites uses available. In cutting tools, SiC whisker-strengthened alumina is widely employed. Over monolithic alumina, the advantage is improved fracture toughness.

Heat exchangers for corrosive and extreme-temperature settings are among the other applications. Parts for abrasive slurry pumps have been made from silicon carbide particle-reinforced alumina to reduce the erosive damage on the pump components, increasing the service life.

CMC are commonly employed in elevated-temperature aeroplane components like exhaust nozzles. Carbon fibre strengthened SiC has been examined as an option for brakes of aircraft, where temperatures can approach 1200° C in emergency brake situations.

In military aircraft engine flaps, usage of SiC matrices strengthened with carbon and SiC fibres is being explored, that can provide a considerable weight reduction over existing nickel-based superalloy. Ceramic matrix composites are expected to play a substantial role in the next generation of aircraft engines. Component weight savings of up to 60% over superalloys have been recorded, with fuel savings of up to 15% expected.

In high-end automobiles, C/SiC brakes are employed. For a range of aeronautical and commercial applications, glass–ceramics strengthened with carbon and SiC fibres are being investigated.

CMC are used in components of heat exchangers and burners. Coated SiC fibres are inserted in a ceramic matrix to provide temperature resistance, toughness, and low density to gas turbine components such as turbine blades, combustion chambers, stator vanes, and turbine engines.

Coated ceramic tiles are used in the aerospace sector to protect body flaps, shrouds, and space shuttle shielding from severe heat.

Engine exhaust systems for commercial aeroplanes, include ceramic exhaust nozzles to extend part life and minimise weight and clatter. Hypersonic aviation vehicles make use of structural materials such ultra-high-temperature CMCs, which are ideal for locations with high heat flux.

9.4.3 Carbon–Carbon Composites

Composites of reinforcement and matrix of carbon can be manufactured with a broad variety of thermal conductivities. The NASA EO1 Earth Observing Satellite carried a demonstration of high-level-conductivity carbon–carbon radiator panel. A carbon–carbon optical bench is featured aboard the GOCE spacecraft. The lack of moisture absorption and outgassing make it a better choice than CFRP.

Glass-manufacturing equipment, heat treatment racks, and wafer-heating components are all examples of industrial carbon–carbon composite usage. Carbon–carbon brakes and clutches are also employed in racing cars and motorcycles.

The space shuttle nose cones experience as high as 1700 °C temperature when the shuttle re-enters into earth's atmosphere. All parts of the space shuttle nose has low density and has materials resistance to high temperature erosion, high thermal conduction to prevent cracking of surface, high specific heat to captivate large heat flux, and significant thermal shock resistance to work at low temperatures in space of –150 to 1700 °C due to re-entry in earth's atmosphere. Carbon–carbon composite is the material of preference for the nose cone to meet this challenging properties requirement. Furthermore, the carbon–carbon nose is unaffected during multiple firing and re-entry, and proven for multiple uses.

9.4.4 Polymer Matrix Composites

The application of Polymer matrix composites ranges from tennis racquets to the space shuttle. Rather than listing all of the applications for polymer-based composites, a few examples from each industry have been chosen to emphasize its importance.

In space application, high specific modulus and strength combined with dimensional stability for a wide range of temperature fluctuations make composites the material of choice. The space shuttle's Graphite/ epoxy-honeycomb cargo bay doors are the best example to showcase the importance of PMCs. Weight savings of up to $2208/kg over standard metal alloys translate to larger payloads. Graphite/epoxy was also chosen for the space shuttles' remote manipulator arm, which deploys and recovers cargo, mostly for load savings and tiny mechanical and thermal variations. Graphite/epoxy PMCs are used in satellite antenna ribs and struts because of its high specific stiffness and ability to meet dimensional stability requirements due to severe temperature excursions in space.

Graphite/epoxy composites coiled on aluminium tubing or chopped S-glass reinforced urethane foam are used in the manufacture of bicycles. The graphite/epoxy combination boosts the tube's specific modulus while reducing the frame's mass significantly. Composites also allow frames to be made up of a single component, improving fatigue life and avoiding stress concentrations at joints, which are common

in metallic frames. Carbon–polymide composite bicycle wheels are lighter and more impact resistant than aluminium wheels.

In field of medical sciences, Glass–Kevlar/epoxy lightweight face masks for epileptic patients is considered to be a major breakthrough. Graphite/epoxy facing sandwiches are employed in X-ray tables because of their rigidity, light in weight, and radiation transparency. The latter feature allows the patient to remain in the same bed for a surgery as well as x-rays, resulting in a lesser radiation dose.

Fibreglass has become a common material for boat building. For increased load savings, vibration damping, and endurance to impact, hybrids of Kevlar–glass/epoxy are gradually substituting fibreglass.

In aerospace applications, polymer composites have largely been pioneered by the military aircraft sector. The use of composite structural materials in F-15 s aircraft in the 1970s was less than 2% which got increased to almost 30% on the AV-8B aircraft in the 1990s. In both instances, the weight savings over metal parts was greater than 20%.

Because of safety concerns, commercial airlines have been reluctant to employ composites in various crucial structures. Composites are only used in secondary structures like the Boeing 767's graphite/epoxy rudders and elevators, as well as Kevlar–graphite/epoxy landing gear doors. Aerial panels and floors are also made of composites. The tail fin of the latter is made of graphite/epoxy and aramid honeycomb. The tail fin's weight was lowered by 300 kg, and the total pieces was reduced from 2000 to 100.

The weight of composite materials has been reduced due to increased competition in model aeroplane flying. Helicopters and tiltrotors use graphite/epoxy and glass/epoxy rotor blades, which not only have a 100 percent longer life than metal blades, but also have higher top speeds.

In many commercial, consumer, and aerospace/defence structural applications, GFRPs strengthened with continuous fibres and textiles have become the standard materials. Rocket motor cases, airplane fairings, interior parts of aeroplane, cargo containers, armours, etc. are all examples of aerospace and defence uses.

Military and commercial aircraft structures unmanned aerial vehicle (UAV) structures, aircraft gas turbine fan blades, spacecraft structures, satellite antennas, optomechanical systems, and ships are all CFRP aerospace/defence applications.

9.5 Conclusion and Future Prospectus

The current study from the chapter reveals that tremendous improvement has been made and is going on with time in the development of aeroplane structural and engine materials. The materials must have adequate mechanical properties and damage tolerance under various conditions in order to meet the design criteria for aeroplane structural materials. For many years, Al-based alloys have been the leading material in this industry due to their well-known mechanical characteristics. The usage of PMC is seen in recent years as compared to Al-based alloys because of significant mechanical

properties polymer has like high specific strength and stiffness. Traditional carbon fibre reinforced PMC, on the other hand, are more prone to stress concentration. Materials for aircraft engines must have sufficient mechanical qualities, density, and resistance to corrosion at elevated temperatures, according to the standards. Ti-based alloys are the dominant materials in the compressor area, where temperatures range from 500 to 600 °C. The high temperature (1400–1500 °C) turbine portion is made primarily of nickel-based superalloys, which can be replaced by titanium aluminide in future as it has at par properties as nickel-based superalloys.

Airbus A380 and Boeing 787 aircraft having more than 25% and 50% use of composite materials respectively. Composite materials have a lot of uses not only in just structural applications, but also in various parts of automotive and aerospace engine. Composite materials are becoming more popular in the aerospace sector as they have very high specific strength and resistance to corrosion and fatigue resistance than conventional metals.

Certain mechanical features and problems, such as wear between moving engine parts, and corrosion, will drive the advancement and selection of next-age group structure materials in the future. Various materials, such as Al-based alloys, Ti-based alloys, steels, and composites, will dominate the airframe raw material. The following topics should be the focus of future study on airframe materials: (i) use diverse tactics, such as controlling refinement microstructure, impurity control, and thermal–mechanical processing, to generate novel metal alloys with greater and precise mechanical properties; (ii) develop new methods to overcome the challenges of metal alloys, such as composition modification, coating, and microstructure control, (iii) develop new composite materials, such as MMC and PMC. The future of aircraft engine materials will be centred on how to survive boosted engine temperatures while maintaining ample mechanical properties. The following topics should be the focus of future work: (i) develop advanced titanium aluminide by alloying with elements that prevent oxidation at high temperatures; (ii) develop advanced CMC with higher fracture toughness by revealing the optimised content of fibres, such as graphene platelet; (iii) improving resistance to high temperature in Ti based alloys by regulating the phases through different alloying elements and thermal–mechanical processing (Zhang et al. 2018).

9.6   Summary

Composites have numerous advantages that include the ability to use a wide range of material combinations and allowing for design flexibility. Composites are developed using different phases of materials and mix in desired combination to get best properties of the phases. In addition, the composites can be tailor made to suit complex shapes which can be directly used in different applications. Composites are lighter in weight than most other conventional materials. While a number of composite materials are currently in commercial stage to suite varying need such as high temperature

application, extreme corroding environment, etc., a large amount of research is still required to meet the growing technical needs in various industrial domains.

References

Almangour B, Grzesiak D, Yang J (2017) In-situ formation of novel TiC-particle-reinforced 316L stainless steel bulk-form composites by selective laser melting. J Alloys Compd. https://doi.org/10.1016/j.jallcom.2017.01.149

Allemang R, De Clerck J, Niezrecki C, Wicks A (2014) Preface. Conf Proc Soc Exp Mech Ser 45(7):577–617

Almangour B, Grzesiak D, Yang J (2017) AC SC. J Alloys Compd. https://doi.org/10.1016/j.jallcom.2017.01.149

Arai Y, Inoue R, Goto K, Kogo Y (2019) Carbon fiber reinforced ultra-high temperature ceramic matrix composites: a review 45:14481–14489. https://doi.org/10.1016/j.ceramint.2019.05.065

Arunachalam R, Kumar P, Muraliraja R (2019) A review on the production of metal matrix composites through stir casting – Furnace design, properties, challenges, and research opportunities 42:213–245. https://doi.org/10.1016/j.jmapro.2019.04.017

Baradeswaran A, Perumal AE (2014) Composites: Part B Study on mechanical and wear properties of Al 7075 / Al 2 O 3 / graphite hybrid composites. Compos PART B 56:464–471. https://doi.org/10.1016/j.compositesb.2013.08.013

Callister WD (2009) Materials Science and Engineering and Introduction, eighth edition, John Wiley and sons, inc. ISBN 978-0-470-41997-7, pp. 626–672

Chen G et al (2018) Microstructures and mechanical properties of in-situ Al3Ti/2024Al composites after solution and subsequent aging treatment. Mater Sci Eng A 724:181–188. https://doi.org/10.1016/j.msea.2018.03.089

Cho D, Kim H, Drzal LT (2014) Surface Treatment and Characterization of Natural Fibers : Effects on the Properties of Biocomposites 3

Dawoud MM, Saleh HM (2019) Introductory chapter: background on composite materials. Charact Some Compos Mater:3–12. https://doi.org/10.5772/intechopen.80960.

Dursun T, Soutis C (2014) Recent developments in advanced aircraft aluminium alloys. Mater Des 56:862–871. https://doi.org/10.1016/j.matdes.2013.12.002

Forintos N, Czigany T (2018) Multifunctional application of carbon fiber reinforced polymer composites: Electrical properties of the reinforcing carbon fibers–a short review. Compos Part B 162:331–343. https://doi.org/10.1016/j.compositesb.2018.10.098

Frankovic I, Lovric I. Rados J (2005) Application of composite materials in aviation. In: Ann. DAAAM Proc. Int. DAAAM Symp, pp 127–128

Gecu R, Karaaslan A (2018) Sliding wear of the ti-reinforced al matrix bi-metal composite: a potential replacement to conventional sic-reinforced composites. Int J Met. https://doi.org/10.1007/s40962-018-0281-9

Gheorghe V, Scutaru ML, Ungureanu VB, Chircan E, Ulea M (2021) New Design of Composite Structures Used in Automotive Engineering, Symmetry, 13, 383. https://doi.org/10.3390/sym13030383

Gradl PR, Valentine PG, Marshall N, Flight S (2017) Carbon-Carbon nozzle extension development in support of in-space and upper-stage liquid rocket engines:1–27. https://doi.org/10.2514/6.2017-5064

Guo Y, Ruan K, Shi X, Yang X, Gu J (2020) Factors affecting thermal conductivities of the polymers and polymer composites: a review. Compos Sci Technol 193:108134. https://doi.org/10.1016/j.compscitech.2020.108134

Gupta R, Chaudhari GP, Daniel BSS (2018) Effect of in-situ formed Al3Ti particles on the microstructure and mechanical properties of 6061 Al alloy. In: IOP Conference Series: Materials Science and Engineering 330(1). https://doi.org/10.1088/1757-899X/330/1/012012

Bryan Harris, (1999) "Engineering Composite Materials," The Institute of Materials, London, pp. 05–31

Hayat MD, Singh H, He Z (2019) Titanium metal matrix composites : an overview 121:418–438. https://doi.org/10.1016/j.compositesa.2019.04.005

Histor of composites, Composites Lab. Retrieved from http://compositeslab.com/composites-101/history-of-composites/

Jin X, Fan X, Lu C, Wang T (2018) Advances in oxidation and ablation resistance of high and ultra-high temperature ceramics modified or coated carbon/carbon composites. J Eur Ceram Soc 38(1):1–28. https://doi.org/10.1016/j.jeurceramsoc.2017.08.013

Joel C, Anand S, Padmanabhan S, Raj YSP (2018) Thermal Analysis of Carbon-Carbon Piston for Commercial vehicle diesel engine using CAE Tool. Int J Ambient Energy:1-8. https://doi.org/10.1080/01430750.2018.1525594

Kaw AK (2006) Mechanics of Composite Materials. Second edition, CRC Press, Taylor & Francis Group, ISBN 0-8493-1343-0, pp. 1–59 chapter-1

Krenkel W, Berndt F (2005) C/C-SiC composites for space applications and advanced friction systems. Mater Sci Eng A 412(1–2):177–181. https://doi.org/10.1016/j.msea.2005.08.204

Krishna V, Kate KH, Satyavolu J, Singh P (2019) Additive manufacturing of natural fiber reinforced polymer composites : processing and prospects. Compos Part B 174:106956. https://doi.org/10.1016/j.compositesb.2019.106956

Ku H, Wang H, Pattarachaiyakoop N, Trada M (2011) Composites : Part B A review on the tensile properties of natural fiber reinforced polymer composites 42:856–873. https://doi.org/10.1016/j.compositesb.2011.01.010.

Kumar S, Ramanathan S, Sundarrajan S (2015) Synthesis , microstructural and mechanical properties of ex situ zircon particles (ZrSiO4) reinforced Metal Matrix Composites (MMCs). Integr Med Res:1–15. https://doi.org/10.1016/j.jmrt.2015.03.003.

Li L (2018) Damage, fracture, and fatigue of ceramic-matrix composites. https://doi.org/10.1007/978-981-13-1783-5_1

Ma Y et al. (2020) Microstructure and mechanical behavior of Al–TiAl3 composites containing high content uniform dispersion of TiAl3 particles. Mater Sci Eng A 786. https://doi.org/10.1016/j.msea.2020.139435.

Manocha LM (2003) High performance carbon–carbon composites 28:349–358

Maurya M, Kumar S, Bajpai V (2019) Assessment of the mechanical properties of aluminium metal matrix composite: a review. https://doi.org/10.1177/0731684418816379

Miracle DB (2005) Metal matrix composites: from science to technological significance. Compos Sci Technol 65(15–16):2526–2540. https://doi.org/10.1016/j.compscitech.2005.05.027

Muraliraja R, Arunachalam R, Al-fori I, Al-maharbi M, Piya S (2018) Development of alumina reinforced aluminum metal matrix composite with enhanced compressive strength through squeeze casting process:1–8. https://doi.org/10.1177/1464420718809516

Nagavally RR (2017) Composite Materials-History, Types, Fabrication Techniques, advantages, and applications (9):82–87

Ngo T (2020) Introduction to composite materials

Padture NP (2016) Advanced structural ceramics in aerospace propulsion. Nat Publ Gr 15(8):804–809. https://doi.org/10.1038/nmat4687

Prakash KS, Thankachan T, Radhakrishnan R (2017) Parametric optimization of dry sliding wear loss of copper−MWCNT composites. Trans Nonferrous Met Soc China 27(3):627–637. https://doi.org/10.1016/S1003-6326(17)60070-0

Reddy PS, Vijaya RKB (2017) Investigation of mechanical properties of aluminium 6061-silicon carbide , boron carbide metal matrix composite. Silicon (6061). https://doi.org/10.1007/s12633-016-9479-8

Ruggles-wrenn MB, Lee MD (2016) Materials Science & Engineering A, "Fatigue behavior of an advanced SiC / SiC ceramic composite with a self-healing matrix at 1300 ° C in air and in steam" Mater. Sci. Eng. A, vol. 677, pp. 438–445. https://doi.org/10.1016/j.msea.2016.09.076

Kalpakjian S, Schmid SR, (2001) "Manufacturing Engineering and Technology," chapter 9-216-233, International Edition. 4th ed. Prentice Hall, Inc.; ISBN 0-13- 017440-8

Soutis CÃ (2005) Fibre reinforced composites in aircraft construction 41:143–151. https://doi.org/10.1016/j.paerosci.2005.02.004

Tang S, Hu C (2017) Design, preparation and properties of carbon fiber reinforced ultra-high temperature ceramic composites for aerospace applications: a review. J Mater Sci Technol 33(2):117–130. https://doi.org/10.1016/j.jmst.2016.08.004

Tjong SC, Ma ZY (2000) Microstructural and mechanical characteristics of in situ metal matrix composites

Johnson Todd (2020) History of Composites. ThoughtCo, thoughtco.com/history-of-composites-820404

Wang P, Liu F, Wang H, Li H, Gou Y (2019) Journal of materials science & technology a review of third generation SiC fibers and SiC f / SiC composites. J Mater Sci Technol 35(12):2743–2750. https://doi.org/10.1016/j.jmst.2019.07.020

Windhorst T, Blount G (1997) Carbon-carbon composites: a summary recent developments an applications 18(1):1115

Yu WH, Sing SL, Chua CK, Kuo CN, Tian XL (2019) Progress in Materials Science Particle-reinforced metal matrix nanocomposites fabricated by selective laser melting : a state of the art review 104:330–379. https://doi.org/10.1016/j.matsci.2019.04.006

Zhang X, Chen Y, Hu J (2018) Recent advances in the development of aerospace materials. Prog Aerosp Sci 97(January):22–34. https://doi.org/10.1016/j.paerosci.2018.01.001

Zoli L, Vinci A, Galizia P, Melandri C, Sciti D (2018) On the thermal shock resistance and mechanical properties of novel unidirectional UHTCMCs for extreme environments. Sci Rep:1–9. https://doi.org/10.1038/s41598-018-27328-x

Zweben C (2015) in Mech. Eng. Handb. Composite Materials (American Cancer Society), pp. 1–37. https://doi.org/10.1002/9781118985960.meh110

Chapter 10
Role of Composite Materials in Automotive Sector: Potential Applications

Dipen Kumar Rajak, D. D. Pagar, A. Behera, and Padeep L. Menezes

Abstract In the 21stcentury, researchers have turned their attention towards composite materials (CMs) concerning lightweight applications in the automobile sector. Researchers have found a way to achieve better fuel efficiency by substituting conventional materials with novel variants. The history and state-of-the-art applications of composite materials in the automotive sector are presented. Material characteristics required for the substitution of composite materials over traditional automobile components are also discussed. The application of novel composite variants for automobiles offers significant advancements in material properties in terms of lightweight, cost, sustainability, and crashworthiness. Weight reduction in an automobile component exhibited by composite materials increased the fuel efficiency with reduced automobile emission. In addition, composite materials offered safety and comfort with improved vehicle performance due to the superior mechanical properties over conventional materials. Bio-composites comprised of natural material in metals and polymers have revealed a positive impact on environmental friendliness retaining its exceptional material properties for desired automotive application.

Keywords Composite materials · Automobile applications · FRPC

D. K. Rajak (✉)
Department of Mechanical Engineering, G H Raisoni Institute of Business Management, Jalgaon, Maharashtra 425002, India

D. D. Pagar
Department of Mechanical Engineering, K. K. Wagh Institute of Engineering Education & Research, Nashik 422003, India

A. Behera
Department of Metallurgical & Materials Engineering, National Institute of Technology, Rourkela 769008, India

P. L. Menezes
Department of Mechanical Engineering, University of Nevada, Reno, NV 89557, USA

10.1   Introduction

The development of the human species is contingent on its characteristic of desire to explore which is strongly associated with individual mobility. Long-distance travel was achieved by riding animals such as horses, camels, elephants, etc., in ancient times until the invention of vehicles in lateral years. The ease in travel, commute, and transportation is predominantly thrived by automobiles these days. An automobile provides mobility, comfort, and safety by means of consuming fossil fuels. Amidst the twentieth century, rapid industrialization swells the automobile sector and subsequently increases the demand for fossil fuels to a large extend. Sudden downfall in the oil prices was also accountable for such great need. Consequently, more people desired to get access to automobiles, which raised more vehicles for the attainment of the demand. Optimum production techniques were developed to reduce the cycle time and cost of an automobile. Most of the vehicles back then make use of conventional materials withdrawn from non-renewable resources. Considering the limited source of such materials, researchers seek sustainable, biodegradable materials for automotive applications, which predominantly increased the utilization of aluminum and its alloys over steel and iron for various automotive components. Further introduction of composite materials changed the whole picture in the automotive sector. Since evolution in the automotive sector prompted a serious global concern of pollution, these high-performance composite materials enhanced the overall efficiency of a vehicle following reduced emissions. The advancement in the efficiency and performance of the vehicle is mainly achieved owing to the material properties offered by the composites (Sinha et al. 2018; Rajak et al. 2019a).

10.1.1   History/Background

Amid World War II, the shortfall of aluminum compels researchers to seek an alternative material for aircraft components, while the automobile sector encountered similar consequences. Therefore, utilization of alternative materials instead of aluminum and steel components in the automobile sector was first undertaken by researchers at Ford Motor Co. in 1941. They used soybean fiber reinforced plastic for automobile body parts which reduced the weight of a car by great means (White 1945). General Motors introduced exterior body panels made of fiberglass in 1953 for their Chevrolet Corvette model. Total 46 components of fiberglass in polyester resin were fabricated, which enhanced vehicle performance through reducing overall weight and superior mechanical properties of material comparing conventional steel and aluminum counterparts. In 1957 Trabant car was made of a monocoque frame structure manufactured in East Germany, which employed cotton fibers reinforced thermoset polymer composite material for the vehicle body. Further introduction of sheet molded composite body panels was substantially employed by premium car manufacturers since the late 1960s (Flax 1991).

The automotive industry flourished in the late 20thcentury as a consequence of the drop in petroleum prices. The numbers of people acquiring an automobile were outbursting. As a result, automobile manufacturers were competing to develop vehicles to entice new buyers. Various big companies gushed into the automotive sector and started introducing novel technologies. Reduction in consumption of fuel or carbon emission was not the primary motive behind developing lightweight vehicles back then; it was rather to attain maximum speed. Daimler Chrysler also started implementing natural fiber composites in 1991. Jute fiber reinforced plastics were applied for the interior door panels of their Mercedes-Benz E-Class model in 1994, and it continued for several succeeding years. Later total 27 number of interior components made of natural fiber-based composites were employed in the 2006 Mercedes Benz S-class. Dutch company Van Eko in the year 2016, developed a battery-operated scooter called 'Be.e', which utilized most of their components made from bio-based materials (Verma and Sharma 2017). Figure 10.1 shows different automobile models in which composite materials are deployed.

The automobile industry is the most influencing industry concerning the global economy. Therefore, novel researches are emerging out to flourish development in the automobile industry. This incorporates improvement in vehicle performance by proposing the optimum structural design of a vehicle, introducing advanced manufacturing techniques to minimize production time, and applying new materials. In this

Fig. 10.1 Application of composite materials in different automobiles (Cape Cod Curmudgeon 2018; Tony Borroz 2009; Maximilian et al. 2020; Mohammed et al. 2015)

context, state-of-the-art composite materials employed in automobile applications since primitive times are presented to understand the advancements and emerging trends in the automotive sector.

10.1.2 Characteristics of Automotive Material

As the world strives to find ways to improve the fuel efficiency of an automobile by ensuring its safety and sustainability, reducing the weight of a vehicle is imperative. Selection of superior material replacing the traditional ones is one of the effective ways of achieving it. In automobile material needs to withstand extreme environments, such as high temperature and pressure, sudden impact, and variable loads. Certainly, it is not always feasible for solitary material to possess such exceptional material properties. Composite material finds extensive applications in the automotive sector, as it combines two or more desirable materials to overcome the demerits of one another. For substituting a composite material, the following aspects need to take into consideration (Todor and Kiss 2016).

Light weight

In an automobile curtailing its overall weight by 10% leads to increased fuel efficiency by approximately 7%, which is also followed by reduced carbon emissions. In addition, reduced overall vehicle weight aids in overcoming inertia forces, consequently saving the power required for accelerating and braking. This further allows designing smaller engines, transmission, and braking systems offering improved vehicle performance by means of rapid acceleration and smaller braking distances. One of the favorable effects of light-weight in automobiles observed was a decline in vehicle drag as its directly proportionate with the weight of the vehicle. Reducing vehicle weight also serves additional gains over vehicle stability and control. Researchers have achieved light-weight in automobiles without losing its functionality by substituting steel components with materials such as aluminum, alloys of aluminum, composite materials, and metallic foams. The only obstruction in employing these light-weight materials with superior mechanical properties over traditional materials is their high cost. The issue can be subdued by seeking advanced manufacturing techniques (Sinha et al. 2018; Ghassemieh 2011).

Sustainability

Researchers these days are obligated to develop environment-friendly products considering the depletion of non-renewable resources. The automobile sector encompasses a large share in the consumption of the world's raw materials. Materials required for the production of an automobile majorly include steel, aluminum, glass as well as various petroleum products. Making use of sustainable materials that are biodegradable or acquired from recycled materials is imperative and such criteria have been set by many countries concerning pollution and limited stock. Aluminum is the most widely recycled material and so is iron and steel, yet natural fibers reinforced

composite materials exhibit remarkable biodegradability. All of these materials are widely implemented in the production of automotive components (Faruk et al. 2017; Muhammad et al. 2021). Moreover, material capability to resist wear and corrosion increases its fatigue life to withstand undesirable environmental conditions.

Cost-effectiveness

The material cost has lion's share in determining the best-fit substitute material for the desired application. Cost of material for automobile component sums up procurement cost, processing cost, and material testing cost. The utilization of naturally occurring substances reduces procurement and processing costs as synthetic materials are intricate and expensive. On the other hand, natural materials are available in abundance, require simple and fewer treatments, and are environment friendly as well. Sometimes it is not always feasible to use cost-effective materials independently considering their functional requirements for desired automotive application. This can be resolved by hybridizing inexpensive materials with finer materials in a certain fraction. Composite materials are accustomed to a similar principle and therefore substantially employed for automobile components (Ghassemieh 2011).

Crashworthiness

Material behavior to exhibit resistance to the deformation on collision to offer occupant safety in an automobile defines the crashworthiness of the material. It is the measure of a material to absorb impact energy retaining its structure against plastic deformation. Meaning material needed to possess high elastic modulus. Nearly 1.35 million people die in a road car accident each year, according to WHO reports. Automobile manufacturers these days are focusing on the safety, comfort, and eco-friendliness of the vehicle (Mallick 2020).Composite materials possess high strength, toughness, and stiffness owing to the combination of their constituents. Compressive loads are taken by the matrix material while tensile loads are carried by the reinforcement materials in a composite structure. This provides resistance to sudden impact during collisions maintaining the high elastic strength of a material.

Moreover with increasing tailpipe emissions have deleterious effects on both environment and human health. Therefore, improving fuel economy is the topmost priority for automobile manufacturers around the world these days. Application of composite materials offers exceptional mechanical, thermal, chemical properties with reduced weight over traditional materials to improve vehicle performance. These properties are tailorable according to the operating conditions of the desired application.

10.1.3   Materials Used for Automotive Applications

As the evolution in automotive materials began, researchers were putting efforts to improvematerial properties of existing materials (iron and steel) used for automobile

fabrication. Cost-effective lamellar cast iron possessing good strength and energy-absorbing characteristics was developed to compete with steel with better tensile properties. However, immanent characteristics of steel and its variants served ease in fabrication and forming ability, which displayed numerous applications in vehicle body applications. Remarkable crashworthiness of high-strength steels (HSS) was observed in vehicle chassis application. Further betterment in steel variants gave rise to anti-corrosive, light-weight yet stronger material called stainless steel. The application of stainless steel can be seen in exhaust systems, fuel tanks, and several other parts. The introduction of aluminum and its alloys have changed the whole picture in the field of automotive applications. Ranging from engine, transmission, and axles, chassis to an exterior body part such as fenders, door panels, hood, and bumper all are made of aluminum alloys (Wilhelm 1993; Sadagopan et al. 2018).

Polymer matrix composite

Usually, polymer matrix materials used for the fabrication of composites are thermosetting or thermoplastic polymers with the inclusion of fibers, particles, preform, or sheets in it. The bond between the matrix material and reinforcements determines the properties of composite materials.

Thermoset

Reinforcements such as continuous or short fibers are easily combined with thermoset polymers at low-pressure conditions as these polymers have a very low viscosity. Therefore simple manufacturing techniques are employed to fabricate composites using thermosetting polymers as a matrix material. However, thermosets are non-reusable and cannot reform after being curing is done. Despite being the most popular matrix material in composites, Epoxy resins are not popular in the automotive industry. Epoxy has low shrinkage, good adhesion, and surface texture, but high-cost and prolonged curing cycles fail Epoxy to implement for mass production in the automobile industry. While Vinylester resins display better energy absorption abilities along with good resistance to temperature, creep, fatigue, and chemicals. On account of low curing time and excellent moldability, vinyl ester resins with glass fibers reinforcements are applied for a variety of large volume automotive applications (Holbery and Houston 2006). E-glass fiber reinforced PU plastic has demonstrated its ability to withstand under extended moisture and temperature conditions for automobile applications (Panaitescu et al. 2019). Reinforcements of carbon fibers in thermoset polymer matrix composites have shown superior properties with greater weight reduction than fiberglass reinforcements.

Thermoplastic

Thermoplastics are inexpensive, reusable, and best fit for mass productions, and they also exhibit longer storage life than thermoset polymers. Also, considering environmental friendliness, thermoplastic polymers are widely deployed for automotive applications. Some thermoplastics such as polystyrene, polyethylene exhibit resistance to certain chemicals, acts as an electrical insulator but are synthetic non-biodegradable plastic. Whereas thermoplastic polypropylene is being quite popular

in automobile applications owing to its remarkable processability and dimensional stability. Polypropylene has a low mass per unit volume and shows resistance to deformation under high temperature and sudden impact loads. Polyesters such as poly(ethylene terephthalate) (PET) and poly(butylenes terephthalate) (PBT) have outstanding wear, abrasion, chemical, and thermal resistance with high strength and moldability when reinforced with fiberglass. Polycarbonate shows amazing light-transmitting ability while having transparency similar to acrylic. It shows resistance to creep, ultraviolet light and possesses good strength, formability and moldability together with dimensional stability. Polyvinylchlorides are low-cost, long-lasting, flame retardant, biodegradable polymers possessing excellent mechanical strength. These are present in amorphous form with great rigidity and hardness, but when combined with plasticizers PVC shows better flexibility and toughness. Polyamide-imides are amorphous polymers and can be categorized as either thermoset or thermo-plastic polymers which show remarkable mechanical properties along with resistance to chemicals and temperature variations. Properties revealed by various polymers in composite materials are displayed in Table 10.1, along with their automobile applications (Hovorun et al. 2017). Wood-plastic composites (WPCs) are referred to as the combination of wood fibers or wood flour with thermoplastic resins. Fibers made of pine wood pulp are blended PLA have displayed superior mechanical properties, an outstanding sound absorption characteristic with the lowest density compared to several other thermoplastics blends (Stark and Cai 2021).

Nanocomposites

Nanocomposites are composites possessing one or more filler materials of dimensions in the nanometer range which is 10^{-9} m. Nanocomposite materials show remarkable physical and mechanical properties due to the high surface area per unit volume of nanoparticles. The incorporation of nano-scaled fillers in the matrix phase is categorized based on their dimensions. One dimensional structure consist of nanofibers or nanotubes such as carbon nanotubes (CNTs), two dimensional fillers contains sheets of graphene or silicate stacked in the matrix material. The third category contains three-dimensional nano-scaled particulates such as spherical silica. The nanofiller materials divert or shorten the cracks and prevent further widening of the crack. This property of nanofiller materials contributes to enhance the strength, fracture toughness, and flexibility of nanocomposites. The characteristics of a nanocomposite material are determined by the type of nanofiller used, the size of the nanoparticle, and the degree of dispersion of nanoparticles in the matrix phase (Stojanović and Ivanović 2015; Fu et al. 2019). Scratch-resistant coating is applied using Al_2O_3, SiO_2, ZrO_2, and TiO_2 nanoparticles. Silicate films, CNTs are used in automobile fabrics to acquire anti-stain and flame retardancy properties (Wu et al. 2020a; Chandra and Kumar 2017).

This state of art review displays various applications of composite materials in the automotive sector incorporating synthetic, natural fiber composite, wood plastic composite, ceramic composite, and metal matrix composites (MMCs).

Table 10.1 Variety of polymers utilizes for automobile applications with their improvement in PMC properties (Gowda et al. 2018; Bouzouita et al. 2017; Patil et al. 2017; Oliver-Ortega et al. 2019)

	Polymer	Properties	Application
Thermoset	Polyurethane (PU)	Improved moisture absorption, increased durability	Seat backrests, armrests, cushions, bumpers, fenders, steering wheels, door panels, hoods, and trunk lid
	Vinyl Ester Resin	Reduced weight	Wheels, seats, cooling rack, and engine valve sleeve
	Polyamides	Improved lifespan with material sustainability	Car door handle,gears, bushes, cams
	Polyamide-imides	High fatigue life, wear and corrosion resistant	Seals, bushings, pistons, and gears
Thermoplastic	Polyvinylchloride (PVC)	Incredible tensile strength	Upholstery, floor mats, auto tops, shields, grips, chemical tanks and electric cables sheathing
	Polypropylene (PP)	High flexural strength, improved fiber-matrix adhesion and insulation properties	Headlights, bumpers, battery boxes, carpets, steering wheels and partitions
	Poly-ethylene terephthalate (PET) & poly-butylene terephthalate (PBT)	Improved strength and rigidity	Housing material, door handles, engine covers, optical fiber cable and other electrical insulating application
	Poly Lactic Acid (PLA)	Heat resistant	Interior trims and door panels
	polyacrylates	Increased plasticity, oils resistance	Coatings, hoses, seals, gaskets, and dampers
	Polycarbonate (PC)	High thermal resistance, toughness, transparent and good processability	Headlamp lens, exterior panels, and wheel covers

10.2 Application of Composite Materials in Automotive Components

10.2.1 Engine Parts

Piston-Cylinder

Engine blocks and heads were previously manufactured of cast iron material on account of their durability. Since piston and cylinder material operate at extremely high pressure and temperature conditions, the coefficient of thermal expansion has to be minimum. Materials with higher thermal expansion coefficient needed more clearance between piston and cylinder which creates more vibrations at high loading conditions leading to failure of the component. Also both cylinder and piston materials needed to be designed to attain operating temperatures as quickly as possible to overcome cold start emission. With the introduction of aluminum, the weight of cylinders drops by more than half as that of cast iron with improved wear properties and thermal conductivity. Piston and cylinder material also encounters acute wear and fatigue failure under cyclic loading. The inclusion of boron nitride, silicon carbide (SiC), graphite, and carbon fibers in the aluminum matrix provides enhanced wear properties by offering solid lubrication. Figure 2a shows the microstructure of graphite inclusions in aluminum matrix composite (AMC). Self-lubricating characteristics of such filler materials in AMCs avoid engine seizure under boundary layer conditions by producing a protective film between moving components (Hassan et al. 2021; Macke et al. 2013; Omrani et al. 2017; Menezes et al. 2018, 2012a, 2013). SiC particles with good forming and machining ability, when added to aluminum alloy matrix, served excellent fatigue strength, wear properties, and thermal stability at high temperatures. Moreover, these composites are light in weight and have low manufacturing costs (Falsafi et al. 2017).

The former cast iron cylinder liner was replaced by aluminium matrix composite (AMC) with the inclusion of nano reinforcement particles of zirconium dioxide (ZrO_2), silicon carbide (SiC), and graphite (Gr). Improvement in the efficiency of diesel engine due to higher cylinder pressure and decline in pollutant emissions of carbon monoxide (CO), hydrocarbons (HC) and smoke was observed along with 43.75% of reduction in weight (Tiruvenkadam et al. 2015).

Driveshaft

In an automobile, drive shafts are referred to power transmitting device which delivers power to the axles from the engine. The Driveshaft is a hollow transverse component carrying torque that produces radial shear stresses. Usually, it is made of steel material due to its prerequisite higher yield strength and toughness values. However, the steel shaft is seen to be heftier in performance and corrosive, which led to consuming additional fuel due to its weight. When it was substituted by the drive shaft made of carbon fiber-reinforced polymer (CFRP) composite material, it showed better perseverance

against torsional loading under prolonged cycle time without fracture. The improvement by means of strength, fatigue life, light-weight in the CFRP composite shaft was observed (Liu et al. 2016). Steel shaft was replaced by an intertwined polymer matrix of vinyl ester and polyurethane reinforced with E-glass fiber mat composite. The result showed increased static torque carrying capacity of the component at 50% reinforcement (Suresh et al. 2020).

Catalytic converter

As mentioned earlier, car manufacturers from the late twentieth century were building high-performance vehicles to attain maximum top speed, disregarding fuel efficiency and pollutants emission. Therefore there was a significant need to set regulations and standards to minimize fuel consumptions and exhaust gas emission causing an environmental hazard. In the United States, the Clean Air Act enacted in 1963 restricted the emission of harmful gases to control national air pollution considering Ozone layer depletion. It compels car manufacturers to reduce emissions by 75% which executed the use of catalytic converter in the exhaust system of a vehicle by the year 1975 in the US. In 1975 United States also commanded Corporate Average Fuel Economy (CAFE) standards to curtail the country's dependency on petroleum imports. As a result, they started penalizing car manufacturers for developing substandard vehicles.

Automobile operates by burning fuel in an internal combustion engine (ICE). The emissions of several types of pollutants from automobiles share more than 60% of air pollution in urban regions. These pollutants include harmful gases liberated by ICEs such as carbon monoxide (CO), hydrocarbons (HC), oxides of nitrogen (NOx) and particulates of sulfur oxide (SOx), and lead (Pb). Air pollution is one of the major concern of countries worldwide as it severely devastate the environment causing global warming and causes dreadful effects on human health. One of the effective ways of battling air pollution is to mitigate automobile emissions. The catalytic converter was initially invented in 1930 by a French researcher and later implemented in automobiles by 1975 in the United States in response to government regulation for restraining tailpipe emissions. A catalytic converter is an apparatus installed in the exhaust system to convert poisonous harmful gases causing greenhouse gas effects into less harmful ones. Inside a catalytic converter, a honeycomb structure coated with porous material provides greater surface area for the redox reactions. The honeycomb structure in a catalytic converter is shown in Fig. 10.2b. The coating material is selected according to the fuel type used for the vehicle ((Mallick 2020; Dey and Mehta 2020)). The ability to disintegrate pollutants emitted from automobiles under visible light is known as the purification efficiency of the catalyst. Hydrocarbons are transformed into hydroxyl radicals to produce CO_2 and water molecules. TiO_2 nanoparticles are commonly used in photogenerated catalysis for the generation of hydroxyl radicals. Tradition metallic semi-conductor material when replaced by non-metallic graphite carbon nitride (g-C_3N_4) catalyst it showed an increase in the efficiency of the converter to purify exhaust gases by a significant amount. The ability of g-C_3N_4 to absorb visible light results in the highest purification efficiency for oxides of nitrogen (Cui et al. 2020). Bismuth vanadate (BiVO$_4$) photocatalystis
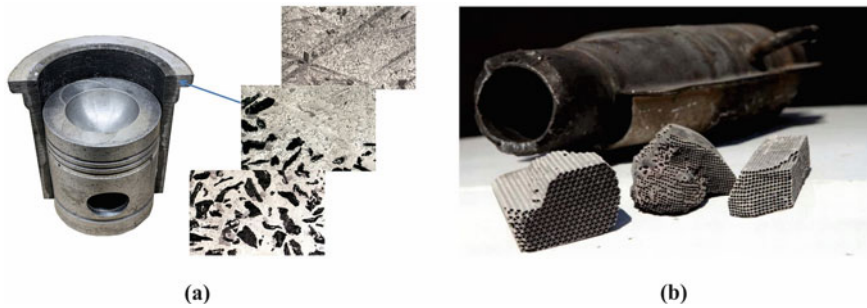
Fig. 10.2 **a** Graphite reinforced AMC for piston-cylinder application (Prateemak—Taken By Dr Pradeep Rohatgi 2012) **b** Honeycomb structure in catalytic converter (Kumar et al. 2015).

generally used for the oxygen evolution combined with graphite carbon nitride (g-C_3N_4) along with the inclusion of 25% by weight of tourmaline powder to form g-C_3N_4/$BiVO_4$/tourmaline powder composite. Purification efficiency for hydrocarbons (HC) and carbon monoxide (CO) to break them down into free radicals to form carbon dioxide (CO_2) and water molecules (H_2O) was increased by 70 percent and that for the oxides of nitrogen by 150 percent compared topure g-C_3N_4 (Li et al. 2020).

Transmission gears

To produce efficacious power transmission in automobiles, gears are the most reliant components. Gears regulate the power output from the IC engine to the drive system. It undergoes repetitive cyclic loading, which causes wear and induces variable stresses significantly affecting the fatigue life of a gear component. Conventional steel gears are substituted with polymer composite gears to attain better durability with minimum noise and vibrations. These gears are inexpensive, less noisy, and provides self-lubricity, high damping resistance, ease in design and fabrication. The addition of nearly 30% by weight glass fibers in polyamide 66 and polyoxymethylene polymers for spur gears have shown a significant decrease in wear rates (Jena 2019). Minimum developments of stresses were observed in composite spur gear fabricated using an aluminum alloy matrix with the inclusion of fly-ash (Rohatgi et al. 2012; Kasar et al. 2020). Compared to the cast steel gear component, composite spur gear displayed enhanced strength and stiffness values with low weight (Saleem et al. 2020). Spur gear made of fiberglass reinforced polymer composite revealed better damping properties compared to gears made of steel alloy and AMC (Aggarwal 2017). For the efficient running performance of electric vehicles, reduction in the weight of automobile components is imperative. Therefore most of the components in electric vehicles are deployed with lightweight components. The gear teeth and the hub part of an electric car were designed of steel to reserve the torque transmission, while the portion in between was introduced of aramid fiber reinforced phenolic composite as shown in Fig. 10.3. A reduction in the weight of the hybrid gear component was achieved with a 43.2% decrease in noise levels against whole steel gear (Kim et al. 2019). Besides engine gears, several other components in the automobile utilize

Fig. 10.3 Hybrid gear made of steel and aramid fiber reinforced phenolic composite (Kim et al. 2019)
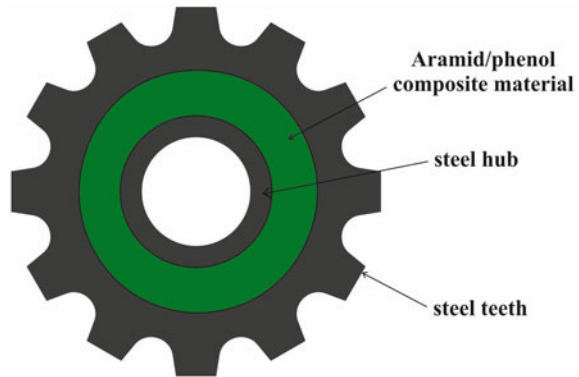
gearing mechanisms such as rack and pinion gear pair in the steering mechanism. Thermoplastic polymer nylon 66 was reinforced with glass fibers to manufacture rack and pinion gear pair for the SAE formula supra car steering mechanism. It offered reduced noise, friction, and weight along with better corrosion resistance and self-lubricity (Chopane et al. 2018).

10.2.2 Braking System

Brake material

The braking unit needs to endure frictional torque and heat dissipation. The material employed for the brake rotor has to sustain in high temperatures and wear environment against thermoplastic deformation. Failure in the braking system is predominantly caused due to heat generation on account of friction between the rotor and braking pads (in the case of a disc braking system) or braking shoe (in case of drum braking system). Any sort of brake material failure will lead to accidents and consequently create a threat to the occupant's life. Formerly asbestos was extensively utilized as a brake material owing to its exceptional heat-absorbing property and abrasive nature. But its carcinogenic nature has later prohibited the use of asbestos and substituted by organic materials (Menezes et al. 2012b). The use of copper was also terminated due to its hazardous effects on marine life. Therefore the implementation of ceramic, aluminum and steel alloys was commonplace for succeeding years until composites were introduced. Composite materials made of fibers of carbon, glass or aramid as reinforcements in graphite or phenolic resins were gaining popularity as an alternative to asbestos for brake pads and brake linings in automobile applications (Jena 2019). Graphite and phenolic resins exhibit superior binding properties while the inclusion of carbon fiber yielded to enhancement in the hardness and specific strength of the brake material. Carbon fibers also provide thermal stability,
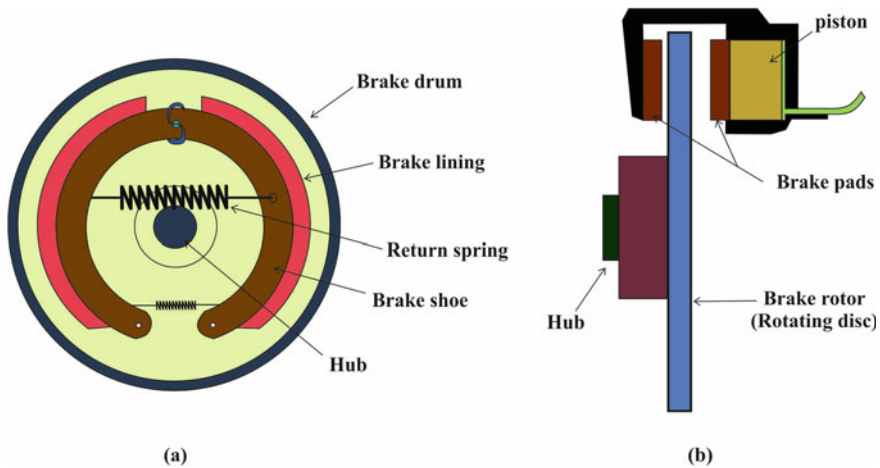
Fig. 10.4 Brake mechanism **a** Drum brake (Padmavathy et al. 2020) **b** Disc brake(Sadagopan et al. 2018)

wear-resistance and less curing time for better heat dissipation (Ahmadijokani et al. 2019).

Brake drum

The drum brake uses the principle where brake shoes or pads are pressed against the rotating drum to decelerate the speed of the drum on account of friction. The drum brake mechanism is displayed in Fig. 10.4a. Initially, brake drums were fabricated using cast iron which was heavyweight and corrodes easily yet displays good wear resistance. Later on, these were replaced by aluminum, a noncorrosive, much lighter, and thermally conductive material than iron. As aluminum wears out easily, brake drums made of aluminum with steel or iron lining on the inner surface were utilized for many years until MMC materials got introduced. Addition of abrasive particles such as alumina (Al_2O_3) and silicon carbide (SiC) into the aluminum matrix curbs the demerits of sole aluminum while retaining its boons. Combining effects of both reinforcement and matrix material revealed excellent strength and tribological properties along with reduced weight and better heat dissipation (Padmavathy et al. 2020; Rajak et al. 2020; Rajak and Menezes 2020; Chaudhary et al. 2020).

Brake rotor

Compressive forces deform the brake rotor profile which induces a vibration and ultimately results in failure. Motorcycle disc brake rotor cast from (AMC) with the 20% SiC reinforcement showed 56% reduction in weight compared to cast iron rotor. Reduced weight in brake rotors signifies lowered inertia forces (Sadagopan et al. 2018). Introducing graphite particles into aluminum alloy matrix manifests excellent wear properties attributed to the self-lubricating characteristic of graphite material. The composite material develops an anti-friction layer at elevated temperatures and

Fig. 10.5 a Interior trims (UFP Technologies 2021) and **b** Exterior trims of an automobile (Jasonstathamnz 2015).

gradually gets stronger, corresponding to further rise in temperature and volume percentage of graphite (Kumar and Kumar 2020).

Brake pads

In disc brakes, brake pads are pressed against the rotating disc under the action of the hydraulic piston, as shown in Fig. 10.4b. As long as operating conditions are concerned, friction and wear phenomenon in brake pads is inevitable. Without undermining the functionality of brake pad materials, wear can be alleviated by introducing composite materials with better performance than harmful asbestos. It is always feasible for the manufacturer to replace brake material despite altering the parameters of braking systems. Basalt fiber-reinforced composite (BFRC) material used as a brake pad material showed advancement in wear resistance and thermal stability as basalt fibers develop a tribo-layer between friction materials at high load conditions (Ilanko and Vijayaraghavan 2016).

When we consider the addition of natural fibers into a composite material to improve the biodegradability of the desired material, few treatments are needed to carry out on account of fiber-matrix compatibility. The selection of natural fibers primarily depends upon the desired characteristic required for the application as well as the availability of fibers in that geographical region which deduces cost with great means. DemostachyaBipinnata fibers were put through silane treatment in order to enhance fiber's surface characteristics for better fiber-matrix bonding and moisture resistance. Bipinnata fibers displayed great hardness number, and shear strength values together with exceptional wear resistance at high load and high-speed situations (Krishnan et al. 2021). Palm kernel fiber, Wheat fiber, and Nile rose fiber are desirable natural fibers combined with aluminum oxide (Al_2O_3) and graphite powder applicable for brake pads in order to enhance wear characteristics and hardness of material (Pujari and Srikiran 2019).

10.2.3 Suspension System

Automobile suspension systems are designed to restrain vertical displacements caused by road surface irregularities. The purpose is to provide comfort for occupants and protect the vehicle from getting damaged against shock loading. The suspension system serves its functionality through strain energy stored in its spring components and aids in making continuous contact with the road surface. Cast aluminum and steel material were broadly used as spring materials for a long time, although superior mechanical properties offered by the composite materials such as high specific strength, stiffness, anti-corrosive nature, high energy storing as well as absorbing capacity makes them the best fit for the spring material in automotive applications (Jena 2019).

Helical spring

Conventionally used steel helical springs as shock absorbing components in light motor vehicles (LMVs) are getting replaced by composite coil springs. About 50 to 80% reduction in weight is observed after substituting composite springs, which subsequently offers an overall decline in vehicle weight. It further offers corrosion resistance which eventually improves the life of the suspension component for a long number of cycles without failure. Various researches manifested the use of carbon fibers along with the glass fibers in epoxy resins have improved the stiffness and specific strength of a helical spring. Nevertheless, the use of basalt fibers instead of glass fibers in hybrid carbon/glass fiber composite has proven significantly better results concerning material sustainability and cost (Ke et al. 2020; Choi and Choi 2015). As fibers convey structural stiffness and strength to the composite material, increased fiber volume in the composite structure enhanced spring stiffness of carbon fiber reinforced epoxy resin composite helical spring. Further, twisted spring manifested minimum stress concentrations, unlike corresponding untwisted ones. It reveals that stress allocation is manageable by controlling twist angle (Wu et al. 2020b).

Belleville springs also serve potential gains helical spring for automobile applications. Polymer composite made of epoxy resin prepreg displayed improvement in vehicle handling and comfort by means of reduced tyre contact patch load variations and acceleration (Foard et al. 2019).

Leaf spring

A leaf spring counts for 10–20% of the unsprung weight of an automobile. Therefore cutting down the weight of the leaf spring will consequently reduce the overall weight of the vehicle to improve its performance. Composite leaf spring comprised of basalt fibers and epoxy resin exhibited phenomenal deduction in weight by 82.27% to that of steel spring retaining its stiffness (Raut et al. 2020). Leaf spring manufactured by stacking 55% vol. of woven carbon fibers into epoxy resin showed an 88.43% reduction in weight comparing to steel counterparts (Raut and Katu 2016). Leaf spring also undergoes friction and wear as it is bolted and clamped to the chassis.

Thus spring material must possess good wear and damping properties. Epoxies resins composite revealed excellent tensile strength and wear resistance in unidirectional reinforcement, while high flexural strength owning to weft reinforcements in 3D woven E-glass prepregs (Khatkar et al. 2020). Two different materials were proposed for leaf spring, AMCwith 25% inclusion of boron carbide and carbon fiber reinforced epoxy composite. Both materials exhibited enhancement in mechanical properties with a reduced weight with higher manufacturing cost compared to steel leaf spring (Singh and Brar 2018).

Tyres

An automobile runs on account of friction between the road surface and tyres. Thus, tyres must hold outstanding wear resistance and durability to maintain their traction on wet or dry roads without skidding. Goodyear, a top tyre manufacturer, introduced corn starch inclusions into tyre material to lower carbon black and silica dependency. Remarkably it decreased the rolling resistance and weight of the tyre, which resulted in minimal noise and rolling inertia further improving fuel economy (Sandstrom et al. 2002). Corn starch, an alternative filler material,was introduced for the most commonly used carbon black to produce tyres. It is a low-cost filler material with outstanding reinforcement capabilities. Addition of corn stover biochar along with corn starch and cornflour in rubber improved tensile properties (Peterson 2012; Kurihara 1995; Akampumuza et al. 2017). Tyres made from graphene-based elastomeric nanocomposites are lightweight and exhibit advanced mechanical properties with decreased rolling resistance which consequently reduced fuel consumption (Mansor and Akop 2020).

10.2.4   Interior Trims

Interior trims refer to all the plastic components or panels that are present inside the automobile cabin. Unlike automobile IC engine components, these components do not undergo high pressure, high temperature, or cyclic loading conditions. The functions of interior trim components are mainly to reduce vibration and noise. Along with the sound absorption characteristic, interior trim material needs to display several other properties, such as flame retardancy, durability, anti-rust, anti-wear, high specific strength, etc. Kevlar fibers are employed for seat textiles because of their high melting point, high kindling point, and thermal resistivity. Nonetheless, a reduction in the weight of any component will improve the vehicle's performance. Reducing weight in interior body panels is achieved by deploying natural fiber composites. Coconut fibers are utilized to manufacture seat bottoms, back cushions, and head restraints, while wood fibers are utilized for backseat cushions and abaca fibers for under-floor body panels. Cotton fibers also offer good sound absorption. Natural fibers composites comprised of plant polyols hold better tear resistance than glass fiber reinforced PU composites. Furthermore, their greater toughness, formability, specific strength over glass fibers makes them a superior candidate for automobile

door trims application (Dahlke et al. 1998; Rajak et al. 2019b; Kumar Rajak et al. 2021).

Interior door panels made of coir fiber in PP composite possessed better dimensional stability, hardness and flame retardancy than GFRP composite. As far as adding 60% of coir fibers resulted in advancement in flexural and tensile strengths of composite material by 26 and 35%, respectively (Ayrilmis et al. 2011). Three different natural fibers hemp, kenaf and flax along with their hybrid combination in epoxy resin were investigated to figure out the best suitable candidate for the fabrication of vehicle door panels. Reinforcement of Flax fiber in epoxy resin composite revealed superior tensile properties and showed better resistance to impact and plastic deformation when the load is applied (Prasad et al. 2021). PU foams are employed for automobile seat cushions and car door trims, while PU foam coated with nanomaterials such as graphene, graphene oxide, and carbon nanotubes exhibit high specific strength and stiffness values (Kausar 2018).

10.2.5 Exterior Trims

Exterior trims refer to plastic components outside the car cabin. They have to withstand impact loads, thermal degradation, and wear. The exterior body parts must hold enough strength and stiffness to resist impact loads on collision for the assurance of occupant safety. Exterior body panels were majorly made from sheet molding compounds (SMCs).

The bumper beam plays a vital role to bear sudden impact at the time of the head-on collision. Thus crashworthiness of the beam component determines occupant safety. By virtue of aramid fiber's incredible characteristics, such as toughness, tensile, flexural, and shear strengths with low density, a bumper beam made from aramid fibers in epoxy resin showed 20% enhancement in the tensile and impact properties to that of stainless steel (Selwyn 2021). Moreover, the combination of glass fibers with hemp fibers in epoxy resin also shows favorable impact strength and hardness requisite for automobile bumper application (Perumal et al. 2018). Kevlar fibers display great resistance to breakage under tensile loads compared to glass or carbon fibers. Former woven fiberglass thermoplastic was replaced by hybridized kevlar-date palm fibers in epoxy resin composite. Combined effects of reinforcing kevlar and date palm fibers raised tensile properties by a great extent which is best suitable for automobile bumper beam material concerning occupant as well as pedestrian safety (Muthalagu et al. 2020).

Front fender

Automobile fenders generally do not go through much stress but need to design for their crashworthiness. Extensively available low-cost sisal fibers treated with alkali solution for the removal of moisture and cellulosic matter showed high surface roughness. The composite material consists of alkali-treated sisal fibers reinforced

with polyester manifested superior tensile and flexural strength over steel counterparts. Alkali treatment offers anti-corrosive characteristics of the composite material, enhancing its fatigue life and rigidity of the component (Alemayehu et al. 2021).

Bonnet

Bonnet durability deteriorates as a consequence of vibrations developed in an automobile while driving. For this reason, automobile bonnet material is required to design for its stiffness against torsion and bending moment. Carbon fiber and glass fiber reinforced composite for an automobile bonnet displayed an increase in strength to weight ratio by 52% when compared with metallic bonnet (Ye et al. 2019). Glass fiber reinforced epoxy resin composite material manifested good tensile properties viable for engine hood material in automobiles (Wagh and Pagar 2018). Composite material's strength, stiffness, hardness, and thermal stability improved with the increased fraction of chopped carbon fibers in PP (Rezaei et al. 2008).

10.3   Other Automobile Applications

Automobile chassis has to sustain under various static and dynamic loads, including occupants and vehicle weight, torsion, and sudden impacts. Therefore, 10% weight reduction with improved rigidity was attained when carbon fiber reinforced thermoplastic composite chassis was substituted for Lotus Elise in place of aluminum chassis (Ishikawa et al. 2018). Glass was used for automobile headlamps and windows owing to its hardness and anti-scratch properties. However, it is replaced by lighter material called polycarbonate, which possesses higher impact resistance and toughness values. Furthermore, an anti-scratch, anti-smudging, hydrophobic coating was applied to polycarbonate by means of nano-particles of aluminum oxide, silica, and titanium oxide to ensure transparency and anti-fogging characteristic for automobile headlamps and windows (Bai et al. 2021). The increase in the percentage content of ZrO_2 in aluminium matrix composite resulted in improved hardness and wear resistance of connecting rod (Ramachandra et al. 2015). Aluminium matrix nanocomposites (AMNC) owing to their incredible strength, stiffness and creep resistance applicable for a variety of automobile components such as connecting rods, brakes, chassis, cylinder liner and exhaust valves (Singh et al. 2020). Ceramic matrix nanocomposites (CMNCs) are employed for nozzles and energy conversion systems where temperature and pressure conditions are extreme. Ceramic matrix incorporating carbon nanofibers displays durability at high temperatures, wear resistance, and are lightweight compared to steel or aluminum (Durowaye et al. 2017).

CFRP fuel pipe served as an outstanding barrier for terminating fuel evaporation and reducing weight by 83% compared to steel alloy (Sinha et al. 2018). Table 10.2 displays several different applications of composite materials in certain vehicles.

Table 10.2 Composite materials automobile applications

Refs	Year	Manufacturer/Model	Material used	Application	Findings
Kurihara (1995)	1980	GM Corvette	GFRP	Leaf springs	Reduced weight by 80% to that of steel leaf spring
	1984	Renault Espace	PMC	Hood, roof	Improved corrosion resistance
	1985	Ford Econoline	CFRP	Propeller shafts	50% weight reduction compared to steel counterparts
Akampumuza et al. (2017)	1995	Opel Corsa	Flax fiber PP composite	Interior door panels	Better soundproofing
	2006	Mercedes Benz S-class	Wood fibers and flax fibers composite	Front door linings, parcel shelves and rear trunk covers	Extended the use of sustainable materials by 73%
	2011	Lexus-CT200	Bio-based polyethylene terephthalate (PET)	Luggage compartment	Increased temperature resistance, durability with reduced susceptibility to shrinkage
Airale et al. (2017)	1981	Chevrolet Corvette C4	Glass fiber reinforced epoxy composite	Leaf spring	Reduced 15 kg of unsprung weight
Sandstrom et al. (2002)	1999	Goodyear (Tyre manufacturer)	Corn starch/plasticizer composite	Tyres	Improved rolling resistance with reduced weight and noise
Carello and Airale (2014)	2012	XAM 2.0	Carbon fiber epoxy resin composite	Wishbone arm in a suspension system	Stiffness improved by 78% with a 5% weight reduction
Schmitt et al. (2017)	2012	Audi AG	GFRP composite	Suspension spring	Reduced weight by 40% compared to steel springs

Table 10.2 (continued)

Refs	Year	Manufacturer/Model	Material used	Application	Findings
Saleem et al. (2020)	2020	Tata Super Ace	Fly ash-AMC	Gears	Minimal stress development with improved strength and stiffness

10.4 Conclusions

The state-of-art review presents a potential application of composite materials in the automobile industry. Owing to their phenomenal advancement in mechanical, thermal and chemical properties over traditional cast iron, steel, and aluminum, composite materials nowadays found their extensive application in almost every automobile component ranging from engine parts to body panels. Leading automobile manufacturers and researchers around the globe are testing for more novel variants of fillers material in metal or polymer matrix to fabricate a composite material for a certain application. The global concern of utilizing more sustainable materials and reducing carbon waste has compelled us to employ natural materials over synthetic ones. Material cost puts significant relevance on a unit price of a vehicle considering mass production in the automobile industry. Bio-composites are cost-effective materials as their constituents are naturally available in abundance. Brittleness of matrix materials was overcome by optimizing the volume fraction of fibers, as natural fibers possess good tensile properties to sustain impact loads following improvement in crashworthiness of automobile components. Moreover, low specific gravity of bio-composite materials remarkably curtails the overall weight of the vehicle improving its fuel efficiency. All four aspects lightweight, sustainability, cost-effectiveness, and crashworthiness of natural composites, have made them the most viable material for automobile application.

References

Aggarwal ML (2017) Experimental investigation into the effect of noise and damping using composite spur gear. Mater Today Proc 4(2):2777–2782

Ahmadijokani F, Shojaei A, Arjmand M, Alaei Y, Yan N (2019) Effect of short carbon fiber on thermal, mechanical and tribological behavior of phenolic-based brake friction materials. Compos B Eng 168:98–105

Airale A, Ferraris A, Xu S, Sisca L, Massai P (2017) Function integration concept design applied on CFRP cross leaf spring suspension. Int J Autom Compos 3(2–4):276–293

Akampumuza O, Wambua PM, Ahmed A, Li W, Qin XH (2017) Review of the applications of biocomposites in the automotive industry. Polym Compos 38(11):2553–2569

Alemayehu Z, Nallamothu RB, Liben M, Nallamothu SK, Nallamothu AK (2021) Experimental investigation on characteristics of sisal fiber as composite material for light vehicle body applications. Mater Today Proc 38:2439–2444

Ayrilmis N, Jarusombuti S, Fueangvivat V, Bauchongkol P, White RH (2011) Coir fiber reinforced polypropylene composite panel for automotive interior applications. Fibers Polymers 12(7):919–926

Bai Y, Zhang H, Shao Y, Zhang H, Zhu J (2021) Recent progresses of superhydrophobic coatings in different application fields: an overview. Coatings 11(2):116

Bouzouita A, Notta-Cuvier D, Raquez JM, Lauro F, Dubois P (2017) Poly (lactic acid)-based materials for automotive applications. Indus Appl Poly (Lactic acid):177–219

Carello M, Airale AG (2014) Composite suspension arm optimization for the city vehicle XAM 2.0. In: Design and computation of modern engineering materials, pp 257–272. Springer, Cham

Chandra AK, Kumar NR (2017) Polymer nanocomposites for automobile engineering applications. In: Properties and applications of polymer nanocomposites, pp 139–172. Springer, Berlin, Heidelberg

Chaudhary A, Gupta V, Teotia S, Nimanpure S, Rajak DK (2020) Electromagnetic shielding capabilities of metal matrix composites

Choi BL, Choi BH (2015) Numerical method for optimizing design variables of carbon-fiber-reinforced epoxy composite coil springs. Compos B Eng 82:42–49

Chopane A, Gupta S, Ajit A, Kakroo S, Salve A (2018) Design and analysis of plastic gears in rack and pinion steering system for formula supra car. Mater Today Proc 5(2):5154–5164

Cui S, Li R, Pei J, Wen Y, Li Y, Xing X (2020) Automobile exhaust purification over g-C3N4 catalyst material. Mater Chem Phys 247:122867

Cape Cod Curmudgeon (2018) 1941 Henry Ford's Soybean Car, Image retrieved from https://todayinhistory.blog/2018/08/13/august-13-1941-henry-fords-soybean-car/. Accessed 12 May 2021

Dahlke B, Larbig H, Scherzer HD, Poltrock R (1998) Natural fiber reinforced foams based on renewable resources for automotive interior applications. J Cell Plast 34(4):361–379

Dey S, Mehta NS (2020) Automobile pollution control using catalysis. Resour Environ Sustain:100006

Duroway SI, Sekunowo OI, Lawal AI, Ojo OE (2017) Development and characterisation of iron millscale particle reinforced ceramic matrix composite. J Taibah Univ Sci 11(4):634–644

Falsafi J, Rosochowska M, Jadhav P, Tricker D (2017) Lower Cost Automotive Piston from 2124/SiC/25p Metal-Matrix Composite. SAE Int J Engines 10(4):1984–1992

Faruk O, Tjong J, Sain M (Eds.) (2017) Lightweight and sustainable materials for automotive applications. CRC Press

Flax AM (1991) Capabilities of sheet molding composite in the automotive industry: an overview. SAE Technical Paper 910383

Foard JHD, Rollason D, Thite AN, Bell C (2019) Polymer composite Belleville springs for an automotive application. Compos Struct 221:110891

Fu S, Sun Z, Huang P, Li Y, Hu N (2019) Some basic aspects of polymer nanocomposites: A critical review. Nano Mater Sci 1(1):2–30

Ghassemieh E (2011) Materials in automotive application, state of the art and prospects. New Trends Develop Autom Indust 20:364–394

Gowda TY, Sanjay MR, Bhat KS, Madhu P, Senthamaraikannan P, Yogesha B (2018) Polymer matrix-natural fiber composites: An overview. Cogent Eng 5(1):1446667

Hassan T, Salam A, Khan A, Khan SU, Khanzada H, Wasim M, Kim IS (2021) Functional nanocomposites and their potential applications: a review. J Polymer Res 28(2):1–22

Holbery J, Houston D (2006) Natural-fiber-reinforced polymer composites in automotive applications. Jom 58(11):80–86

Hovorun TP, Berladir KV, Pererva VI, Rudenko SG, Martynov AI (2017) Modern materials for automotive industry. J Eng Sci 4(2)

Ilanko AK, Vijayaraghavan S (2016) Wear behavior of asbestos-free eco-friendly composites for automobile brake materials. Friction 4(2):144–152

Ishikawa T, Amaoka K, Masubuchi Y, Yamamoto T, Yamanaka A, Arai M, Takahashi J (2018) Overview of automotive structural composites technology developments in Japan. Compos Sci Technol 155:221–246

Jasonstathamnz (2015) why should I buy second hand car parts?, Image retrieved from https://jasons tathamnz.wordpress.com/2015/07/14/why-should-i-buy-second-hand-car-parts/. Accessed 25 May 2021

Jena H (2019) Study of tribo-performance and application of polymer composite. In: Automotive Tribology (pp. 65–99). Springer, Singapore

Kasar AK, Gupta N, Rohatgi PK, Menezes PL (2020) A Brief Review of Fly Ash as Reinforcement for Composites with Improved Mechanical and Tribological Properties. Jom 72(6):2340–2351

Kausar A (2018) Polyurethane composite foams in high-performance applications: A review. Polym-Plast Technol Eng 57(4):346–369

Ke J, Wu ZY, Liu YS, Xiang Z, Hu XD (2020) Design method, performance investigation and manufacturing process of composite helical springs: A review. Compos Struct 252, 112747

Khatkar V, Behera BK, Manjunath RN (2020) Textile structural composites for automotive leaf spring application. Compos Part B Eng 182:107662

Kim H, Kim C, Kim S, Kim B, Lim C (2019) Novel steel and aramid/phenol composite gear for a transmission with optimum design and FEM vibration analysis. Int J Automot Technol 20(4):749–754

Krishnan GS, Kumar JP, Shanmugasundar G, Vanitha M, Sivashanmugam N (2021) Investigation on the alkali treatment of Demostachya Bipinnata fibers for automobile applications-A green composite. Mater Today Proc 43:828–831

Kumar TV, Balaji S, Babu KM, Gautham KH (2015) Performance of magnetic fuel induction technology to reduce the exhaust emission. ARPN J Eng Appl Sci 10 (14)

Kumar M, Kumar A (2020) Sliding wear performance of graphite reinforced AA6061 alloy composites for rotor drum/disk application. Mater Today Proc 27:1972–1976

Kumar Rajak D, Pagar DD, Pruncu CI (2021) Failure Mechanisms of Biobased Composites: Biobased Composites: Processing, Characterization, Properties, and Applications:87–106

Kurihara Y (1995) Polymer matrix composite materials in automobile industries. Adv Compos Mater 4(3):209–219

Li Y, Xing X, Pei J, Li R, Wen Y, Cui S, Liu T (2020) Automobile exhaust gas purification material based on physical adsorption of tourmaline powder and visible light catalytic decomposition of g-C3N4/BiVO4. Ceram Int 46(8):12637–12647

Liu J, Xian Y, Cao D, Su J, Liao W, Ding M, Su Z (2016) Study of the design and torsion performance for carbon fiber composite material automobile drive shaft. In: Society of automotive engineers (SAE)-China congress (pp 303–312). Springer, Singapore

Macke A, Schultz BF, Rohatgi PK, Gupta N (2013) Metal matrix composites for automotive applications. In: Advanced composite materials for automotive applications: structural integrity and crashworthiness, pp 311–344

Mallick PK (Ed) (2020) Chapter 1—Overview. In Materials, design and manufacturing for lightweight vehicles (pp. 1–36). Woodhead publishing

Mansor MR, Akop MZ (2020) Polymer nanocomposites smart materials for energy applications. In: Polymer nanocomposite-Based smart materials (pp. 157–176). Woodhead Publishing

Johannes Maximilian—Own work (2020). Trabant 601, GFDL 1.2, Image retrieved from https://commons.wikimedia.org/w/index.php?curid=87864157 . Accessed 12 May 2021

Menezes PL, Rohatgi PK, Lovell MR (2012) Self-lubricating behavior of graphite reinforced metal matrix composites. In: Green tribology (pp. 445–480). Springer, Berlin, Heidelberg

Menezes PL, Rohatgi PK, Lovell MR (2012) Studies on the tribological behavior of natural fiber reinforced polymer composite. In: Green tribology (pp. 329–345). Springer, Berlin, Heidelberg

Menezes PL, Reeves CJ, Rohatgi PK, Lovell MR (2013) Self-lubricating behavior of graphite-reinforced composites. In: Tribology for scientists and engineers (pp. 341–389). Springer, New York, NY

Menezes PL, Rohatgi PK, Omrani E (eds) (2018) Self-Lubricating Composites (pp. 75–103). Springer, Berlin

Mohammed L, Ansari MN, Pua G, Jawaid M, Islam MS (2015) A review on natural fiber reinforced polymer composite and its applications. Int J Polymer Sci

Muhammad A, Rahman MR, Baini R, Bakri MK B (2021) Applications of sustainable polymer composites in automobile and aerospace industry. In: Advances in sustainable polymer composites (pp 185–207). Woodhead Publishing

Muthalagu R, Murugesan J, Kumar SS, Babu BS (2020) Tensile attributes and material analysis of kevlar and date palm fibers reinforced epoxy composites for automotive bumper applications. Mater Today Proc

Oliver-Ortega H, Julian F, Espinach FX, Tarrés Q, Ardanuy M, Mutjé P (2019) Research on the use of lignocellulosic fibers reinforced bio-polyamide 11 with composites for automotive parts: Car door handle case study. J Clean Prod 226:64–73

Omrani E, Rohatgi PK, Menezes PL (2017) Tribology and applications of self-lubricating materials. CRC Press

Padmavathy S, Kamalakannan R, Manikandan A (2020) Tribological and mechanical properties of AA6061 reinforced with SiC and graphite for automobile applications. Mater Today Proc 21:24–29

Panaitescu I, Koch T, Archodoulaki VM (2019) Accelerated aging of a glass fiber/polyurethane composite for automotive applications. Polym Testing 74:245–256

Patil A, Patel A, Purohit R (2017) An overview of polymeric materials for automotive applications. Mater Today Proc 4(2):3807–3815

Perumal CI, Sarala R, Muthuraja R, Senthilraja R (2018) A review on characteristic of polymer composites with natural fiber used as a reinforcement material. Int J Res Appl Sci Eng Technol 6(1):1213–1217

Peterson SC (2012) Evaluating corn starch and corn stover biochar as renewable filler in carboxylated styrene–butadiene rubber composites. J Elastomers Plast 44(1):43–54

Prasad SV, Kumar GA, Sai PY, Basha SV (2021) Design and fabrication of car door panel using natural fiber-reinforced polymer composites. Trends Manufact Eng Manag:331–343

Prateemak (2012) Taken By Dr Pradeep Rohatgi aluminum graphite particle composite piston and cylinder liner UWM Center for Composite Materials, CC BY-SA 4.0, https://en.wikipedia.org/w/index.php?curid=62445252. Accessed 17 May 2021

Pujari S, Srikiran S (2019) Experimental investigations on wear properties of Palm kernel reinforced composites for brake pad applications. Defence Technol 15(3):295–299

Rajak DK, Pagar DD, Kumar R, Pruncu CI (2019a) Recent progress of reinforcement materials: a comprehensive overview of composite materials. J Market Res 8(6):6354–6374

Rajak DK, Pagar DD, Menezes PL, Linul E (2019b) Fiber-reinforced polymer composites: Manufacturing, properties, and applications. Polymers 11(10):1667

Rajak DK, Wagh PH, Menezes PL, Chaudhary A, Kumar R (2020) Critical overview of coatings technology for metal matrix composites. J Bio Tribo-Corros 6(1):1–18

Rajak DK, Menezes PL (2020) Application of metal matrix composites in engineering sectors. Encyclopaedia of Mater Compos Elsevier

Ramachandra M, Abhishek A, Siddeshwar P, Bharathi V (2015) Hardness and wear resistance of ZrO2 nano particle reinforced Al nanocomposites produced by powder metallurgy. Proc Mater Sci 10:212–219

Raut LB, Katu AR (2016) Experimental analysis of different compositions of carbon fiber/epoxy composite and its application in leaf spring. In: International conference on advanced technologies for societal applications techno-societal 2016 (pp. 699–707). Springer, Cham

Raut LB, Jadhav SV, Jagadale VS, Swami V, Gavali SR, Gade SB (2020) Experimental investigation of basalt fiber/epoxy composite for automobile leaf spring. In: Techno-Societal (pp 777–787). Springer, Cham

Rezaei F, Yunus R, Ibrahim NA, Mahdi EDOSCFRPCFCB (2008) Development of short-carbon-fiber-reinforced polypropylene composite for car bonnet. Polymer Plast Technol Eng 47(4):351–357

Rohatgi PK, Menezes PL, Lovell MR (2012) Tribological properties of fly ash-based green friction products. In: Green tribology (pp 429–443). Springer, Berlin, Heidelberg

Sadagopan P, Natarajan HK, Kumar P (2018) Study of silicon carbide-reinforced aluminum matrix composite brake rotor for motorcycle application. Int J Adv Manufact Technol 94(1):1461–1475

Saleem M, Ashok Raj J, Sam Kumar GS, Akhila R (2020) Design and analysis of aluminium matrix composite spur gear. Adv Mater Process Technol:1–9

Sandstrom PH (2002) U.S. Patent No. 6,391,945. U.S. Patent and Trademark Office, Washington, DC

Schmitt J (2017) U.S. Patent No. 9,604,515. U.S. Patent and Trademark Office, Washington, DC

Selwyn TS (2021) Formation, characterization and suitability analysis of polymer matrix composite materials for automotive bumper. Mater Today Proc 43:1197–1203

Singh H, Brar GS (2018) Characterization and investigation of mechanical properties of composite materials used for leaf spring. Mater Today Proc 5(2):5857–5863

Singh M, Bhandari D, Goyal K (2020) A review of the mechanical performance of nanoparticles reinforced aluminium matrix nanocomposites. Mater Today Proc

Sinha M, Tyagi RK, Bajpai PK (2018) Weight reduction of structural members for ground vehicles by the introduction of FRP composite and its implications. In Proceedings of the international conference on modern research in aerospace engineering (pp 277–290). Springer, Singapore

Stark N, Cai Z (2021) Wood-based composite materials: panel products, glued laminated timber, structural composite lumber, and wood–nonwood composites. Chapter 11 in FPL-GTR-282, 11–1

Stojanović B, Ivanović L (2015) Application of aluminium hybrid composites in automotive industry. Tehnički Vjesnik 22(1):247–251

Suresh G, Srinivasan T, Bernard SS, Vivek S, Akash RM, Baradhan G, Anand B (2020) Analyzing the mechanical behavior of IPN composite drive shaft with E-glass fiber reinforcement. Mater Today Proc:1107–111

UFP Technologies (2021) Case study: automotive interior trim components. Image retrieved from https://www.ufpt.com/resource-center/automotive-interior-trim-components/. Accessed 25 May 2021

Tiruvenkadam N, Thyla PR, Senthilkumar M, Bharathiraja M, Murugesan A (2015) Synthesis of new aluminum nano hybrid composite liner for energy saving in diesel engines. Energy Convers Manage 98:440–448

Todor MP, Kiss I (2016) Systematic approach on materials selection in the automotive industry for making vehicles lighter, safer and more fuel–efficient. Appl Eng Lett 1(4):91–97

Tony Borroz (2009) 'June 30, 1953: Corvette Adds Some Fiber, Flair to American Road', The very first Corvettes roll off the assembly line at the Chevrolet plant in Flint, Michigan. Image retrieved from, https://www.wired.com/2009/06/dayintech-0630/. Accessed 12 Apr 2021

Verma D, Sharma S (2017) Green biocomposites: a prospective utilization in automobile industry. In: Green biocomposites (pp 167–191). Springer, Cham

Wagh PH, Pagar DD (2018) Investigation of mechanical and tribological behavior of composite material filled with black epoxy resin and aluminium tri-hydroxide using reinforcement of glass fiber. In: AIP Conference Proceedings (vol. 2018, No. 1, p. 020025). AIP Publishing LLC

White LJ (2013) The automobile industry since 1945. Harvard University Press

Wilhelm M (1993) Materials used in automobile manufacture-current state and perspectives. Le J De Phys IV 3(C7):C7-31

Wu Q, Miao WS, Gao HJ, Hui D (2020a) Mechanical properties of nanomaterials: a review. Nanotechnol Rev 9(1):259–273

Wu L, Chen L, Fu H, Jiang Q, Wu X, Tang Y (2020b) Carbon fiber composite multistrand helical springs with adjustable spring constant: design and mechanism studies. J Market Res 9(3):5067–5076

Ye H, Liu C, Yan K (2021) Optimization design of the structure of the automobile bonnet made of fiber composite material. In: Proceedings of China SAE congress 2019: selected papers (pp. 675–693). Springer, Singapore

Chapter 11
Modeling of a Closed Loop Hydrostatic Transmission System and Its Control Designed for Automotive Applications

Santosh K. Mishra and Purushottam Kumar Singh

Abstract This control strategy can be quite handful in practical situations where constant rpm is the primary need, especially in case of heavy drilling machines/automobiles being employed in drilling large stone quarry in mines. In such a situation, the drilling needs to be performed at a predetermined speed only and major fluctuations in the speed can lead to undesirable results. To realize the same control strategy in real terms, the physical model of a closed loop HST (Hydrostatic Transmission system) system consisting of a variable displacement pump and a fixed displacement motor has been developed. Conventionally, the rpm of the motor decrease upon loading the pump as load pressure increases. This can severely affect the performance of the overall system as it is assumed that the system works excellently or is designed for certain range of rpm which should be more or less constant. Hence in view of the situation, a feedback control mechanism is applied via means of PID (Proportional, Integral and Derivative) controller which keeps track of the decline in rpm of the motor and through certain control strategy sends a command signal to the pump. Based on the received feedback signal, the inclination of the swash plate of the pump is varied resulting in the increase of the flow rate from the pump which consequently increments the rpm of the motor to match the demand requirements resulting in the constant rpm. Furthermore, an advanced PID controller constructed on the basis of neural network following has the capability of approximating nonlinearities. The devised controller has been found to be quite effective during simulations and has edge in regulating the parameters, better robustness and minimizing nonlinearities, fluctuations and errors. Performance indicators such as correlation coefficient (R), variance and root mean square error (RMSE) are computed for the model under multiple regression analysis.

Keywords Closed loop · Hydrostatic Transmission System · Swashplate · PID · Neural Network · Friction

S. K. Mishra (✉)
Department of Production Engineering, National Institute of Technology, Trichy 620015, India

P. K. Singh
Department of Mechanical Engineering, BIT Sindri, Dhanbad 828123, India

11.1 Introduction

In this present scenario, the utility of pumps especially axial piston pumps in hydraulic systems becomes very crucial because of its pressure control applications (Costopoulus 1992; Rexroth 1986). These pumps have certain features which makes it handy such as providing regulated flow according to consumer requirement which leads to higher efficiency and minimizing the temperature of the oil with controlled pressure. The variable displacement axial piston pump in association with various valves such as servo or proportional valves makes provides effectiveness and ease of operation to modern hydraulic system. Sophisticated hydraulic control systems are modeled keeping in mind the static and dynamic characteristics of these pumps (Kaliafetis and Costopoulos 1995). Monitored hydraulic power supplies as well as hydrostatic transmission drives are two key areas dealing in fluid power which finds predominant application of these pumps. The ability to vary its displacement along with its high power to weight ratio makes it more desired component for controlling systems utilizing highest level of power (Karkoub et al. 1999). From design perspective, they are comparatively simple and reliable; however, their main attracting feature involves varying the displacement at the output.

Meanwhile, for accomplishing the task of controlling the hydraulic component such as hydro-motor, the need of the hour is to follow controlling methods which can turn out to be quite effective such as PID (Çetin and Akkaya 2010; Knohl and Unbehauen 2000), fuzzy (Liu et al. 2014; Hassan and Kothapalli 2012; Kalyoncu and Haydim 2009), neural network (Wu et al. 2009; Taormina et al. 2012; Jia et al. 2013) etc. PID is widely used in hydraulic systems because of having some specific features such as uncomplicated structuring, ease in execution and comprehensive analytical analysis. The most essential part involved in PID control is the efficient tuning of the three adaptable gains, the proportional gain Kp, integral gain Ki and derivative gain Kd.Nevertheless, PID is empowered to deal with systems which are having linear attribute and is incompetent to deal with systems which are having nonlinear behavior alone such as friction. However, in recent past the trend has changed and lot of artificial intelligence techniques have evolved which can be applied as optimizers in order to tune the PID gains for dealing with complex and nonlinear systems. Karam et al. (Elbayomy et al. 2008) suggested the genetic algorithm (GA) in order to monitor the angular position related to electro-hydraulic servo actuator online by optimizing tuning the PID controller gains. Chang (2013) deployed the artificial bee colony (ABC) algorithm for searching the parameters of PID control. Das et al. (2017) devised a control approach using PID along with the feed forward for the tracking of an electro-hydraulic actuation system having a nonlinear model which considered the frictional effects originating from a geometrically symmetric hydraulic cylinder and the variation in the openings associated with the metered ports of a solenoid-driven proportional valve. Kaddissi et al. (2007) analyzed the modeling of an electro-hydraulic servo system along with its control in real time. They applied nonlinear backstepping algorithm as their controlled strategy and observed that under the conditions when the system loading is exceptionally high, then the PID controller

does not perform efficiently as compared to a nonlinear controller designed on the basis of backstepping scheme.

Neural Networks (NN) has been found to be another viable modeling option which yields quite satisfactory results for the system which dealing with nonlinearities like viscous friction. This method attempts to work on the same pattern as the brain does in retrieving information. Karkoub and Elkamel (1997) applied a neural network model for predicting the distribution of pressure inside a rectangular shaped gas bearing. The prediction results in terms of pressure distribution along with the load bearing capacity furnished by the proposed model proved to be way ahead in comparison with the existing tools. Gharbi et al. (1995) envisaged an important oil recovery by applying neural networks. In contrast to the traditional regression or finite difference techniques, the performance of the NN model was remarkably appreciable. Li et al. (1995) utilized NNs in association with the Powell's optimization method for controlling single and double link inverted pendulums. The authors got substantial results. Panda et al. (1996) employed NNs for modeling fluid contacts around Prudhoe Bay oil fields. The model developed by them gave a better estimation of the circulation of the fluid and precisely in contrast with the conventional regression-based methods. Aoyama et al. (1996) deduced an NN model for predicting the response related to a non-minimum phase system. The model put forwarded by them was employed in Van de Vuss reactor and a continuous stirred tank bioreactor and encouraging results were obtained.

Off late PIDNN controller is considered one of the well-known techniques involved in the controlling of nonlinear and intricate systems. Various techniques which are considered robust and can be auto tuned have been devised in order to further refine the control and robust functioning linked with the PIDNN controller (Jung et al. 2015; Skoczowski et al. 2005; Zhao et al. 2015; Chen et al. 2015). An adaptive PIDNN controller (Kang et al. 2014) has been proposed for improving the converging speed and to avoid the trapping of the weights in the local optima, the particle swarm optimization (PSO) is followed for initializing the neural network. The experimental results are observed to be effective justifying the devised algorithm. The PSO algorithm takes a fair bit of time during the course of initializing the weights. Cong et al. (2009) examined the consequences of the learning rates in terms of stability of a closed loop system. The weight updating of the proposed controller is done based on the errors induced by unsettled factors of the system under consideration. The proposed controller has been found to be robust while considering parameter uncertainty. Ho et al. (2006) developed an optimization problem with the aim to establish a fuzzy neural network model (FNNM) with the objective of effectively tune the PID controllers of a plant having under damped nature. Nevertheless, the algorithm put forwarded need considerable effort as the number of parameters needs to be ascertained before its final implementation. A novel design of PID controller established in association with neural network based on minimum norm least square has been proposed by Vikas et al. (2014). The gains of the PID controller are updated online by means of recursive least square. The implementation of the controller is quite simple and it requires minimum number of parameters to be tuned before implementing.

The methodology proposed by Guo et al. (2009) has been used for tuning and regulating the parameters of the proposed controller, nevertheless the validation of the methodology is done by its implementation in a closed loop hydraulic set up for controlling the speed of the hydraulic motor.

11.2   System Description

The flow is catered towards motor via cross line relief block by means of a swash plate controlled variable displacement pump (SCVDP) which is shown in Fig. 11.1. There is a provision for the connection of the pump with the motor via return line. In order to compensate for the leakage of the system, a small refilling charge pump is provided which is integral of the system. The capacity of the charge or feed pump both in terms of pressure and flow is very small. In order to permit make up fluid to reach the main pump via return line, the cross-line relief valve is provided in the circuit which also keeps the high-pressure side isolated. The make-up circuit relief valve is designed at the maximum system pressure of the circuit and has to act according to the necessities of the main pump. Plenum is considered as the amount of volume of fluid in between the outlet of source pump and the inlet of directional control valve. It is assumed that for the smooth free working of the motor, surging effect is provided by the plenum in association with the flexible conduit. The inertial and viscous loads are driven by the low speed high torque (LSHT) motor. The pictorial view of actual experimental set up is depicted in Fig. 11.2.
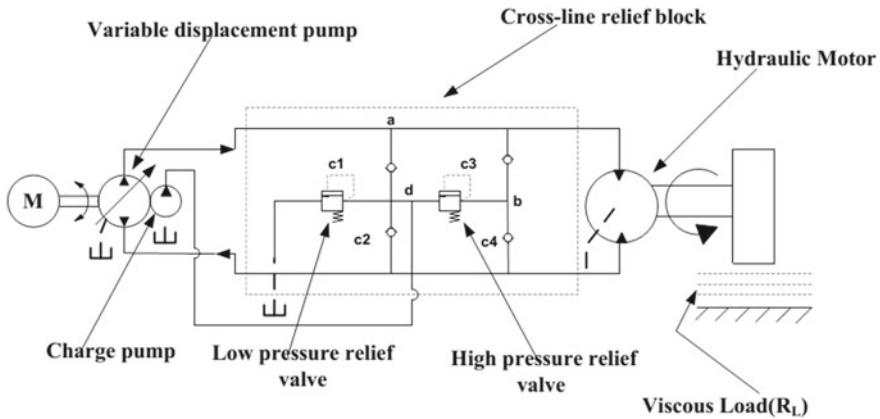
Fig. 11.1 Experimental test set-up (overall circuit)

Fig. 11.2 Experimental test set-up

11.3 Experiment Description

The experiment has been accomplished in a closed loop hydrostatic transmission primarily comprising of SCVDP and LSHT motor under LabView environment through controller (cRIO). The control approach utilized for the experimentation has been depicted in Fig. 11.3. With reference to Fig. 11.3, it can be observed that the demand or reference signal and the sensor response signal pertaining to hydraulic motor 's speed undergoes algebraic operation in the summation block. Consequently, the voltage signal is being supplied to SCVDP for the excitation of swash plate. The arithmetic operations are executed under the core algorithm block.

The response is being plotted at dissimilar command signals (being supplied to the PRV) as shown in Fig. 11.4 that monitors the flow and pressure behavior of the valve and indirectly the viscous friction coefficient as discussed earlier. As the command voltage gets incremented, there is increase in resistances also.

11.3.1 The Hydraulic System Modeling and Experimental Validation

The modeling of the proposed system has been carried out in MATLAB-Simulink. The Simulink model of the proposed system has been provided in Fig. 11.5.

The simulated as well as the experimental response of the hydraulic motor speed pertaining to the HST has been traced in Fig. 11.6. The model is managed in such a way that the rotational speed of the motor always tries to catch up with the excitation
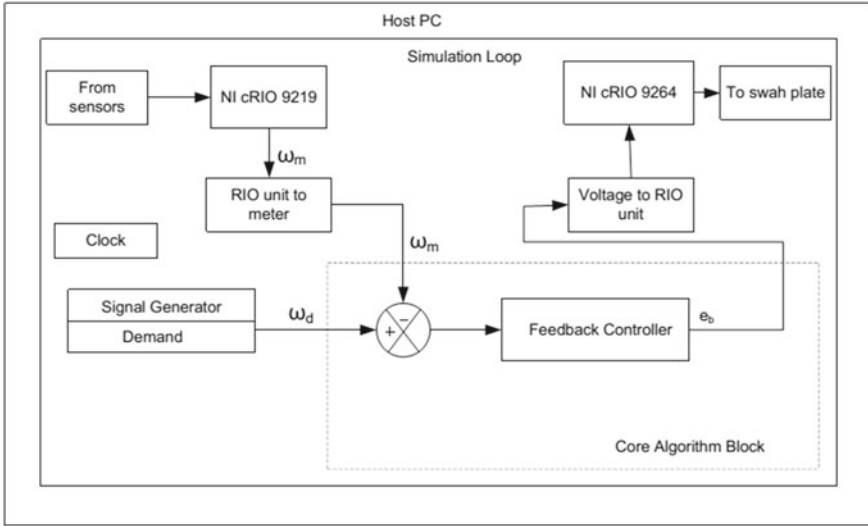
Fig. 11.3 Control strategy using PID control
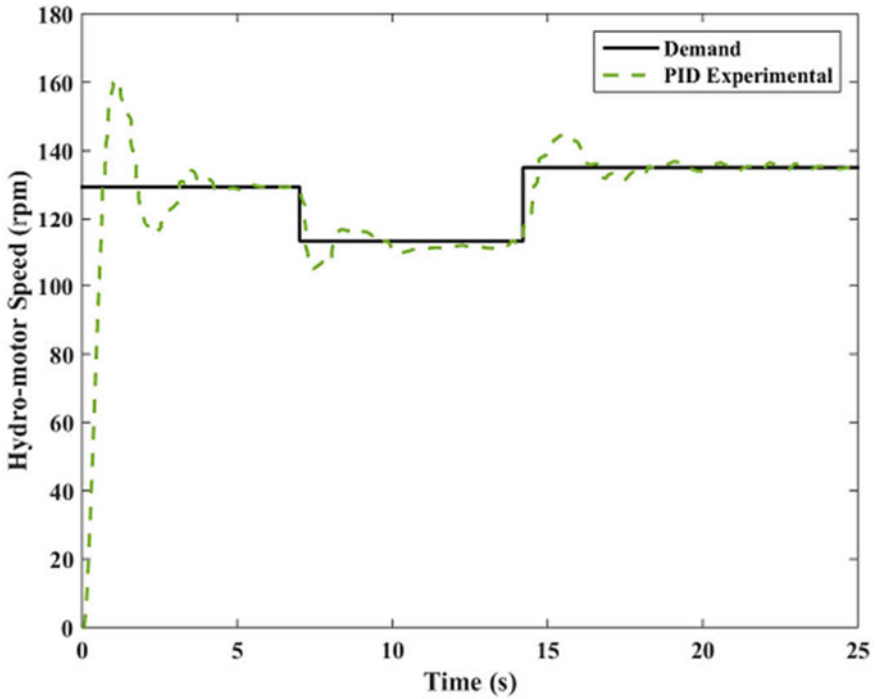
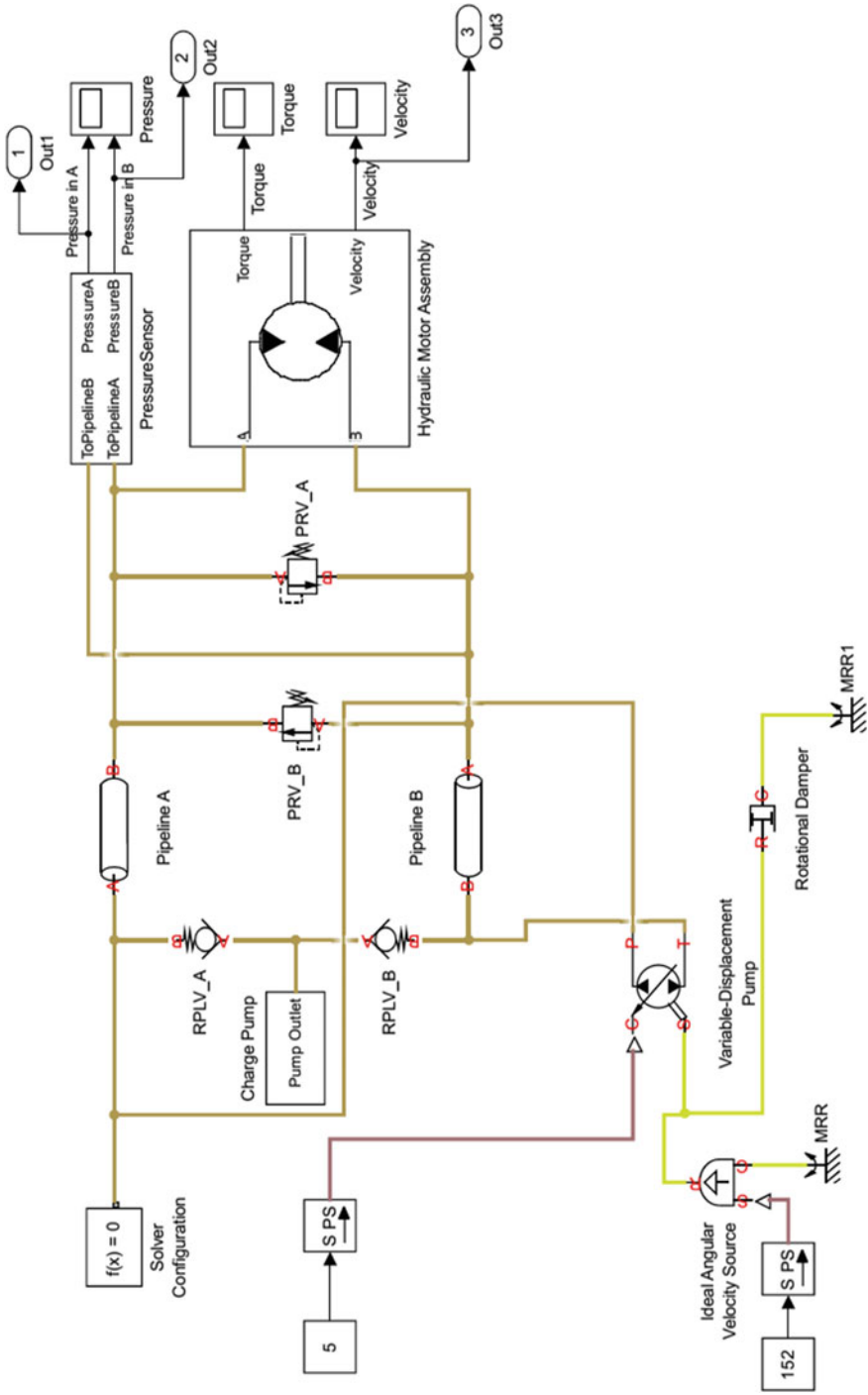**Fig. 11.4** Variation of experimental motor speed with time

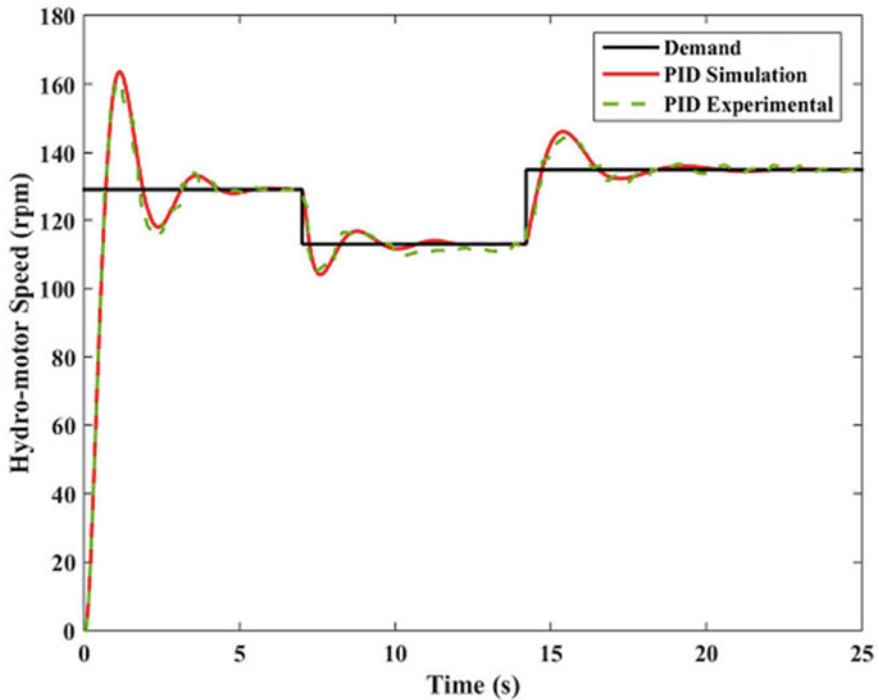**Fig. 11.5** Simulink model of the proposed system

Fig. 11.6 Comparison between predicted and the experimental motor speed

step signal i.e. whenever the rpm of the motor falls below the demand or desired threshold value of the rpm, the pump is held responsible for the basic or primary adjustment of transmission. Hence, the feedback mechanism gets activated via means of PID control which automatically results in the altering of the capacity of the pump by means of the change in the swash plate angle. The feedback mechanism gets triggered by sensing the rotational speed of the motor which eventually gets affected due to the load applied by varying the settings of the PRV. The excitation step signals have been superimposed by the response rotational speed of the motor in the various step signal zones. The permissible range of rotational speed of the hydraulic motor has been determined for the model in consideration.

The dynamic nature of the system was taken into consideration which emphasized: the effect of step type signal of rpm being overlapped over by the hydraulic motor by considering the adjustment made in view of feedback signal undermining the variable pump's capacity, addressing both the cases of presence of error and with no error along with its compensation. It has been shown in 1st part of the curve 6.1. The same feature has been observed for other steps which are getting overlapped by the hydraulic motor and hence getting their flow adjustment determined by the capacity of variable displacement pump as shown in 2nd and 3rd part of the curve 6.

11.4 Traditional Pid Control of the Closed Loop System

With the intention of controlling the speed of the hydraulic motor for tracking its reference demand speed, PID control is utilized in the pumping section as shown in Fig. 11.7. The general PID control scheme can be put forward as a function of time in the following way:

$$e(t) = \omega_r(t) - \omega(t) \tag{11.1}$$

$$u(t) = K_p e(t) + K_i \int_0^t e(t)dt + K_d \frac{de(t)}{dt} \tag{11.2}$$

where e represents the error between the reference speed and the actually obtained speed, parameters K_p, K_i and K_d stands for proportional gain, integral gain and derivative gain, respectively.

Ziegler-Nichols second method fits suitable here and hence has been employed to obtain the parameters K_p, T_i and T_d. The transfer function of PID controller as tuned by means of second method of Ziegler–Nichols rules (Ogata 2003) is given by:

$$G(s) = K_p(1 + 1/T_i s + T_d s) \tag{11.3}$$

The complete procedure of tuning is provided below:

(i)   Firstly, the values of parameters are set as T_i=0 and T_d=∞.
(ii) The proportional gain K_p comes into action as its value is increased from 0 to a critical value K_{cr} where sustained oscillations are firstly displayed by the output. In this way, the control gain K_{cr} and the corresponding period P_{cr} are ascertained via experimentation.

Ziegler-Nichols proposed for the setting of the parameters .

Type of Controller	K_p	K_i	K_d
PID controller	$0.6K_{cr}$	$K_p/0.5P_{cr}$	$0.125K_p P_{cr}$

$P_{cr} = 0.56$, $K_{cr} = 0.00083$.

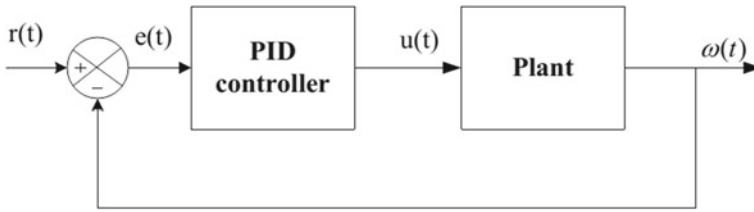| Type of Controller	K_p	K_i	K_d
PID controller	4.9800e-04	0.0018	3.4860e-05

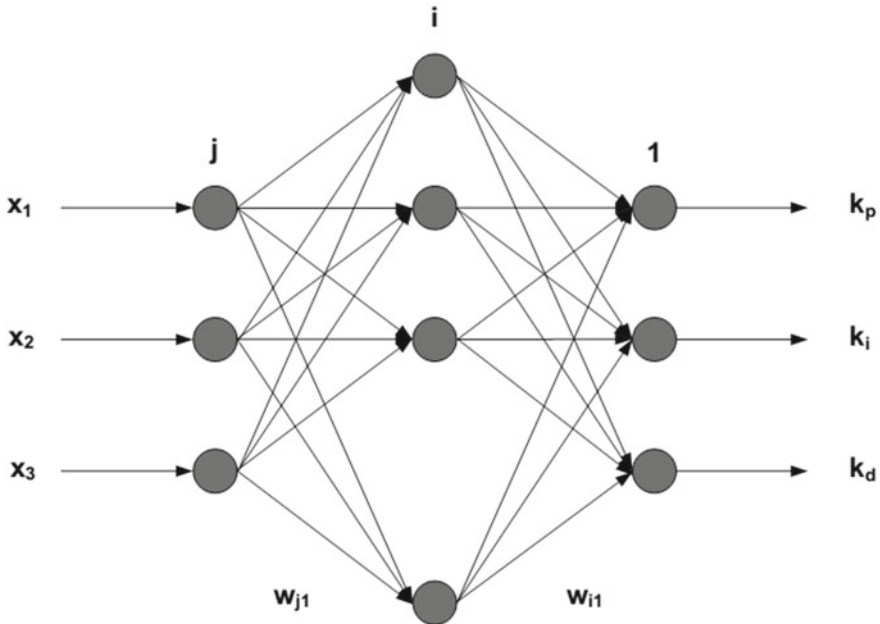**Fig. 11.7** Closed loop HST system with PID controller

Fig. 11.8 Architecture of the Neural Network structure

11.4.1 PID Controller Based on the Artificial Neural Network

The conventional PID control extensively used in industrial processes since its method of controlling is simple, straightforward and robust. But, some drawbacks are related with PID control. First of all, sometimes it's gets very tedious to control the three gains associated with the PID controller i.e. Kp, Ki and Kd. Secondly, PID control is generally employed in linearized systems and hence when the situation arises such that it has to deal with nonlinear, time varying or the system possessing large inertia; in such cases it has found to be less effective. Therefore, to deal with the nonlinearities and fine tuning the gains of the PID controller, artificial neural networks (ANN) are employed. They possess the features of self-adaptation with learning, nonlinear representation, robustness and fault tolerant behavior. A PID

controller which is tuned by ANN has been devised in this paper (Guo et al. 2009). The results obtained through simulation indicate that the can be applied with ease and is quite handy in regulating the parameters of PID.

The back-propagation algorithm (BP) is utilized to build an ANN model. After assessing the real time condition of the control system under observation, the perquisite is to design an ANN network having three layers in structure i.e. input, hidden and output layers. The architecture of BP neural network is shown in Fig. 11.8, whose exact numbers are ascertained based on the complexity linked with the controlled plant. Input layer represents the first layer. The neurons present in the middle layer represent the hidden layer. The output layer is represented by the third layer which contains the parameters of the PID i.e. kp, ki and kd.. The input and the output layers of the ANN network are linked by means of hidden layer nodes, which relate the true associations present involving the theses two layers. For the sake of simplicity, the hidden layers as minimum as possible and for the network under investigation 8 hidden layers have been taken into consideration. It is a matter of experience or using hit and trial method for getting the hidden layer nodes practically. The activation function of the neuron representing the input layer is considered linear function $f_i(x) = x$; while Sigmoid function $f_h(x) = \frac{1}{1+e^{-x}}$, is considered for the hidden layer and again linear function $f_o(x) = x$ is used for the output layer.

With a focus on closed loop control related to industrial sector, the (PID) controller is the most versatile controller used nowadays. The algorithm based on digital incremental PID is given below:

$$u(k) = u(k-1) + k_p(e(k) - e(k-1)) + k_i e(k) + k_d(e(k) - 2e(k-1) + e(k-2))$$
(11.4)

The weights w_1, w_2 and w_3 corresponding to the neurons will be operating as like as gains of the PID controller. By means of some learning rule, the weights linked with the neural network are changed in order to achieve the desired objective. The proportional, integral and integral errors are represented by $x_1(k)$, $x_2(k)$ and $x_3(k)$ respectively and are jotted down below:

$$x_1(k) = e(k) - e(k-1)$$
(11.5)

$$x_2(k) = e(k)$$
(11.6)

$$x_3(k) = e(k) - 2e(k-1) - e(k-2)$$
(11.7)

where K represents a constant used to speed up or slow down the response of the closed loop.

The learning algorithm for neural network based on back propagation is reported in the following way:

$x_j(1, 2……, n)$ represents the input corresponding to the network. The input and output pertaining to the hidden layer is given as:

$$net_h(k) = \sum_{j=0}^{m} w_{ij}x_j \qquad (11.8)$$

$$O_h(k) = f(net_h(k)), h = 1, 2 \ldots, n \qquad (11.9)$$

where w_{ij} stands for the weights assigned to the hidden layer. The activation function related to the hidden layer follows sigmoidal function.

$$f(x) = \frac{1}{1 + e^{-x}} \qquad (11.10)$$

The inputs and outputs linked with the output layer are computed in the following way:

$$net_o(k) = \sum_{j=0}^{m} w_{ij}o_h \qquad (11.11)$$

$$O_o(k) = g(net_o(k)), h = 1, 2 \ldots, n$$
$$O_1 = k_p; \; O_2 = k_i; O_3 = k_d. \qquad (11.12)$$

The different steps involved in tuning a PID controller by means of ANN are given by:

Step 1: Random values are selected for the weights.

Step 2: The error is computed by subtracting the reference input with the output.

Step 3: The gains associated with the PID controller are determined through supervised delta learning method, employing the error signal.

Step 4: For obtaining an improved closed loop response, the multiplication of the output of the individual neuron i.e. Δu is done with a gain K.

Step 5: The updated weights will assume the role of the proportional gain, the integral gain and the derivative gain respectively.

The supervised delta learning rule used in order to update the weights has been provided by Giacomino et al. (2011):

$$w_1(k) = w_1(k - 1) + \eta_P e(k - 1)u(k - 1) \qquad (11.13)$$

$$w_2(k) = w_2(k - 1) + \eta_I e(k - 1)u(k - 1) \qquad (11.14)$$

$$w_3(k) = w_3(k - 1) + \eta_D e(k - 1)u(k - 1) \qquad (11.15)$$

η_P, η_I and η_D stands for the proportional, integral and the derivative learning rates.
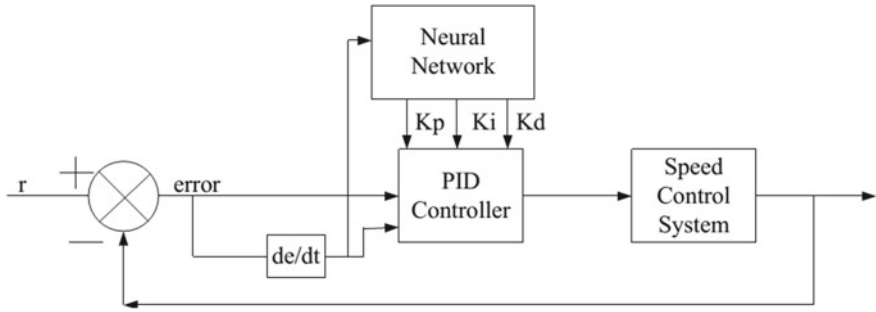
Fig. 11.9 Schematic of Neural Network tuned PID control system

The controlling technique is adaptive PID control established on back propagation neural network. The basic architecture of adaptive PID control developed on the basis of back propagation neural network is depicted in Fig. 11.9.

11.5 Multiple Linear Regression (MLR)

Through Multiple linear regression (MLR), a mathematical expression can be achieved showing the linear association between a dependent variable and several independent variables (Giacomino et al. 2011). The dependent variable is occasionally referred as predict and the independent variables as predictors.

Multiple regression analysis basically aims to create a choice between the available independent variables for obtaining the best suitable model equation which describes the dependent variable appropriately based on its usage (Harrell 2001). Considering the bivariate correlation, measurements such as flow rate, pump pressure, motor pressure, supply voltage, loading voltage etc. taken from the hydraulic test set up that are closely correlated with the predicted speed of the hydraulic motor at a confidence level of 95% are chosen for constructing the model. Each and every independent variable was utilized for identifying the apt regression model and in this regard various empirical relations such as exponential and power, logarithmic and linear were attempted in order to constitute a regression linking motor speed employing every independent variable. The results suggested that linear relations were suited for the experimental data having higher correlation coefficient (r^2). MLR is established on the ground of least squares: the model is considered fit if all the sum of squares of differences of observed and predicted values are as small as possible. Hence for the present study, multiple regression model is considered as linear and can be expressed as:

$$Y = \beta_0 + \beta_1 X_{1i} + \beta_2 X_{2i} \ldots\ldots\ldots\ldots\ldots + \beta_n X_{ki} + \varepsilon \qquad (11.16)$$

where Y is the predicted value corresponding to the response, X_1, X_2, and X_n are the predictors and β_1, β_2, and β_n are the regression coefficients of X_1, X_2, and X_n, the parameter β_0 is constant representing the value of y when all the independent variables are zero.

11.5.1 Performance Evaluation for the Models

In order to evaluate the performance of the model predicted by ANN, mean square error (MSE) was employed and computed by means of equation:

$$MSE = \frac{1}{N} \sum_{i=1}^{N} (t_i - td_i)^2 \qquad (11.17)$$

where t_i represents the measured value of the experimental samples, td_i is the predicted value, and N denotes the total number of samples.

The normalization of the data sets is an essential step and must be carried out in order to equalize the significance of variables before the commencement of the training of the network. Therefore, the normalization of the training and testing data sets were done by means of their least and highest values under the range of -1 and 1because of using hyperbolic tangent sigmoid function in the model. At last, the outputs obtained were changed to their initial scale employing a reverse normalizing process for calculating the results. The normalization process was done utilizing Eq. (11.18)

$$X_{norm} = \frac{X - X_{\min}}{X_{\max} - X_{\min}} - 1 \qquad (11.18)$$

where X norm denotes the normalized value of a variable, X is actual value of the variable, and X_{max} and X_{min} are the highest and least values of X, respectively. The prediction performance with respect to ANN and MLR models was measured with the help of graphical comparison. The mean absolute percentage error (MAPE), the root mean square error RMSE) and coefficients of determination (R^2) were utilized for assessing the robustness of the predicted models. The MAPE, RMSE and R^2 values were computed using Eqs. (11.19)–(11.21), respectively. The prediction models were selected on the basis of the criteria of best predicted values. In case of Eq. (11.21), $\bar{t}$ denotes the average of predicted values.

$$MAPE = \frac{1}{N} \left(\sum_{i=1}^{N} \left[\left| \frac{t_i - td_i}{t_i} \right| \right] \right) \times 100 \qquad (11.19)$$

$$\text{RSME} = \sqrt{\left(\frac{1}{N}\sum_{i=1}^{N}(t_i - td_i)^2\right)} \tag{11.20}$$

$$R^2 = 1 - \frac{\sum_{i=1}^{N}(t_i - td_i)^2}{\sum_{i=1}^{N}\left(t_i - \bar{t}\right)^2} \tag{11.21}$$

The mean square errors corresponding to the ANN model possessing 7 and 8 hidden neurons have been shown in Fig. 11.10. The results imply that the errors corresponding to the test set and validation set possess similar features and it does not point that considerable over-fitting has taken place. Therefore, the results obtained through ANN are appropriate. The plots among the evaluated and the predicted values corresponding to the ANN network have been presented in Fig. 11.11. The ANN model developed for seven and eight hidden layers have furnished predicted values which closely approximates the measured values as the correlation coefficients (r) are 0.90412 and 0.90664, respectively. Since the regression value corresponding to eight hidden neurons is little bit better than with having seven neurons. So, eight hidden neurons have been considered here.

11.6   Comparative Analysis of the Speed Response of Hydraulic Motor

The initial and foremost step in the designing of any control system is the development of mathematical model which depicts the dynamics associated with the system along with the motive of controlling it. The precise the dynamic model, more improved the performance linked with the controlled process or system. A closed-loop system is considered in order to make easier the determination of model parameters. It is obvious from Fig. 11.10 that the simulated response along with the experimental response related to the system is closely associated and justifies each other. While designing the desired response, it was taken in consideration that the response should be devoid of overshoot and steady state error along with the rise time to be considered as small as possible.

Step response is convenient to be applied and hence the reduction of error for the complete step response can lead to both lowering of rise time and overshoot. The PID controller is tuned and designed using MATLAB in such a way that the overshoot does not go over 10% with minimum or zero steady state error. Meanwhile, it can be observed that during the various course of speed range of motor rpm, the system turns oscillatory as minor oscillations or fluctuations are quite apparent. However, any attempt made towards improving the response nature with overshoot of zero along with steady state approaching zero will lead to substantial increase in rise and settling time linked with the response. The experimental response/result obtained with the help of PID control seems to be consistent with the simulation

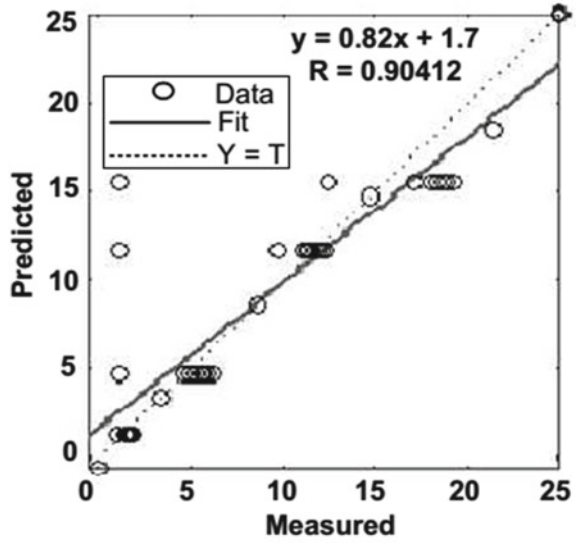**Fig. 11.10** Network errors for 7 and 8 hidden neuron neural network **a** 7 hidden-neuron **a** 8 hidden-neuron
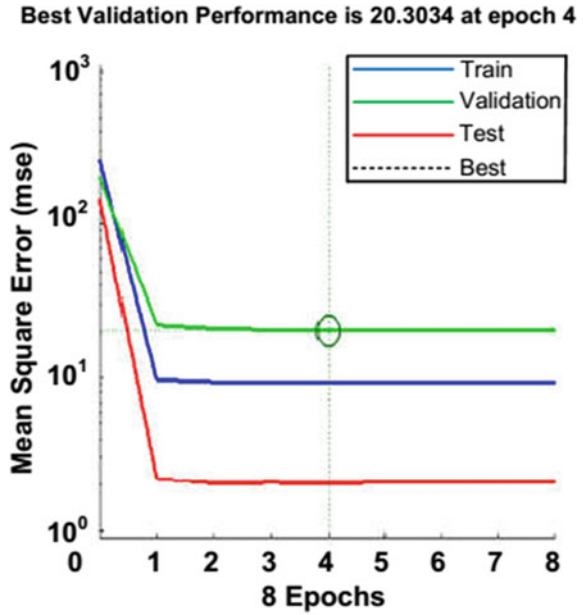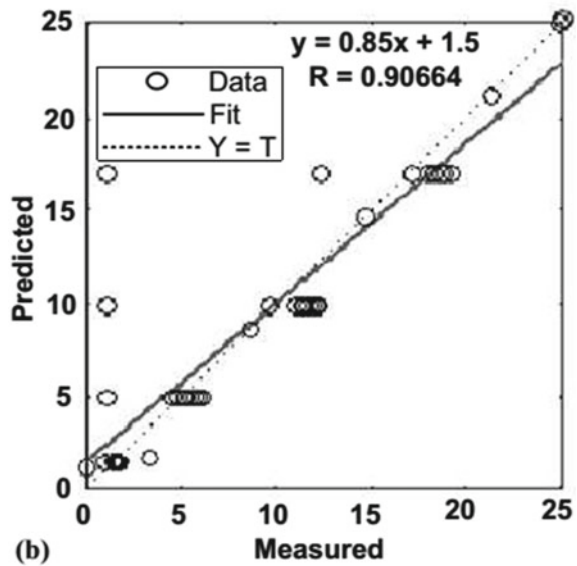

(a)
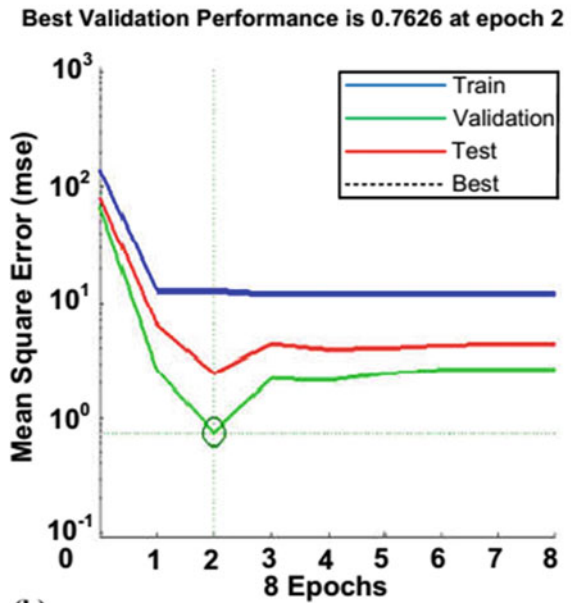
(b)

Fig. 11.11 Scatter plots for ANN model neuron employing 7 and 8 neurons **a** 7 hidden-neuron **b** 8 hidden-neuron

(a)

(b)

one. Time lag and overshoot seems to be the factors causing major differences in experimental and simulation results. PID control has the distinct character of ameliorating the response speed and unique precise control because it can monitor the PID parameters continuously based on the demand requirements by suitably adjusting the error values. In this way, PID control can give prompt, quick and precise response. Considering the case of a closed loop control system, where the step response speed tuned in by PID parameters gets incremented along with the steady decrement of the steady state error, due to the increment in the values of K_p and K_i and decrement in the value of K_d. The overshoot and vibration features will be there which will eventually lead to the extension of the adjustment time.

The neural network within the closed loop as shown in Fig. 11.9 is employed for updating the parameters of the PID controller i.e. proportional, integral and derivative gains. The nature of a second order closed loop system response depicting the motor speed having self-tuned PID controller utilizing the neural network approach along with the PID motor speed responses obtained via both simulation and experimentally have been depicted in Fig. 11.12. The plots corresponding to change in error is shown in Fig. 11.13. It is evident that the motor speed employing neural network approach (dash line) possesses less fluctuations and oscillations prior to reach the steady state
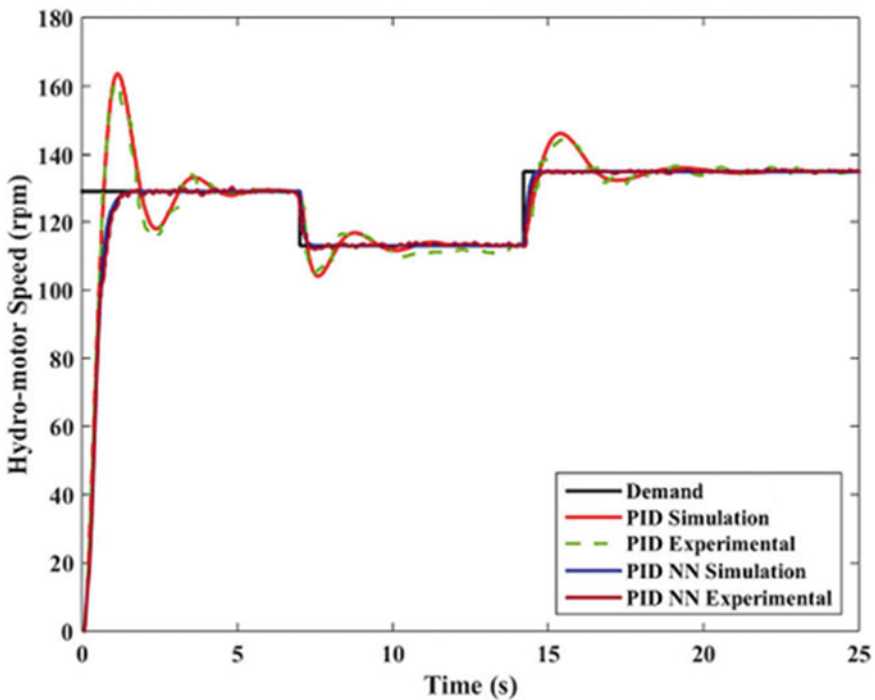

Fig. 11.12 Contrast of speed response of hydraulic motor with step command signal
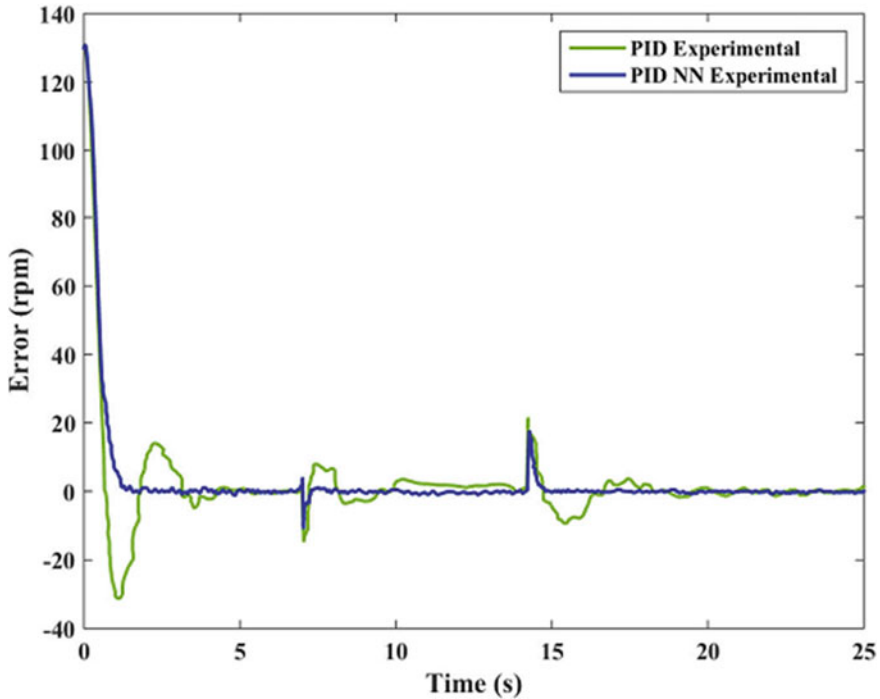
Fig. 11.13   Variation in error in hydraulic motor speed with time

in comparison to the simulated (solid line) and experimental (dash dot) motor speeds using PID.

References

Aoyama A, Doyle FJ, Venkatasubramanian V (1996) Control-affline neural network approach for non minimum-phase nonlinear process control. J Process Control 6(1):17–26

Çetin Ş, Akkaya AV (2010) Simulation and hybrid fuzzy-PID control for positioning of a hydraulic system. Nonlinear Dyn 61(3):465–476

Chang WD (2013) Nonlinear CSTR control system design using an artificial bee colony algorithm. Simul Model Pract Theory 31:1–9

Chen YM, He YL, Zhou MF (2015) Decentralized PID neural network control for a quad rotor helicopter subjected to wind disturbance. J Central South Univ 22:168–179

Cong S, Liang Y (2009) PID-like neural network nonlinear adaptive control for uncertain multivariable motion control systems. IEEE Trans Industr Electron 56(10):3872–3879

Costopoulus T (1992) Hydraulics and pneumatics. Symeon, Athens

Das J, Mishra SK, Saha R, Mookherjee S, Sanyal D (2017) Nonlinear modeling and PID control through experimental characterization for an electrohydraulic actuation system: system characterization with validation. J Braz Soc Mech Sci Eng 39(4):1177–1187

Elbayomy KM, Zongxia J, Huaqing Z (2008) PID controller optimization by GA and its performances on the electro-hydraulic servo control system. Chin J Aeronaut 21(4):378–384

Gharbi R, Karkoub M, ElKamel A (1995) An artificial neural network for the prediction of immiscible flood performance. Energy Fuels 9(5):894–900

Giacomino A, Abollino O, Malandrino M, Mentasti E (2011) The role of chemometrics in single and sequential extraction assays: a review Part II. Cluster analysis, multiple linear regression, mixture resolution, experimental design and other techniques. Analytica Chimica Acta 688(2):122–139

Guo B, Liu H, Luo Z, Wang F (2009) Adaptive PID controller based on BP neural network. In: International joint conference on artificial intelligence, 2009 (JCAI'09). IEEE, pp 148–150

Harrell FE (2001) Regression modeling strategies: with applications to linear models. Survival Analysis and logistic regression. Springer-Verlag, New York

Hassan MY, Kothapalli G (2012) Interval Type-2 fuzzy position control of electro-hydraulic actuated robotic excavator. Int J Min Sci Technol 22(3):437–445

Ho SJ, Shu LS, Ho SY (2006) Optimizing fuzzy neural networks for tuning PID controllers using an orthogonal simulated annealing algorithm OSA. IEEE Trans Fuzzy Syst 14(3):421–434

Jia CY, Shan XY, Cui YC, Tao BAI, Cui FJ (2013) Modeling and simulation of hydraulic roll bending system based on CMAC neural network and PID coupling control strategy. Int J Iron Steel Res 20(10):17–22

Jung JW, Leu VQ, Do TD, Kim EK, Choi HH (2015) Adaptive PID speed control design for permanent magnet synchronous motor drives. IEEE Trans Power Electron 30(2):900–908

Kaddissi C, Kenne JP, Saad M (2007) Identification and real-time control of an electrohydraulic servo system based on nonlinear backstepping. IEEE/ASME Trans Mechatron 12(1):12–22

Kaliafetis P, Costopoulos T (1995) Modelling and simulation of an axial piston variable displacement pump with pressure control. Mech Mach Theory 30(4):599–661

Kalyoncu M, Haydim M (2009) Mathematical modelling and fuzzy logic-based position control of an electrohydraulic servosystem with internal leakage. Mechatronics 19(6):847–858

Kang J, Meng W, Abraham A, Liu H (2014) An adaptive PID neural network for complex nonlinear system control. Neurocomputing 135:79–85

Karkoub M, Elkamel A (1997) Modeling pressure distribution in a rectangular gas bearing using neural networks. Tribol Int 30(2):139–150

Karkoub MA, Gad OE, Rabie MG (1999) Predicting axial piston pump performance using neural networks. Mech Mach Theory 34(8):1211–1226

Knohl T, Unbehauen H (2000) Adaptive position control of electrohydraulic servo systems using ANN. Mechatronics 10(1):127–143

Kumar V, Gaur P, Mittal AP (2014) ANN based self-tuned PID like adaptive controller design for high performance PMSM position control. Expert Syst Appl 41(17):7995–8002

Li CJ, Lilai Y, Chbat NW (1995) Powell's method applied to learning neural network control of three unknown dynamic systems. Optimal Control Appl Methods 16(4):251–262

Liu Z, Gao Q, Niu H (2014) The research on the position control of the hydraulic cylinder based on the compound algorithm of fuzzy & feed forward-feedback. Sensors Transducers 162(1):314–324

Ogata K (2003) Modern control engineering, 4th edn. Prentice Hall

Panda MN, Zaucha DE, Perez G, Chopra AK (1996) Application of neural networks to modeling fluid contacts in Prudhoe Bay. SPE J 1(3):303–312

Rexroth M (1986) The hydraulic trainer volume 2- proportional and servo valve technology

Skoczowski S, Domek S, Pietrusewicz K, Broel-Plater B (2005) A method for improving the robustness of PID control. IEEE Trans Industr Electron 52(6):1669–1676

Taormina R, Chau KW, Sethi R (2012) Artificial neural network simulation of hourly groundwater levels in a coastal aquifer system of the Venice lagoon. Eng Appl Artif Intell 25(8):1670–1676

Wu CL, Chau KW, Li YS (2009) Methods to improve neural network performance in daily flows prediction. J Hydrol 372(1):80–93

Zhao Y, Du X, Xia G, Wu L (2015) A novel algorithm for wavelet neural networks with application to enhanced PID controller design. Neuro Computing 158:257–267

Chapter 12
Study of Tribo-Corrosion in Materials

Hemalata Jena and Jitendra Kumar Katiyar

Abstract Tribocorrosion is a combined action of chemical and mechanical which causes material degradation during sliding, fretting, rolling, impingement etc. in a corrosive medium. It is very important to study the tribocorrosion behaviour and its testing conditions for the materials. These materials may be either ceramics or polymers or alloys. Further, it is found that tribochemical reactivity of metal is more as compare to ceramic and polymer. Moreover, polymer coatings are helpful to reduce the chemical reactivity of the metal in the presence of a corrosive medium. Therefore, tribocorrosion is an important factor among other factors to decide the application of materials in different environments. Hence, the present chapter has deliberated the tribocorrosion on different materials such as alloy, ceramics, and polymers and remedies suggested by different researchers to avoid tribocorrosion.

Keywords Tribocorrosion · Ceramic · Alloys · Polymers

12.1 Introduction

Tribology is an interdisciplinary subject that addresses the interaction between the surfaces which are in a relative motion. Due to relative motion, at the interface friction occurs which causes the wear. To reduce friction and wear from the interface, lubricant is applied. The lubricant may be either solid, semi-solid or liquid in nature.

There are different types of wear modes i.e. erosive, adhesive, abrasive, surface fatigue, corrosive, fretting etc. The most basic mechanisms of wear are shown in Fig. 12.1. Abrasive wear is a material loss from the surface when two body slides under pressure wherein the case of adhesive wear, materials get removed due to mutual affinity between two rubbing body. Tribo-chemical wear mechanism deals

H. Jena
School of Mechanical Engineering, KIIT Deemed To Be University Bhubaneswar, Odisha 751024, India

J. K. Katiyar (✉)
Department of Mechanical Engineering, SRM Institute of Science and Technology, Kattankulathur, Tamil Nadu-603203, India
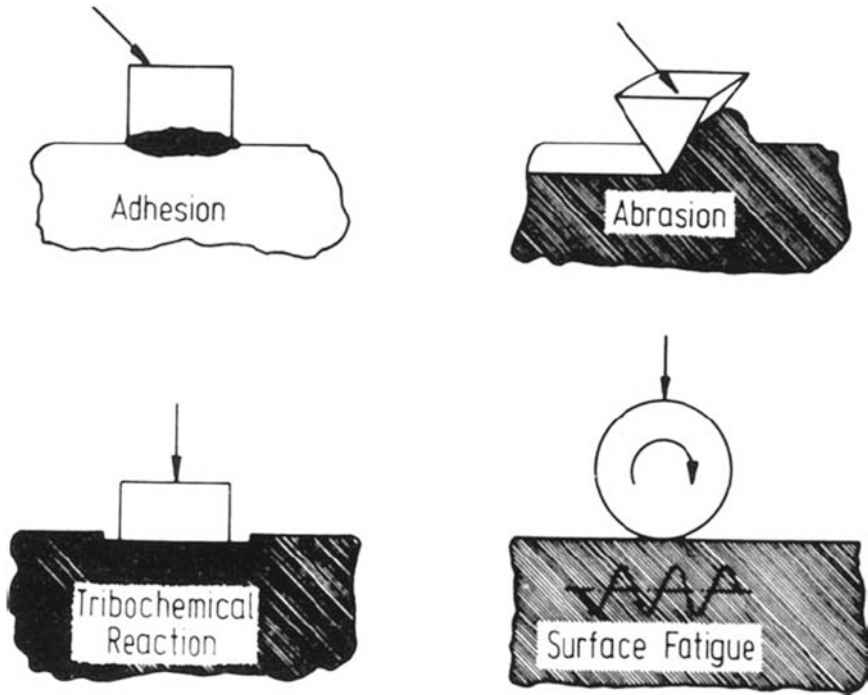e-mail: jitendrv@srmist.edu.in

Fig. 12.1 Schematic description of four basic wear mechanisms (Peterson 1980)

with the mechanical aspects as well as chemical aspects of the counter body. Hence, the wear mechanism in tribocorrosion is tribo-chemical. In this chapter, the emphasis will be on tribo-chemical wear. These mechanisms are described by the different researchers as shown in Table 12.1. To know the wear property, tribo-testers are required. For different wear modes, different wear tests are available which is shown in the Table 12.2.

Tribocorrosion is the material degradation during sliding, fretting, rolling, impingement etc. in a corrosive medium. The basic concept of tribocorrosion is shown in Fig. 12.2. A tribochemical reaction generates a reaction layer on the surface of the workpiece in the presence of corrosive liquids or gases. The wear rate of this case is found by considering the amount of reaction layer removed by the subsequent friction. Tribocorrosion may be Two- or Three-body contacts depending upon the presence of lubrication on the sliding between the two body. If there is no lubrication and one body is slides over another directly it is termed as Two-body. In the presence of lubricant or wear particles in between two body, it is known as Three-body contact. In the Three-body contact case, abrasives particles are locked in between the two surfaces which are free to roll and slide. Due to rubbing action of the abrasive particles, it causes the material degradation from the mating surface. Both Two-

Table 12.1 Research on wear mechanism

S. No	Name of researchers	Wear mechanisms	Ref
1	Burwell and Strang	Abrasive wear, Adhesive wear, Corrosive Wear, Surface Fatigue, Fretting, Erosion and Cavitation	Burwell and Strang (1952)
2	Jahanmir	Delamination, Adhesion, Fretting, Abrasion, Impact Wear, Surface Fatigue, Erosion, Diffusive Wear, Electric Contact Wear and Corrosive Wear	Burwell (1957)
3	Rice	Adhesion, Abrasion, Fatigue, Erosion, Corrosion or Oxidation and Electrical	Jahanmir (1980)
4	Godfrey	Delamination, Damage due to cavitation, Mild and severe adhesion, Abrasion, Erosion, Fatigue, Corrosion and Polishing	Godfrey (1980)

or Three-body contacts are responsible for the degradation of material in the tribo-corrosion. Different authors have reviewed the tribological behaviour and its test conditions and parameters (Nirmal et al. 2011, 2015; Jena 2019). Different materials show different tribological properties. Table 12.3 shows the tribological characteristic of different materials under various categories. In tribocorrosion mechanism, various chemical reactions take place at interface when bodies are in relative motion. In addition, a metastable reaction product is very important at interface because it developed a stable layer at interface and such layer is removed because of friction. Moreover, the various parameters that affect tribocorrosion are shown in Fig. 12.3. Stack (2002) has also reported that the corrosive environment may be complex. He has also concluded that various mechanistic maps have been generated which shows the transition between tribo-corrosion regimes with respect to the tribological and corrosive variables. According to him, there are three regimes of tribocorrosion. Those are active corrosion, passivation, or no corrosion which depends mostly on variables.

Present paper have reviewed nature of tribocorrosion on different materials and its scope. Novelty of this study is to give an overview of different authors what they have suggested for the remedies of tribocorrosion and its origin.
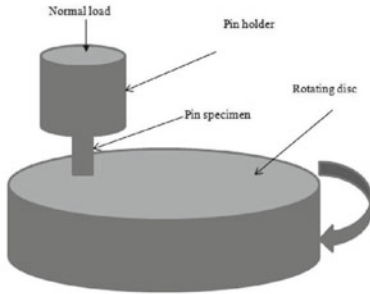
12.2 Tribocorrosion in Materials

A material undergoes tribocorrosion process when the relative motion of two contact surfaces under corroded medium results in wear-corrosion of the material. This increases or reduces the material loss of contacting surfaces as compare to individual degradation mechanisms which lead to unpredictable material behaviour
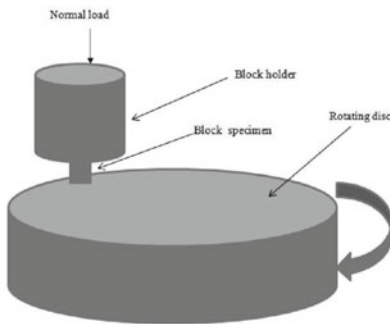
Table 12.2 Tribo testing equipments (Jena 2019)
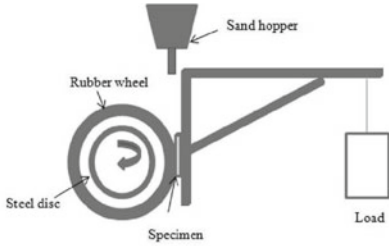
Rubber wheel abrasion test

(i)Rubber wheel test

 (i)Dry Sand Rubber Wheel (DSRW) follows ASTM-G65

(ii)Wet Sand Rubber Wheel (WSRW) follows ASTM -G105

(iii) Sand/Steel wheel (SSW) test in wet/dry conditions follows ASTM- B 611

- Abrasive wear behaviour of materials under three-body conditions.
- The dimension of the specimen is 70mm x 20mm x 7mm
- The rubber wheel get in touch with the specimen under a load
- Silica sand particles (i.e. fine, grain or coarse) are then introduced between the specimen and a rotating rubber wheel
- Used also for adhesive testing
- Operating parameters: applied load, rubber hardness, sliding speed.
- Applications: tyres, bushes, bearings and rollers

(ii)Pin-on-disk test

- Pin-on-disc abrasion test follows ASTM G99-05
- Dimension of the specimen is 10mm x 10mm 20mm.
- The test specimen is set perpendicular under loading against the rotating counterface.
- The contact area is not varying with respect to sliding time.
- Operating parameters: sliding velocity, sliding distance, normal load, wet or dry sliding, abrasive or adhesive contact condition.
- Application: sliding wear of various materials where constant contact area of interest.

Pin-on-disk abrasion test


Block on disc test

(iii)Block on disc test

- Block on Disc Test follows ASTMG99
- The dimension of the specimen is 10mm x 10mm 20mm.
- The test specimen is placed vertically to the counterface which is rotating.
- An infrared thermometer can be used for measuring interfaces temperatures during the interaction of sample and counterface.
- Contact area is not varying with respect to sliding time.
- Test can be adhesive and abrasive.
- Operating parameters: sliding velocity, sliding distance, normal load, wet or dry sliding, abrasive or adhesive contact condition.
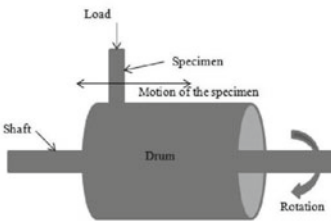- Applications: sliding wear of various materials

(continued)

Table 12.2 (continued)
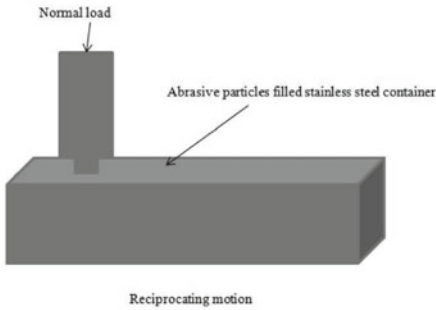
Linear Reciprocating Abrasion Testing
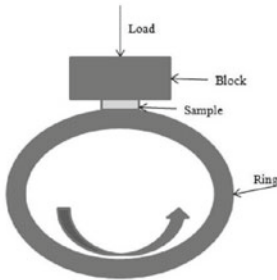
Block on ring test

Pin on drum test

where constant contact area of interest.

iv)**Linear reciprocating test**

Linear reciprocating abrasion test follows ASTM G133-05e1.

Abrasive wear behavior of materials under three-body conditions.

It has space for a variety of sample geometries to form point, line and area contacts.

Stainless steel container filled with abrasive moves linearly with the help of the power screw which is directly coupled to the motor and the specimen slides in the abrasive particles filled container.

- Test is abrasive in the presence of abrasive particles in the stainless steel container otherwise, the test is purely adhesive
- Operating parameters: sliding velocity, wet or dry sliding, abrasive types, applied load
- Application: linear sliding of window panels, door handles, lock mechanisms

(v)**Block on ring test**

- Block on Ring Test follows ASTM G77, G137-95 standards.
- Dimension of the specimen is 10mm x 20mm x 50mm.
- Test sample place parallel to the side of the counterface and contact surface varies with the sliding time.
- Operating parameter: sliding velocity, sliding distance, applied load, temperature, wet or dry sliding
- Applications: crankshafts, camshafts, piston pins, connecting rods, suspensions, lubricants.

(vi)**Pin on drum test**

- Pin on drum test follows ASTM A514
- Specimen travels linearly which is placed horizontally against a rotating drum.
- The drum is covered with abrasive paper. Without abrasive paper, test is simply adhesive.
- Operating parameters: sliding distance, sliding velocity, applied load, wet or dry sliding, abrasive or adhesive contact condition.
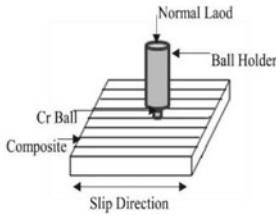- Applications: conveyor belts, rotating rollers etc.

(continued)

under a simultaneous effect of mechanical force and corrosion. This wear-corrosion behaviour of the metal can be shown in the following equation (Landolt et al. 2004).

$$T = W + C + S \tag{12.1}$$

Table 12.2 (continued)

	(vii)**Low-amplitude oscillating test**

Low-amplitude oscillating Test

- Known as Fretting wear
- 10 mm x10 mm x 3-4 mm
- A polished chromium steel ball having surface roughness values in the range 0.01–0.015 μm oscillates against the specimen. The diameter of the ball is 10 mm.
- Operating parameter: Load, sliding velocity, number of cycles, slip amplitude, slip, frequency, contact geometry, material properties, environment.
- Application: Bearings, gears, bushes, flanges, multilayer leaf springs, palliatives
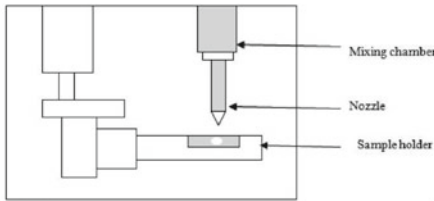
(viii)**Erosion test**
- Erosion test follows ASTM: G76–07
  Dimension of the specimen 20mm×20mm
  The dry and compressed air with the solid sand particles hit on the test sample at various speeds and angle at constant feed rate through converging nozzle.
  Stand of distance is 10 mm.
  Operating parameters: impingement angle, impact velocity, erodent type
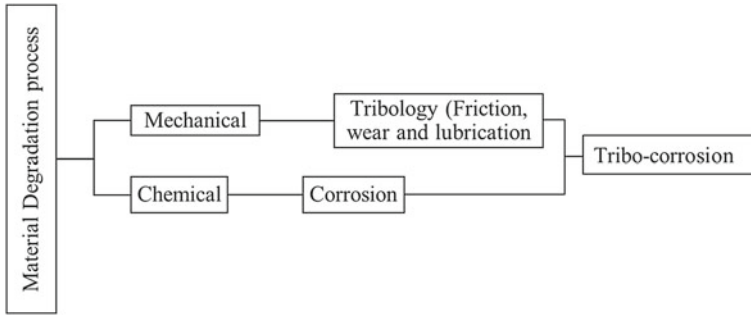- Application: rotor blade, convener belt

Erosion test

Fig. 12.2 Basic concept and definition of tribocorrosion

Table 12.3 Tribological characteristics in relation to material types (Czichos et al. 1995)

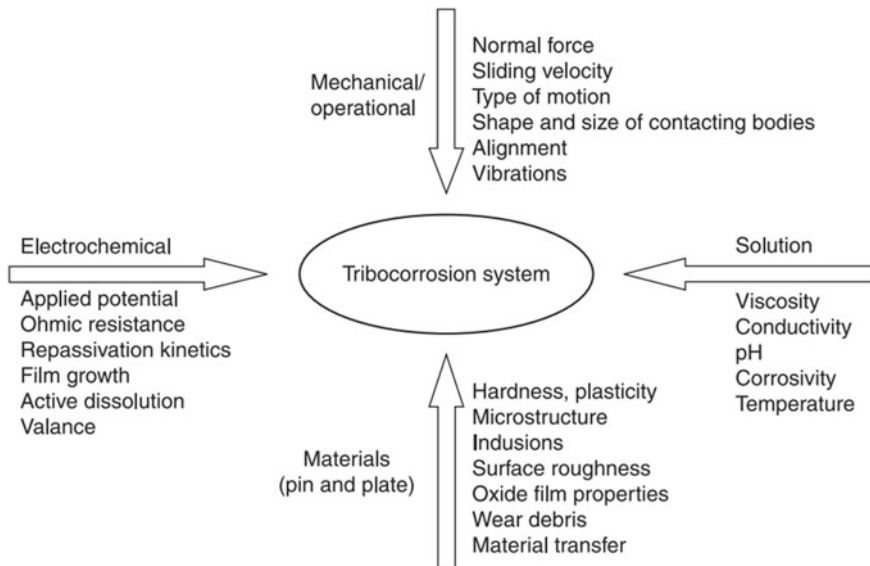| Mass forces	$F_{polymer} < F_{ceramic} < F_{metal}$
Hertzian pressure	$F_{polymer} < F_{metal} < F_{ceramic}$
Friction-induced temperature increase	$< F_{metal} < F_{polymer} < F_{ceramic}$
Adhesive energy (surface tension)	$Ad_{polymer} < Ad_{metal} < Ad_{ceramic}$
Abrasion	$Ab_{ceramic} < Ab_{metal} < Ab_{polymer}$
Tribochemical reactivity	$R_{polymer}, R_{ceramic} < R_{metal}$

Fig. 12.3 Various parameters which affect the tribocorrosion system is sliding contact under electrochemical environment (Wood 2017)

where T = Total volume losses by tribocorrosion (mm^3), W = Loss of volume due to mechanical wear (mm^3), C = Loss of volume due to electrochemical corrosion (mm^3), and S = Loss of volume due to the synergy of wear and corrosion (mm^3).

The term S which is known as total wear-corrosion synergism further divided into two components. The one component represents the increase in mechanical wear due to corrosion and second component represents the increase in corrosion due to mechanical wear. Various parameters like the nature of contact, the contacting material and the environment have influenced tribocorrosion behaviour. Berradja et al.(2006) have studied the influence of contact frequency on tribocorrosion behaviour of the steel in corrosive medium. They have concluded that an increase in contact frequency causes the reduction of open-circuit potential and improvement of anodic current. This may be due to the involvement of more active material in the electrolyte at higher contact frequency due to the less time between two successive contacts in the worn path. A detailed discussion on tribocorrosion of materials is explained in the following section about the testing procedure and influence of process parameters on tribocorrosion of alloy, ceramic and polymer.

12.2.1 Tribocorrosion in Alloys

Alloys have been received interest in various applications such as aerospace and automotive application for their high strength-to-weight ratio. Magnesium (Mg) alloys

have good machinability, high thermal conductivity, but have poor wear resistance in corrosive environments which limits their applications (Liu et al. 2021). Hence, to reduce the wear and friction under corrosive environment, alloys are needed to coat for protection. Sun et al. (2009) have coated polymer on CoCrMo alloy and studied its tribocorrosion behaviour under body fluid. Mischler and Pax (2002) have studied the surface degradation due to friction between bone and Titanium alloy (implant material) under body fluid conditions.

Corrosion wear of alloys has been calculated by immersion test, open circuit potential (OCP), potentiodynamic polarization, and anodic polarization as shown in Fig. 12.4. The immersion test is conducted as per ASTM G31 (Ayyagari et al. 2018). It is a simple technique to measure the loss of mass or gain in mass of the alloy under the corrosive environment. The following relation is used to calculate the corrosion rate (Ayyagari et al. 2018).

$$\text{Corrosion rate} = \frac{k \times w}{A \times t \times \rho} \quad (12.2)$$

where, k = Constant, t = Time of exposure (hrs.), A = Area (cm^2), w = Mass loss/gain (g), ρ = Density of metal (g/cm^3). In Fig. 12.4, the working electrode is the pin, however, either the pin or the disc/plate can be the working electrode based on the material to be tested. Three electrodes are used in tribocorrosion tester: one is a reference electrode, second is a working electrode (sample), and third is a counter electrode. The reference electrode may be Saturated Calomel Electrode (SCE), Ag/AgCl electrode, or Standard Hydrogen Electrode (SHE). The counter electrode may be platinum or graphite. These three electrodes are immersed inside the electrolytes and supplied with potential and current cell which is known as potentiostat.
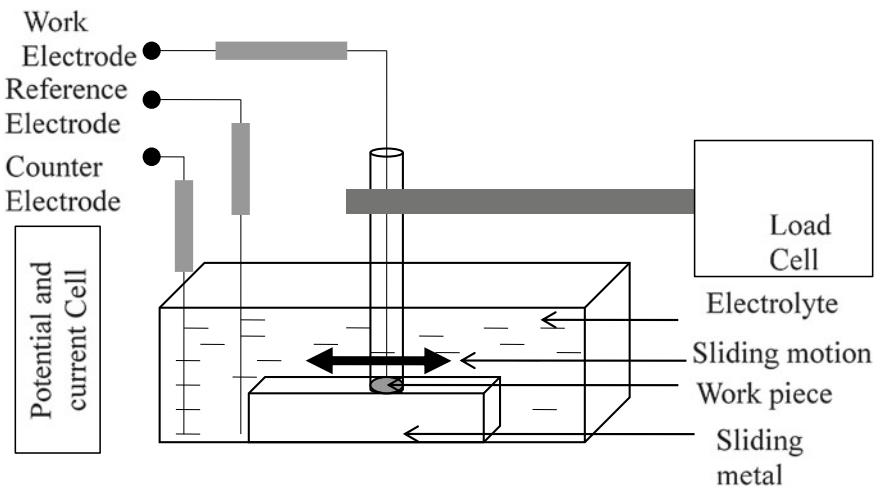

Fig. 12.4 Tribocorrosion tester

To avoid the electrochemical corrosion of the workpiece sample, a potential difference of -0.8 V for stainless steel is applied during the test which is known as cathodic protection. The mass loss of metal by cathodic protection is known as pure mechanical wear. Electrochemical techniques for the study of tribocorrosion of metal are as follows: Open Circuit Potential (OCP) measurement, potentiodynamic polarization and electrochemical corrosion tested on the worn surface. In OCP, there is no external current or potential is applied to the metal which is deep in an electrolyte. In this condition, the developed potential at the surface of the electrode during deep inside the electrolyte is known as the Open Circuit Potential (OCP). In OCP, the system obtains the equilibrium condition where the net current is considered as zero. From the equilibrium condition, it is taken as a reference condition for considering the potential and potential changes in the system relating to standard electrodes i.e. Standard Calomel Electrode (SCE).

In potentiodynamic polarization, the system has to maintain in OCP for one hour first. In the test, the sample undergoes a potential sweep ranging at a particular scan rate which is different for different alloys. Beyond the potentiodynamic polarization voltage range, it causes anodic reactions, like fail of the protective surface oxides, coating and pitting.

The following relation is used to calculate the corrosion rate (Ayyagari et al. 2018).

$$\text{Corrosion rate} = \frac{k \times i_{corr} \times EW}{\rho} \tag{12.3}$$

where, $k = 3.27 \times 10^{-3}$ mm g/(μA.cm.year), i_{corr} = corrosion current density (A/m^2) and EW = equivalent weight (g). Corrosion behaviour is caused by the intrinsic properties of the coating. The coating on steel and other metal is a technique to protect them in tribocorrosion environment. The porosity of the coating helps to determine the extent of corrosion. The porosity of the coating can be calculated by using the potentiodynamic polarization method which is developed by Mathes et al.(1991):

$$P = \left(R_{pm}/R_p\right) \times 10^{|\nabla E_{corr}/\beta_a|} \tag{12.4}$$

where, R_{pm} = Polarization resistance of the substrate, R_p = Polarization resistance of coating-substrate, ∇E_{corr} = Corrosion potential difference between the substrate and coating layer, and β_a = Anodic Tafel constant of substrate. Similarly, efficiency of the coating is calculated by using following relation (Nozawa and Aramaki 1999):

$$P_i = 100(1 - i_{corr}/i_{corr}^*) \tag{12.5}$$

where i$_{corr}$ and i*$_{corr}$ are corrosion current density (A/m^2) with and without coating, respectively.

Table 12.4 Experimental conditions of tribocorrosion of alloys

Workpiece	Wear test condition	Electochemical Corrosion test condition	Potentiodynamic measurements	Observation	Ref
Ti6Ak4V coated with and without Diamond Like Carbon(DL)	**Pin-on-plate** Al_2O_3 ball = 5 mm diameter Normal load = 4 N, 16 N Sliding velocity = 8 mm/s, 32 mm/s Sliding distance = 8 mm	Electrolyte = PBS (pH 7.1) Counter Electrode = Platinum Wire Reference electrode = SCE	Scan rate = 0.167 mV/s at 400 mV	DLC improve the corrosion resistance but reduces the life of coating at simultaneous effect of wear and corrosion	Manhabosco and Muller (2009)
Low alloy steel (one ferritic and one martensitic)	**Pin-on-disc** Al_2O_3 ball Load = 20 N Linear sliding speed = 0.2 m/s	Electrolyte = simulated waste solution (pH 4.5) Counter Electrode = platinum ring Reference electrode = Ag/AgCl	− 600 mV to 800 mV at a sweep rate of 0.5 mV/s **For ferritic Steel** Cathodic potential = − 700 mV vs. Ag/AgCl Anodic potentials = − 600, − 400 and − 200 mV vs. Ag/AgCl, **For martensitic Steel** Cathodic potential = − 650 mV vs. Ag/AgCl Anodic potentials = − 450, − 300 and − 100 mV vs. Ag/AgCl	Ferritic grade low alloy steel showed higher wear corrosion as compared to the martensitic grade Low alloy steel	Mantyranta et al. (2019)

Table 12.4 (continued)

Workpiece	Wear test condition	Electochemical Corrosion test condition	Potentiodynamic measurements	Observation	Ref
Aluminium bronze	**Pin-on-disc** Load = 10 N,20 N	Electrolyte = 3.5 wt.% NaCl solution Counter Electrode = platinum ring Reference electrode = Ag/AgCl	– 600 mV to 800 mV at a sweep rate of 0.5 mV/s	The sliding load causes the plastic deformation and abrasive wear	Huttunen-Saarivirta et al. (2018)
Ti-6Al-4 V	**Reciprocating ball-on-plate** Al₂O₃ ball = 10 mm diameter Load = 1 N Frequency = 1 Hz Stroke length = 3 mm	Electrolyte = PBS Reference electrode = SCE	-	Tribocorrosion of Ti-6Al-4 V made by Laser Engineered Net Shaping shows better wear resistance as compared to the parts made by casting and hot pressing	Buciumeanu et al. (2018)
ASTM-F67Gr1 titanium alloy	**Pin-on-flat reciprocating sliding** Silicon nitride indenter = 6 mm Load = 4.85 N, 9.71 N Speed = 9,3,23.3 mm/s	Electrolyte = Ringer solution Counter Electrode = platinum ring Reference electrode = SCE	Scan rate = 1 V/s Anodic potential = 2.3 V Cathodic potential = – 0.8 V	Speed and the applied load affect the titanium degradation, corrosion decreases the mechanical wear except under the condition of highest applied load and sliding speed	Ferreira et al. (2019)

*saturated calomel electrode (SCE)
* Phosphate Buffered Saline (PBS)

Table 12.4 show the experimental conditions for tribocorrosion of alloys. There is broad research on wear of the coatings in different environment condition like humidity, water, lubricant, corrosive and physiological environment etc. Manhabosco and Muller (2009) have performed tribocorrosion of a DLC-coated Ti alloy in a simulated physiological environment i.e. PBS solution. Coatings show high protection efficiency against corrosion of the alloy. In marine and mining industry, tribocorrosion plays an important role for metal like steels. Under tribocorrosion, most of the alloys like stainless steel and titanium- or cobalt-based medical alloys behave passively. When the contact between the workpiece and the probe material makes electrochemical analysis difficult, direct and indirect ultrasonic vibratory cavitation system is adopted to measure the tribocorrosion. In direct ultrasonic vibratory cavitation system, the sample is fixed to the sonotrode and indirect system, the sample is rigidly fixed on a device with an offset distance between the sonotrode and the sample. The vibratory device produces oscillations of small amplitude (50 μm) and high frequency (20 kHz) on the surface of a sample immersed in liquid. The vibration of the devices produces the oscillation of sample and the sonotrode which creates cavitations bubbles. The breakage of the bubbles on the sample surface results in cavitations erosion. Various authors have studied the ultrasonic vibratory cavitation system on steel. Basumatary et al. (2015) have conducted erosion-corrosion test on duplex stainless steel (DSS) and nickel aluminium bronze (NAB) under distilled water and saline water by indirect ultrasonic vibratory cavitation system.

12.2.2 Tribocorrosion in Ceramics

Ceramic is an inorganic non-metallic solid material that is widely used for pottery, cement, porcelains, glass, refractories and abrasives and glass. Ceramic has good mechanical, thermal, tribological property and possesses chemical inertness. It performs excellently in high heat applications. Hence, coating of ceramic particles with an alloy matrix (cermets) are methods to improve the hardness, corrosion and chemical resistance, toughness and ductility of the metals. Figure 12.5 shows the basic principles of tribocorrosion of different ceramics and their behaviours
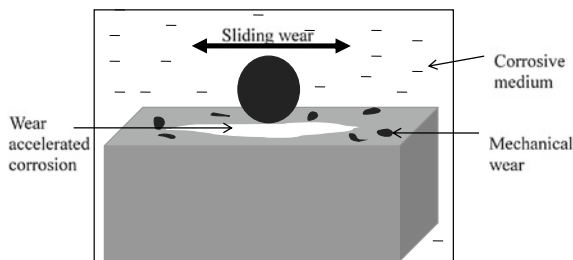

Fig. 12.5 Tribocorrosion of ceramic under corrosive medium

under corrosive medium. Ceramic materials slide with another materials, the wear on ceramic particles are accelerated due to the presence of corrosive medium. Silicon nitride is a tribological material in especially rolling applications and the strongest material. Renz et al. (2016) have investigated the wear property of cutting tools made of ceramic material i.e. SiAlON and SiC whisker reinforced with alumina in dry sliding action with the work material of Inconel 718. The wear rate of SiAlON exponentially decreases with an increase in frictional power and the wear rate of Al_2O_3–SiC is lesser than that of SiAlON at high frictional power. This may be due to the chemical stability of the Al_2O_3 matrix and the development of stable lubricous tribo-layers. The wear coefficient of non-oxidative ceramic sliding against themselves is calculated by using the following relation where it is believed that heating due to rubbing between two bodies also increases the chemical reaction at the contact interface (Kitaoka et al. 1997).

$$K_c = \frac{A}{\rho v} \exp\left(-\frac{Q}{R_g T}\right) \tag{12.6}$$

where, Q = Activation energy (J), Rg = Gas constant 8.314 J/ mol·K, T = Reaction temperature, ρ = Density of oxide, and v = Sliding velocity. Table 12.5 shows the experimental condition of wear-corrosion of ceramics which indicates the influence of experimental conditions on the wear-corrosion behaviour of ceramics.

12.2.3 Tribocorrosion in Polymers

Polymers are well known for their non-degradability, low weight, adhesive in nature etc. In the recent era, plastic industries boom in the market for their wide acceptability and applicability. It may be natural or synthetic in nature which is classified into as thermoplastic, thermosetting, and elastomers. Polymers and their composite show good tribocorrosion resistance properties in special applications like biomedical, aerospace, shipbuilding. Titanium-based materials are widely used in orthopaedics, implantology, but it releases metallic ions to surrounding tissue when it comes to contact with saliva and body fluid. This is the reason for tissue inflammatory reactions which is harmful to the human body. Poly-ether-ether-ketone (PEEK) polymer coating is used on the metal to improve the tribcorrosion resistance because of its good resistant to a wide variety of organic and inorganic fluids (Kim et al. 2004).

It is observed that corrosion of hip replacement bearing material for metal-on-metal is higher than metal-on-polymer under the condition of 0.35% NaCl and bovine serum solutions (Hesketh et al. 2012). Metal on polymers can help to avoid the formation of metallic debris in total hip joint application during metal-on-metal bearing. Hence metal-on-polymer is the emerging technology in this area of research. Stack

Table 12.5 Experimental conditions of tribocorrosion of ceramics

Ceramics	Tribo test	Medium	Observation	Ref
Ionic ceramics (Al_2O_3 and ZrO_2) Covalent ceramics (Si3N4 and SiC) (Rubbing against Al2O3 ball)	**Ball-on-disk** Sliding speed = 0.30 m/s Load = 2.5 N Sliding distance = 800 m	CF_3CH_2F (HFC-134a)	CF_3CH_2F gas reduces the friction and wear of all the ceramic	Cong et al. (2002)
Al_2O_3 ZrO_2 (Rubbing against Ni)	**Linear reciprocal sliding motion** 30 min with a Frequency = 1 Hz Load = 2.74 N Contact pressure = 667 MPa Stroke length = 5 mm. Sliding velocity = 20 mm/s	Citrate buffer solution (pH 4.5)	The formation of mixed nickel and aluminium/zirconium oxides is suggested as the wear mechanism of alumina and zirconia	Du et al. (2019)
Zirconia (two material: Brittle and Taugh) (Rubbing against Zirconia)	**Pin-on-disk** Normal load = 9.8 N Sliding speed = 1 mm/s	Air, Water, Hexadine, Stearic acid, Nitrogen	Different materials behave differently in various corrosive medium	Fischer et al. (1988)
Si_3N_4 (Rubbing against Si_3N_4)	**Ball-on-block** Load = 9.8 N Sliding speed = 2.4 mm/s	Deionized water, purified n-alcohols, water–methanol and methanol-nonanol	Water causes highest friction and wear on Si3N4	Hibi and Enomoto 1989)
SiC (Sliding against Mo)	**Linear reciprocal sliding motion** Stroke distance = 3 mm Speed = 0.2 mm/s Load = 0.5 N Contact pressure = 0.7GPa	Gas: SO_2, O_2 or H_2S at a gas pressure 4–40 Pa	Produces low friction, lubricating films under this gas medium	Singer et al. (1996)

et al. (2005) have applied polymer coating in steel under carbonate/bicarbonate solution for the hip joint. Sampaio et al. (2016) have added a veneering poly-ether-ether-ketone (PEEK) over titanium-based metal for enhancement of wear and corrosion properties of biocompatible prosthetic structures. They have conducted the test on reciprocation ball-on-plate tribometer at 30 N normal load under 1 Hz reciprocation frequency. They have reported that PEEK protected titanium alloy from corrosion when submerged in artificial saliva, lower friction coefficient and higher wear resistance by applying PEEK over titanium alloy. Under tribocorrosion conditions, PEEK has a lower coefficient of friction against Alumina (0.07) than that of Titanium-based metal (0.36). Xu et al. (2018) have conducted the tribocorrosion behaviours of (PEEK) and its composite composites sliding against stainless steel in seawater conditions. It is found that PEEK reinforced with short carbon fibres (SCF) when added with 5 vol% hexagonal boron nitride nanoparticles (h-BN) considerably improves the wear resistance. Further added SCF and SCF/h-BN into the PEEK has shown the higher wear resistance when sliding under seawater than in deionized water. Filler plays an important role to decide the tribological property of the polymer. Different authors have taken various filler added in the polymer and tested the wear behaviour under the lubricated with deionized and seawater (Chen et al. 2008; Yan et al. 2013). It is found that polymer composite having filler as an important phase which synergistically improves the wear and corrosion performance of the polymer.

12.3   Future Scope

Tribocorrosion has developed into a promising area of research with biomedical and bioengineering applications. It is a combination of mechanical and environmental effects. From the literature, it is seen that the relative occurrence of tribocorrosion in engineering parts is 10% where abrasion, adhesion, surface fatigue, corrosion and erosion are 30, 15, 15, 12, 10 and 8% respectively (Celis 2017). This is the main factor of economic loss due to friction and wear. Tribocorrosion can be seen largely from the engineering part to medical application. Hence, more research should be addressed to develop the analytical or simulation model to know the occurrence, caused and alternatives should be raised for reduction of this complex wear and friction phenomenon. The study and research on tribocorrosion have been started for the last 30 decades, but improvement of a standard test method is still a major apprehension. In this area of research, momentous developments have been found in the collaborations between researchers around the globe as shown in Fig. 12.6. More scope of tribocorrosion is in the clinical application where more challenges are there. Hence multidisciplinary research must be diversified.
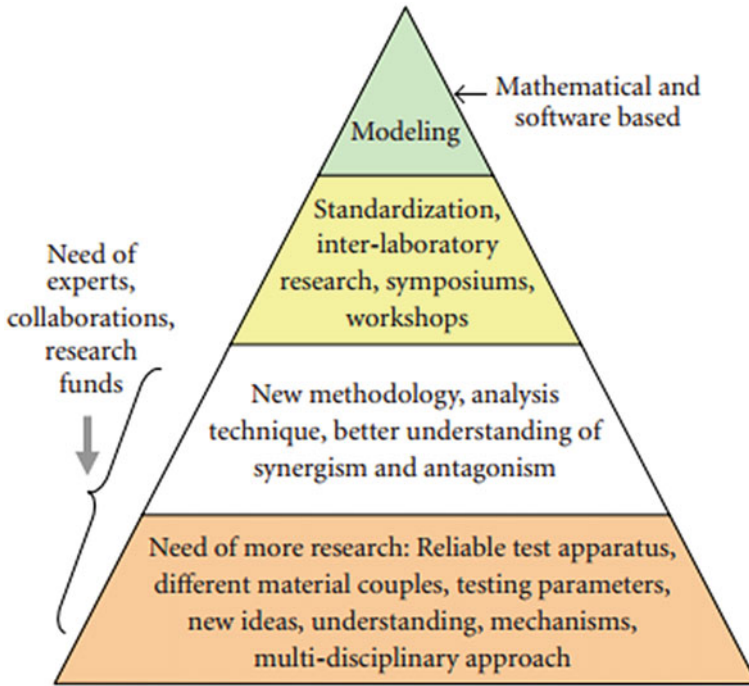
Fig. 12.6 Future scope of tribocorrosion research (Mathew et al. 2009)

12.4 Conclusions

Tribocorrosion is a very important phenomenon to address with respect to various materials such as polymers, ceramics, and alloys. The present chapter reveals that:

- Tribocorrosion is a combined action of chemical and mechanical processes which causes the material degradation during sliding, fretting, rolling, impingement etc. in a corrosive liquids or gases. A tribochemical reaction creates a reaction layer on the surface of the workpiece in the presence of corrosive medium. The wear rate of this case is found by considering the amount of reaction layer removed by the subsequent friction.
- Tribocorrosion has been evaluated by various methods such as immersion test, open circuit potential (OCP), potentiodynamic polarization, and anodic polarization. Moreover, surface coatings can reduce it. Furthermore, a detailed study can be performed on the cathodic and anodic reaction of the metal in a wear-corrosion test for a better understanding of tribochemical reaction at interface.

References

Ayyagari A, Hasannaeimi V, Grewal HS, Arora H, Mukherjee S (2018) Corrosion erosion and wear behaviour of complex concentrated alloys: a review. Metals 8(603):1–40

Basumatary J, Nie M, Wood RJK (2015) The synergistic effects of cavitation erosion–corrosion in ship propeller materials. J Bio- Tribo-Corrosion 1(12)

Berradja A, Bratu F, Benea L, Willems G, Celis J-P (2006) Effect of sliding wear on tribocorrosion behaviour of stainless steels in a ringer's solution. Wear 261:987–993

Buciumeanu M, Bagheri A, Shamsaei N, Thompson SM, Silva FS, Henriques B (2018) Tribocorrosion behaviour of additive manufactured Ti-6Al-4V biomedical alloy. Tribol Int 119:381–388

Burwell JT Jr (1957/58) Survey of possible wear mechanisms. Wear 1:119–141

Burwell JT, Strang CD (1952) On the empirical law of adhesive wear. J Appl Phys 23:18–28

Celis J-P (2017) Testing tribocorrosion of passivating materials supporting research and industrial innovation: a handbook. CRC Press, United Kingdom

Chen J, Jia J, Zhou H, Chen J, Yang S, Fan L (2008) Tribological behaviour of short fiber-reinforced polyimide composites under dry-sliding and water-lubricated conditions. J Appl Polym Sci 107:788–796

Cong P, Li T, Mori S (2002) Friction–wear behavior and tribochemical reactions of different ceramics in HFC-134a gas. Wear 252:662–667

Czichos H, Klaffke D, Santner E, Woydt M (1995) Advances in tribology: the materials point of view. Wear 190:155–161

Du J, Cao S, Munoz AI, Mischler S (2019) Tribological and tribocorrosion behaviour of nickel sliding against oxide. Wear 426–427:1496–1506

Ferreira DF, Ale Almeida SM, Soares RB, Juliani L, Bracarense AQ, Cunha Linsb VF, Junqueira RMR (2019) Synergism between mechanical wear and corrosion on tribocorrosion of a titanium alloy in a Ringer solution. J Mater Res Technol 8(2):1593–1600

Fischer TE, Anderson MP, Jahanmir S, Salher R (1988) Friction and wear of tough and brittle zirconia in nitrogen air, water, hexadecane and hexadecane containing stearic acid. Wear 124:133–148

Godfrey D (1980) Diagnosis of wear mechanisms. In: Peterson MB, Winer WO (eds) Wear control handbook. ASME, New York, pp 283–311

Hesketh J, Hu X, Dowson D, Neville A (2012) Tribocorrosion reactions between metal-on-metal and metal-on-polymer surfaces for total hip replacement. Proc Instit Mech Eng Part J J Eng Tribol 226(6):564–574

Hibi Y, Enomoto Y (1989) Tribochemical wear of silicon nitride in water, n-alcohols and their mixtures. Wear 133:133–145

Huttunen-Saarivirta E, Isotahdon E, Metsajoki J, Salminen T, Carpen L, Ronkainen H (2018) Tribocorrosion behaviour of aluminium bronze in 3.5 wt.% NaCl solution. Corrosion Sci 144:207–223

Jahanmir S (1980) On the wear mechanisms and the wear equations. In: Suh NP, Saka N (eds) Fundamentals of triblogy. MIT Press, Cambridge, pp 455–467

Jena H (2019) Study of tribo- performance and application of polymer Composite. In: Automotive tribology. Springer Science and Business Media LLC, , pp 65–99. ISBN 978–981–15–0434–1

Kim S, Lee K, Seo Y (2004) Polyetheretherketone (PEEK) surface functionalization by low-energy ion-beam irradiation under a reactive O2 environment and its effect on the PEEK/copper. Langmuir 10:157–163

Kitaoka S, Tsuji T, Yamaguchi Y, Kashiwagi K (1997) Tribochemical wear theory of non-oxide ceramics in high-temperature and high-pressure water. Wear 205:40–46

Landolt D, Mischler S, Stemp M (2004) Third body effects and material fluxes in tribocorrosion systems involving a sliding contact. Wear 265:517–524

Liu S, Li G, Qi Y, Peng Z, Ye Y, Liang J (2021) Corrosion and tribocorrosion resistance of MAO-based composite coating on AZ31 magnesium alloy. Journal of Magnesium and Alloys. https://doi.org/10.1016/j.jma.2021.04.004

Manhabosco TM, Muller L (2009) Tribocorrosion of Diamond-Like Carbon Deposited on Ti6Al4V. Tribol Lett 33:193–197

Mantyranta A, Heino V, Isotahdon E, Salminen T, Huttunen-Saarivirta E (2019) Tribocorrosion behaviour of two low-alloy steel grades in simulated waste Solution. Tribol Int 138:250–262

Mathew MT, Pai PS, Pourzal R, Fischer A, Wimmer MA (2010) Significance of tribocorrosion in biomedical applications: overview and current status. Adv Tribol. Article ID: 250986

Matthes B, Brozeit E, Aromaa J, Ronkainen H, Hannula SP, Leyland A, Matthews A (1991) Corrosion performance of some titanium-based hard coatings. Surf Coat Technol 49(1–3):489–495

Mischler S, Pax G (2002) Tribological behaviour of titanium sliding against bone. Eur Cell Mater 3(1):28–29

Nirmal U, Hashim J, Lau STW (2011) Testing methods in tribology of polymeric composites. Int J Mech Mater Eng 6(3):367–373

Nirmal N, Hashim J, Megat Ahmad MMH (2015) A review on tribological performance of natural fibre polymeric composites. Tribol Int 83:77–104

Nozawa K, Aramaki K (1999) One and two dimesional polymer films of modified alkanethiol monolayers for preventing iron from corrosion. Corros Sci 41(1):57–73

Peterson MB (1980) Classification of wear processes. In: Peterson MB, Winer WO (eds) Wear control handbook. ASME, New York, pp 9–15

Renz A, Khadera I, Kailer A (2016) Tribochemical wear of cutting-tool ceramics in sliding contact against a nickel-base alloy. J Eur Ceram Soc 36(3):705–717

Sampaio M, Buciumeanu M, Henriques B, Silva FS, Souza Julio CMJ, Gomes R (2016) Tribocorrosion behaviour of veneering biomedical PEEK to Ti6Al4V structures. J Mech Behav Biomed Mater 54:123–130

Singer IL, Mogne TL, Donnet C, Martin JM (1996) Friction Behaviour and Wear Analysis of SiC Sliding Against Mo in SO2, O2 and H2S at Gas Pressures Between 4 and 40 Pa. Tribol Trans 39(4):950–956

Stack MM (2002) Mapping tribo-corrosion processes in dry and in aqueous conditions: some new directions for the new millennium. Tribol Int 35:681–689

Stack MM, Jawan H, Mathew MT (2005) On the construction of micro-abrasion maps for a steel/polymer couple in corrosive environments. Tribol Int 38(9):848–856

Sun D, Wharton JA, Wood RJK, Ma L, Rainforth WM (2009) Microabrasion-corrosion of cast CoCrMo alloy in simulated body fluids. Tribol Int 42(1):99–110

Wood RJK (2017) Marine wear and tribocorrosion. Wear 376–377:893–910

Xu Y, Qi H, Li G, Guo X, Wan Y, Zhang Ga (2018) Significance of an in-situ generated boundary film on tribocorrosion behaviour of polymer-metal sliding pair. J Colloid Interf Sci 518:263–276

Yan L, Wang H, Wang C, Sun L, Lin D, Zhu Y (2013) Friction and wear properties of aligned carbon nanotubes reinforced epoxy composites under water lubricated condition. Wear 308:105–112